Thesis for the degree of Doctor of Philosophy

Fluorescent Calixarenes as Molecular Receptors

Carol Lynam B.Sc.

Dublin City University
School of Chemical Sciences

August 2002

Supervisor: Prof. Dermot Diamond

I hereby certify that this material, which I now submit for assessment on the programme of study leading to the award of Doctor of Philosophy is entirely my own work and has not been taken from the work of others save and to the extent that such work has been cited and acknowledged within the text of my work.

Signed: Carol Lynam I D No.: 97970476

Carol Lynam

Date: 17th Sept. 2002

Table of Contents

Declaration ii
Table of Contents iii
Dedication vii
Acknowledgements viii
Abbreviations x
Abstract xi

1 Calixarenes and Host-Guest Chemistry: Introduction and Literature 1

1.1 Calixarenes – Introduction and Historical Aspects 2
1.2 One-Pot Procedures - Base Catalysed Reactions 3
1.2.1 Reaction Pathway 4
1.2.2 Cyclisation Pathway 5
1.3 One-Pot Procedures - Acid Catalysed Reactions 8
1.4 Stepwise Synthesis 8
1.5 The Conformations of Parent Calixarenes 9
1.6 Upper Rim Functionalisation 13
1.7 Lower Rim Functionalisation 15
1.8 Introduction to Chirality 20
1.8.1 Labelling of chiral molecules 21
1.9 Chiral Calixarenes 22
1.9.1 Asymmetric Calix[4]arenes by O-Alkylation with Chiral Residues 22
1.9.2 Asymmetric Calixarenes - Inherent Chirality 23
1.9.3 Asymmetric Calix[4]arenes with a Single meta-substituted Phenolic Unit 24
1.9.4 Asymmetric Calix[4]arenes by O-Alkylation with Achiral Residues 25
1.10 Host–Guest Chemistry and Molecular Recognition 27
1.11 Historical Aspects of Host –Guest Chemistry and Molecular Recognition 28
1.11.1Definitions used in Host –Guest Chemistry 29

1.12 Principle of Complementarity 31
1.13 The Role of Solvent 32
1.14 The physical chemistry of molecular recognition 33
1.15 Types of Hosts 36
1.16 Host-Guest Complexes 39
1.17 Substitution Effects in Macrocyclic Hosts 48
1.18 Literature Survey- Introduction 54
1.19 Calixarenes as Hosts – Binding Metal Ions 55
1.19.1 Calixarenes as Chromionophores 55
1.19.2 Fluorogenic Calixarenes 59
1.20 Calixarenes as Hosts – Molecular Binding 63
1.21 Chiral Calixarenes as Hosts 70
1.22 References 76

2 Synthesis of Fluorescent Calixarenes 86
2.1 Introduction 87
2.2 Results and Discussion 90
2.2.1 Synthesis of calix[4]arene amides from acids via acid chlorides 90
2.2.2 Synthesis of calix[4]arene amides directly from acids 95
2.2.3 Synthesis of novel calix[4]arene tetra-amides via acid chlorides 97
2.2.4 Synthesis of calix[4]arene amides by appending pre-formed amides via phenol hydroxy groups 98
2.3 Conclusion 106
2.4 Experimental 107
2.4.1 Procedure and Equipment 107
2.4.2 Synthetic Procedures 108
2.5 References 120

3 Molecular Recognition and Enantiomeric Discrimination based on Fluorescence Quenching of Chiral Calixarene L1 121
3.1 Fluorescence Introduction 122
3.2 Importance of chirality 127

3.2.1 Chiral discrimination in fluorescence quenching 129
3.3 Experimental Section 134
3.3.1 Equipment and Materials 134
3.3.2 Procedure for Fluorescence Measurements 134
3.3.3 Preparation of solutions for Fluorescence Lifetime Measurements 134
3.3.4 Procedure for Fluorescence Measurements of Propranolol label 136
3.3.5 Procedure for Fluorescence Measurements of di-functionalised R-propranolol amide calix[4]arene 136
3.4 Results and Discussion 137
3.4.1 Excitation and Emission Spectra 137
3.4.2 Linear Response range 139
3.4.3 Linear range of Stern-Volmer plot 139
3.4.4 Variation of Stern-Volmer plot with enantiomeric composition 141
3.4.5 Variation of two-dimensional emission intensity contour plots with enantiomeric composition 146
3.4.6 Variation of fluorescence lifetimes with enantiomeric composition 149
3.4.7 Variation of Stern-Volmer plot of propranolol label with enantiomeric composition 154
3.4.8 Variation of Stern-Volmer plot of a partially functionalised calix[4]arene with enantiomeric composition 157
3.5 Conclusion 163
3.6 References 164

4 Host-Guest Behaviour of Ion-Complexes of Calix[4]arene Host L1 165

4.1 Introduction -Fluorescent cyclodextrins as host molecules 166
4.2 Experimental Section 171
4.2.1 Equipment and Materials 171
4.2.2 Procedure for Fluorescence Measurements 171
4.3 Effect of Ion-Complexation on Chiral Discrimination by L1 172
4.4 Results and Discussion 175
4.4.1 Linear Response range 175

4.4.2 Variation of Stern-Volmer plot with enantiomeric composition 178
4.4.3 Variation of Kapp with R-phenylalaninol concentration 181
4.5 Conclusion 192
4.6 References 193

5 Solvent effects on Enantiomeric Discrimination of Chiral Calixarene L1 195
5.1 Solvent effects on electronic spectra 196
5.2 Experimental Section 199
5.2.1 Equipment and Materials 199
5.2.2 Procedure for Fluorescence Measurements in Acetonitrile 199
5.2.3 Procedure for Fluorescence Measurements in Chloroform 200
5.2.4 Procedure for Fluorescence Lifetime Measurements in Chloroform 200
5.3 Fluorescence studies in Acetonitrile 201
5.3.1 Excitation and Emission Spectra 201
5.3.2 Linear Response range in Acetonitrile 203
5.3.3 Linear range of Stern-Volmer plot. 204
5.3.4 Variation of Stern-Volmer plot with enantiomeric composition 206
5.4 Fluorescence studies in Chloroform 210
5.4.1 Excitation and Emission Spectra 210
5.4.2 Linear response range in Chloroform 212
5.4.3 Linear range of Stern-Volmer plot. 212
5.4.4 Variation of Stern-Volmer plot with enantiomeric composition 213
5.4.5 Variation of fluorescence lifetimes with enantiomeric composition 218
5.5 Conclusion 221
5.6 References 222

6 Conclusions and Future Work 223
6.1 Conclusions 224
6.2 Future Work 227

Appendix A

Dedicated to my parents Ray and Loretta

Acknowledgements

The time has finally come to say farewell to the glorious student days! Some words of thanks are therefore necessary to a few people. Firstly I would like to thank Dermot for his faith in me, encouragement when the going was tough, generous financial support and in particular for the marvellous holiday in Australia, cheers Dr. D.

Thanks also go out to Prof. Tony McKervey who supervised my duration in Queens University Belfast, and to all there working and living with me at the time. Thanks to Dr. Tia Keyes and her research group who graciously allowed me the use of the facilities in DIT (Kevin ST.), for the lifetime measurements in particular, and to Dr. Kieran Nolan, for his constant help and direction.

Now that the formalities are taken care of I'd like to extend heartfelt thanks to all in the chemistry department, staff and postgrads, over the past few years who have made working there easier, either by their generous help or good sense of humour. To the technicians, Mick, Maurice and Damien, thanks for all your help and making me laugh, also to Ann, Veronica and John for their help and support. And thanks to Ambrose, we'd all be lost without you at the hatch. Gratitude also to all the staff of the NCSR, in particular Celine and Declan, you've been great.

Cheers to all the members of the DD-RG, past and present, including Teresa, Paddy, Darren "eating is cheating" Fayne, Fran, Brendan (big bren), Aogan, Karl, Karen, Rachel, Liam, Michaela, Susan, Valerie, Brendan, Kim, Gillian and all of whom I've forgotten to mention. The "old crew" also deserve a mention for showing us the ropes, slippery ones an' all, Bronagh, Christine, Luke, Conor, Ben, to mention just a few. To all of you who remember the parties of "666" Dean Swift Road, aka the house of hags! To the lads who are there now, cheers for keeping me smiling, if at times all I wanted to do was cry with frustration, Scott, Marco, Adrian, Wesley, Ray, Karl, Robbie, Ian, Yang, Johnny, Shane, Kieran, Richard, Johan, Darren, Mary, Lorraine, Marion, Kathleen, Maura, Emer and to all my feather-brain head can't recall. To the "lunch-time posse" and my good friends in general, thanks for being there guys and for keeping the jokes rolling (whatever hour on the clock it happened to be!), Ger, Shaggy (Neil), Jenny, Helen, Davnat, Mairead, Molser and Edel, cheers guys for being good friends and putting up with me over the past year, I know it hasn't been easy!!!

To Colm, thanks for everything, I'd never have made it without the daily phone calls to see how I was, cheers dude. Finally thanks to my family, in particular my parents Ray and Loretta, and Raychel, for their never-ending support, financial and otherwise. You've always encouraged me in whatever I chose to do, and for that I'm forever grateful.

Abbreviations

BTMA	benzyltrimethylammonium cation
BTMAN	*p*-nitro-benzyltrimethylammonium cation
CD	cyclodextrin
DCC	dicyclohexyl carbodiimide
ESIMS	electrospray ionisation mass spectrometry
GC	gas chromatography
HPLC	high performance liquid chromatography
I.R.	infra red
LC	liquid chromatography
m.p.	melting point
NMR	nuclear magnetic resonance
PA	phenylalaninol
PEA	phenylethylamine
PG	phenylglycinol
TLC	thin layer chromotography
TMA	*N*,*N*,*N*,-trimethylanilinium cation

Abstract

The synthesis of calixarene **L1** is described. This molecular sensor incorporates a fluorescent naphthyl moiety, the necessary fluorophore for optical transduction, whose fluorescent intensity alters to differing degrees on binding of enantiomers. Means of distinguishing between enantiomers of a chiral molecule are of critical importance in many areas of analytical chemistry and biotechnology, particularly in drug design and synthesis. Fluorescent quenching studies of calixarene **L1** in methanol demonstrated no enantiomeric selectivity in a short chain amino acid, phenylglycinol, while excellent selectivity was observed for a longer chain, phenylalaninol. Fluorescent lifetime studies of this calixarene with phenylalaninol guests confirmed that a static quenching mechanism is responsible for the decrease in fluorescence intensity of **L1** in methanol upon addition of phenylalaninol. Calix[4]arenes are well-known to possess ion-binding properties. The formation of metal ion complexes of the p-allyl calix[4]arene propranolol amide derivative is shown to induce a more regular and rigid cone conformation in the calix[4]arene macrocycle, which generates a significant enhancement in the observed enantiomeric discrimination.

The effect of solvent on the fluorescent properties of this calixarene has been studied with regard to methanol, acetonitrile and chloroform. While enantiomeric selectivity is observed in methanol, no discrimination is achieved in acetonitrile, and although there appears to be a 1:1 association with the guest in the latter solvent, in the case of methanol the guest must be far in excess of the host to achieve enantiomeric discrimination. Upon addition of the R-enantiomer of the guest in chloroform a new band is formed, which would suggest a charge transfer complex between this guest and the calixarene, an effect, which is not observed with the S-enantiomer. Fluorescence lifetime studies in chloroform indicate a static quenching mechanism of **L1** by both enantiomers of phenylalaninol, which would suggest that exciplex formation is not responsible for the new band at 440nm upon addition of R-phenylalaninol. This new band has been attributed to the presence of two different conformations of calixarene **L1**, which is reinforced by the ^{1}H-NMR studies and molecular modelling studies in chapter 4.

After the successful performance of calixarene **L1** with respect to enantiomeric discrimination (chapters 3, 4 and 5), an attempt was made to prepare a series of calixarene sensor molecules that possess similar properties to **L1**, but are prepared from inexpensive starting materials. Using DCC as a coupling agent to form amides directly from calixarene tetra-acids does not however, achieve tetra-substituted amides. An alternative route was taken to produce calixarene tetra-amides which involved two steps:

1. formation of the amide moiety
2. attachment of amide moieties to calixarene backbone

The first of these two steps was carried out successfully and led to the formation of three amide subunits however the second step suffered from partial substitution, and resulted in a series of mono-, di- and tri-substituted fluorescent calixarenes. A five-fold excess of the amide moiety was used which is not sufficient to complete the tetra-substitution.

1 Calixarenes and Host-Guest Chemistry: Introduction and Literature

"Pleasantest of all ties is the tie of host and guest"

: Aeschylus, Athenian poet and dramatist (approx. 5BC)

1.1 Calixarenes – Introduction and Historical Aspects

As early as 1912, Raschig speculated that calixarenes might exist as constituents of the commercial plastic called Bakelite. This hard resinous solid, which resulted from the reaction of phenol and formaldehyde under fairly strenuous conditions, was named after Leo Bakeland who discovered and exploited this substance. Whether Bakelite actually included calixarene structures in its composition is not clear, but it is now certain that the condensation of certain *p*-substituted phenols with formaldehyde undoubtedly yields calixarene products.

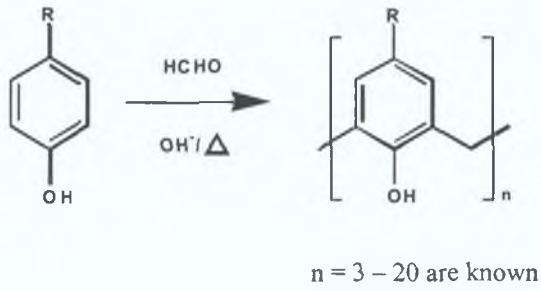

Figure 1-1 *Formation of Calixarenes with phenol, formaldehyde and base*

Calixarenes are macrocycles like cyclodextrins and crown ethers, whose conformational isomers offer a great number of unique cavities, with great variety in size and shape. These compounds favourably adopt a so-called cone-type conformation due to stabilisation of this conformation due to intramolecular hydrogen-bonding interactions among their phenoxy hydroxyl groups. They are very similar in structure to spherands, the difference being the length of the spacer connecting the phenyl units. This implies that calixarenes should be good hosts for complexing to guests with complementary functionalisation.

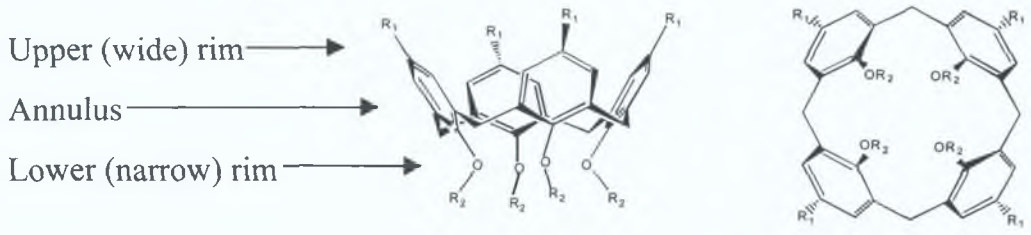

Figure 1-2: *View of calixarene cavity; side-on view and through the annulus*

It was in the 1970's with the increasing interest in "enzyme mimics" that David Gutsche was inspired to investigate calixarenes as potential candidates for molecular baskets. The idea of enzyme mimic building is to construct a receptor for a substrate molecule and equip the receptor with functional groups that are appropriate for interacting in some manner with the substrate molecule. Reasons why they are attractive as hosts include their ready availability, with multigram quantities producible on a laboratory scale in a relatively simple manner from cheap starting materials, with numerous options for their structural variation. This makes them different from many of the other synthetic macrocycles, and makes them particularly attractive as potential hosts.

It was during their investigations of the "curing" phase of the Bakelite process, that Zinke and Ziegler first demonstrated the formation of macrocycles [**1**]. The curing step heated the initially formed phenol-formaldehyde condensate, to produce the final resin. They treated *p-tert*-butylphenol with aqueous formaldehyde and sodium hydroxide at various temperatures, and eventually yielded an acetyl derivative with a molecular weight of 1725. No structure was suggested for this product, but in retrospect they seemed to have isolated the cyclic octamer.

Following work by Cornforth [**2**] and Gutsche [**3**, **4**, **5**, **6**], it was confirmed that the Zinke reaction yielded a mixture of products and that the size of the macrocycle is dependant on the reaction conditions employed. The cyclic tetramer, which was one of the products from the aforementioned reaction, bore a remarkable resemblance in shape to a Greek vase called a Calix Crater. It was for this reason that Gutsche and Muthukrishnan assigned the name calixarene (arene, indicating the incorporation of aromatic rings in the macrocyclic array) to this class of compounds, with the size of macrocycle specified by a bracketed number inserted between calix and arene.

1.2 One-Pot Procedures - Base Catalysed Reactions

The Petrolite procedure, which was devised to simulate the factory production of phenol/formaldehyde resins, yields 60-70% crystalline *p-tert*-butylcalix[8]arene from *p-tert*-butylphenol. While attempting to solve the mystery of the condensation of *p-tert*-butylphenol and formaldehyde, it was discovered that instead of the catalytic amount of base used in the original Petrolite procedure, a stoichiometric amount of

base yielded the cyclic hexamer as the major product (70-75%). The cyclic tetramer however, is produced in irregular yields when employing the Zinke reaction, from almost nothing to anything up to 45%.

The optimal amount of base for the formation of the tetramer and octamer is about 0.03 mole of NaOH per mole of *p-tert*-butylphenol, with tetramer yields of 50% when higher temperatures are used (diphenyl ether, reflux ~220°C) than in the case of the octamer (63% yield-xylene, reflux ~145°C). Larger amounts of base are required for the formation of the hexamer, 0.4 moles KOH per mole *p-tert*-butylphenol. The odd-numbered calixarenes are more difficult to quantitatively obtain than their even-numbered counterparts, with reasons for the formation of particular calixarenes virtually unknown. Though calixarenes are now known with repeating units up to twenty in number, to date the majority with analytical interest have been tetramers, with hexamers to a less significant extent.

1.2.1 Reaction Pathway

Although little is known about the total mechanism of cyclic oligomer formation, the initial stages of the sequence appear reasonably unambiguous. It is relatively certain that the first step in the overall reaction involves the condensation of the phenolate anion with formaldehyde, to form a hydroxymethylphenol.

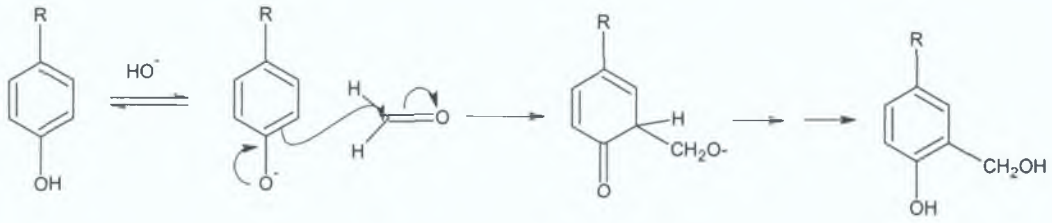

Figure 1-3: *Formation of hydroxymethylphenol from phenol*

Subsequent condensation of the previous product with the starting phenol then ensues to form linear dimers, trimers, tetramers etc., with this process capable of taking place under relatively mild conditions. A Michael-like reaction was postulated, whereby phenolate anions and *o*-quinonemethide intermediates form by loss of water from the hydroxymethylphenols.

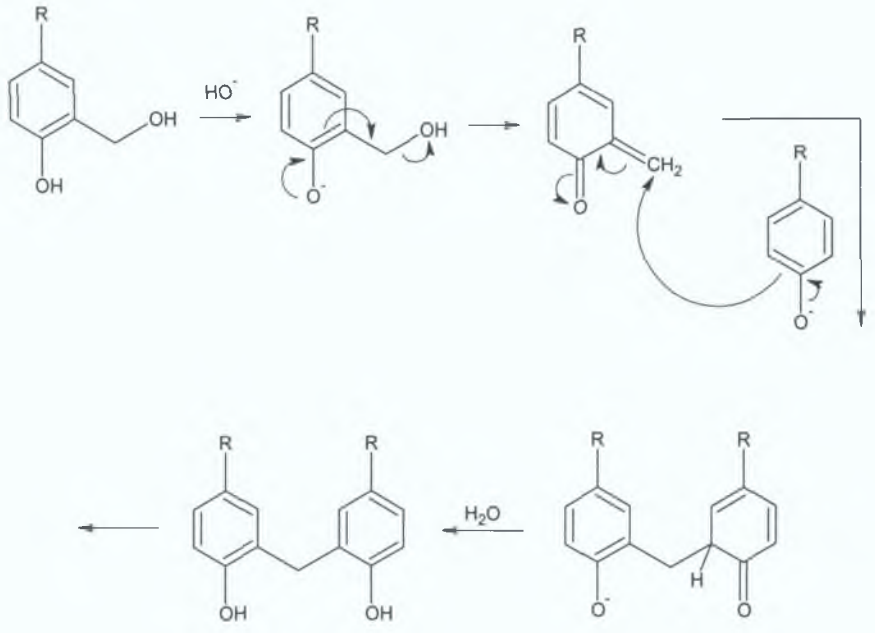

Figure 1-4: *Formation of diphenylmethanes via o-quinonemethide intermediates*

Dibenzyl ethers are concomitantly formed with the diphenylmethanes previously mentioned, as a consequence of intermolecular dehydration.

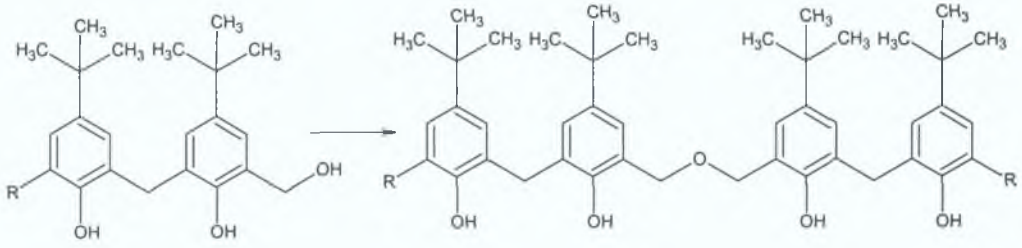

Figure 1-5: *Formation of dibenzylethers from hydroxymethylphenols*

1.2.2 Cyclisation Pathway

How this mixture of hydroxymethyl-diphenylmethanes and dibenzyl ethers are transformed to the macrocyclic calixarene is still unclear. Certain arguments however, seem to suggest that hydrogen bonding plays a vital role. Another argument states that since it is known that tetramers are formed as a result of heating octamers in the presence of base, that the octamer is the primary cyclisation product, with an increase in temperature producing the tetramer [**7**].

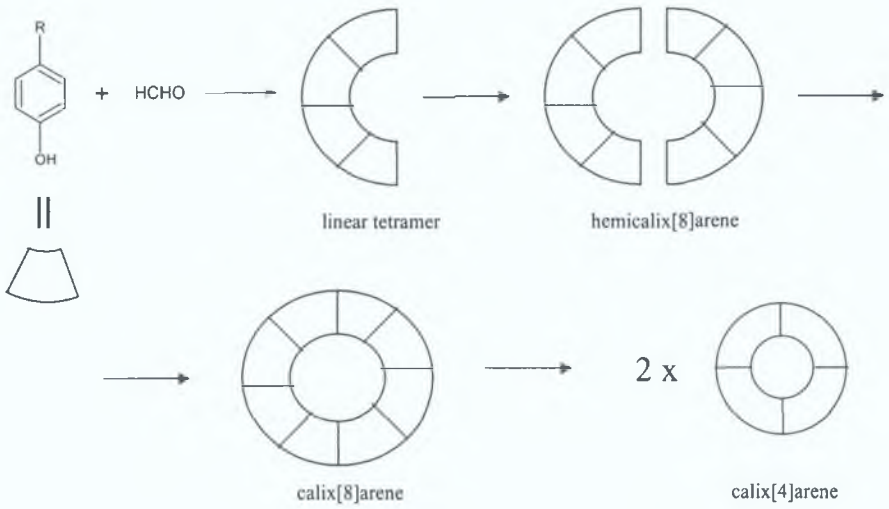

Figure 1-6: *Possible cyclisation pathway to calix[4]- and calix[8]arenes*

In the case of calix[6]arene formation however, a template effect has been postulated, similar to that in crown ether chemistry, since higher yields of cyclic hexamers have been obtained with RbOH as base than with CsOH, KOH, or NaOH [**6**]. However the differences between these four bases is not spectacular, and it seems that the function of the base is other than merely acting as a template. From space filling molecular models it is suggested that it may be possible for the cyclic hexamer to achieve the "pleated loop" conformation of the octamer, with removal of hydrogen to form the monoanion of the calixarene, thereby strengthening the hydrogen bonding within the system. It is therefore proposed that the principal functions of the base include:

(a) creation of the monoanion of a linear hexamer, which becomes a "pleated loop" pseudocalix[6]arene as a preface to cyclisation, or

(b) the formation of the monoanion of a linear trimer, which could associate with a neutral trimer to form the hemicalix[6]arene anion to undergo cyclisation.

However if other *p*-alkyl or even *p*-arylphenols are used in the synthesis, a mixture that contains no discernable amount of tetramer is produced, with *p*-halophenols yielding products, which do not seem to be calixarenes. If the previously described pathways for cyclisation are correct, then the *p*-substituent should not exert a huge effect on the process, since they are quite far apart in the "pleated loop" conformation. Even presuming that the conversion from calix[8]arene to calix[4]arene probably involves close contact of such substituents, the fact that smaller

substituents than *t*-butyl (methyl) as well as larger (phenyl, adamantly, cumyl), do not favour tetramer cyclisation, would appear to imply that steric differences are not particularly responsible for the outcome of the reaction [**7**].

Influences on the reaction of calixarene formation, include:

(a) solvent effect- formation is favoured by non-polar solvents (xylene, tetralin, diphenylether) and inhibited by polar solvents (quinoline)

(b) base concentration effect- the cyclic octamer and tetramer are favoured by a catalytic amount of base whereas a stoichiometric amount is favoured by the cyclic hexamer

(c) temperature effect- the cyclic octamer and hexamer are produced preferentially at lower temperatures (refluxing xylene ~145°C) than the cyclic tetramer (refluxing diphenyl ether ~220°C).

Gutsche presents an argument, which encompasses the aforementioned reaction pathways, and states that the calix[8]arene is produced through kinetic control, the calix[4]arene is a product of thermodynamic control, with the calix[6]arene formed in part by a template effect. However the exact proceedings that take place in the final phase of the sequence leading to the cyclisation products remains somewhat of a mystery. It is certain that the linear oligomers lose water and formaldehyde in the process of cyclisation, but the immediate precursors of the cyclic products are not known.

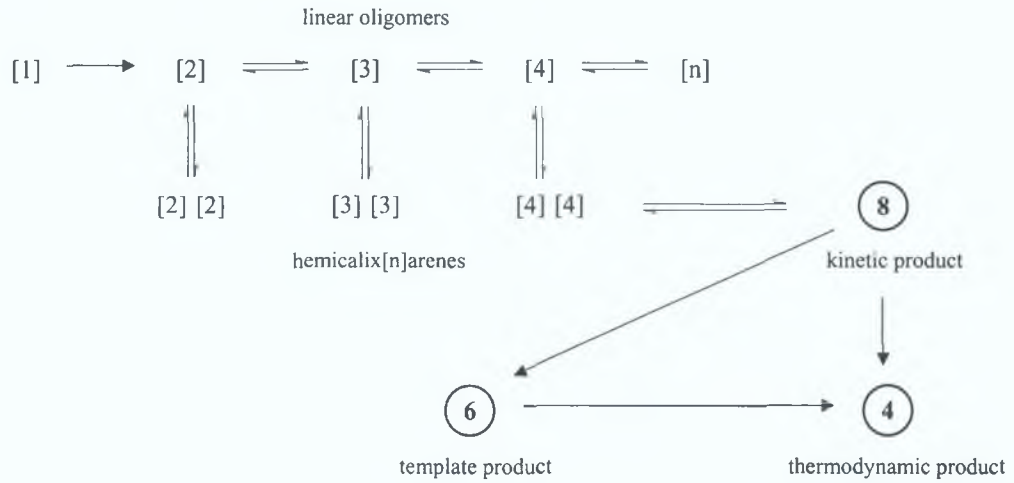

Figure 1-7: Cyclisation pathway proposed by Gutsche, [n] = ^{n}repeat linear units; (n) = ^{n}repeat cyclic units.

1.3 One-Pot Procedures - Acid Catalysed Reactions

The synthesis of calixarenes via acid-catalysed phenol-formaldehyde condensation reactions has been achieved with such starting materials as 1,3,5-trimethyl benzene and 1,2,3,5-tetramethyl benzene [**8**], in the presence of formaldehyde and acetic acid, with the former reaction product also obtainable from 2-chloromethyl-1,3,5-trimethyl benzene with aluminium-chloride as catalyst [**9**].

1.4 Stepwise Synthesis

The stepwise synthesis described in 1956 by Hayes and Hunter [**10**] and optimised sometime later by Kämmerer, Happel et al [**11**, **12**, **13**, **14**], allowed for the synthesis of calixarenes from different alkylphenol units, therefore generating a range of functionalities on either the upper or lower rim. This synthesis starts from *o*-bromo-*p*-alkylphenol and employs a series of alternating hydroxymethylation and condensation steps to assemble a linear oligomer with a hydroxymethyl group on one end. This can in turn undergo cyclisation after the *o*-position has been made available by de-halogenation.

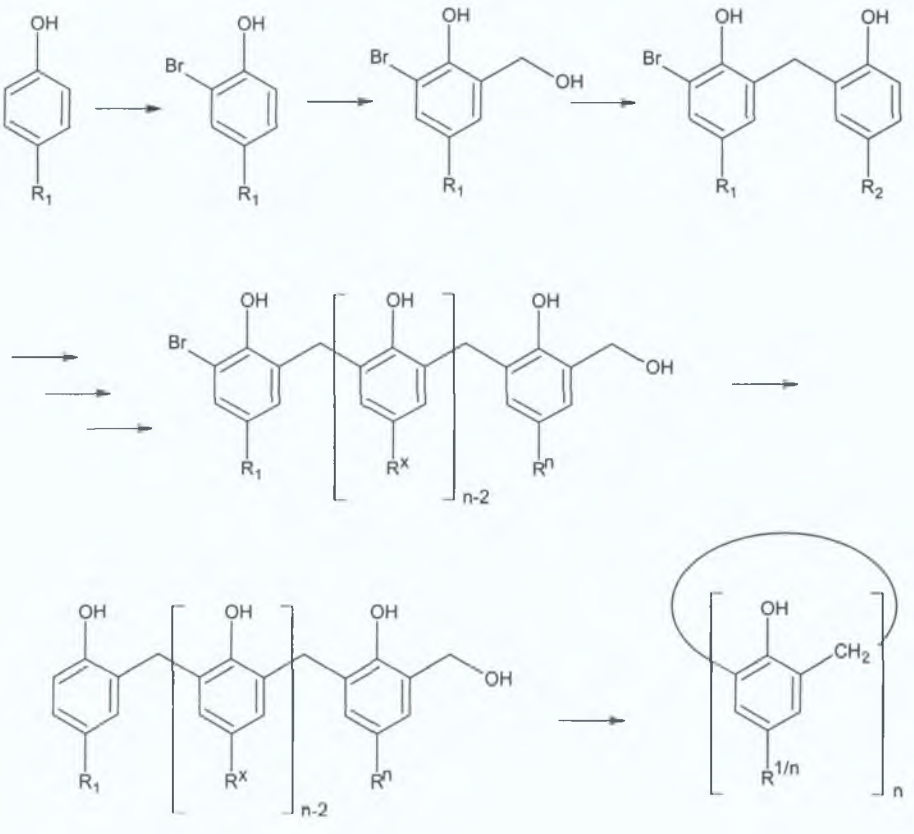

Figure 1-8: *Kämmerer's non-convergent stepwise synthesis*

This procedure however, is very time consuming and suffers from poor yields. Volker Böhmer's convergent stepwise synthesis improved on Kämmerer's non-convergent one by delivering better yields of variably substituted calixarenes in a stepwise method. This involves condensations involving the "3+1" [**15**, **16**, **17**, **18**,] and "2+2" principle [**19**].

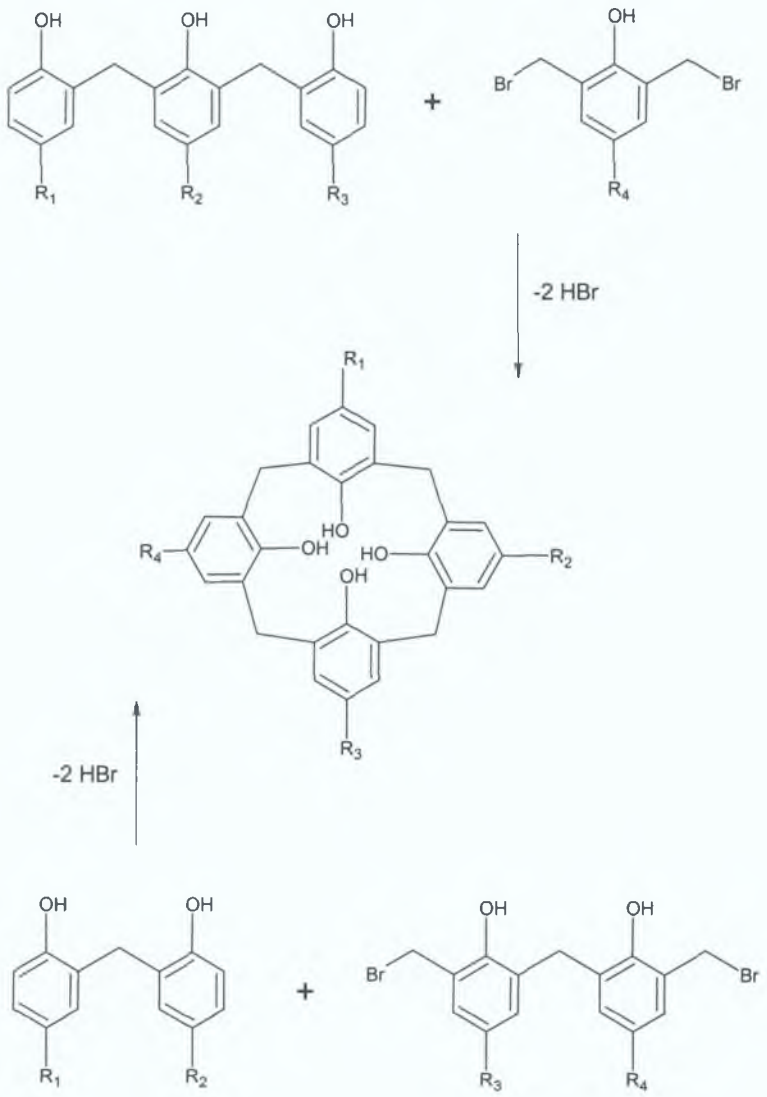

Figure 1-9: *Böhmer's convergent stepwise synthesis*

1.5 The Conformations of Parent Calixarenes

The cyclic tetramer is actually amoeboid in character and can exist in several other shapes as well as the cone. The variety of conformations, which they can assume, is one of the most interesting features of the calixarenes, and is allowed by the rotation about the σ-bonds of the Ar-CH_2-Ar groups. This was first reported by Megson [**20**] and Ott and Zinke [**21**], but it was not until Cornforth et al [**22**] that these adumbrated

versions were advanced upon. Cornforth demonstrated that four discrete forms of calixarene can exist, which are referred to as "cone", "partial- cone", "1-2-alternate", "1-3-alternate".

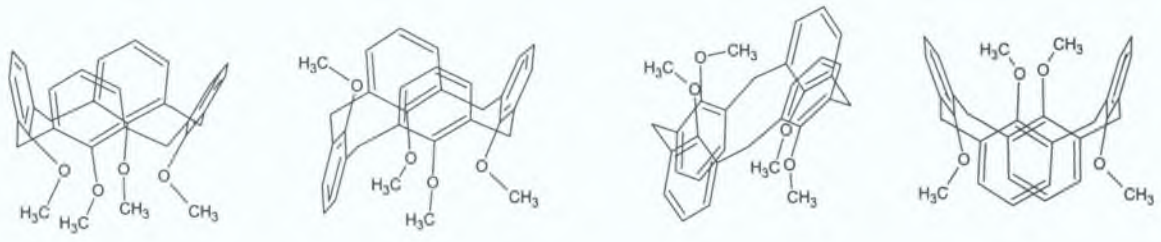

cone *partial cone* *1,2-alternate* *1,3-alternate*

Figure 1-10: *The four principle conformations of calix[4]arenes*

Kämmerer et al carried out dynamic ^{1}H NMR studies of p-alkylcalix[4]arenes which demonstrated that the aforementioned conformations were readily inter-convertible [**11**, **12**]. The cone conformation is adopted by calix[4]arenes with free OH-groups, since they are stabilised by intramolecular hydrogen bonds between the hydroxy groups. This is confirmed by crystal structures so far reported, including compounds containing different phenolic units [**23**, **24**, **25**]. Shaping the basket plays a vital role in the design of calixarene molecules as enzyme mimics, with host-guest interactions depending on complementarity of shape as well as functionality.

All calixarenes are conformationally mobile at room temperature, with degrees of mobility varying with degrees of substitution. However, solvent polarity has generally a greater influence on rate of conformational inversion of the tetramer than the effect of the para-substituent. In non-polar solvents such as chloroform, toluene, benzene, bromobenzene and carbon disulfide, the barriers of rotation are greater than in more polar solvents (e.g. acetone and acetonitrile). The difference is attributed to the differing abilities of calixarenes to form endo-complexes with the solvent [**26**], and is also a result of the disruption of the intramolecular hydrogen bonding, which contributes to maintaining the calixarene in the cone conformation.

The effect of hydrogen bonds is more apparent with structures of calix[4]arenes with less than 4 endo-hydroxy groups. While the aminophenol calixarene **1** (c) still exists in the cone conformation [**27**], the diphenol **1** (a) and the OH-free compound **1** (b) assume the 1,3-alternate conformation [**28**].

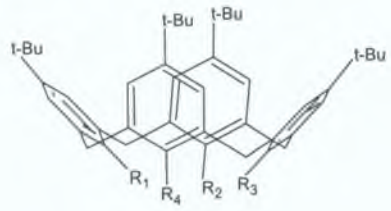

	R^1	R^2	R^3	R^4
(a)	OH	OH	H	H
(b)	H	H	H	H
(c)	OH	H	NH_2	OH

1

Cram defined 'cavitand' as a synthetic compound containing an 'enforced cavity' (conformationally mobile baskets) large enough to engulf ions or molecules [**29**, **30**]. Calixarene tetramers meet Cram's criterion of synthetic accessibility, but are not quite permanent baskets; they must therefore be frozen into the cone conformation to make constant calix's. The most obvious manner in which to curb mobility and curtail inversion through the annulus of the macrocyclic ring is to replace the phenoxy-OH moieties with larger or longer functionalities. Mobility or conformational change is also dependent to a certain extent on the size of the para-substituent, as rotation can also occur this way.

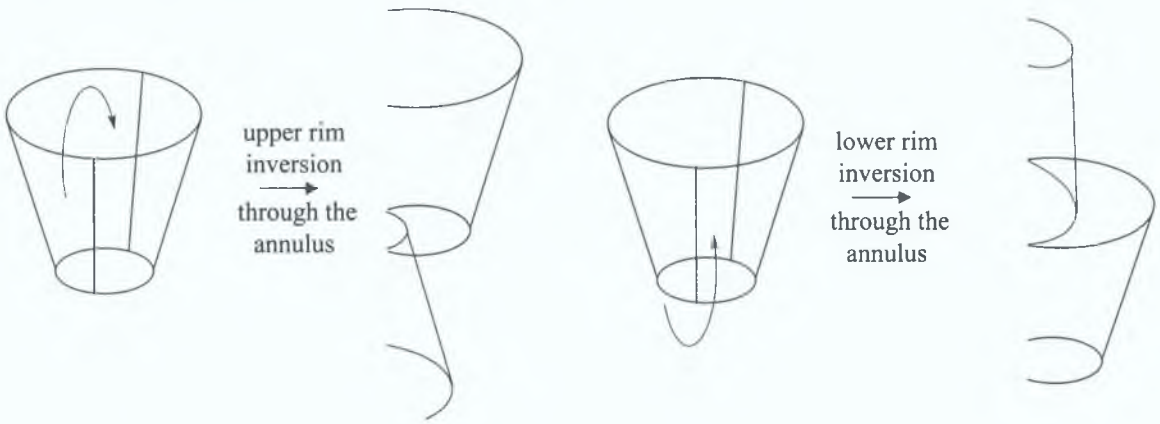

Figure 1-11: *Mobility through the annulus of the macrocyclic ring*

Each of the four isomeric conformations of the calix[4]arenes has characteristic resonances in ^{1}H NMR spectroscopy, which allows easy assignment of structure. Acetylation of (**2**) yields the tetra-acetate (**4**a), which is shown by ^{1}H NMR to be in the 1,3-alternate conformation. However among derivatives of the tetrahydroxycalix[4]arenes, the 1,3-alternate conformation seems quite rare, with "partial-cone" and "cone" generally more favourably adopted. The tetra-acetate derivative of the *p-t*-butyl calix[4]arene (**3**) is fixed in the "partial-cone" conformation (**5**a), which has been verified by x-ray crystallography [**31**]. Methylation and ethylation

of (**2**) and (**3**), and allylation of (**2**) produce the corresponding ethers (**4**b, **4**c, **4**d, **5**b and **5**c) which exist in the "partial-cone" conformation.

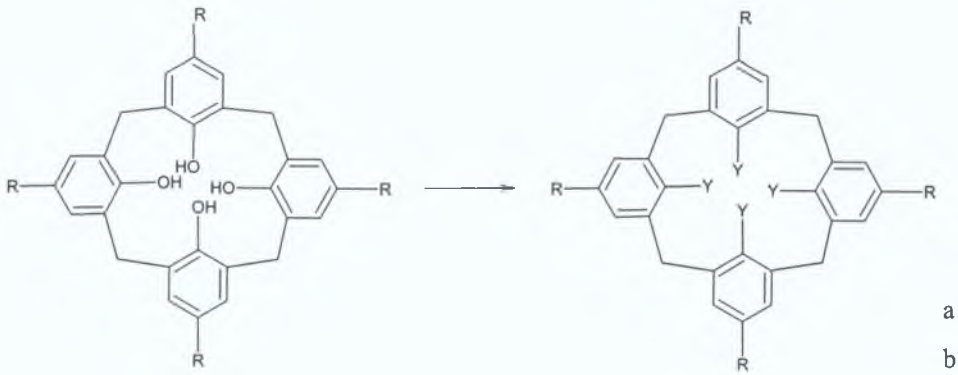

(**2**): R = H

(**3**): R = t-butyl

(**4**): R = H

(**5**): R = t-butyl

Y

a $OCOCH_3$

b OCH_3

c OC_2H_5

d $OCH_2CH{=}CH_2$

The tetramethyl ethers are surprisingly almost as flexible as calixarenes with four free OH groups, with a mixture of conformations generally existing in solution due to the lack of intramolecular hydrogen bonding. While (**2**) is found in the "cone" conformation when transformed to the analogous tetrabenzyl ether or tetra tosylate, cone conformations are established for (**3**) when converted to its tetra-allyl ether, benzyl ether or trimethyl ether. Consequently, acetylation appears to favour "partial-cone" conformations, while benzylation and trimethylsilylation seem to prefer products in the "cone" conformation.

The above-mentioned reaction effects allow a contoured design (with relative confidence in the outcome) of the cavity prior to its synthesis. The calix[6]arenes and calix[8]arenes are however, conformationally more mobile than their tetrameric counterparts, even after certain derivatisation reactions.

Regardless of conformational freezing, derivatisation of calixarenes is desirable to facilitate the introduction of various types of functional groups, to increase their usefulness as potential enzyme mimics. Therefore chemical modification of calixarenes permits the synthesis of new host molecules in conjunction with control of their conformation and hindrance of conformational inversion.

Modification of calixarenes derived from phenol can be achieved in two ways

1. Electrophilic substitution in the para position with respect to the phenolic hydroxy group (subsequent to de-alkylation of the tert-butyl groups).

2. Introduction of residues at the phenolic hydroxy groups

1.6 Upper Rim Functionalisation

The t-butyl groups can be easily removed by $AlCl_3$-catalysed transalkylation in the presence of toluene as acceptor [**32**]. *Ipso* substitution of t-butyl groups is a possible alternative route to upper-rim functionalised calix[4]arenes. Virtually all common substitution reactions, which are successfully carried out on phenols, may then be applied to calixarenes. The substituents can further undergo reaction, which when combined with suitable reactions at the phenolic OH-groups, yield numerous possible derivatives of calixarenes.

The transbutylation reaction is an important one considering the large variety of calixarenes obtainable by subsequent electrophilic substitution of the *p*-position. Halogenation [**33**, **34**, **35**], sulfonation [**36**, **37**], sulfochlorination [**38**], formylation, acylation [**39**, **40**], chloromethylation [**41**], aminomethylation [**42**, **43**], nitration [**44**], and coupling with diazonium salts [**45**, **46**]. Further reactions of these residues make even more novel calixarenes possible, e.g. haloform reactions of acetyl groups, aryl-aryl coupling by the Suzuki reaction, reduction of nitro-, and azo-, or acyl groups, further substitution at chlorosulfone and chloromethyl groups, to name just a few.

Claisen rearrangements of allyl ethers and Fries rearrangements have also been carried out [**32**, **47**], which can in turn lead to isomerisation and/or ozonolysis of the allyl groups [**32**]. Another alternative to electrophilic substitution by a direct route uses the nucleophilic character at the *p*-position of phenolates. A Mannich type reaction occurs when calix[4]arenes are reacted with formaldehyde and various amines. Further quaternization of the aminomethylcalix[4]arene followed by elimination of the amine moiety, produces a highly reactive p-quinomethide, which will react with whatever nucleophile that is added to the reaction mixture.

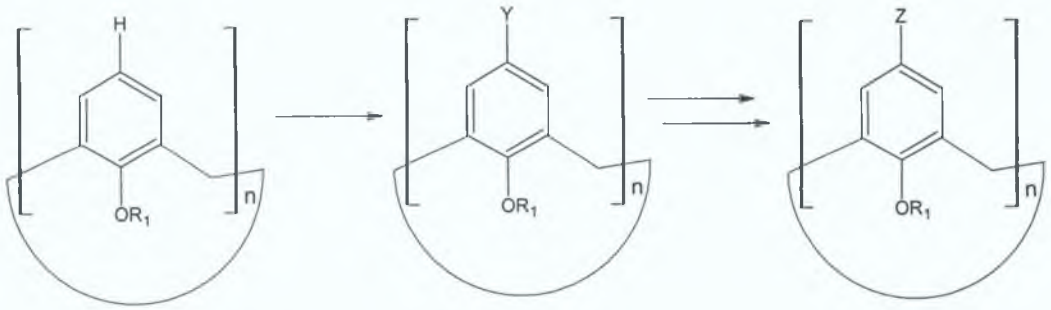

Entry	R^1	Y	Z
A	Alkyl	Br	Li, CO_2H, CN, Ar
B	H	SO_3H	NO_2
C	H	NO_2	NH_2
D	Alkyl	COR^2	CO_2H
E	H	CH_2NR^2	$CH_2NR^2{}_2Me^+$, CH_2CN, CH_2OMe
F	H	$CH_2CH{=}CH_2$	CH_2CHO, CH_2CH_2Y, CH=CHMe, CHO
G	H or Alkyl	CH_2Cl	Me, Et, CH_2Ar, $CH_2PO(OR)_2$, $CH_2NR^2{}_3^+$
H	Alkyl	CHO	CH_2OH, CH_2X, CO_2H
I	Alkyl	I	Ar, $C{\equiv}CR_2$, CO_2R^2, NH_2
J	H	N=NAr	NH_2

Figure 1-12: *Functionalisation of calixarenes on the "upper rim"*

1.7 Lower Rim Functionalisation

Zinke and Ziegler first reported the synthesis of calixarene esters, with their acetate derivative [**1**]. Since then ester, amide and ketone derivatives have been readily obtained by reaction with such reagents as Br-CH_2-COOR [**48**, **49**], Cl-CH_2-$CONR_2$ [**50**, **51**, **52**, **53**, **54**], and Cl-CH_2-COR [**48**, **55**] respectively, yielding tetra-alkylated calixarenes solely in the "cone" conformation which have been established as important ionophores. Using alkyl halides, NaH and DMF or THF/DMF as base and solvents respectively, yields alkylated calix[4]arenes invariably fixed in the "cone" conformation [**56**, **57**].

Methyl, ethyl, ally and benzyl ethers have been prepared in high yields employing this method. The sodium cation appears to play a part as a template, with the proximal 1,2-dialkylated products considered as intermediates. Compounds in the 1,3-conformation are affected by the use of caesium carbonate in acetonitrile solution [**58**], whereas employing potassium t-butoxide in benzene generates partial cone products [**56**]. Generally the "cone" conformation is favoured over the others by factors, which increase the rate of alkylation (substrate, solvent, cation, alkyating agent) or decrease the rate of ring inversion (solvent, templating cation).

Direct and selective alkylation of calixarenes at the lower rim, takes advantage of the difference in acidity of each phenolic hydroxy group. It has been concluded that the first hydroxy group is considerably more acidic than the others, due to the stabilisation of its conjugate anion by two intramolecular hydrogen bonds, with the second reaction occurring at the opposite (distal) position. A good yield of monoalkoxy calixarenes has been obtained by using 1.2 equivalents of a weak base such as CsF in DMF, or K_2CO_3 in acetonitrile with an excess of alkylating agent [**59**].

Formation of 1,3-dialkylated calix[4]arenes has been achieved through excess of a weak base in acetonitrile, which paved the way for the synthesis of very selective receptors for alkali metal cations [**60**, **61**, **62**]. The direct proximal (1,2) dialkylation of calix[4]arenes has been accomplished using sodium hydride as base in DMF with 2.2 equivalents of alkylating agent [**63**, **64**]. Trialkoxy calix[4]arenes are obtained when alkyl halides are reacted with calix[4]arenes in the presence of BaO-$Ba(OH)_2$ [**65**, **66**]

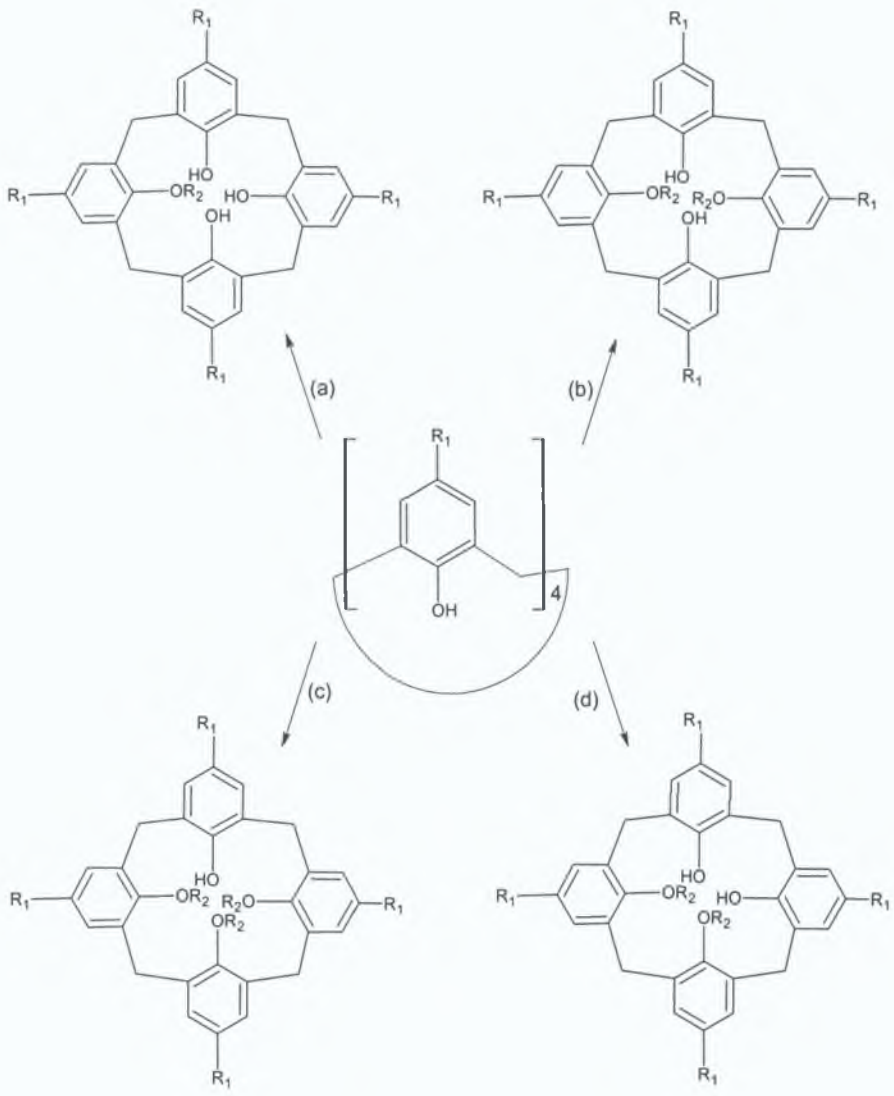

(a) (c) BaO, $Ba(OH)_2$, DMF (d) NaH, DMF

(b) CsF, DMF (b) K_2CO_3, MeCOMe or MeCN

Figure 1-13: *Selective functionalisation of calixarenes on "lower rim"*

Selective 1,3-dialkylation of calix[4]arenes in the presence of weak base can be explained by the fact that in these conditions only the monoanion of the calix[4]arenes and of their monoalkylethers can be formed (see Figure 1-14; a and b). When the base removes a proton from the calix[4]arene, the monoanion is stabilized as a result of strong intramolecular hydrogen bonds of the adjacent hydroxide groups, which are consecutively stabilised by hydrogen bonds with the remaining hydroxide moiety.

The tetraphenolic species of p-t-butylcalix[4]arene in THF show a pK_a = 4.11, which is similar to the monomethyl ether with a pK_a = 3.98, but considerably lower than the corresponding di- and trimethyl derivatives (pK_a > 12). Removal of a second proton by a weak base is generally found to produce a monoanion opposite to that of the monoalkylated site, which allows hydrogen bonds on either side of the anion to stabilise this intermediate. In the presence of a stronger base however (NaH in DMF), di-anions are formed which favour a second alkylation in the proximal position (1,2) (see Figure 1-14; c and d). In these conditions however, the 1,3-dialkylated products appear to react faster than their 1,2-isomers, probably due to the lack of stabilising hydrogen bonds for the opposite di-anion intermediate (see Figure 1-14c) yielding fully alkylated products.

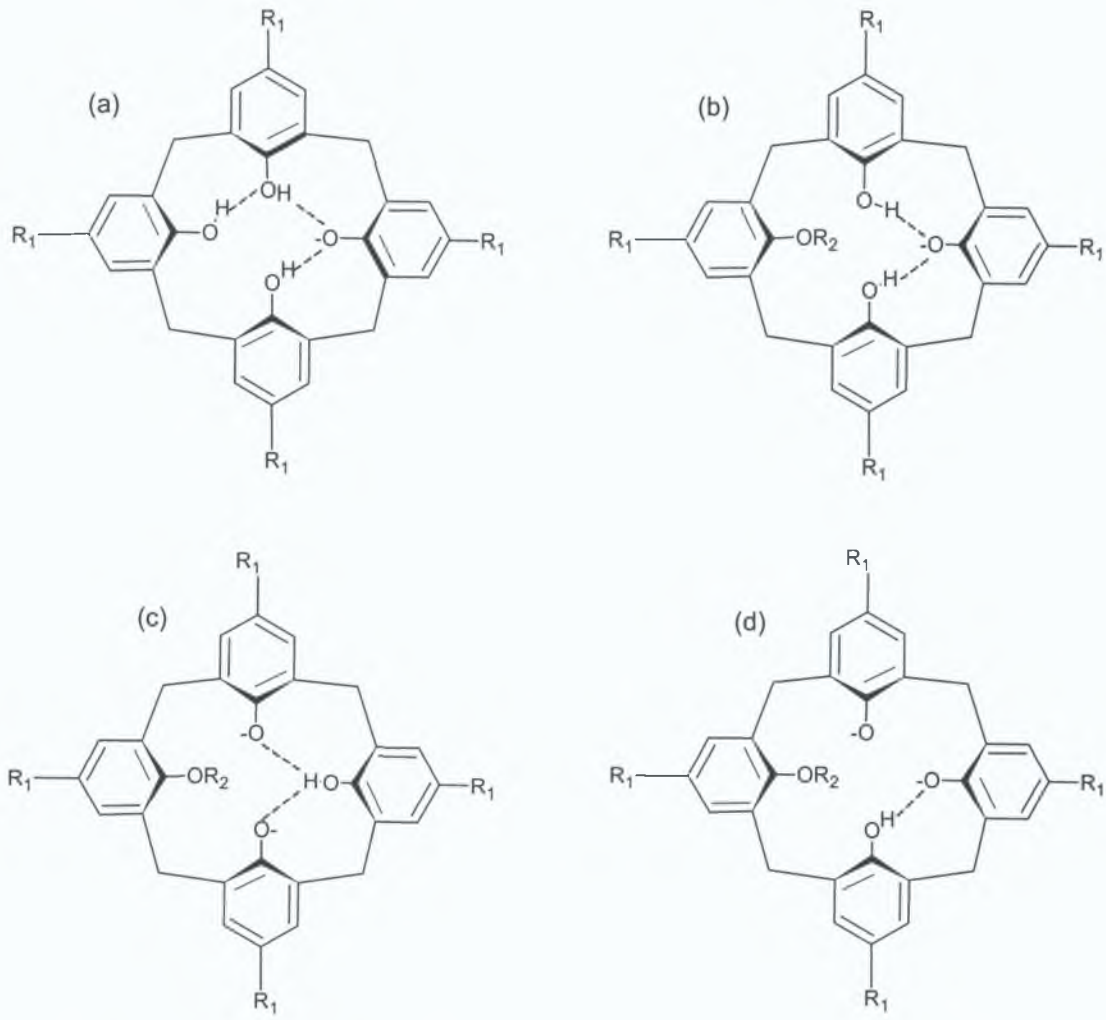

Figure 1-14: *Selective functionalisation of calixarenes on "lower rim" via anion formation*

Indirect methods of selectively synthesising monoalkyl- and 1,2-dialkylcalix[4]arenes have been accomplished by treating 1,3-dialkyl- and tetraalkylcalix[4]arenes with one or two equivalents of iodotrimethylsilane in chloroform respectively. Good yields of monoalkylcalix[4]arenes were attained [**67**], with the proximal 1,2-dialkylcalix[4]arenes obtainable by the action of $TiBr_4$ on tetraalkylderivatives [**68**]. Recently a study by Wall has described the synthesis of 1,3-dialkylcalix[4]arenes by treating calix[4]arenes with two equivalents of alkylating agent and one equivalent of base *in acetonitrile.* Good yields of these di-alkylated calix[4]arenes have been obtained by this method [**69**].

A Summary of Substitution Reactions of Calixarenes [**70**].

(a, h, i): formation of various ethers/ esters: OH → OX

(b): transbutylation: t-butyl → H

(c): oxidation to quinones

(d): hydrolysis of ester groups, reduction of ester/ amide/ nitrile groups: OX → OY

(e): ipso-substitution (e.g. nitration): t-butyl → R

(f): sulfonation

(g): electrophilic substitutions (halogenation, sulfonation, sulfochlorination, formylation, acylation, coupling with diazonium salts, chloromethylation, and aminomethylation)

(k): Claisen/ Fries rearrangements

(l): reduction of nitro groups, aryl-aryl coupling, haloform oxidation, transformation of allyl groups: R → S

(m): nucleophilic substitution of quaternary ammonium groups: R → Q

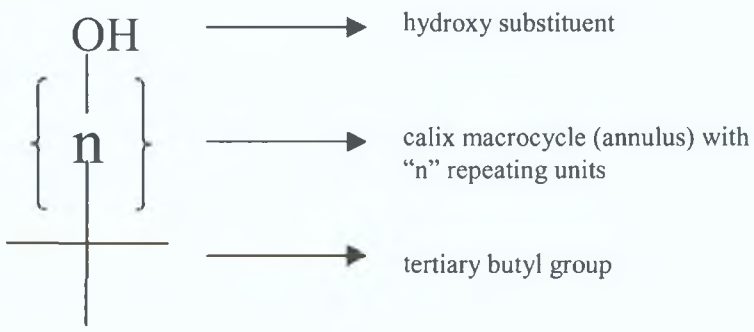

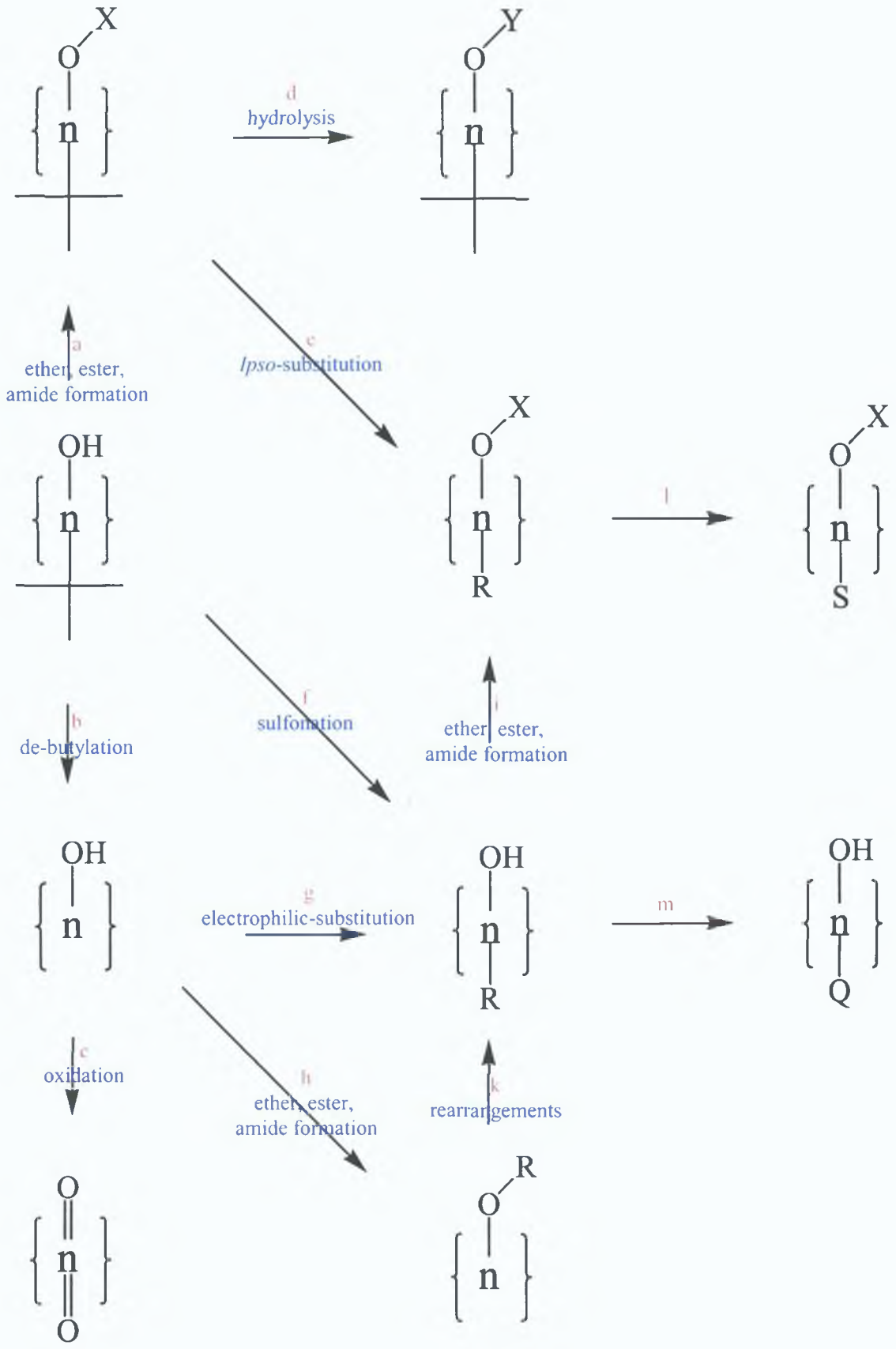
X
O
n
d
hydrolysis
Y
O
n
a
ether, ester,
amide formation
c
Ipso-substitution
OH
n
X
O
n
R
l
X
O
n
S
f
sulfonation
i
ether, ester,
amide formation
b
de-butylation
OH
n
OH
n
g
electrophilic-substitution
OH
n
R
m
OH
n
Q
e
oxidation
h
ether, ester,
amide formation
k
rearrangements
O
n
O
R
O
n

1.8 *Introduction to Chirality*

A molecule or an object is chiral if it cannot be superimposed on its mirror image. The term chiral was derived from cheir, the Greek for hand by Thompson in 1884. A molecule and its non-superimposable mirror image are known as enantiomers (*enantio* Greek for "opposite"), and such molecules are devoid of a centre of symmetry and a plane of symmetry. Enantiomers are related to each other as a right hand is related to a left hand and therefore chirality occurs as a result of dissymmetry or asymmetry. Apart from their reactions with chiral agents such as enzymes, enantiomeric molecules differ only in the way in which they interact with plane-polarised light and are said to be optically active. One enantiomer (in liquid form or solution) may rotate the plane of polarised right to the left (*laevo* or (-) or l), while the other may rotate the plane to the right (*dextro* or (+) or d). A racemic mixture consists of equal measures of each enantiomer and therefore shows no net rotation of polarised light.

If in a molecule a carbon atom is bonded to four different atoms or groups of atoms (R_1, R_2, R_3, R_4), the spatial orientation around the central carbon (or chiral carbon) can be arranged in two ways (see Figure 1-15). The two molecules shown have opposite configurations around the chiral carbon and are therefore non-identical mirror images, or enantiomers (also known as optical isomers).

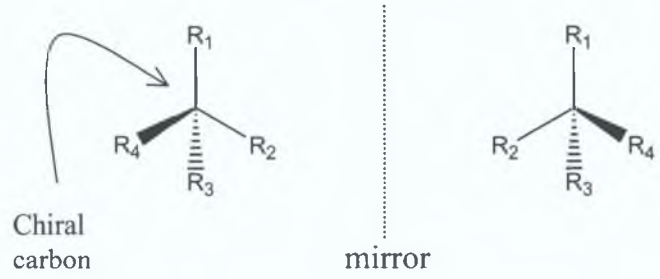

Figure 1-15: *The chiral carbon and its two mirror-image forms.*

A more general name for molecules that differ in their spatial orientation is stereoisomers. If a molecule possesses more than one chiral centre then the maximum number of stereoisomers, which are possible in a molecule containing n chiral carbon atoms, is 2^n. These isomers may be enantiomers or stereoisomers that are not enantiomers, otherwise known as diastereoisomers. Diastereoisomers are thus defined as stereoisomers that do not relate to each other as mirror images and this includes isomerism owing to the presence of double bonds, e.g. *cis*- and *trans*-

isomers. As a result all enantiomers are stereoisomers, but not all stereoisomers are enantiomers.

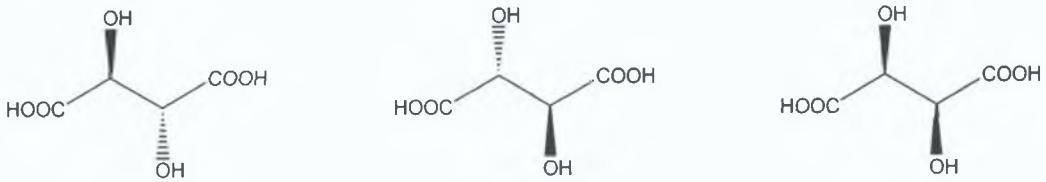

S, R (i) R, S (ii) Meso (iii)

Figure 1-16: *Stereoisomers of tartaric acid; (i) and (ii) are enantiomers, whereas (iii) is a meso compound (a diastereomer of (i) an (ii)).*

1.8.1 Labelling of chiral molecules

Enantiomers may be labelled as (+)/(-), d/l, D/L or R/S. The first two terms refer to the direction to which the enantiomer rotates plane-polarised light, (+) or d signifies rotation to the right, with (-) or l denoting rotation to the left. The D/L and R/S labels refer to the absolute configuration around the chiral centre. The D/L notation provides a parallel between the configuration of the chiral molecule and the configuration of glyceraldehydes, and is mainly reserved for amino acids and carbohydrates. A monosaccharide, which has it's highest numbered chiral carbon (penultimate carbon atom) with the same configuration as D-glyceraldehyde is assigned D, while one, which has the same configuration as L-glyceraldehyde is labelled L.

The R and S system, devised by Cahn, Ingold and Prelog, offers an unambiguous method of defining absolute configuration, using a set of rules, "sequence rules" which determine the order of priority of groups surrounding a chiral carbon. These rules include

1. higher atomic number is given priority.
2. higher atomic mass is given priority.
3. *cis* is prior to *trans.*
4. like pairs [(R, R) or (S, S)] are prior to unlike pairs [(R, S) or (S, R)].
5. lone pair electrons are regarded as an atom with atomic number zero.

The groups around the chiral carbon are then ordered in a sequence 1 >2 >3 >4 according to the list of rules above, and are then viewed in such a manner that the group designated 4 (that is of lowest priority) is pointing backwards, or away from the viewer. The remaining groups are then studied. When the group priorities follow a clockwise direction, the chiral centre is labelled R, and when the group priorities follow an anti-clockwise direction, the chiral centre is labelled S.

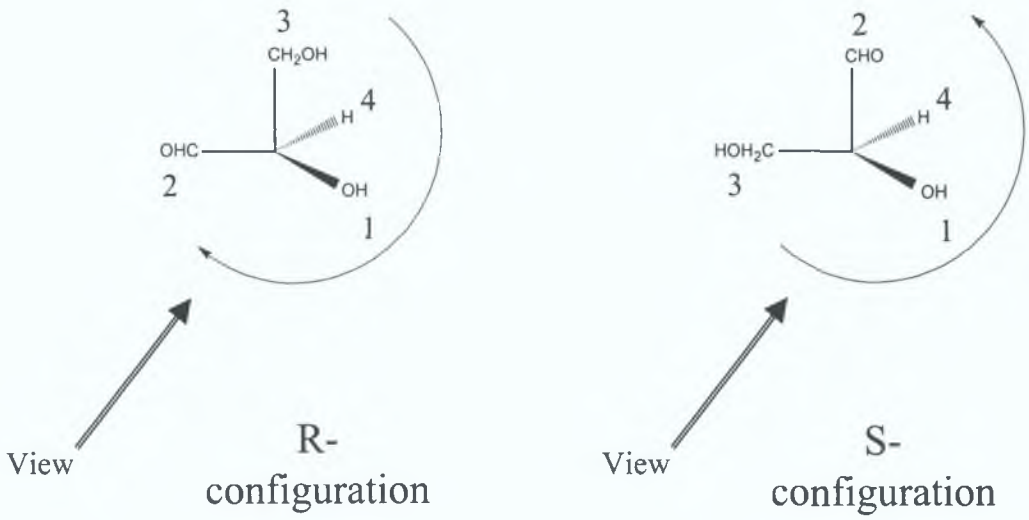

Figure 1-17: *The R and S nomenclature system.*

1.9 Chiral Calixarenes

1.9.1 Asymmetric Calix[4]arenes by *O*-Alkylation with Chiral Residues

The introduction of chiral substituents can convert calixarenes into chiral derivatives. This can be accomplished at either the phenolic hydroxy group or the para position, in calixarenes derived from phenols. Providing enantiomerically pure reagents are used and that derivatisation proceeds without racemisation, pure enantiomeric calixarene products can be obtained in good yield [**71**, **72**]. The chirality of these compounds is however, due solely to the chirality of the individual substituents. The non-planar molecular structure of calixarenes can nonetheless be taken advantage of, resulting in inherently chiral calix[4]arenes, which are based on the absence of a plane of symmetry, or an inversion centre in the molecule and not merely a chiral subunit [**73**].

1.9.2 Asymmetric Calixarenes - Inherent Chirality

Calix[4]arene derivatives with three [**19**] or four [**16**] (sequentially AABC {where $R^1=R^2$ or $R^3=R^4$} or ABCD respectively) different *para*-substituents were among the first inherently chiral calix[4]arenes synthesised. This was achieved by (3+1) or (2+2) condensation of appropriate trimers with bisbromomethylated phenols, or apposite dimers with bisbromomethylated dimers respectively (see below). Compounds with functional groups such as methyl, *t*-butyl, *n*-alkyl, cyclohexyl, phenyl, COOR, CH_2COOR and Cl have been synthesised in this fashion, with the final cyclisation step yielding 25-35% of product [**19**, **16**, **74**].

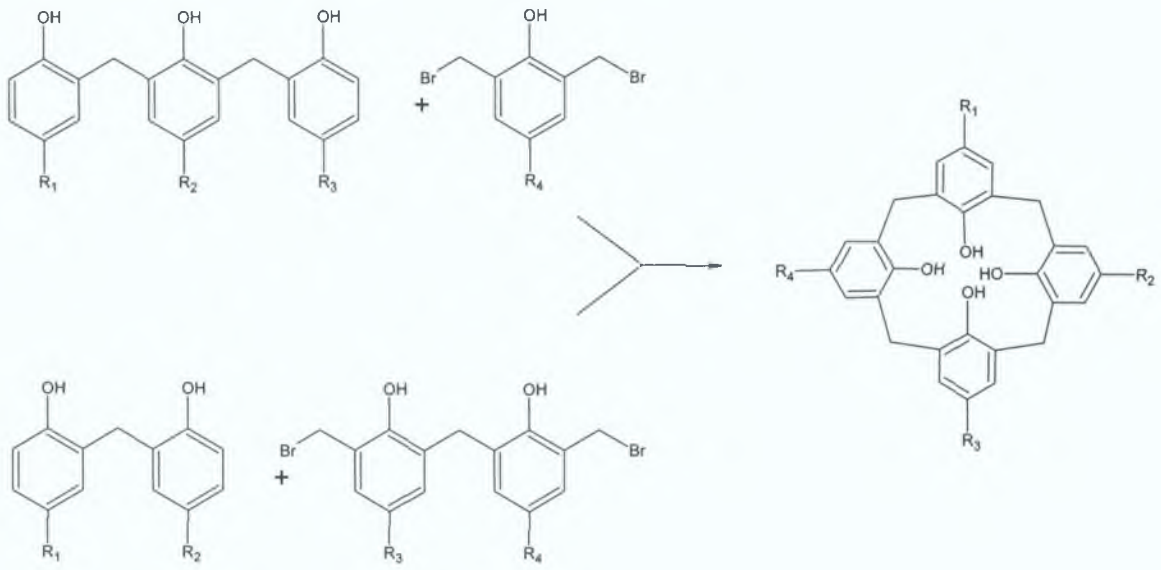

Figure 1-18: *"3+1" and "2+2" formation of inherently chiral calix[4]arenes*

However in order to prevent racemisation (or ring inversion in the case of calixarenes), sufficiently large groups must be introduced at the phenol hydroxy sites. Suitable bridges between the *para*-positions may also suppress racemisation by ring inversion. This was illustrated by the bridged calixarene below (**6**), which due to the disparity of the residues in the *para*-positions (methyl, t-butyl) is asymmetric. In the presence of Pirkle's reagent, the splitting of ^{1}H-NMR signals establishes the existence of stable enantiomers; with single crystal *x-ray* analysis indicating each enantiomer exists in the cone conformation. Even with the likelihood of flexibility in solution, and therefore the possibility that the molecule could undergo changes in conformation from cone ↔ partial cone ↔ 1,2-alternate, the fixed molecular skeleton prohibits conversion into the reverse cone-conformation [**75**].

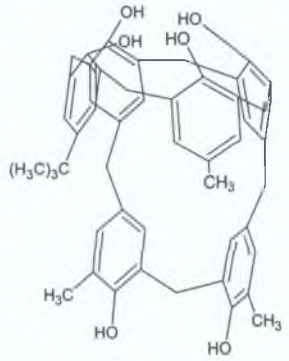

(**6**)

1.9.3 Asymmetric Calix[4]arenes with a Single *meta*-substituted Phenolic Unit

An idea first realized by Vicens et al. was that the introduction of a single *meta*-substituted phenolic unit would result in an asymmetric calix[4]arene (**7**) [**76**, **77**]. These compounds have been prepared by "3+1" fragment condensation reactions.

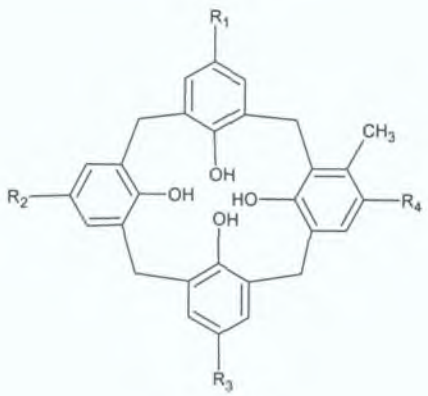

	R^1	R^2	R^3	R^4
a	Me	Me	Me	Me
b	iPr	iPr	iPr	iPr
c	iPr	Phe	iPr	iPr
d	tBu	tBu	tBu	iPr

(**7**)

The tetrapropyl ether was prepared in the cone conformation from compound d, and resolved by chiral chromatographic stationary phases [**78**, **79**]. The tetrapropyl ether chains appended at the lower rim were large enough to curtail inversion of the macrocycle through the annulus, which in turn prevented racemisation of the compound, thus yielding the first distinct enantiomer of an inherently chiral calixarene. Further results were achieved with a *meta*-hydroxyl group incorporated in the 2,6-position, i.e. with a single resorcinol unit [**80**]. Calix[4]arenes with *meta*-substituted phenolic units were synthesised by Gutsche from the corresponding monoquinone derivatives, e.g.:

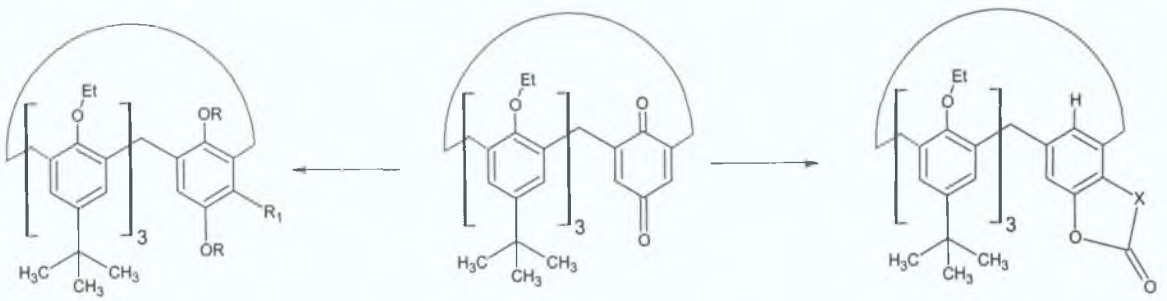

R = H, $R^1 = S\text{-}C_6H_4\text{-}CH_3$

R = Ac, $R^1 = O\text{-}Ac$

X = S, CHR, SCH_2

Figure 1-19: *Asymmetric calixarenes with meta-substituted phenolic units*

1.9.4 Asymmetric Calix[4]arenes by O-Alkylation with Achiral Residues

A similar asymmetric configuration, AABC or ABCD, can be acquired by adding three of four different substituents to the phenolic oxygens, via alkylation or acylation, which is advantageous from the point of view that chirality is achieved concurrently with a fixed conformation, rendering racemisation impossible [**81**, **82**, **83**].

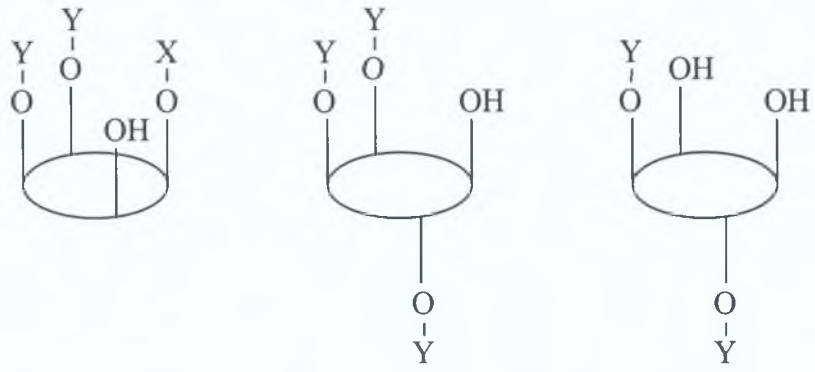

(**8**) (**9**) (**10**)

At least two different pendent groups are necessary for an all *syn*-arrangement of the *O*-alkyl groups (**8**), but this is not essentially the case if some of these groups are in the anti position. In the latter situation numerous possibilities exist, including compounds (**9**) and (**10**) with one kind of *O*-alkyl group, which are asymmetric and dissymmetric respectively ((**10**) having effectively C_2 symmetry). Shinkai *et al.* [**81**, **82**] and Pappalardo *et al.* [**84**] have produced such examples of caiixarenes, with some resolved by chromatographic techniques [**85**, **86**]. Since the hydroxy group in the above compounds can still pass through the annulus, an incompletely *O*-alkylated calix[4]arene can, in principle, assume different conformations. For example (**8**) can exist in *cone* and *partial cone* conformations, with *partial cone* and *1,2-alternate* possibilities for (**9**), while (**10**) could exist in all conformations except *cone*.

Therefore it has been suggested that the terms cone, *partial cone*, *1,2-alternate* and *1,3-alternate*, should be reserved for descriptions of tetra-ether compounds only, and also for conformational assignments, while syn and anti or the superscripts α and β should denote the mutual arrangement of the *O*-alkyl groups [**73**].

Condensation of calix[4]arenes with two different p-substituted phenolic units ("2+2 " for AABB, "3+1 " for ABAB) generate products which, when in the cone conformation possess C_S and C_{2V} symmetry. 1,3-Diethers are readily prepared from calix[4]arenes [**56**], and can also be obtained in high yields from calixarenes of type AABB, illustrating another variety of chiral calixarenes [**87**]. The chirality of the molecule is due to its asymmetry, since the plane of the calix substructure is not coincidental with the plane of symmetry of the *O*-alkyl groups. The aforementioned chirality (i.e. symmetry issues) also holds true in the case of 1,2-diethers of calix[4]arenes of type ABAB. 1,3-di-*O*-alkylation is however, far more selective than 1,2- di-*O*-alkylation rendering the latter synthesis rather difficult. If even slight amounts of the two possible mono, 1,3-di or triether products were formed, it would make for quite a complex reaction mixture.

Mild oxidation ($Me_3PhN^+Br_3^-/NaHCO_3$ in CH_2Cl_2) can convert t-butyl calix[4]arenes into spirodienones, which are yet again another example of inherently chiral calix[4]arenes [**88**, **89**, **90**]. The structure of the monospirodienone (**11**) was confirmed by x-ray crystal analysis, with the ^{1}H-NMR spectrum showing two signals for the different OH groups and four different AX systems for the methylene bridges.

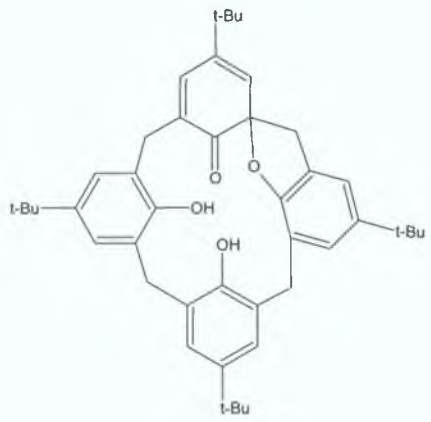

(**11**)

The chirality of this compound is due to the asymmetrically substituted spirocarbon atom, implying that this calix[4]arene is not inherently chiral. It is however similar to

calix[4]arenes having three different phenolic units in the sequence AABC (two hydroxyl groups in proximal positions, one carbonyl group and an ether group).

1.10 Host–Guest Chemistry and Molecular Recognition

"Evolution has produced chemical compounds exquisitely designed to accomplish the most complicated and delicate of tasks. Many organic chemists viewing crystal structures of enzyme systems or nucleic acids and knowing the marvels of specificity of the immune systems must dream of designing and synthesising simpler organic compounds that imitate working features of these naturally occurring compounds." – D.J. Cram, Nobel Lecture [**91**].

Supramolecular chemistry was defined by Lehn as "chemistry beyond the molecule" or "the designed chemistry of the intermolecular bond". Central to the comprehension of supramolecular chemistry is the phenomenon of molecular recognition, or how certain molecules and ions select to associate with specific partners in particular ways. One of the most fundamental processes in biology, in addition to chemistry, is molecular recognition between molecules, and this makes the principle important. One of the fundamental components of systems that exhibit molecular recognition is non-covalent interactions [**92**]. Such interactions involve a subtle interplay of entropic and enthalpic effects that are difficult to separate.

Living processes depend essentially on non-covalent interactions, which are responsible for many of the structural features of biological molecules (for example their assembly into whole organisms) and for the chemical transformations that allow organisms to function and replicate. Extremely diverse ranges of systems whose actions depend on the recognition phenomenon include enzymes, receptors, antibodies, membranes, cells, carriers and channels [**93**]. Macrocyclic architectures that are purposefully synthesised can provide convergent, preorganised recognition sites, which can cooperatively act on an enclosed substrate, and can therefore, to a certain extent, mimic the natural recognition processes occurring at the binding sites of enzymes and biological receptors. The study of these recognition processes can help to gain an insight into, or improve in the understanding of the mechanisms of molecular recognition phenomena. Among these phenomena is chiral recognition,

simple in concept but often difficult in practice, whereby a chiral host molecule selectively binds one enantiomer of a racemic mixture.

1.11 Historical Aspects of Host –Guest Chemistry and Molecular Recognition

The recognition and complexation of guest molecules by biotic receptors has been studied since about 1900. It began essentially in 1894 when E. H. Fischer postulated a stereospecific interaction between a sugar and a fermenting agent, thereby formulating the "lock and key" notion (see Figure 1-20) for the interaction of an enzyme and a substrate [**94**], (for which he received the Nobel Prize in 1902). This concept maintains that molecular recognition images the complementarity of a lock and key- the lock being the molecular receptor and the key being the substrate that is recognized to give a defined receptor-substrate complex.

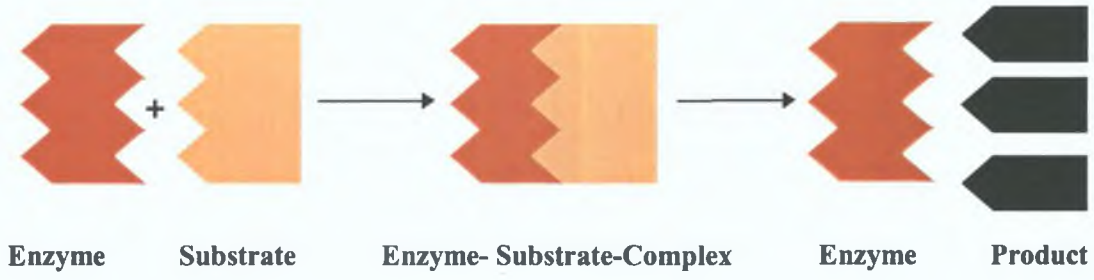

Figure 1-20: *illustration of "lock and key" theory of Emil Fischer.*

The model of molecular interactions between an active drug and a protein receptor was developed by J.N. Langley in 1906 [**95**], while early experiments conducted in the 1930's of associations in solution led to the use of the term "Übermolekeln" (supermolecules). In essence however, the field only rapidly expanded around the 1960's, from studies of molecular recognition of alkali metal ions using natural antibiotics and synthetic macro(poly)cyclic polyethers. Roots however can be traced back to when Paul Ehrlich postulated cross-reactions between molecules competing for the same binding site at the same chemoreceptor, as a result of investigations based on immunized animals and stained living tissue [**96**]. In a paper in 1900, he reasoned that toxins possessed two different combining groups, a heptaophore that

bound the toxin to the cell and a toxophore that was responsible for the toxic action [**97**].

A significant contribution was made in 1957 in Zurich by the group of Waser et al., in working out the mechanisms of the activity of T-curarin and related compounds at the neuronal fibre terminal of the muscle [**98**]. Büchi postulated a receptor model for the binding of local anaesthetics, and proposed complementary molecular structures of drugs fitting the receptors [**99**]. His model of the receptor geometry was confirmed by the pharmacological activity profile of compounds, and structure-activity relationships were explored by chemical tailoring of such compounds and studying the pharmacokinetic properties of various derivatives. These early investigations of molecular recognition led scientists to investigate the basic properties of the molecular processes involved in nature.

Although Cram's pursuit of the imitation of natural systems ca. 1959 did not lead to the observation of intercalated structures [**100**, **101**], they did recognise that central to simulation of enzymes by relatively simple organic compounds would be the investigations of highly structured complexes. Inclusion compounds and the whole area of "host-guest" chemistry was initiated in 1967, when Pedersen published papers which reported the formation of highly structured complexes when alkali metal ions bind crown ethers [**102**, **103**]. At approximately the same time (1969), Lehn, Sauvage and Dietrich published papers on the design, synthesis and binding properties of the cryptands, representing further developments in complexation chemistry [**104**, **105**]. In 1977 the terms **host**, **guest**, **complex** and their binding **forces** were defined by Cram [**106**]:

"Complexes are composed of two or more molecules or ions which are held together in unique structural relationships by electrostatic forces other than those of full covalent bonds."

1.11.1 Definitions used in Host –Guest Chemistry

The **host** component is defined as an "organic molecule or ion where binding sites converge in the complex, whereas the **guest** component is one whose binding sites diverge in the complex". Hosts are synthetic counterparts of the receptor sites of biological chemistry and guests the counterparts of substrates, inhibitors and

cofactors. Simple guests are abundant, and small in comparison to hosts, but hosts are usually bigger and in order to complex existing guests, must often be designed and synthesised. Guests may be organic molecules or ions, metals or metal ions or metal-ligand assemblies. Hosts are open chain, cyclic, bicyclic or polycyclic compounds, and frequently contain repeating units.

A highly structured molecular **complex** is comprised of at least one host and one guest component. A host-guest association involves a complementary stereoelectronic arrangement of binding sites in both the host and guest. The interactions between molecules depend on forces that are much weaker than those which hold molecules together [**107**]. The covalent bonds broken and made during syntheses are typically of the order ca. 350 KJ mol^{-1} (for a C-C bond), which are in stark contrast to the forces employed in associations in supramolecular chemistry, which range from 50 KJ mol^{-1} downward. Multiple binding sites are therefore usually required to produce a highly structured complex, since the forces at any one binding site are (in comparison to covalent bonds) small.

It can often be useful to classify complexes in relation to the extent to which a host envelops a guest in a complex. In crystals, both the host and guest compounds are completely enveloped; therefore terms borrowed from crystallography would be inaccurate as descriptions. Cram et al have suggested the term "*perching complex*" to typify complexes in which well under half the guest surface contacts the host [**108**]. A structure in which over half of the guest surface contacts the host is termed a "*nesting complex*", while the term "*capsular complex*" is applied to structures in which the guest surface is enclosed sufficiently by the host, to prevent solvent or external ligand molecules from contacting the guest.

Molecular complexes are usually held together by **forces** such as hydrogen bonding, ion pairing, π-π interactions, metal to ligand binding, van der Waals attractive forces, solvent reorganising, and by partially made and broken covalent bonds (transition states). The electron pair donor-acceptor interactions (see Figure 1-21) between basic ligands and metal ions are amongst the strongest of the aforementioned associations. For example, the Zn(porphyrin)-pyridine bond described by Walker and Benson, may be estimated at 42 KJ mol^{-1} [**109**].

M = metal

L = ligand atom (O, N, S, P etc.)

Figure 1-21: *electron pair donor-acceptor interactions of ligands and metals*

Hydrogen bonds and electrostatic interactions (which are usually mediated through the former) are also relatively strong, up to 30 KJ mol^{-1} [**107**].

D = H-bond donor atom

A = H-bond acceptor

Figure 1-22: *hydrogen-bonding interactions between donor and acceptor atoms.*

These interactions, that of ligand-to-metal and hydrogen bonding, are of interest not only because of their strength, but also because their specificity and directionality allows for significant control over their exploitation. Charge-dipole, dipole-dipole, and dipole-induced dipole interactions may be weak individually, but they can yield strong and specific bonding when operating collectively between extended rigid units such as π-π interactions between aromatic systems [**110**].

1.12 Principle of Complementarity

For molecules to associate in a pre-programmed fashion, it is necessary to establish specific complementarity between the different components. Therefore conformational control is a central issue in the design of supramolecular systems. Using well-defined three-dimensional structures, with the recognition sites arranged can help to achieve this complementarity. Employment of such rigid architectures can also limit the possibilities of intramolecular quenching of binding sites, and can minimize the loss of entropy on complex formation.

In some cases it is desirable to retain a degree of flexibility, in order to obtain a perfect "fit" of components, by relaxation in each other's presence. Since however flexibility is extremely difficult to avoid, it is rarely an obstacle in receptor design. Elemental compositions, component structures, solubilities and examination of Corey-Pauling-Koltun (CPK) molecular models of possible complexes, allowed

general structures of the first host-guest complexes to be estimated. Cram and co-workers used CPK molecular models to investigate potential complexes [**111**] and subsequently synthesised hosts to establish if they possessed the desired guest-binding properties.

While using molecular models to anticipate host structures the "principle of complementarity" was kept in mind: "to complex, hosts must have binding sites which cooperatively contact and attract binding sites of guests without generating non-bonded repulsions" [**112**]. By 1986 the crystal structures of over 50 complexes and another 25 hosts had been determined by Trueblood, et al [**113**]. These crystal structures were examined to compare the theoretical models with the host-guest structures observed experimentally, and good similarities were found. Studies of the crown-alkali metal salt complexes by Truter [**114**] and Dunitz [**115**], and work done by Weiss [**116**] on cryptand-alkali metal complexes also provided firm evidence of complex structures in crystalline state.

The design of macrocycles capable of molecular recognition is invariably influenced by the proposed choice of solvent. Synthetic receptors are generally intended to operate either in water (for genuinely bio mimetic recognition) or in non-polar organic media such as chloroform (which is held to mimic the conditions in biological membranes).

From spectral results on both the hosts and their metal-salt complexes by Dale [**117**] and Chan [**118**], structures in solution could subsequently be compared to those in solid state.

1.13 The Role of Solvent

While forces such as van der Waals interactions, hydrogen bonding and metal to ligand interactions are among the first to be considered in molecular recognition, the factor of solvent must also be taken into account. For simple processes the first of the two equations below is usually used (1), however the second is probably a more accurate description, with the explicit mention of solvent (see (2)).

$$A + B \rightarrow A \cdot B$$ **Equation 1-1**

$$A \cdot solvent + B \cdot solvent \rightarrow A \cdot B + solvent \cdot solvent$$ **Equation 1-2**

In the case of a non-polar organic solvent, generalised intermolecular attractions are unlikely to be effective in driving complex formation, because the energy gained on forming 'A.B' and 'solvent.solvent' is lost when A and B are desolvated. It is usually necessary in complex formation for A and B to contain particular features, which complement each other without greatly promoting the affinity of either for solvent molecules. In non-polar media ligand-metal and hydrogen bonding interactions are promoted, while π-π and cation-π interactions can also be very effective. However engineering the poor solvation of A and B may also be taken advantage of, in particular if the solvent molecules are large or awkwardly shaped [**119**, **120**].

A supplementary force for complex formation is achieved when the solvent molecules have a high affinity for each other. When the self-association of solvent molecules is a more favourable interaction than the solvent with A and B, equation 1-2 will be driven to the right. In solvents capable of hydrogen bonding (among which the most important is water) such solvophobic effects are particularly important. In water, the dominant interaction for molecular association is often hydrophobic binding, while intermolecular hydrogen bonding is relatively ineffective due to the solvation of recognition sites.

1.14 The physical chemistry of molecular recognition

The laws that govern all physical chemical processes are also applicable to molecular recognition. ΔG represents the Gibbs free energy, a term which is equivalent to the binding energy and which is composed of two opposing terms, ΔH, which is the enthalpy component and ΔS the entropy component.

$$\Delta G = \Delta H - T\Delta S$$ **Equation 1-3**

(where T is the absolute temperature)

When ΔG is negative, there exists a thermodynamically spontaneous process. This can happen if

1. ΔH and ΔS are both negative and the absolute magnitude of ΔH is greater than that of $T\Delta S$, or
2. if ΔH is negative and ΔS is positive

The hydrophobic effect, which was mentioned earlier, derives from a favourable entropic effect when non-polar moieties are de-solvated [**121**]. The change in entropy which results on complex formation or molecular assembly is therefore another factor to be considered. Entropy will usually work against the formation of organized assemblies, as rotational and translational freedom is commonly lost when molecules associate. However ensuring that the loss in internal degrees of freedom is maintained as small as possible may minimize the damage. For this reason the use of rigid architectures, with the recognition moieties being held in correct positions for binding (preorganised) is gainful, with the intention of as little loss in freedom as possible when complexation takes place.

Strong or tight binding, which can be driven by a large decrease in enthalpy, generally equates with components that cannot move in relation to each other. This situation is of course less entropically favoured than a weak association where there is greater freedom within the complex, but it should be noted that entropic factors tend to moderate the effect of enthalpic forces [**122**]. The process of binding requires that the drug and receptor molecules have a complementarity of shape and charge, which leads to an overall negative interaction energy ($\Delta G<0$). The relation between the free energy of dissociation (free energy at constant pressure of Gibbs free energy) to an equilibrium constant K, governs bimolecular complex formation.

$$\Delta G = -RT \ln K \qquad \textbf{Equation 1-4}$$

(Where R is the gas constant and T is the absolute temperature)

Apart from making a significant contribution to the binding energy, electrostatic effects are also involved in the orientation of molecules and the recognition

processes that lead to binding. With reference to host-guest reactions, Spichiger-Keller examined the variations between thermodynamics, electrostatic interactions and solvent [**123**] and proposed that fast kinetics are required in order to apply host-guest chemistry to sensor technology.

The thermodynamic properties of a large variety of ionophores was studied and a positive ΔS at $\Delta H=0$ was found, which implies an entropy stabilised association mechanism where the predominant conformer of the free ionophore in pure solvent is less stabilised than that of the complex, which means the association is entropically favoured [**124**]. The polarity and hydrogen donicity of the solvent exert a strong influence on the preformation of the ionophore, and therefore the free energy of the interaction.

1.15 Types of Hosts

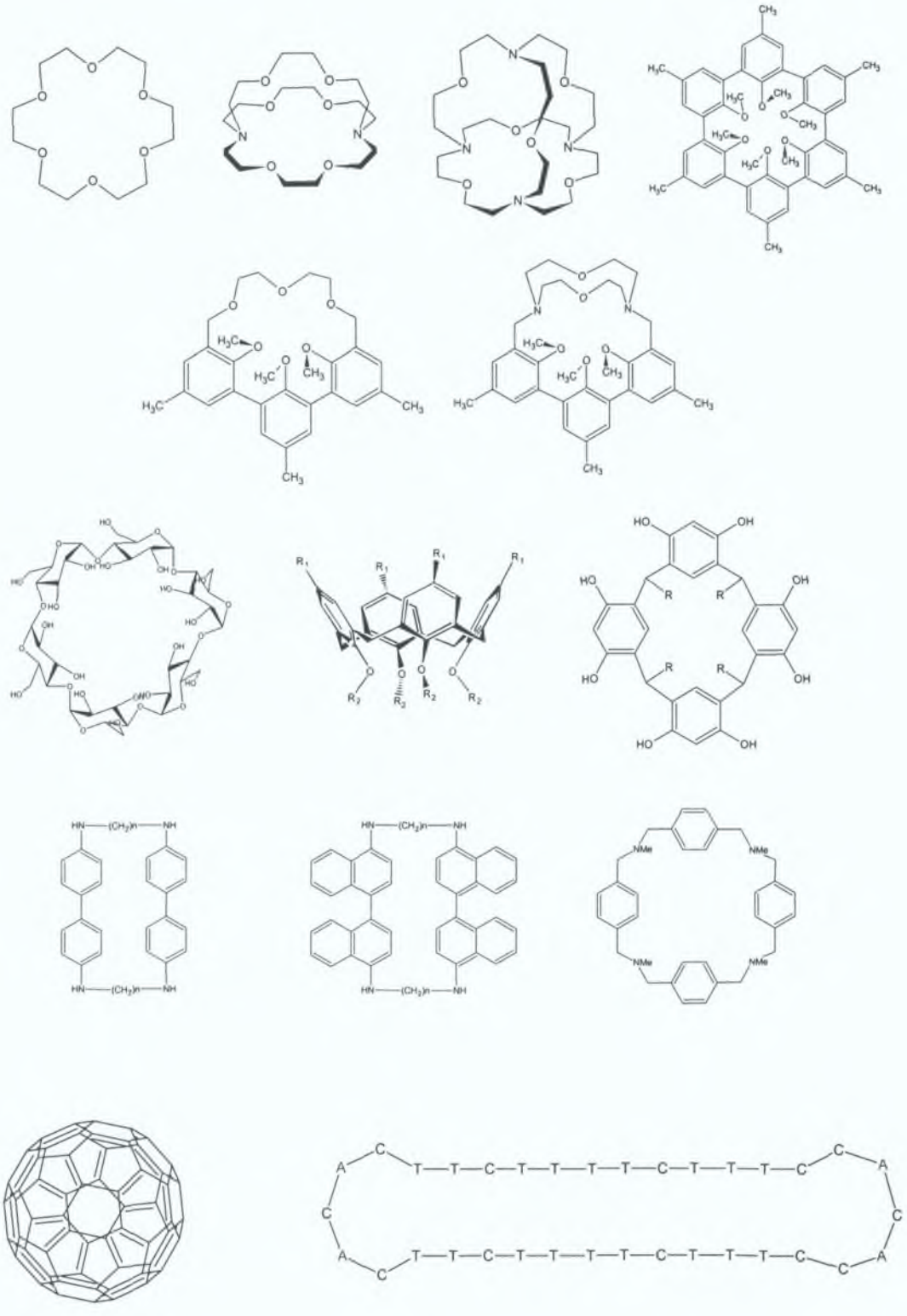

Figure 1-23: *from left to right, top to bottom: Crown, Cryptand, Spherand, Spherand, Hemispherand, Cryptaspherand, Cyclodextrin, Calixarene, Resorcarene, 3 Cyclophanes, Fullerene-C_{60}, Circular DNA (A, C, T = Adenine, Cytosine and Thymine).*

Crown ethers and cryptands are hosts with polyethyleneoxy units, with the latter making a bridge between the nitrogen bridgeheads of bi- or polycyclic hosts. Modified crowns or cryptands are terms used when the crown or cryptand structure dominates with other units being substituted for the CH_2CH_2, CH_2OH, $N(CH_3)$, or $CH_2OCH_2CH_2OCH_2$ groups. Spherands are defined as hosts conformationally organised prior to complexation, and therefore must contain more rigid components than those of crowns or cryptands. Lehn's earliest spherand (pictured above) is aliphatic in nature, and differs dramatically from the spherand designed and prepared by Cram, who took a different approach to this type of encapsulating compound. Hemispherands are composed of mobile and rigid parts, with the latter part determining the conformation, while podand is the name given to the family of acyclic hosts. While all of the above-mentioned hosts are preorganised for binding, not all of them are conformationally organised (have the correct contour or shape) prior to complexation.

Other types of macrocycles that have been used as host molecules include those pictured previously. Cyclodextrins (CD's), are macrocyclic oligosaccharides, produced by the enzymatic catabolism of starch consisting of 6(α), 7(β) or 8(γ) α-D-glucopyranose units connected by 1,4-glycosidic bonds. It is known from crystal structure and spectroscopic analyses that CD's exist in an approximately round conical shape (see Figure 1-23), in solution as well as in the solid state [**125**]. They are inherently chiral and form inclusion complexes with a variety of organic compounds in aqueous solution, accommodating a guest molecule in their central cavity [**126**, **127**, **128**]. Calixarenes and resorcarenes are macrocycles like crown ethers and cyclodextrins, whose conformational isomers offer a great number of unique cavities, all of different size and shape. They are very similar in structure to the spherands, implying that these condensation products should be good hosts for complexation. Cyclophanes, or bridged aromatic compounds have also been employed as hosts, which form both stacked-type and inclusion complexes. In contrast to the previously mentioned hosts, the fullerene series could act only as capsular hosts. Though large in comparison to the rings so far referred to, the DNA macrocycle pictured in Figure 1-23, has been found to bind complementary linear strands by simultaneous Watson-Crick and Hoogsteen base pairing.

The discovery of recognition phenomena, which have involved most of the aforementioned host categories, has permitted an understanding of the properties of more complex natural products. This has involved investigation of the occurrence of these general properties amongst the natural ionophore macrocycles. Detailed analysis therefore of the orientation of substituents attached to the macrocycle and also control of this orientation has led to general concepts concerning the properties required for a biological channel. Among these general concepts is that of ion transport capability. Ionophores can be characterised as receptors that form stable complexes with charged species (e.g. Na^+, K^+ and Ca^{2+}), thereby allowing transport of these ions across lipophilic phases, in particular membranes. There are several classes of natural ionophores:

- Cyclodepsipeptides formed from alternating α–amino acids and α–hydroxy acids
- Cyclopeptides formed solely from α–amino acids
- Cyclodepsides which consist only of α–hydroxy acids

Cyclodepsipeptides are macrocycles characterised by having lipid side chains and polar groups in the chain (amide, ester, ether). This class of compounds are cyclic antibiotics including the archetypal natural ionophore Valinomycin and also Beauvericin, Enniatin A and Enniatin B. Cyclopeptides are another class of macrocyclic compounds, very commonly met in biological systems. In comparison to cyclodepsipeptides, relatively few natural cyclopeptides are complexing agents for alkali and alkaline earth metal cations. However, synthetic cyclopeptides have been prepared and have been found to complex a range of alkali, alkaline earth and even some transition metal ions. Another class of natural compounds, unlike those mentioned above, contain only ester type links (lactone) together with ether groups but no peptide bonds. The nactins are 32-membered cyclic tetralactones, which belong to this family of molecules, and have been found to complex metal ions and the ammonium cation. A series of macrotetrolides of structure related to that of the nactins has been synthesised. They exhibit ionophoric properties, and some of them do possess ion transport abilities, though less important than those for crown ethers.

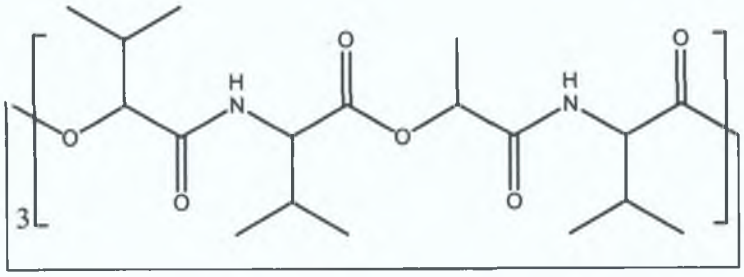

(a)

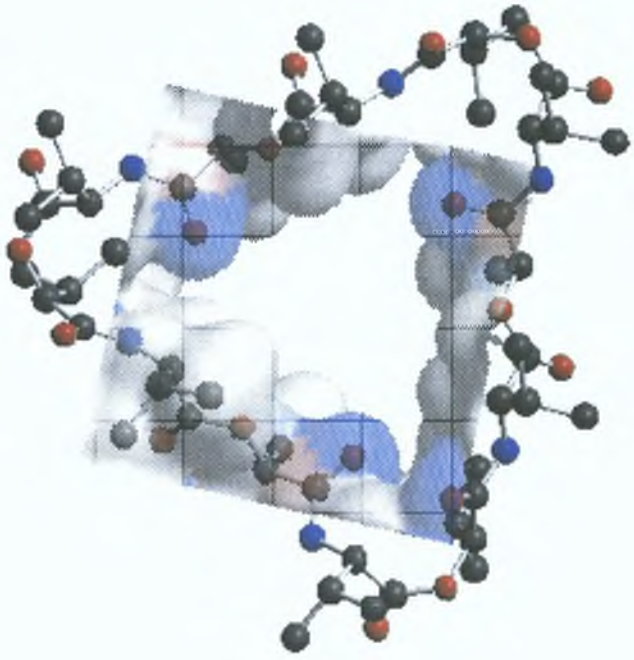

(b)

Figure 1-24: (a) *Structure of natural K^+ ionophore Valinomycin,* ***(b)*** *energy minimised structure of valinomycin, using Chem3D Pro software -version 6.0, showing partial charge surface in grey squared area.*

1.16 Host-Guest Complexes

One of the first complexes that proved of practical interest was a complex between [18]crown-6 and acetonitrile. When [18]crown-6, or partially purified [18]crown-6 is stirred with acetonitrile, it forms a colourless complex, which has been used for final purification of the crown [**129**]. The complex was first reported in 1974 but the crystal structure was not solved until 1988 (Figure 1-25) [**130**].

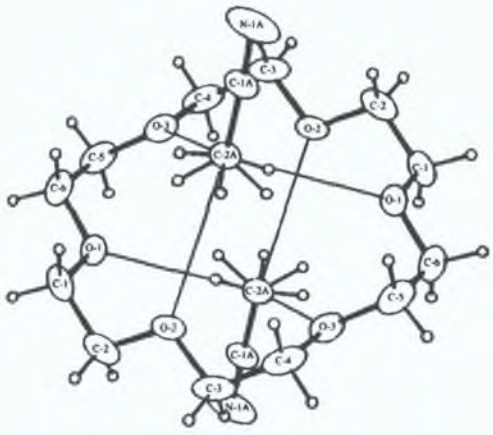

Figure 1-25: *Crystal structure of the [18]crown-6-acetonitrile complex.*

Crystal structures of Pedersen's [18]crown-6 (**12a**) and Lehn's [2.2.2]cryptand (**13a**) show that they do not contain cavities or convergently arranged binding sites in their uncomplexed states. The free macrocycles fill their internal void by turning two of their methylene groups inward. However indications that the act of complexation must be accompanied by host reorganisation and desolvation are evident by comparing the energy minimised (Chem3D Pro –version 6.0) structures of the [18]crown-6 host (**12b**) with that of its K^+complex (**13b**).

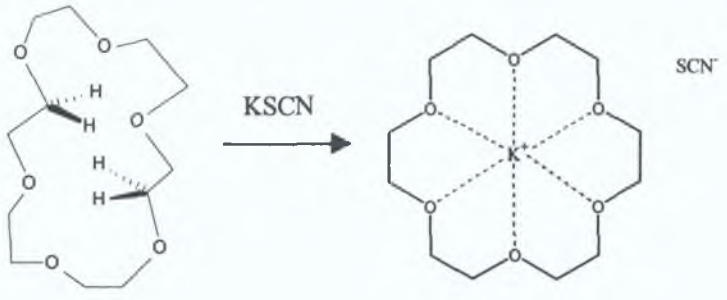

(**12a**) (**13a**)

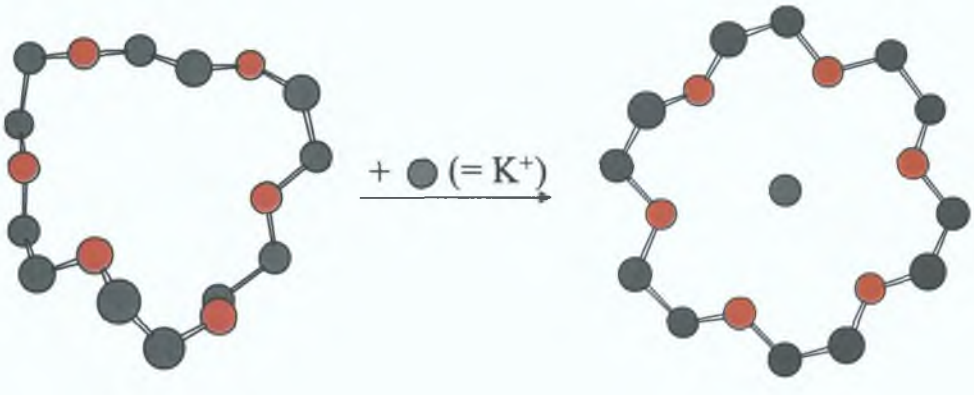

(**12b**) (**13b**)

The complexes (**13**) and (**16**) are good examples of what are termed by Cram et al, as "nesting complexes" with the guest totally engulfed by the host cavity [**108**]. A different type of complex is called a "perching-complex", thus designated since the guest component is too large to fit into the host and must perch on rather than be encapsulated by the host [**108**]. An example of this is the complex (**14**), in which the acidic hydrogen's of the methylammonium guest ion are hydrogen bonded to three alternate oxygen's of the [18]crown-6 host in a tripod arrangement. The nitrogen atom and bonded methyl group project above the plane of the host, where it appears to "perch".

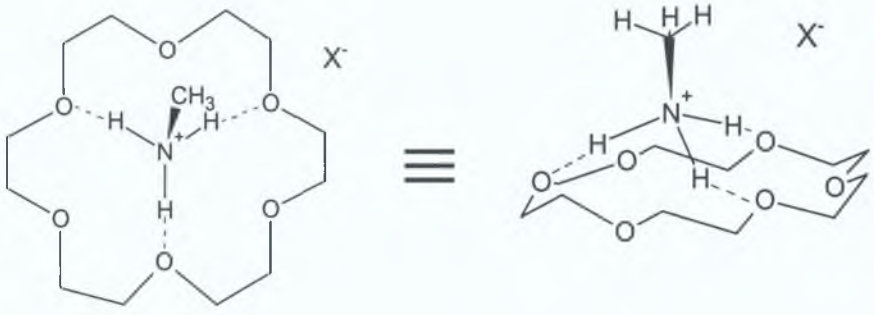

(**14**)

Apart from complex formation involving metal ions, crown ethers have been shown to associate with a variety of other guests molecules, both charged and uncharged. Typical guests include ammonium salts, the guanidium ion, diazonium salts, water, alcohols, amines, molecular halogens, substituted hydrazines, p-toluene sulfonic acid, phenols, thiols and nitriles.

The aim of cryptand synthesis has generally been the elaboration of a ligand displaying good complexation properties towards a specific cation. The first cryptand [2.2.2] (**15**) was designed to complex the potassium ion, which it did successfully, see energy minimised (Chem3D Pro –version 6.0) K^+complex (**16b**) [**131**].

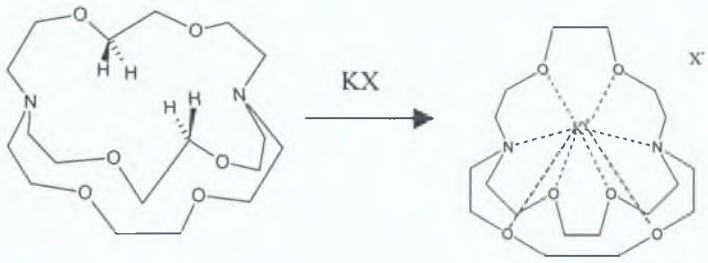

(**15a**) (**16a**)

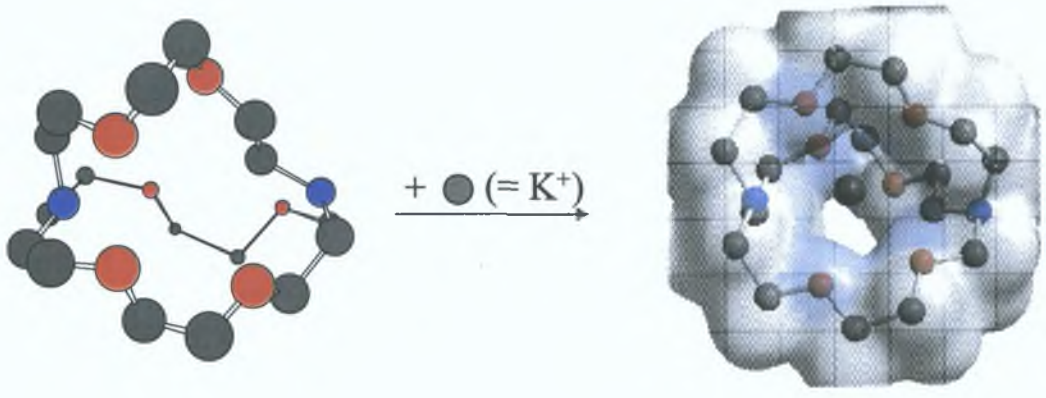

(15b) **(16b)**

The [1.1.1] cryptand (**17**) possesses excellent acid-base and proton transfer properties. This bicycle strongly binds one or two protons as shown by structures (**18**) – (**22**). The presence of a cryptate (cryptand complex) type structure is indicated both by NMR spectral analysis and by the high resistance of the complex to deprotonation. If (**18**) is heated at 60°C in 5M KOH for 80 hours it only partially yields the monoprotonated form (**19**). Even the reaction of sodium in liquid ammonia on (**18**) was found to give rise to only a very small amount of (**19**) [**132**].

(18) **(19)**

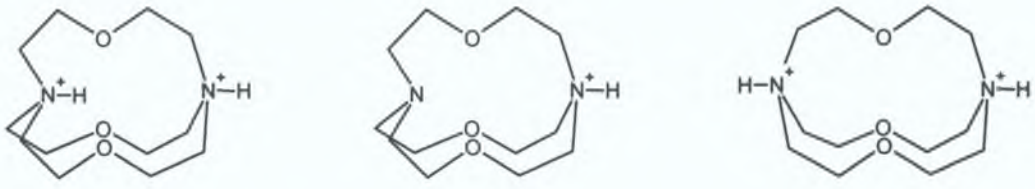

(20) **(21)** **(22)**

Crystallographic studies of the compounds [1.1.1], [H^+, 1.1.1] and [$2H^+$, 1.1.1] have shown that the protons are located inside the cavity as in (**18**) and (**19**) [**133**]. Other cations, which the various cryptand type hosts bind, include, Li^+, Na^+, Ca^{2+}, Mg^{2+}, Zn^{2+}, Ag^+, Tl^+, Rb^+, Cs^+, heavy metals, lanthanides, actinides and the ammonium ion.

A more elaborate type of encapsulating structure is illustrated by the spherands, which defines ligands with an enforced spherical cavity. Spherand (**23**) was designed to be complementary to Li^+ and Na^+ ions. The syntheses of (**23**) - (**25**) and their

crystal structures are reported [**134**]. (**23**) contains a cavity lined with 24 electrons, which are shielded from solvation by 6 methyl and 6 aryl groups. The crystal structures (**26**) and (**27**) are almost identical, and render compound (**23**) the first ligand system that was completely organised for complexation during synthesis, rather than during complexation.

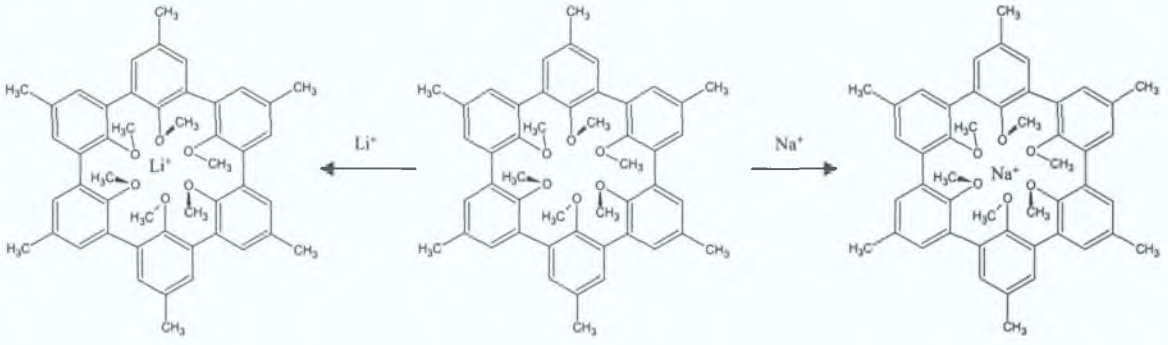

(**24**) (**23**) (**25**)

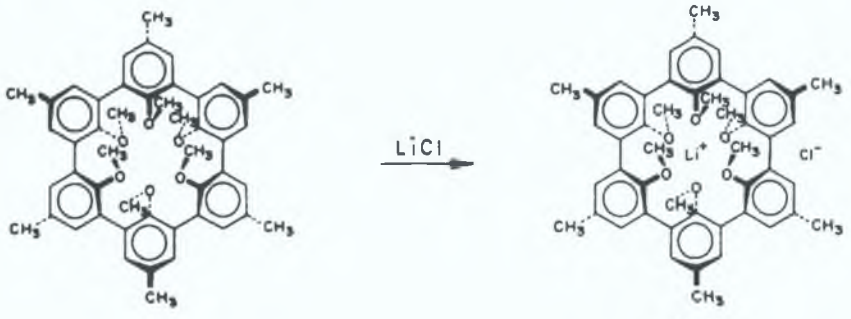

(**23**)
Molecular model of host
(spherand)

(**24**)
Molecular model of complex
(lithiospherium chloride)

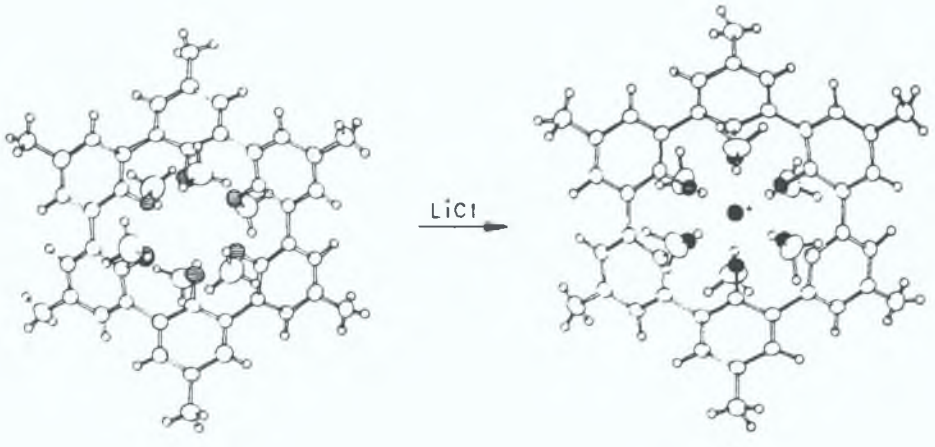

(**26**)
Crystal structure of host
(snowflake)

(**27**)
Crystal structure of complex

In general, free energies of lipophilic hosts (*H*) towards guest picrate salts can be estimated when guest salts (*G·picrate*) are partitioned between $CDCl_3$ and D_2O at 25°C in the absence and presence of host (*H*); thereby allowing K_a [mol^{-1}] and $-\Delta G°$ values [kJ mol^{-1}] to be calculated:

$$H + G \cdot picrate \underset{k_1}{\overset{k_{-1}}{\rightleftharpoons}} H \cdot G \cdot picrate$$

$$K_a = k_1 / k_{-1}$$

$$-\Delta G° = RT \ln K_a$$

Free energies of host (**23**) towards guest picrate salts of Li^+, Na^+, K^+, Rb^+, Cs^+, NH_4^+, $CH_3NH_3^+$, t-$BuNH_3^+$, were estimated when guest salts were partitioned between $CDCl_3$ and D_2O at 25°C in the absence and presence of host (**23**). While spherand (**23**) binds Li-picrate (>23 kcal mol^{-1}) and Na-picrate (19.3 kcal mol^{-1}), it totally rejects the other standard ions, as well as a variety of di- and trivalent ions [**112**].

Podand (**28**), the open-chain counterpart of spherand (**23**) binds Li-picrate and Na-picrate with $-\Delta G°$ <6 kcal mol^{-1} [**135**]. The only constitutional difference between (**23**) and (**28**), is the two hydrogen atoms at each end of the chain in (**28**) in place of one Ar-Ar bond in (**23**). The conformational disparity and state of solvation however is enormous. The ideally arranged single conformation of the spherand for binding Li and Na, contrasts greatly with the flexible chain of the podand, which can exist in principle in thousands of conformations.

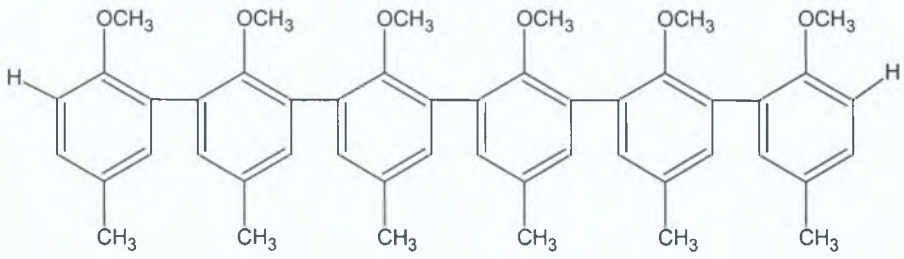

(**28**)

The variation in binding powers of spherand (**23**) and podand (**28**) with Li^+ is 17 kcal mol^{-1}, which corresponds to a differentiation of a factor of $>10^{12}$ in K_a. Similar values

concerning sodium binding yield a $-\Delta G°$ difference of >6 kcal mol^{-1}, corresponding to a difference in K_a of a factor $>10^{10}$. These dramatic variations in binding power led Cram and co-workers to conclude that "preorganisation is a central determinant in binding power". The principle of preorganisation states that the more highly hosts and guests are organised for binding and low solvation prior to complexation, the more stable will be their complexes. This preorganisational feature is the reason why spherand (**23**) is a more powerful binder with 6 binding sites than cryptand (**29**) or hemispherand (**30**) with 7 binding sites, or even the augmented crown (**31**) with 8. The oxygens in spherand (**23**) have no choice but to be arranged around an enforced spherical cavity, which is complementary to Li^+ and Na^+ ions.

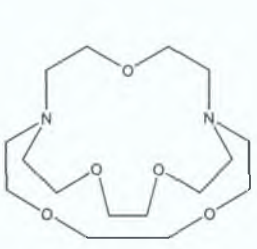

(**29**)

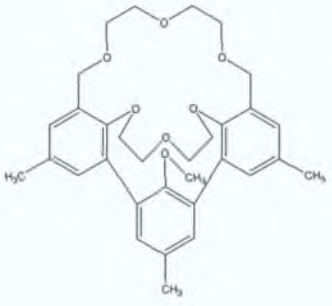

(**30**)

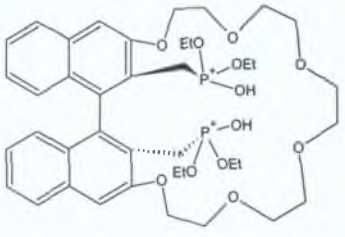

(**31**)

Cyclophanes or bridged aromatic compounds first commanded consideration in the 1950's with interest in small cyclophanes and their respective properties. In 1955 Stetter and Roos reported a number of larger cyclophanes, which possessed the possibility of the formation of inclusion compounds with organic guests, based on their strong interactions with solvent molecules in the crystalline state [**136**].

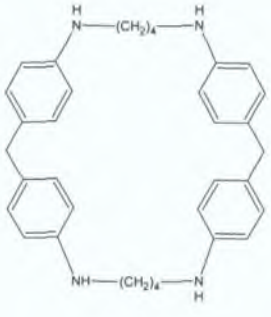

(**32**)

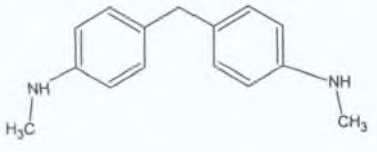

(**33**)

Host (**32**) is soluble in water in acidic solutions of pH<2, by multiple protonation. An examination of host guest interactions can therefore be carried out in aqueous media at this low pH. When the fluorescence spectrum of guest (**34**) is examined in the presence and absence of the host a marked difference can be seen. Not only is there an intensity increase in the spectrum of this guest; 8-anilino-1-naphthalenesulfonate,

but there is also a blue shift. Since such a fluorescence shift of guest (**34**) is quite common when bound to a protein or biomembrane, the above mentioned effects would indicate that this guest is transferred into a nonpolar environment in the presence of (**32**), namely the cavity of the cyclophane.

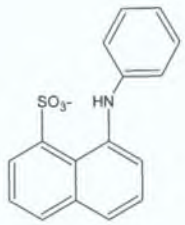

(**34**)

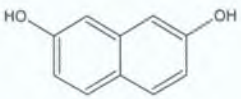

(**35**)

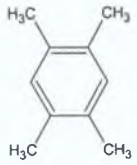

(**36**)

When guest (**35**), 2,7-dihydroxynaphthalene is observed by ^{1}H-NMR spectroscopy in the absence and presence of host (**32**), marked upfield shifts of the guest signals were observed (D_2O-DCl solution, pD 1.2). Such large upfield shifts in ^{1}H-NMR spectra can be ascribed to a strong anisotropic effect due to the ring currents of the aromatic rings of the host (**32**) (see Figure 1-26).

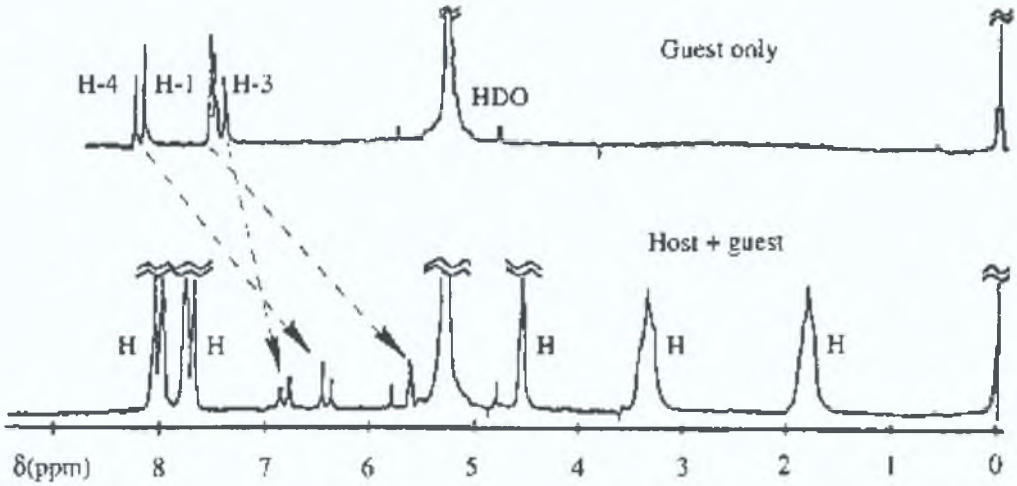

Figure 1-26: *^{1}H-NMR spectrum of guest (**35**) (upper spectrum) and ^{1}H-NMR spectrum of guest (**35**) in the presence of host (**32**).*

In the presence of the acyclic reference host (**33**) under the same conditions, negligible changes were observed in the fluorescence and ^{1}H-NMR spectra of the guests. This result strongly supports the inclusion of the guests in the hydrophobic cavity of host A.*n*H$^+$ in aqueous solutions. The crystal structure of host (**32**) with durene (**36**) was isolated, which shows clearly that the guest is indeed included in the cavity of this host cyclophane.

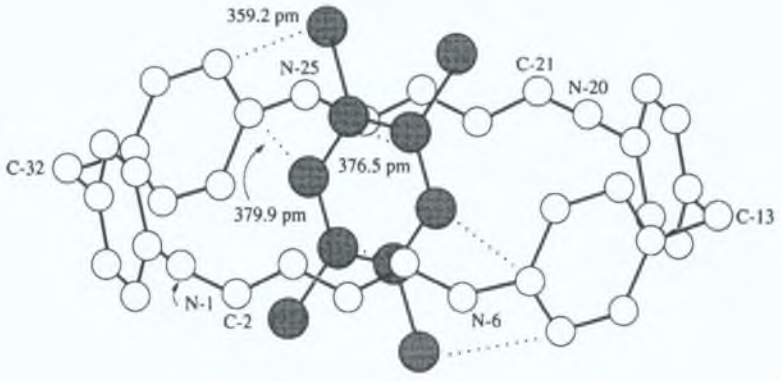

Figure 1-27: *Crystal structure of host (**32**) and guest (**36**) complex.*

Families of hosts can be arranged according to their $-\Delta G^{\circ}$ values with which they bind their most complementary guests:

spherands > cryptaspherands > cryptands > hemispherands > coronands > podands

Coronand is the name given to the family of modified crown-ethers. Although the character and numbers of binding sites influence the values of binding power, the degree of preorganisation appears to dominate the above sequence. Just as preorganisation is the central determinant of binding power; complementarity is the central determinant of structural recognition. In potential complexing partners both binding sites and steric barriers must be complementary to each other in terms of electronic character and geometry. Complementary positions of binding sites in complexing partners determine the number of contacts between host and guest. Since the binding energy at a single contact site (at most a few kcal mol^{-1}) is small, compared to that of a covalent bond, several contacts between host and guest are required for structuring of complexes.

Spherand (**23**) binds sodium better over potassium by a factor as high as $>10^{10}$, whereas cryptaspherand (**37**) follows the same pattern by a factor of 13000. The somewhat larger more flexible hosts however, cryptaspherand (**38**) and hemispherand (**39**), bind potassium better over sodium by factors of 11000 and 2000 respectively. A similar but less strictly adhered to sequence than that of preorganisation, is observed for classes of hosts with decreasing order of ability to select between the alkali metal ion guest:

spherands > cryptaspherands ~ cryptands > hemispherands > corands > podands

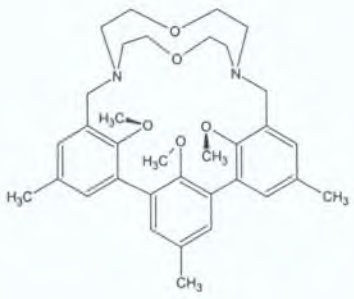

(37)

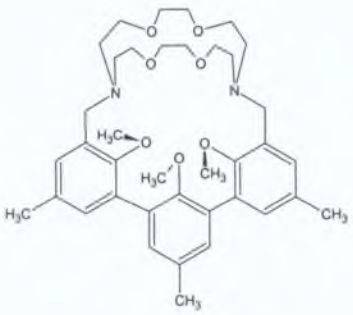

(38)

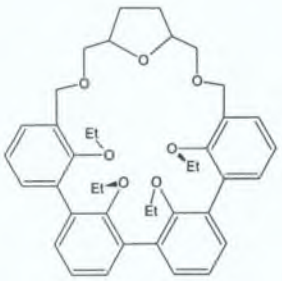

(39)

1.17 Substitution Effects in Macrocyclic Hosts

Substitution of sulphur atoms for oxygen in the simple crown ether leads to thiacrowns, with the presence of nitrogen atoms in the ring giving azacrowns (2 nitrogen equals diazacrown etc.). The behaviour of [18]crown-6 is greatly altered by such substitutions. The introduction of sulphur slightly expands the size of the macroring, and its soft donor qualities enhances the rings affinity for transition metals, while reducing the attraction for alkali and alkaline earth metals.

Substitution of appropriate heterocycles for CH_2OCH_2 units in [18]crown-6 leads to hosts with powerful binding abilities. Take for example the following hosts (**41**) – (**44**), which at least equal or better [18]crown-6 in K^+ or RNH_3^+ binding. These units place heteroatoms with unshared electron pairs in positions to bind metal or alkylammonium ions.

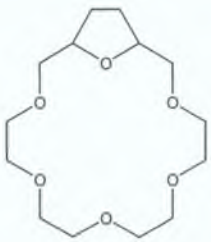

(40)

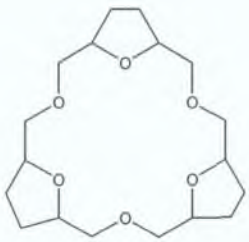

(41)

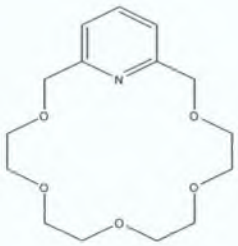

(42)

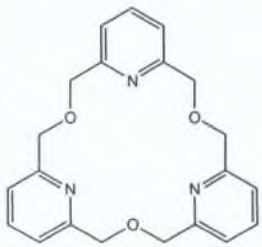

(43)

Host	K_a for NH_4^+, [mol^{-1}]
(**12**) ([18]crown-6)	7.5×10^5
(**40**)	1.1×10^6
(**42**)	1.4×10^6

The presence of pyridine (**42**) and (**43**) as a constituent renders the crown more rigid and basic. The fact that pyrido nitrogens are better hydrogen bonding sites than the ether oxygens was confirmed by comparisons of the free energies of association of a series of hosts with $(CH_3)_3CNH_3^+SCN^-$ [**137**].

Complexation strength is not notably altered with the introduction of a single furan ring into the macrocycle (**44**), even though in this case oxygen is part of an aromatic heterocycle. This is not surprising considering the oxygen is still effectively positioned for successful binding. Significantly different however is the position of oxygen in a phenol-substituted crown (**45**), with the binding power dependent upon pH, since ionisation of the phenolic hydroxyl may readily occur in a basic environment. Although the size of cavity formed by the oxygen array appears smaller than in the case of [18]crown-6, effective binding can still occur as phenol can tilt out of the plane. Apart from rigidifying the crown, binding is diminished nearly 60-fold when a benzo group is fused to [18]crown-6 (**46**). This is due in part to delocalisation of oxygen electrons into the benzo group and to the electron withdrawing nature of the benzo group relative to an alkyl group, which reduces the donicity of the attached oxygen atoms.

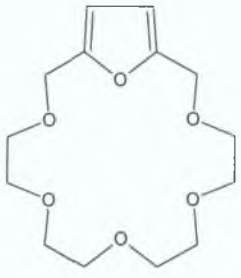

(**44**)

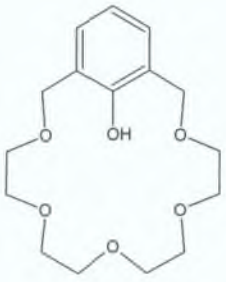

(**45**)

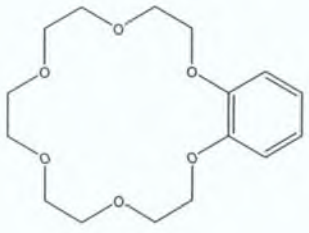

(**46**)

Each of the three subsequent hosts (**48**), (**49**) and (**50**), contains three heterocyclic subunits which will somewhat rigidify the typical crown arrangement. All three hosts display tripod type binding of $Me_3CNH_3^+$. The trifurano host (**48**) binds this guest less strongly than the other hosts in this series. The partial positive charge on each of the three furano oxygens certainly weakens its binding potential. When however, the three furano units are reduced to tetrahydrofuran units as in (**49**), the binding energy more than doubles.

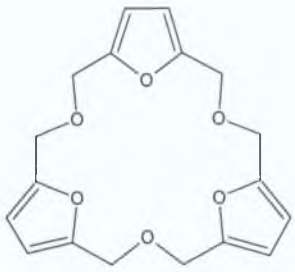

(48)

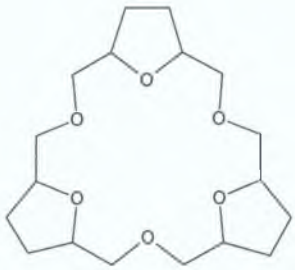

(41)

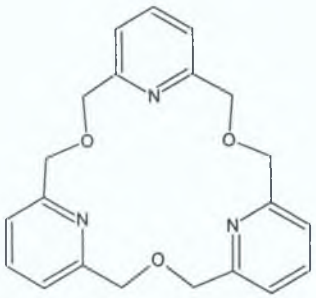

(43)

Host	-ΔG° for $(CH_3)_3CNH_3^+SCN^-$, [kcal mol^{-1}]
(**48**)	4.1
(**41**)	9.0
(**43**)	8.8

An interesting study compared the following series with their interactions with the guest $(CH_3)_3CNH_3^+SCN^-$, by measuring the -ΔG° values [kJ mol^{-1}] at ~25°C in $CDCl_3$ saturated with D_2O [**137**]. Unlike metal salts, this guest interacts with the less lipophilic hosts such as [18]crown-6 to form complexes distributed mainly in the $CDCl_3$ layer, allowing ^{1}H-NMR determinations of complexes possible. The open-chain polyether (**49**) differs by only two hydrogen atoms and a single C-C bond in comparison to cyclic (**50**), but the difference in binding free energies amounts to 6 kcal mol^{-1}. This difference can be attributed to the organisation of binding sites in each host. While the binding sites in (**49**) are collected, they are both collected and partially organised for a tripod-type of binding in (**50**) (which the crown ethers seem to adopt when binding to $(CH_3)_3CNH_3^+SCN^-$; see (**14**)). The structural changes in (**51**) and (**52**), mainly the lack of one oxygen, reduce the binding energy by 18.84 kJ mol^{-1} and 17.17 kcal mol^{-1} respectively, from that of (**50**). This considerable reduction in binding power can be explained if one takes into account the fact that the ammonium ion complex probably interacts with both sets of oxygen's in (**50**). The ammonium ion is deprived of one oxygen binding site in the alternate arrangement in the cases of hosts (**51**) and (**52**).

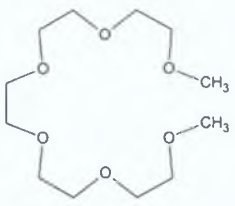

(**49**)

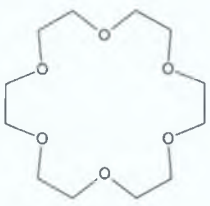

(**50**)

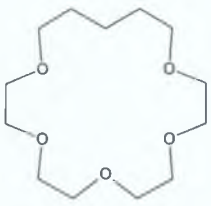

(**51**)

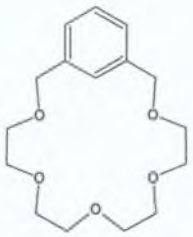

(**52**)

Host	-ΔG° for $(CH_3)_3CNH_3^+SCN^-$, [kcal mol^{-1}]
(**49**)	2.9
(**50**)	8.9
(**51**)	4.4
(**52**)	4.8

Analogous arrays of adapted cryptands are known, with benzyl groups, chiral bi-naphthyl bridges, and pyridyl units, among others, incorporated as subunits of the macroring. Chromionophores (**53**) and (**54**) have been synthesised, and display high Li^+ selectivity. In particular they give no measurable response to solutions containing molar concentrations of the biologically important ions, Na^+, K^+, Mg^{2+}, or Ca^{2+}. These cryptands are for this reason well adapted for use in biological sensing of Li^+ [**138**].

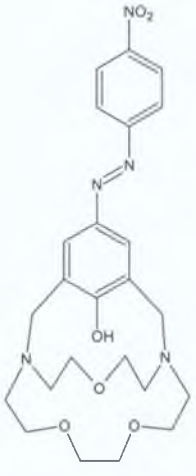

(**53**)

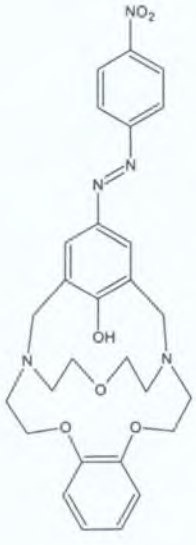

(**54**)

The solid state structures of the following aza-cryptands (**55**) - (**57**) when complexed to Li^+ have been solved and reveal that the complexes are of the cryptate type with

the cation located inside the central cavity and penta-coordinated with short Li-N distances [**139**].

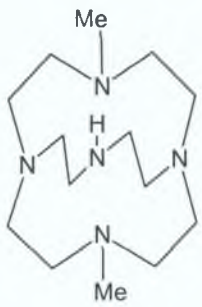

(**55**)

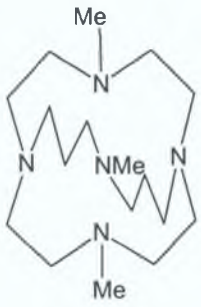

(**56**)

(**57**)

The complexation of Ag^+ ions has been studied in order to investigate the effect of soft metal cations on several types of cryptand. This ion forms very stable complexes with many cryptand ligands. Of interest is how the change in number of nitrogen or oxygen atoms in the ligand alters the stability of the complex.

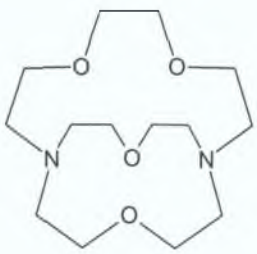

(**58**)

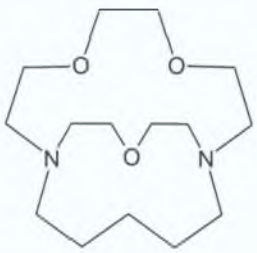

(**59**)

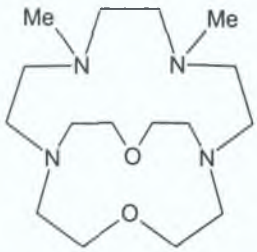

(**60**)

For example the following hosts (**58**) - (**60**) bind Ag^+ ions with log K_s values of 8.52, 6.0 and 7.69 respectively. The absence of one oxygen in cryptand (**59**) decreases the binding power significantly. The replacement also of two of the ether oxygens with two tertiary nitrogens (**60**) improves on the previously discussed host (**59**), but still does not quite match the binding of the first host in the row (**58**) [**140**].

The two types of cryptands pictured below (**61**) and (**62**) exhibit interesting features on binding to calcium and strontium ions. The 2-hydroxypropylene series (**62**) of cryptands form more stable complexes with the alkaline earth cations (with the exception of Ba^{2+}) than do the propene (**61**) analogues. This can be attributed to the fact that the 2-hydroxy-series (**62**) have more binding sites than do the unsubstituted cryptand series (**61**), with the oxygen atoms of the hydroxy groups participating in binding. These additional binding sites are important with respect to the divalent cations, which have a high coordination number (hydration number of eight). It can be seen from the table below that the monovalent cations do not display a similar

increase in stability, because they do not require as many binding sites due to their lower hydration number of 6.

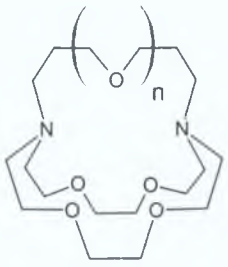

(a) n=1
(b) n=2
(c) n=3

(61)

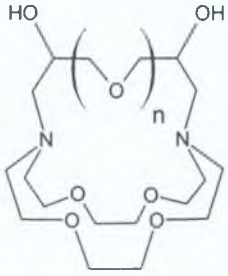

(a) n=1
(b) n=2
(c) n=3

(62)

Ligand	*log* K_s, Ca^{2+}	*log* K_s, Na^{+}	*log* K_s, Sr^{2+}	*log* K_s, K^{+}	*log* K_s, Ba^{2+}
(**61**) a	5.20	6.13	5.81	5.11	5.05
(**62**) a	**5.92**	4.01	**5.95**	3.4	3.63
(**61**) b	3.75	4.36	4.81	5.47	7.53
(**62**) b	**6.64**	5.75	**7.21**	5.13	8.62
(**61**) c	4.12	4.65	6.53	5.15	6.64
(**62**) c	**8.73**	5.15	**8.94**	5.63	8.43

In conclusion, it can be seen from these results that apparently small structural changes in the substitution of host molecules can lead to dramatic changes in guest selectivity or the magnitude of binding constants.

1.18 Literature Survey- Introduction

Calixarenes are very similar in structure to spherands, the difference being the length of the spacer connecting the phenyl units. This implies that calixarenes should be good hosts for complexation. Reasons why they are attractive as hosts include their ready availability, with multigram quantities producible on a laboratory scale in a relatively simple manner from cheap starting materials. This makes them different from many of the other synthetic macrocycles, and makes them particularly attractive as potential hosts. It was in the 1970's with the increasing interest in "enzyme mimics" that David Gutsche was inspired to investigate calixarenes as potential candidates for molecular baskets.

The idea of enzyme mimic building is to construct a receptor for a substrate molecule and equip the receptor with functional groups that are appropriate for interacting in some manner with the substrate molecule. Gutsche introduced the name calixarenes, because of the beaker-like shape of the most stable conformation of the tetramer (calix means beaker in Greek and Latin). This bowl-like or cone conformation provides a cavity for possible guest inclusion in calixarene molecules. Gutsche regarded calixarenes as cavity-containing substances and therefore appropriate as enzyme mimics, more so than crown ethers because in their simplest form they are mere loops rather than cavities. Also in comparison to the cyclodextrins, calixarenes are synthetic products, and more easily prepared in the laboratory than the aforementioned natural products.

As mentioned previously one of the most interesting features of calixarenes is their ability to act as molecular baskets, that is their ability to interact with small molecules and ions reversibly. Fine-tuning of selectivities is possible by varying the nature, length and position of the alkoxy groups. Tetraesters in the cone conformation are selective for Na^+, while other conformations, invariably the partial cone, favour K^+ [**141**]. In contrast to ester and ketone derivatives, amides are stronger complexing agents for alkaline earth metal ions. While however, tertiary amides bind alkali metal ions considerably more strongly than esters, they do so at the cost of selectivity.

1.19 Calixarenes as Hosts – Binding Metal Ions

The following calix[4]arenes were synthesised and found to show remarkable selectivity among alkali and alkaline earth metal ions for Ca^{2+} and Sr^{2+} which are quantitatively complexed at pH 6-7 [**142**]. The affinity of the ligands (**63**), (**64**) and (**65**) for Ca^{2+} and Sr^{2+} were evaluated from the percentages of free metal ion in solution as a function of pH and led to the following order:

(**65**) > (**63**) > (**64**) for Ca^{2+} and

(**63**) ≈ (**65**) > (**64**) for Sr^{2+}

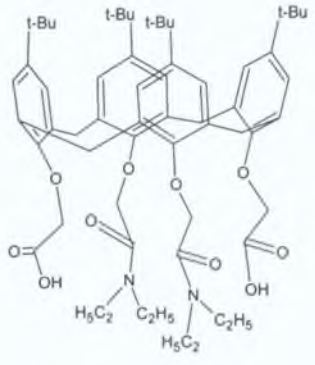

(**63**)

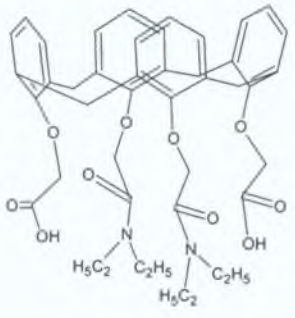

(**64**)

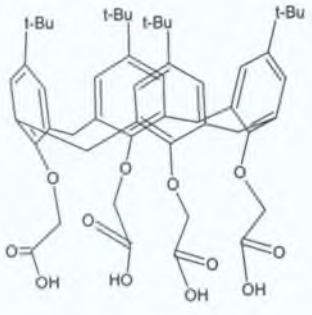

(**65**)

The spectroscopic detection of metal ions is important in terms of analytical chemistry and in the molecular design of ion sensors and signal transduction. The metal-induced coloration process serves as a transducer of the chemical signal (i.e. metal concentrations) to the physical signal (i.e. spectral parameters), which has been well represented by the family of chromogenic crown ethers. Calixarenes are also capable of selective metal binding if the OH groups on the lower rim are appropriately modified.

1.19.1 Calixarenes as Chromionophores

Synthetic chromoionophores that give rise to specific colour changes on complexation with alkali and alkaline earth cations have been utilised as spectrophotometric reagents for the detection of cations. Calixarenes are useful building blocks in the design of artificial receptors [**143**, **144**]. Kubo and co-workers [**145**] synthesised (**66**), with an absorbance maximum at 609nm. However the addition of $Ca(SCN)_2 4H_2O$ to this compound in solution causes a large bathochromic shift with an increase in absorption intensity. A new absorption band in the NIR

region at 719nm was observed at a ratio of $[Ca^{2+}]$ to [**66**] of 100: 1. The addition of NaSCN, KSCN or $Mg(ClO_4)_2$ however, caused only minor changes in the absorption spectra, suggesting a significant selectivity of (**66**) for Ca^{2+}. The authors also used IR spectroscopy to discern the co-ordination structure, with the frequency of both C=O (ester) and C=O (quinone) absorption's for the Ca^{2+}·(**66**) complex lower than those of the free ligand by 34-35 cm^{-1}. This suggests that (**66**) forms an encapsulated complex with Ca^{2+} on the lower rim of the calixarene backbone, and it is also shown to be more sensitive to Ca^{2+} than to Na^{+}, K^{+}, Mg^{2+}.

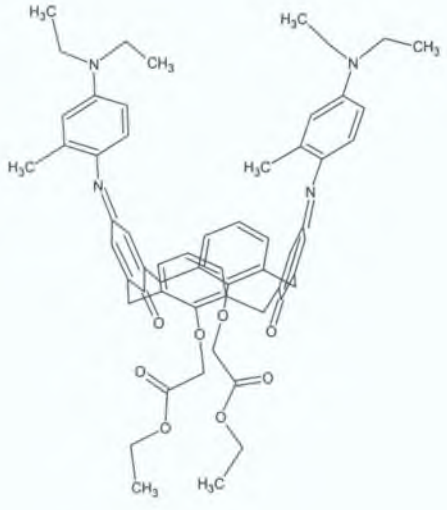

(**66**)

In an earlier publication Kubo [**146**] describes the synthesis of a chromoionophore having indoaniline and calix[4]arene segments (**67**), the ethylacetate derivative of which shows a high selectivity for Na^{+}. The addition of NaSCN (30 equiv.) to this tetraester in 99% ethanol solution caused a bathochromic shift of 42nm with an increase in absorption intensity.

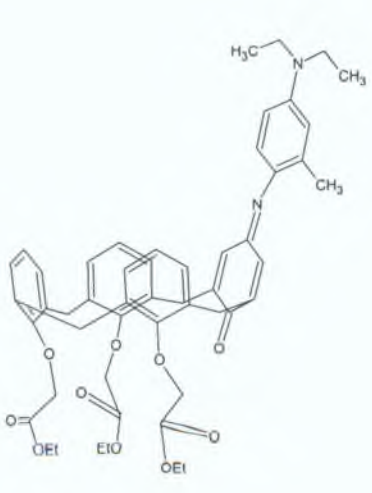

(**67**)

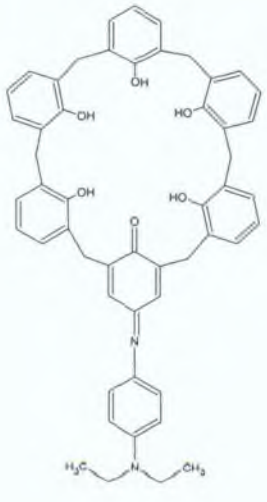

(**68**)

The authors also describe the synthesis of a similarly derived hexamer (**68**) (with one indoaniline unit bridging five phenol units). This calix[6]arene has a visible absorption band with λ_{max} = 665nm (99% ethanol solution). The addition of base, 1,8-diazobicyclo[5.4.0]undec-7-ene (DBU) caused a hypsochromic shift of 37nm, which was attributed to the removal of intramolecular hydrogen bonding between the quinone carbonyl of indoaniline and the adjacent phenolic hydroxy groups. This calix[6]arene was then investigated as a chromionophore for the detection of the uranyl ion (UO_2^{2+}). The addition of UO_2^{2+} to calixarene (**68**) in solution causes a large bathochromic shift with an increase in absorption intensity. At a ratio of host: guest, 1:1000 a new band appeared at 687nm. The addition of other metal ions such as Li^+, Na^+, K^+, Cs^+, Sr^{2+}, Ba^{2+} caused little or no change in the host's absorption spectrum, indicating a significant selectivity for the uranyl ion by this calix[6]arene.

The bridged calixarene (**69**) has been examined as an ion carrier for electrochemical K^+ sensors. Modification of this structure to give the ionisable chromoionophore (**70**) appeared as a promising K^+ selective optical-fibre based sensor. The modified structures (**70**) a and b extracted K^+ ions from aqueous solution into chloroform with a colour change associated with the formation of the corresponding salts. This data shows how (**70**) a and b are both highly selective chromoionophores for K^+ in the presence of the other physiologically important ions, Na^+, Mg^{2+}, Ca^{2+}.

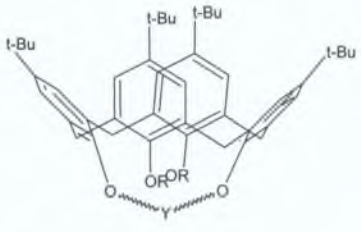

$Y=OCH_2[CH_2OCH_2]_3CH_2O$

(**69**)

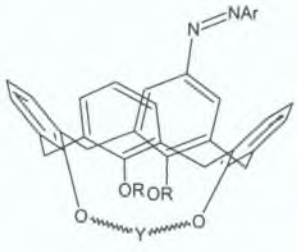

$Y=OCH_2[CH_2OCH_2]_3CH_2O$

(**70**)

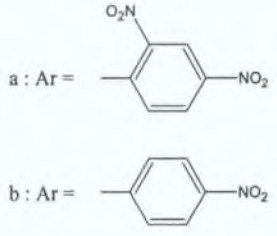

The following hosts (**71**) - (**73**) have U.V. maxima at 270nm (attributed to π - π^* transitions occurring in the aromatic rings of the calixarenes) and little change is seen in their absorption spectra upon the addition of various metal ions (Na^+, K^+, Rb^+, Cs^+, Ag^+) in methanol solution. The fluorescence spectra of (**71**) and (**72**) in methanol show a maximum at 310nm (λ_{exc}= 270nm). Even though the addition of metal ions caused only weak effects on the absorption spectra of these hosts, significant changes in the emission intensity and wavelength maxima of the

fluorescence bands of (**71**) and (**72**) were observed after the addition of metal ions to these hosts in solution. The fluorescence intensity of the alkali metal ion complexes follow a similar trend for hosts (**71**) and (**72**), that is decreasing with increasing atomic number from Na^+ to Cs^+. Such changes have been attributed to cation - π interactions between the metal ion and two of the aromatic rings of the calixarene pointing towards it.

Calixarene (**73**) was used as a control to evaluate the effect on the photophysics due to the phenolic oxygens involved in metal ion binding, which in the cone conformation does not allow any possible cation - π interactions. Even in the presence of a large excess of cation, no significant changes were observed in the luminescence spectra of (**73**), therefore the involvement of the phenolic oxygens in binding does not alter the fluorescence properties, further proving the cation - π interaction theory of the authors [**147**].

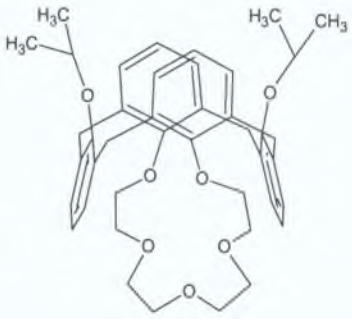

(**71**)

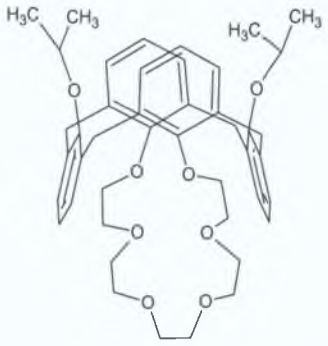

(**72**)

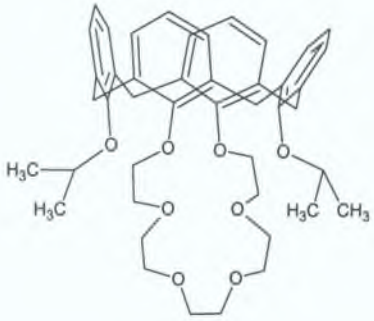

(**73**)

Chawla and Srinivas [**148**] report how their success in calix[8]arene-cerium(IV) promoted biomimetic hydroxylation of simple phenols [**149**] prompted them to obtain other calix[8]arene derivatives with selectively functionalised hydroxyl groups and chromophores. They report the first examples of chromogenic calix[8]arenes in which the opposite phenyl rings are bridged by the biphenyl bisazo linkage. (**74**) shows a strong absorption band at 382nm, and when this solution is made alkaline (with NaOH), the solution changed from pale yellow to red with a bathochromic shift of 98nm, with a new peak appearing at 433nm. (**74**)b, (**74**)c, and (**74**)d have strong UV absorption bands at 329nm, 342nm and 334nm respectively, however no such bathochromic shifts are observed in their UV spectra under alkaline conditions.

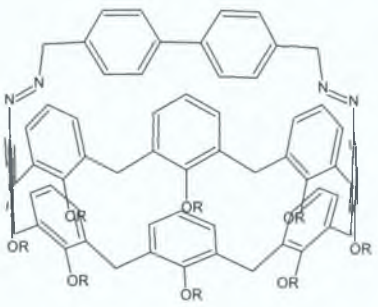

a: R = H , b: R = CH_3,
c: R = $COCH_3$, d : R = COPh

(**74**)

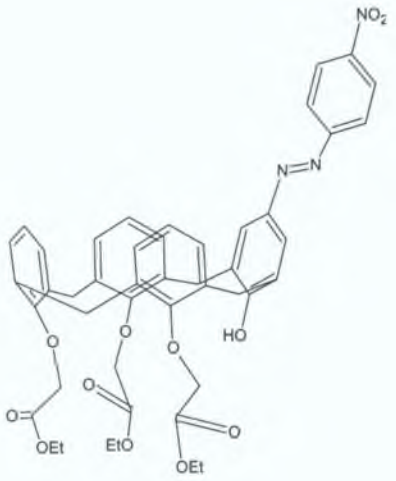

(**75**)

Shinkai et al. describe how their synthesis of (**75**), which has a 4-(4-nitrophenol) azophenol unit [**150**, **151**], and showed a new absorption maximum at *ca*. 600nm upon metal binding, with a high Li^+ selectivity.

1.19.2 Fluorogenic Calixarenes

This work then inspired the authors to design a fluorogenic calixarene tetramer, whereby a trace amount of the metal ion under investigation could be more sensitively detected than by an absorption method of spectroscopy. The fluorogenic calixarene (**76**) prepared has a benzothiazole unit as the chosen fluorophore. This compound has an absorption maximum at 327nm in chloroform, which was unaffected by the addition of triethylamine (up to 1,000-fold excess), implying in chloroform the basicity of triethylamine is not strong enough to dissociate the OH groups of the calixarene. Alkali-metal perchlorates (Li^+, Na^+, K^+, Rb^+ and Cs^+) were added as salts to solutions of calixarene (**76**) in chloroform, and in the absence of triethylamine, the metal ions were not extracted and the absorption spectra hardly affected. The presence of triethylamine however, allowed the extraction of Li^+ which in turn changed the absorption maximum to 356nm. This effect was not duplicated by the other ions tested, presenting (**76**) as a Li^+ -selective chromogenic calix[4]arene.

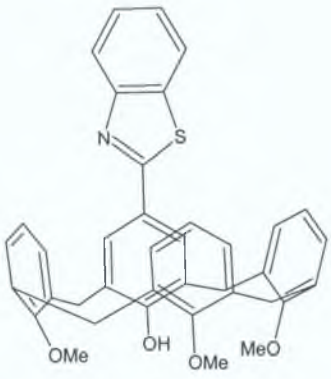

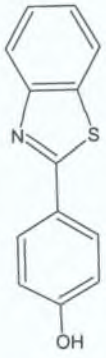

(76) **(77)**

Such a Li^+ induced spectral change was not observed by the authors for reference compound (**77**), indicating the importance of the ionophoric cavity constructed on the lower rim. In chloroform (**76**) gave a fluorescence maximum at 391nm when excited at 332nm, and showed no change in spectrum upon addition of triethylamine. This band almost disappeared and a new one emerged at 422nm in the presence of $LiClO_4$ and triethylamine, which was not induced by the other alkali perchlorates listed previously [**152**].

Calixarene derivatives including ionophoric functional groups linked by the phenolic oxygens express some excellent properties as receptors for metal ions, due to stable complex formation and size-related selectivity. These properties prompted Diamond et al. [**153**] to prepare fluorescent calixarenes, having an anthracene moiety with the specific ability to complex alkali metal ions. Anthracene was chosen as the fluorophore due to its fluorescence efficiency. (**78**) was synthesised as a tetraester, with four anthracene units appended to the lower rim, as shown below.

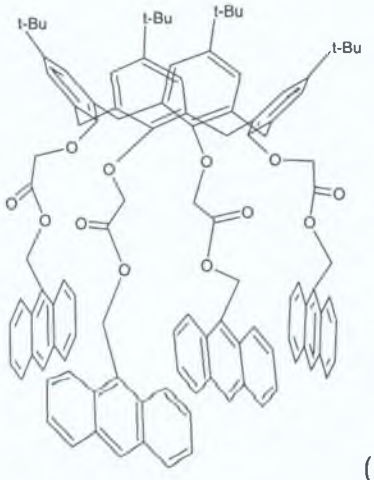

(78)

Monomer emission with a fluorescence maximum at 418nm is observed when the above molecule (**78**) is excited at 388nm. After the addition of Li^+ or Na^+ salts, the fluorescence intensity of the full spectrum decreases dramatically with increasing salt concentration. While the addition of K^+ causes the maximum at 418nm to decrease with increasing salt concentration, an increase at 443nm is observed. The interesting optical responses according to the authors, to K^+, Li^+ and Na^+ could form the basis of an optical sensor for the determination of these ions.

Dual emission, resulting from the excimer (480nm) and monomer (390nm) pyrene species is characteristic of the fluorescence spectrum of the free ligand (**79**) in MeOH-THF (15:1 v/v) solution. In the free ligand, excimer emission dominates with the intensity ratio of excimer to monomer emission about 4. The addition of NaSCN however, reverses this trend and in the concentration ranges studied, excimer emission intensity decreases 9-fold with monomer emission intensity increasing 3.7-fold. Other alkali metal ions were tested in the presence of Na^+ (K^+, Li^+, Rb^+, Cs^+) and gave rise to only slight changes (only 1% in the case of the latter three ions). These results indicate the suitability of (**79**) as a fluorescent sensor for selective Na^+ detection in non-aqueous solution.

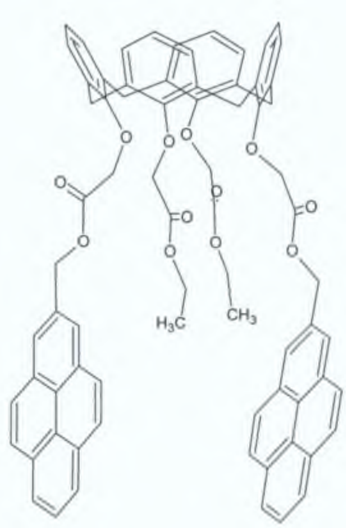

(**79**)

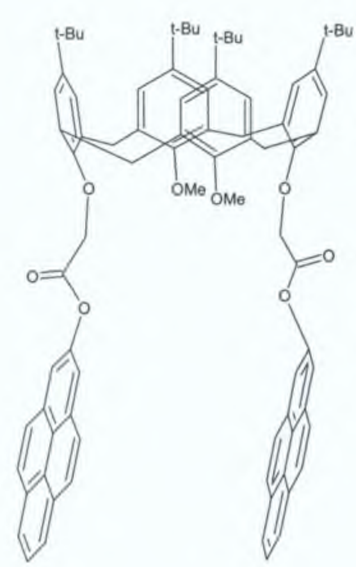

(**80**)

Shinkai et al. [**154**] found the ratio of monomer vs. intramolecular excimer emission intensity of calixarene (**80**) is affected by solvent polarity and metal ion addition. Monomer emission (380nm) increases with increasing solvent polarity, with excimer emission (480nm) decreasing. In methanol monomer emission dominates, while the

two emissive intensities are approximately equal in propan-2-ol, whereas in hexane excimer emission dominates. The authors also found that excimer emission decreases with the addition of metal ions, like in the previous example mentioned. This calixarene forms 1:1 complexes with Na^+, K^+ and Li^+ (log K_{ass} /dm^3 mol^{-1}; 5.34, 4.06 and 4.73 respectively).

The proximity of the nitrophenol group in the free ligand of (**81**) causes intramolecular quenching between the excited pyrene fluorophore and the nitrobenzene quencher. The presence of the sodium ion interrupts this proximity and an increase in the signal is observed upon complexation [**155**]. In the free ligand the ester groups can freely rotate and probably allow interaction of the pyrene ring and nitrobenzene quencher. However after the addition of Na^+ ions the carbonyl groups must turn inward to bind with the metal in the ionophoric cavity. The authors claim this metal-induced reorientation dramatically reduces the collisional probability between the pyrene fluorophore and nitrobenzene quencher, thus increasing the fluorescence intensity. The fact that the chemical shifts of the protons of the nitrobenzene in the free ligand are at 6.8ppm and 7.6ppm would suggest an effect of the ring current from the pyrene system. This is further demonstrated by the lower magnetic field shifts of these protons in the Na-complex, 7.6ppm and 8.3ppm respectively.

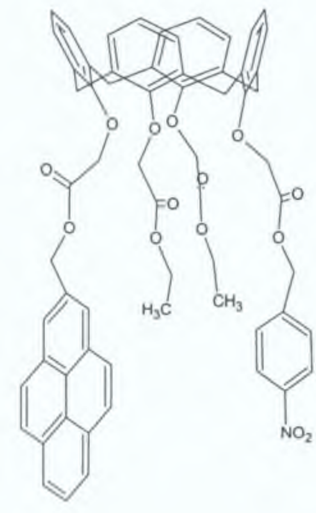

(**81**)

For calixarenes ion selectivity depends on ring size and conformation, whereas successful interaction with guest molecules is dependent on the length of the pendant chains. In the cone conformation of the tetramer, a cavity is present which can host neutral molecules of complementary size. For various water-soluble

calixarenes unspecific complexation of aromatic hydrocarbons has been described, however some selectivity is achieved with varying ring size.

1.20 Calixarenes as Hosts – Molecular Binding

Many calixarenes form complexes in the solid state, amongst them some of the simple phenol derivatives, e.g., p-tert-butyl-calix[4]arene form inclusion compounds with such solvent molecules as chloroform [**141**], acetone, acetonitrile, methanol water and arenes(benzene, anisole, pyridine, tetraline, toluene, xylene) [**143**]. Most of them have a well-defined host-guest stoichiometry (usually 1:1), and the complexation behaviour seems to be determined by the conformational mobility of the calix and by the nature of the R group present at the upper rim.

Host	Recrystallisation solvent mixture (50:50 v/v)	Ratio of Included aromatic guest
(**1a**) R = Bu^t	p-xylene : m-xylene	80 : 20
	p-xylene : o-xylene	100 : 0
	p-xylene : toluene	90 : 10
	p-xylene : anisole	75 : 25
	Anisole : toluene	80 : 20
	Benzene : p-xylene	75 : 25
	Benzene : anisole	90 : 10
(**1a**) R = *t*-octyl	Benzene : toluene	50 : 50
	p-xylene : o-xylene	45: 55
	p-xylene : m-xylene	55 : 45

Table 1 *Guest selectivity properties of p-t-butylcalix[4]arene ((1), R = Bu^t) and p-octylcalix[4]arene ((1), R = t-octyl) towards aromatic molecules in the crystalline state.*

Table 1 reports the guest selectivity properties of these macrocycles towards aromatic molecules, established by competitive crystallisation experiments in the presence of equal volumes of two competing guests [**156,157**]. The results show high

selectivity for host *p*-t-butylcalix[4]arene ((1), R = Bu^t). Benzene is the preferred guest included in the cavity of this macrocycle, although it is remarkable how much shape-selective discrimination is observed between *p*-xylene and the *ortho* and *meta* isomers. For the xylene isomers a similar pattern is shown by *p-i*-propylcalix[4]arene ((1), R = Pr^i), however the p-octylcalix[4]arene ((1), R = *t*-octyl) shows very little selectivity and it is unable to distinguish between the various xylene isomers. It has been discovered if alkyl groups are removed from the upper rim of calix[4]arenes their ability to form intramolecular inclusion complexes with aromatic guest species drops dramatically and no such complexes have been observed so far with calix[4]arene, although it exists in the cone conformation [**158**].

Evidence reported in the mid-1990's suggests that calixarenes [**159**, **160**] and oxacalixarene derivatives complex tetraalkylammonium salts in organic media. N-methylpyridinium cation is bound to conformationally mobile calix[4]-, calix[6]- and calix[8]arene methoxy derivatives in a 10: 1 mixture of $CDCl_3$:CD_3CN, whereas alkyltrimethylammonium cations show a more marked preference for calix[6]arene derivatives.

Gutsche and co-workers report the complexation of aliphatic amines by alkylcalix[4]arenes in CD_3CN, examples of the complexation of aromatic ammonium cations have appeared. However evidence for complexation of organic molecules in organic solvents is rare. Several reasons may be responsible for the fact that complexation of neutral organic molecules by calix[4]arenes in solution has not been very successful. The cavity is too small to engulf the guest and the stabilizing forces are not strong enough to compete effectively with the solvent. Moreover, the cavity of the parent calix[4]arene is not rigid and a continuous ring inversion process occurs in solution. This may be overcome by immobilisation of the calixarene in a cone conformation by the introduction of substituents at the lower rim. This approach is based on the use of calix[4]arenes as a lipophilic molecular platform for building molecular receptors for organic molecules, on which binding sites can be organised, introduced by selective functionalisation.

Calix[4]arenes containing two fluorescent pyrene moieties on the lower rim were synthesised: the recognition site was introduced by skilful arrangement of hydrogen bond acceptors. (**82**)a and (**82**)b have etherial and esterial oxygens as hydrogen-

bond acceptors, and two pyrenes as fluorescent reporters, which could deliver a fluorescence signal change upon binding, by means of hydrogen bonds, of guest molecules. Upon excitation, monomer pyrene emission is observed at 380nm and excimer pyrene at 480nm. Upon inclusion of TFA (trifluoroacetic acid) monomer emission increases while emission of the excimer decreases. The addition however, of ethyl-TFA shows no effect on the fluorescence of either calixarene displaying a very specific interaction for TFA, through hydrogen bonds, which will interfere with the interaction of the two pyrene moieties. This paper [**161**] describes how upon inclusion of a guest molecule, the ratio of monomer to excimer emission changed specifically and sensitively.

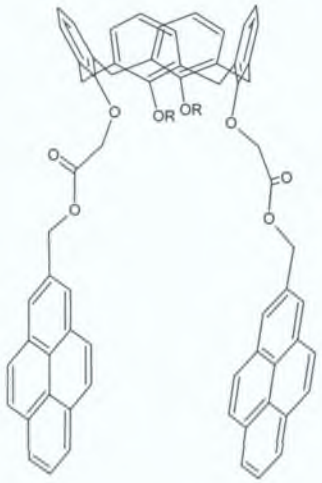

a: R = Me
b: R = CH_2CH_2Me

(82)

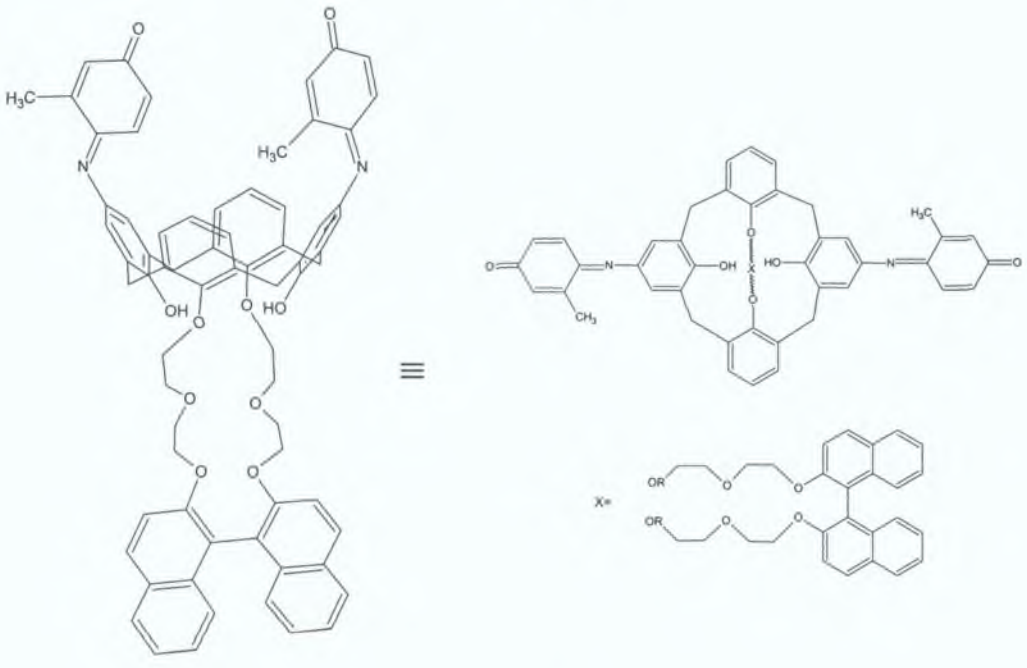

(83)

Kubo and co-workers' interest in synthetic chromogenic receptors, which deliver a specific colour change on selective complexation with guest species, led to the development and subsequent synthesis of a chromogenic bi-naphthyl-derived calix[4]crown derivative (see (**83**)), in which the steric or electrostatic effects of the 1,1-binaphthyl unit could be useful for the molecular recognition of amines. Upon addition of Bu^tNH_2, the solution of this calixarene turns from red (absorbance maximum at 512.5nm) to blue with a bathochromic shift of 148nm. They carried out similar measurements for other butylamines and a marked difference between their respective association constants was observed, which the authors attributed to the shape of the butyl substituents. The tetramer (**83**) interacts with butylamines in the following order: -

$$Bu^t >> Bu^s > Bu^i > Bu^n.$$

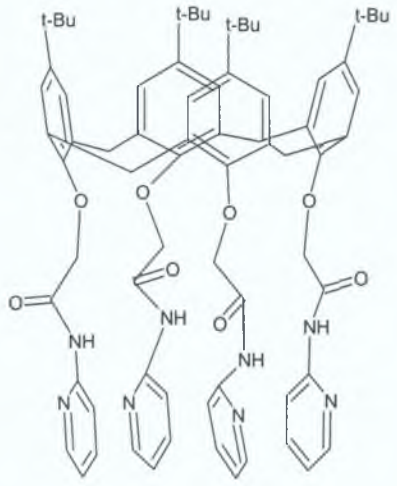

(**84**)

(**84**) has a hydrogen bonding receptor site next to its ionophoric site, with NMR data implying communication between two sites. This is supported by the fact that in (**84**) the δ_{NH} (-50°C) appears at 10.21ppm whereas the δ_{NH} for the monomeric species is found at 9.79ppm. This data suggests that the NH protons in (**84**) are subject to intramolecular hydrogen bonding, since this causes OH and NH protons to shift to lower magnetic field. New signals were observed after the addition of sodium perchlorate at -50°C for the (**84**).Na^+ complex, resulting in an upfield shift suggesting a partial disruption in the intramolecular hydrogen bonding.

When a guest molecule is added (γ-butyrolactam – a specific guest for (**84**)), only the NH signal for (**84**).Na^+ moves to a lower magnetic field, indicating intermolecular

hydrogen bonding with the guest amide. This suggests that complexation with sodium induces an 'open' receptor state, on what was in its free state a 'closed' form. It is known that in calix[4]aryl tetraesters and tetraamides, the four carbonyls are turned outward to reduce electrostatic repulsion among carbonyl oxygens, whereas Na^+ complexation induces the carbonyls to point inward in order to bond the metal ion. In (**84**) movement of the carbonyls to bind Na^+ disrupts the intramolecular hydrogen bonding and then facilitates binding of the guest molecule via intermolecular hydrogen bonds.

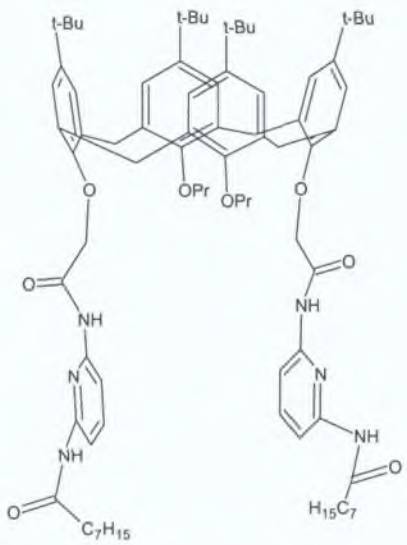

(**85**)

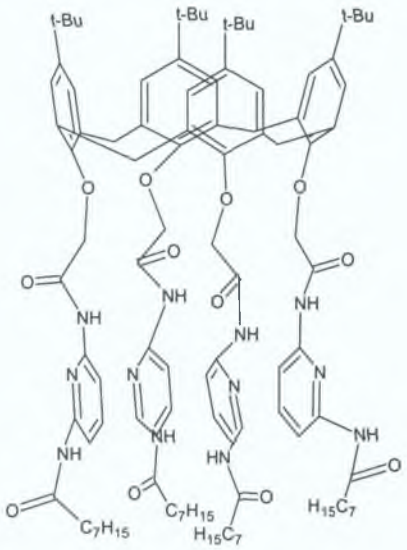

(**86**)

The calixarene (**85**) (with NH signals at 9.03ppm and 10.07ppm) can be mixed with guest (**87**) in solution, and no change in the ^{1}H-NMR signals are observed. The lowfield signals of the NH protons in (**85**) are due to strong intramolecular hydrogen bonds, which are not affected by the presence of guest (**87**). When however, sodium ions are introduced to this solution, it complexes with (**85**) and a large highfield shift in the signal corresponding to the calixarene NH is observed, to 8.31ppm and 9.14ppm respectively. This is due to disruption of intramolecular H-bonds in the calixarene, to facilitate the metal ion co-ordination, which then allows intermolecular hydrogen bonding between the calixarene host and the guest (**87**) (dimethyl (a)/ dioctylbarbituric acid (b)). The binding sites in (**86**) are exposed after the addition of Na+ and create oligomeric clusters with guest (**87**a).

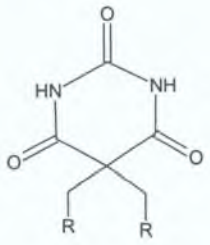

(a): R = H

(b): R = C_7H_{15}

(**87**)

In order to allow a deeper understanding of the basic forces involved in host-guest recognition processes in a solvent where most biological processes occur, water-soluble macrocycles, as hosts are important. Arena and Casnati [**162**] have shown that their water-soluble derivatives of calixarenes, which often after functionalisation are used for the recognition of neutral molecules, metal ions and anions, recognise the trimethyl-ammonium group or the benzene ring of aromatic cations. Two water-soluble calix[4]arenes (**89**) and (**90**) were studied at neutral pH by ^{1}H-NMR spectroscopy in regard to their complexation of *N*,*N*,*N*,-trimethylanilinium (**TMA**), benzyltrimethylammonium (**BTMA**) and *p*-nitro-benzyltrimethylammonium (**BTMAN**) cations.

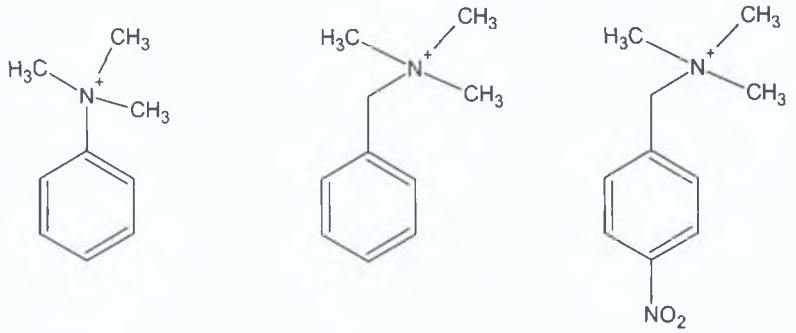

TMA **BTMA** **BTMAN**

(**88**) specifically binds the (**TMA**)-$\underline{N^+(CH_3)_3}$ group, whereas (**89**) recognises only the aromatic ring of (**TMA**), both in contrast to the conformationally mobile (**90**) which binds both the phenyl and ammonium methyl moieties, but unselectively [**163**]. The introduction of a spacer between the charged polar group and the aromatic residue (**BTMA**) or an electron-withdrawing group on the aromatic moiety (**BTMAN**) does not alter the selectivity for (**88**), but in the case of (**89**), it selectively recognises the $N^+(CH_3)_3$ group of (**BTMAN**), but complexes (**BTMA**) both by the $N^+(CH_3)_3$ group and the aromatic moiety, thereby unselectively.

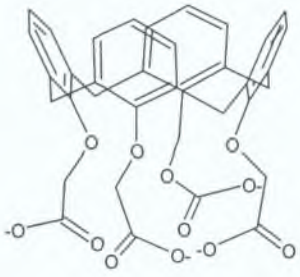

(88)

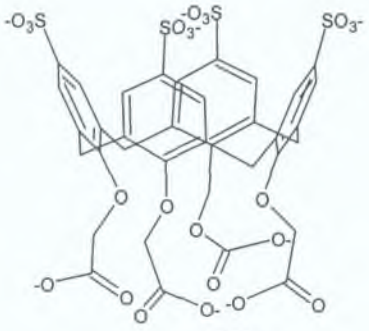

(89)

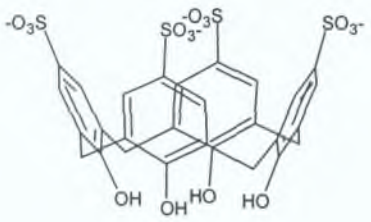

(90)

The hosts (**88**), (**89**) and (**90**) also exhibited different behaviours upon inclusion of ethanol in aqueous solution [**164**]. Ethanol is included into the hydrophobic cavity of the water-soluble calixarenes (**89**) and (**90**), with the alkyl residue pointing in towards the cavity, leaving the hydroxyl group facing the bulk solvent. In contrast no inclusion is detected for (**88**), which the authors attribute to the sulfonate groups acting as anchoring points.

The summation of the aforementioned data, allowed the authors to establish the crucial role played by the sulfonate groups on the upper rim, in assisting the guest inclusion in the calixarene apolar cavity. This prompted them to extend their studies to the use of L-α-amino acids as guests. The complexation of the -α-amino acids transpires by insertion of the aromatic or aliphatic apolar (R) group into the calixarene cavity, which allows the charged group of the amino acids to be exposed to the polar medium. The amino acid guests examined included L-Ala, L-Val, L-Leu (R-aliphatic), L-Phe, L-Tyr, L-His, L-Trp (R-aromatic). Upon inclusion the aromatic protons of the guest experienced a large upfield shift in comparison with the free guest, with L-Ala not undergoing complexation with these hosts, which the authors assign to the small size of the R methyl group **[165]**. They also describe how no inclusion is observed for L-Tyr either, which is explained by the polarity of the R group. In fact no inclusion was observed with any of these guests and calixarene (**88**), while L-His is complexed only by (**90**). The authors describe how calixarenes (**89**) and (**90**) show comparable efficiency, with the cone calixarene (**89**) being slightly more efficient in the recognition of L-Leu.

1.21 Chiral Calixarenes as Hosts

Calixarenes differ significantly from cyclodextrins by their lack of inherent chirality, but can be converted into inherently chiral compounds by dissimilar substitution at the lower rim. They can also be converted into chiral derivatives by the introduction of chiral substituents. This was first achieved by Muthukrishnan and Gutsche [**166**] who prepared the mono- and di-camphorsulfonyl esters (**91**)a and (**91**)b respectively, of p-tert-butyl-calix[8]arene.

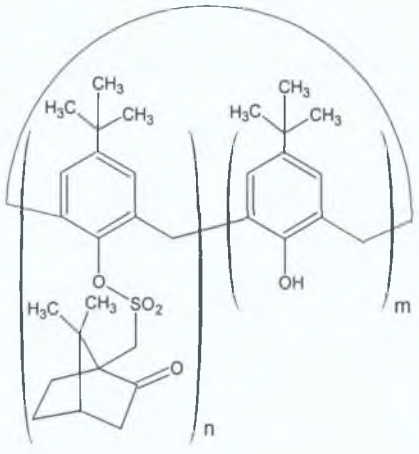

(a): n=1, m=7

(b): n=2, m=6

(**91**)

Shinkai has described further examples of such chiral compounds [**167**]. They introduced chirality, by treating p-sulfonatocalix[4]arene with (S)-1-bromo-2-methylbutane to produce (**92**) which was subsequently used in complexation studies [**168**]. The authors chose aliphatic alcohols as guest molecules and observed no change in the CD-spectrum of the calixarene, after the addition of these guests. They did however observe that the ^{1}H-NMR chemical shifts of these guests move to a higher magnetic field in the presence of (**92**) indicating that a host-guest complex is formed.

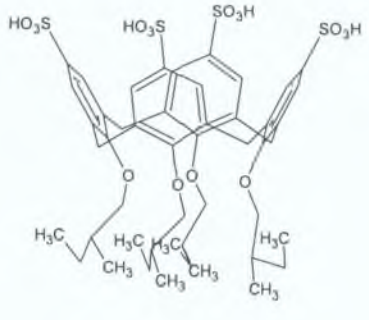

(**92**)

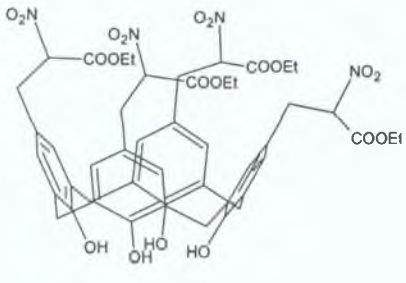

(**93**)

Upper rim functionalisation containing four chiral centres achieved by Gutsche is represented by (**93**) [**169**]. In the design of asymmetric reagents, the reaction centre is often surrounded by a chiral moiety and a recognition site, the latter controlling the substrate selectivity and the former, the stereoselectivity of the process. Binaphthyl derivatives offer a wide range of possibilities and are among the most popular chiral building blocks used. In the separation of amino acid esters Cram used binaphthyl-derived crown ethers [**170**], with binaphthyl-derived cyclophanes by Diederich complexing quinine derivatives [**171**] and pyranosides [**172**], whereas in binding tartaric acid derivatives Hamilton et al. [**173**] used binaphthyl-containing clefts. Since calixarenes are widely used for the selective recognition of ions and small molecules it seemed attractive to Casnati and Ungaro to link them with the binaphthyl moiety in the synthesis of new chiral ligands [**174**].

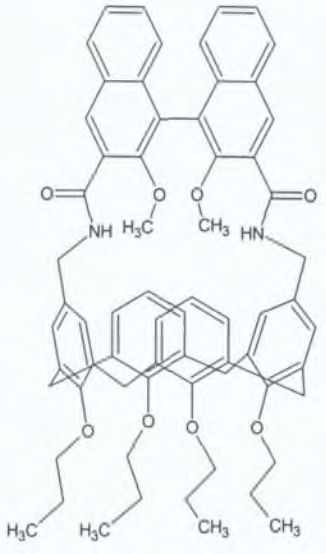

(**94**)

Complexation studies were carried out with a series of neutral guest molecules, ammonium salts and metal ions. Complexation with (**94**) was observed only in CCl_4 with guests having acidic C-H groups such as nitromethane and acetonitrile. The upfield shifts of the methyl groups of the binaphthyl unit suggest that these guests are accommodated in the apolar cavity of (**94**). Concerning metal ions, the silver cation is strongly and selectively complexed by this ligand, while no complexation occurs with alkali metal cations as in lower-rim bridged calixcrowns and calixspherands.

Kubo and co-workers [**175**] desire to achieve visual discrimination between enantiomers led them to design a molecular sensor which would translate an

enantioselective molecular recognition event into a discernible colour change. They regarded calixarenes as particularly attractive frameworks for the construction of optical sensing systems, because chromophores can be appended to the calixarene platform, and that such systems could be useful in the construction of sensors that allow the visual detection of and enantiomeric discrimination of amines and amino acids. (**83**) and (**95**) were therefore synthesised, altering the length of the ether spacers in these calixarenes, allowing the binaphthyl unit of (**95**) to be closer to one of the indophenols than the other. This means having two distinct indophenol groups, which, they hoped, would translate into a powerful chromogenic response with binding of chiral substrates generating different signals.

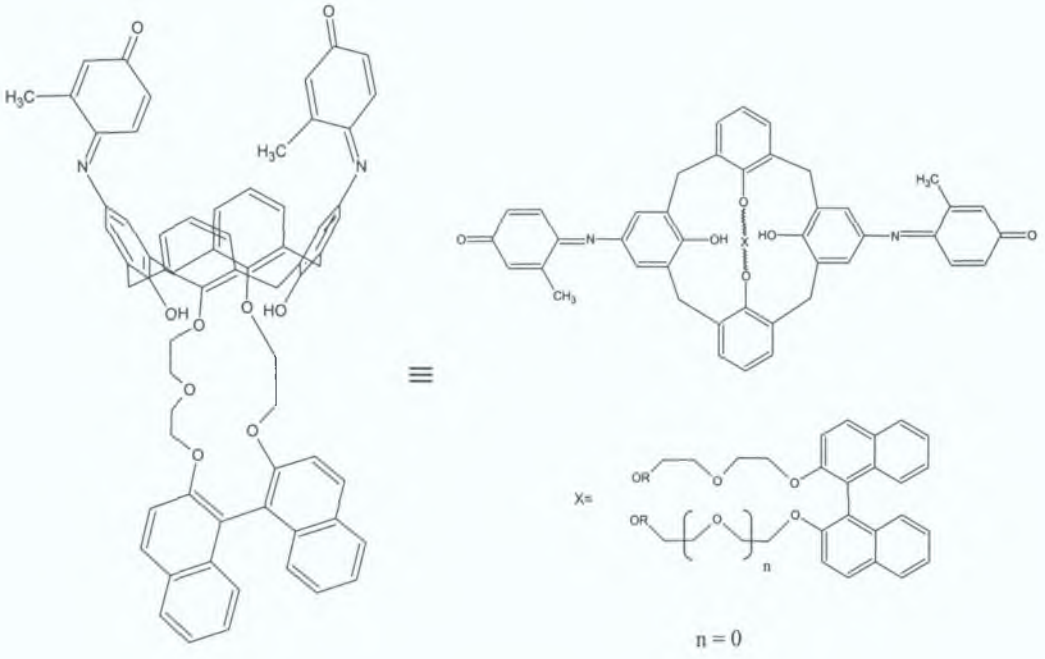

(**95**)

(R)-phenylglycinol was added to a solution of (**95**), which resulted in an immediate colour change from red to blue-violet and a new absorption band at 650nm, which was previously at 515.5nm. However, when (S)-phenylglycinol was added, almost no detectable change in the spectrum was observed, which results in very successful distinction between enantiomers with the naked eye. (**83**) however, yielded association constants of a quarter the value for the unsymmetrical calixarene with the R-enantiomer, indicating that complexation takes part in the cavity with the etherial oxygens and phenolate oxygens of the indophenol unit. No selectivity was observed for (**95**) with the enantiomers of phenylethylamine, but good selectivity was achieved with this compound and the enantiomers of phenylalaninol and phenylglycine.

The synthesis of a new type of chiral stationary phase was reported by Glennon et al. [**176**], where they describe the application of a silica-bonded derivative of (**96**), functionalised at the lower rim with L-(-)-ephedrine, and packed into an LC column for chiral separations.

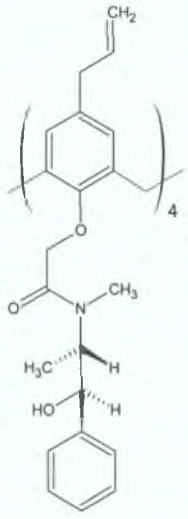

(**96**)

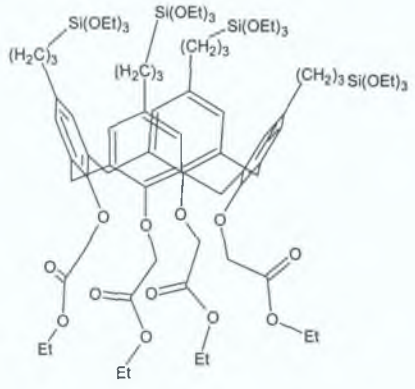

(**97**)

The authors intended that these new types of stationary phases be employed in the separation of enantiomeric substances, by the formation of diastereomeric host-guest adsorbates. They injected racemic mixtures of (+) and (-)-1-cyclohexylethanol and of R(-) and S(+)-1-phenyl-2,2,2-trifluoroethanol onto a column with the derivatised calixarene as stationary phase and obtained successful resolution of both pairs of enantiomers. In a previous publication [**177**] the authors describe how a silica bonded calix[4]arene tetraester (**97**) has been utilised in the HPLC separation of alkali metal ions and a series of amino acid esters. Good separation was achieved when a test mixture of benzamide, benzophenone and biphenyl was injected onto a column packed with (**97**) as stationary phase. They were also successful in the separation of NaCl and KCl, along with ester derivatives of L-aspartyl-L-phenylalanine, β-alanine and D-tryptophan.

The two isomers (+) and (-) of the following calix[3]arene were optically resolved by chiral HPLC, with the first fraction ((-)-anti-(**98**)) and second fraction ((+)-anti-(**98**)) giving symmetrical CD spectra, θ_{max} = ±2θ200 deg cm^2 dmol^{-1} at λ_{max} 232nm. The association constants of these calixarenes were measured with various chiral amines. The association constants for the L-configured amines were greater with ((-)-

anti-(**98**)) than for ((+)-anti-(**98**)) , displaying good chiral selectivity (see Table below) [**178**].

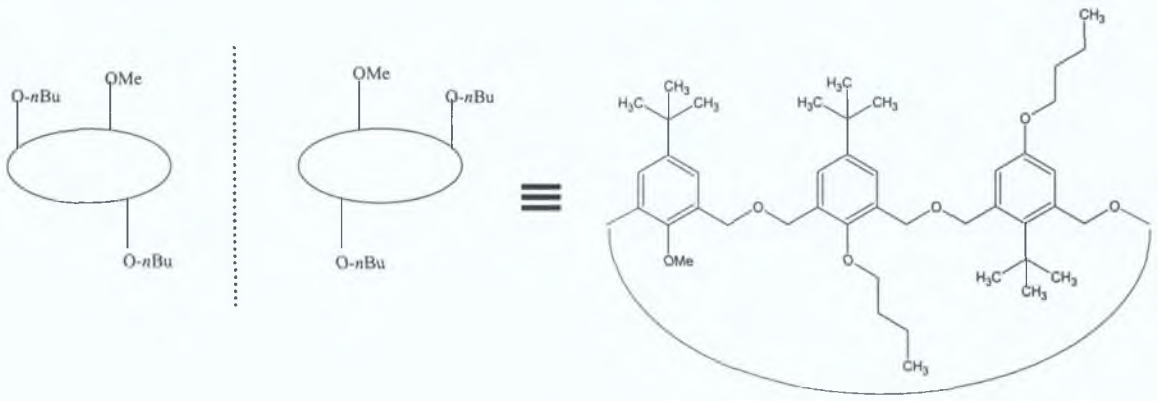

(**98**)

Picrate Salt	K_{ass} (-)-(98)	K_{ass} (+)-(98)	K_{ass}(large)/ K_{ass}(small)
L-alanine methyl ester picrate	4500	3200	1.4
L-phenylalanine methyl ester picrate	1200	180	6.7
(R)-1-phenylethylamine picrate	2200	3000	1.4
(R)-1-naphthylethylamine picrate	2000	2400	1.2

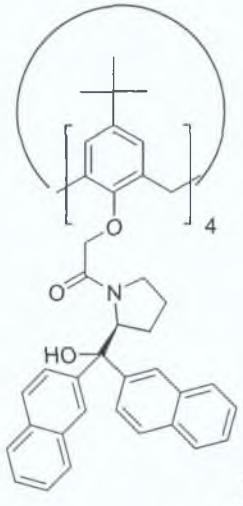

(**99**)

Calixarene (**99**) exhibits much larger Stern-Volmer constant (K_{SV}) differences with regard to the enantiomers of phenylethylamine than do calixarenes (**100**) and (**101**) [**179**]. Calixarene (**99**) also possesses the ability to discriminate between the enantiomers of norephedrine, whereas (**100**) and (**101**) do not.

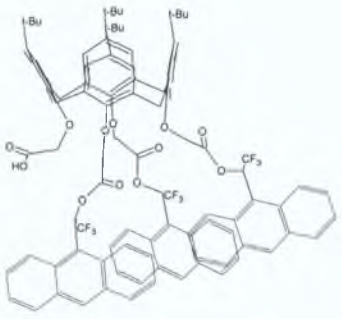

(**100**)

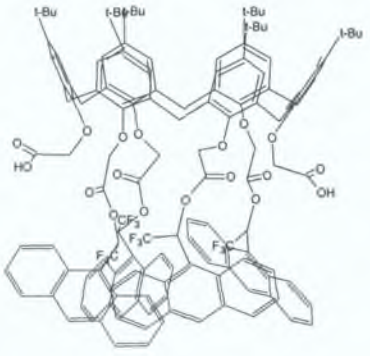

(**101**)

Subsequently Diamond et al. describe a system involving the (S)-di-naphthylprolinol calix[4]arene (**99**), as the stationary phase in capillary electrophoresis. They have achieved the chiral separation of the enantiomers of 2-phenylglycinol with this system, employing methanol as the mobile phase [**180**]. Recently Diamond and Jennings have reported the successful chiral discrimination of phenylglycinol by (**99**), whereas the similar phenylalaninol (differing only by one $-CH_2-$ group) does not even quench the luminescence of the aforementioned calixarene. The authors ascribe this occurrence to the longer chain length of phenylalaninol, which prevents the intimate contact necessary with the excited naphthalene groups to allow interaction with the phenyl ring of the longer amino alcohol. The fact that the aromatic ring is necessary in this instance is proven by results in the paper describing how the aliphatic cyclic derivative of phenylethylamine (already discussed); cyclohexylethylamine does not quench the fluorescence of (**101**) [**181**].

In conclusion, fluorescent calixarenes have been reported as successful sensor molecules with regard to ion-recognition/ selectivity and molecular/ chiral recognition. This is due in part to their well-defined cavities and also the simultaneous polar (usually lower rim) and non-polar regions (usually at the upper rim). Because of these properties calixarenes can form inclusion compounds with a wide range of guests species. The results reviewed here inspired the synthesis of a fluorogenic calix[4]arene, which differed from (**99**) by a methylene spacer group, and with the aid of fluorescence spectroscopy to study whether this new ligand would successfully discriminate between the enantiomers of phenylalaninol. We also considered that the response of this new ligand with respect to phenylglycinol (which is shorter than phenylalaninol by one methylene spacer) would present an interesting comparison to the results of (**99**) mentioned previously.

1.22 References

1 A. Zinke, E. Ziegler, *Berichte*, **1941**, 74, 1729.

2 J. W. Cornforth, P. D'Arcy Hart, G. A. Nicholls, R. J. W. Rees, J. A. Stock, *Brit. Pharmacol.* **1955**, 10, 73.

3 C. D. Gutsche, R. Muthukrishnan, *J. Org. Chem.* **1978**, 43, 4905.

4 C. D. Gutsche, R. Muthukrishnan, K. H. No, *Tetrahedron Lett.* **1979**, 2213.

5 R. Muthukrishnan, C. D. Gutsche, *J. Org. Chem.* **1979**, 44, 3962.

6 C. D. Gutsche, B. Dhawan, K. H. No, R. Muthukrishnan, *J. Am. Chem. Soc.* **1981**, 103, 3782.

7 M. Izatt, J. J. Christensen, *Synthesis of Macrocycles; The Design of Selective Complexing Agents*, John Wiley and Sons, New York, **1987**.

8 J. L. Balard, W. B. Kay, E. L. Propa, *J. Paint Technol.* **1966**, 38, 251.

9 F. Bottino, G. Montaudo, P. Maravigna, *Ann. Chim.* (Rome) **1967**, 57, 972.

10 B. T. Hayes, R. F. Hunter, *J. Appl. Chem.* **1958**, 8, 743.

11 H. Kämmerer, G. Happel, F. Caeser, *Makromol. Chem.* **1972**, 162, 179.

12 G. Happel, B. Mathiasch, H. Kämmerer, *Makromol. Chem.* **1975**, 176, 3317.

13 (a) H. Kämmerer, G. Happel, *Makromol. Chem.* **1975**, 179, 1199, (b) *ibid.* **1981**, 182, 759, (c) *ibid.* **1980**, 181, 2049.

14 H. Kämmerer, G. Happel, H. Mathiasch, *Makromol. Chem.* **1981**, 182, 1685.

15 V. Böhmer, P. Chhim, K. Kämmerer, *Makromol. Chem.* **1979**, 180, 2503.

16 V. Böhmer, F. Marschollek, L. Zetta, *J. Org. Chem.* **1987**, 52, 3200.

17 J. de Mendoza, P. M. Nieto, P. Prados, C. Sanchez, *Tetrahedron*, **1990**, 46, 671.

18 K. N. No, K. L. Hwang, *Bull. Korean Chem. Soc.* **1993**, 14, 753.

19 V. Böhmer, L. Merkel, U. Kunz, *J. Chem. Soc. Chem. Commun.* **1987**, 896.

20 N. R. L. Megson, *Oesterr. Chem.* Z. **1953**, 54, 317.

21 R. Ott, A. Zinke, *Oesterr. Chem.* Z. **1954**, 55, 156.

22 J. W. Cornforth, P. D'Arcy Hart, G. A. Nicholls, R. J. W. Rees, J. A. Stock, Brit. *J. Pharmacol.* **1955**, 10, 73.

23 M. Perrin, D. Oehler, "Conformations of Calixarenes in the Crystaline State", in *Calixarenes. A Versatile Class of Macrocyclic Compounds*, (Eds. J. Vicens, V. Böhmer), Kluwer, Dordrecht, **1991**.

24 G. D. Andreetti, F. Ugozzoli, *Inclusion Properties and Host-Guest Interactions of Calixarenes in the Solid State.*

25 N. Ehlinger, S. Lecocq, R. Perrin, M. Perrin, *Supramol. Chem.* **1993**, 2, 71.

26 C. D. Gutsche, L. J. Bauer, *J. Am. Chem. Soc.* **1985**, 107, 6052.

27 F. Grynszpan, O. Aleksiuk, S. E. Biali, *J. Org. Chem.* **1994**, 59, 2070.

28 (a) F. Grynszpan, Z. Goren, S. E. Biali, *J. Org. Chem.* **1991**, 56, 532, (b) F. Grynszpan, S. E. Biali, *Tetrahedron Lett.* **1991**, 32, 5155.

29 J. R. Moran, S. Karbach, D. J. Cram, *J. Am. Chem. Soc.* **1982**, 104, 5826.

30 D. J. Cram, *Science*, **1983**, 219, 1177.

31 C. Rizzoli, G. D. Andreetti, R. Ungaro, A. Pochini, *J. Molec. Structure*, **1982**, 82, 133.

32 C. D. Gutsche, J. A. Levine, P. K. Sujeeth, *J. Org. Chem.* **1985**, 50, 5802.

33 C. D. Gutsche, P. F. Pagoria, *J. Org. Chem.* **1985**, 50, 5795.

34 M. Conner, V. Janout, S. L. Regen, *J. Org. Chem.* **1992**, 57, 3744.

35 F. Hamada, S. G. Bott, G. W. Orr, A. W. Coleman, H. M. Zhang, J. L. Atwood, *J. Incl. Phenom. Mol. Recogn.* **1990**, 9, 195.

36 S. Shinkai, K. Araki, T. Tsubaki, T. Arimura, O. Manabe, *J. Chem. Soc. Perkin Trans.1*, **1987**, 2297.

37 A. Casnati, Y. Ting, D. Berti, M. Fabbi, A. Pochini, R. Ungaro, D. Sciotto, G. G. Lombardo, *Tetrahedron*, **1993**, 49, 9815.

38 Y. Morzherin, D. M. Rudkevich, W. Verboom, D. N. Reinhoudt, *J. Org. Chem.* **1993**, 58, 7602.

39 S. Shinkai, T. Nagasaki, K. Iwamoto, A. Ikeda, G.-X. He, T. Matsuda, M. Iwamoto, *Bull. Chem. Soc. Jpn.* **1991**, 64, 381.

40 Z. T Huang, G.-Q. Wang, *Chem. Ber.* **1994**, 127, 519.

41 M. Almi, A. Arduini, A. Casnati, A. Pochini, R. Ungaro, *Tetrahedron*, **1989**, 45, 2177.

42 C. D. Gutsche, K. C. Nam, *J. Am. Chem. Soc.* **1988**, 110, 6153.

43 C. D. Gutsche, I. Alam, *Tetrahedron*, **1988**, 44, 4689.

44 K. No, Y. Noh, *Bull. Korean Chem. Soc.* **1986**, 7, 314.

45 S. Shinkai, K. Araki, J. Shibita, O. Manabe, *J. Chem. Soc. Perkin Trans.1*, **1989**, 195.

46 M. Yeh, F. Tang, S. Chen, W. Liu, L. Kin, *J. Org. Chem.* **1994**, 59, 754.

47 (a) K. No, Y. Noh, Y. Kim, *Bull. Korean Chem. Soc.* **1986**, 7, 442. (b) T. Arimura, S. Shinkai, T. Matsuda, Y. Hirata, H. Satoh, O. Manabe, *Bull. Chem. Soc. Jpn.* **1988**, 61, 3733.

48 A. Arduini, A. Pochini, S. Reverberi, R. Ungaro, G. D. Andreetti, F. Ugozzoli, *Tetrahedron*, **1986**, 42, 2089.

49 F. Arnaud-Neu, E. M. Collins, M. Deasy, G. Ferguson, S. J. Harris, B. Kaitner, A. J. Lough, M. A. McKervey, et al. *J. Am. Chem. Soc.* **1989**, 111, 8681.

50 S.-K. Chang, I. Cho, *J. Chem. Soc. Perkin Trans.1*, **1986**, 211.

51 S.-K. Chang, S.-K. Kwon, I. Cho, *Chem. Lett.* **1987**, 947.

52 G. Calestani, F. Ugozzoli, A. Arduini, E. Ghidini, R. Ungaro, *J. Chem. Soc. Chem. Commun.* **1987**, 344.

53 A. Arduini, E. Ghidini, A. Pochini, R. Ungaro, G. D. Andreetti, G. Calestani, F. Ugozzoli, *J. Incl. Phenom.* **1988**, 6, 119.

54 F. Arnaud-Neu, M.-J. Schwing-Weill, K. Ziat, S. Cremin, S. J. Harris, M. A. McKervey, *New. J. Chem.* **1991**, 15, 33.

55 G. Ferguson, B. Kaitner, M. A. McKervey, E. M. Seward, *J. Chem. Soc. Chem. Commun.* **1987**, 584.

56 J.-D. van Loon, W. Verboom and D. N. Reinhoudt, *Org. Prep. Proceed. Int.* **1992**, 24, 437.

57 S. Shinkai, *Tetrahedron*, **1993**, 49, 8933.

58 W. Verboom, S. Dotta, Z. Asfari, S. Harkema, D. N. Reinhoudt, *J. Org. Chem.* **1992**, 57, 5394.

59 L. C. Groenen, B. H. M. Ruël, A. Casnati, W. Verboom, A. Pochini, R. Ungaro, D. N. Reinhoudt, *Tetrahedron*, **1991**, 47, 8379.

60 D. N. Reinhoudt, P. J. Dijkstra, P. J. A. in't Veld, K.-E. Bugge, S. Harkema, R. Ungaro, E. Ghindini, *J. Am. Chem. Soc.* **1987**, 109, 4761.

61 P. J. Dijkstra, J. A. J. Brunink, K.-E. Bugge, D. N. Reinhoudt, S. Harkema, R. Ungaro, F. Ugozzoli, E. Ghindini, *J. Am. Chem. Soc.* **1989**, 111, 7567.

62 E. Ghindini, F. Ugozzoli, R. Ungaro, S. Harkema, A. El-Fadl, D. N. Reinhoudt, *J. Am. Chem. Soc.* **1990**, 112, 6979.

63 L. C. Groenen, B. H. M. Ruël, A. Casnati, P. Timmerman, W. Verboom, S. Harkema, A. Pochini, R. Ungaro, D. N. Reinhoudt, *Tetrahedron Lett.* **1991**, 32, 2675.

64 F. Bottino, L. Giunta, S. Pappalardo, *J Org. Chem.* **1989**, 54, 5407.

65 K. Iwamoto, K. Araki, S. Shinkai, *Tetrahedron*, **1991**, 47, 4325.

66 C. D. Gutsche, B. Dhawan, J. A. Levine, K. H. No, L. J. Bauer, *Tetrahedron*, **1983**, 39, 409.

67 A. Casnati, A. Arduini, E. Ghindini, A. Pochini, R. Ungaro, *Tetrahedron*, **1991**, 47, 2221.

68 A. Arduini, A. Casnati, L. Dodi, A. Pochini, R. Ungaro, *J. Chem. Soc. Chem. Commun.* **1990**, 1597.

69 G. McMahon, R. Wall, K. Nolan, D. Diamond, *Talanta*, **2002**, 57, 1119.

70 V. Bohmer, *Angew. Chem. Int. Ed. Engl.* **1995**, 34, 713.

71 T. Arimura, H. Kawabata, T. Matsuda, T. Muramatsu, H. Satoh, K. Fujio, O. Manabe, S. Shinkai, *J Org. Chem.* **1991**, 56, 301.

72 A. Ikeda, T. Nagasaki, S. Shinkai, *J. Phys. Org. Chem.* **1992**, 5, 699.

73 V. Böhmer, D. Kraft, M. Tabatabai, *J. Incl. Phenom. Mol. Recogn.* **1994**, 19, 17.

74 L. Zetta, A. Wolff, W. Vogt, K. -L. Platt, V. Böhmer, *Tetrahedron*, **1991**, 47, 1911.

75 V. Böhmer , R. Dörrenbacher, W. Vogt, L. Zetta *Tetrahedron Lett.* **1992**, 33, 769.

76 H. Casabianca, J. Royer, A. Satrallah, A. Taty.C, J. Vicens, *Tetrahedron Lett.* **1987**, 28, 6595.

77 P. A. Reddy, C. D. Gutsche, *J. Org. Chem.* **1993**, 58, 3245.

78 S. Shinkai, T. Arimura, H. Kawabata, H. Murakami, K. Araki, K. Iwamoto, T. Matsuda, *J. Chem. Soc. Chem. Commun.* **1990**, 1734.

79 S. Shinkai, T. Arimura, H. Kawabata, H. Murakami, K. Iwamoto, *J. Chem. Soc. Perkin Trans.1*, **1991**, 2429.

80 M. Tabatabai, W. Vogt, V. Böhmer, *Tetrahedron Lett.* **1990**, 31, 3295.

81 K. Iwamoto, A. Yanagi, T. Arimura, T. Matsuda, S. Shinkai, *Chem. Lett.* **1990**, 1901.

82 K. Iwamoto, H. Shimizu, K. Araki, S. Shinkai, *J. Am. Chem. Soc.* **1993**, 115, 3997.

83 L. T. Burne, J. M. Harrowfield, D. C. R. Kockless, B. J. Peachey, B. W. Skelton, A. H. White, *Aust. J. Chem.* **1993**, 46, 1673.

84 S. Pappalardo, L. Giunta, M. Foti, G. Ferguson J. F. Gallagher, B. Kaitner, *J. Org. Chem.* **1992**, 57, 2611.

85 S. Pappalardo, S. Caccamese, L. Giunta, *Tetrahedron Lett.* **1991**, 32, 7747.

86 S. Caccamese, S. Pappalardo, *Chirality*, **1993**, 5, 159.

87 V. Böhmer , A. Wolff, W. Vogt, *J. Chem. Soc. Chem. Commun.* **1990**, 968.

88 O. Aleksiuk, F. Grynszpan, S. E. Biali, *J. Chem. Soc. Chem. Commun.* **1993**, 11.

89 A. M. Litwak, S. E. Biali, *J. Org. Chem.* **1992**, 57, 1943.

90 A. M. Litwak, F. Grynszpan, O. Aleksiuk, S. Cohen, S. E. Biali, *J. Org. Chem.* **1993**, 58, 393.

91 D. J. Cram, *Angew. Chem. Int. Ed. Engl.* **1988**, 27, 1009.

92 A. D. Buckingham, A. C. Legon, and S. M. Roberts (eds.), *Principle of Molecular Recognition*, Blackie Academic, Glasgow, **1993**.

93 S. M. Roberts (ed.), *Molecular Recognition- Chemical and Biochemical Problems*, Royal Society of Chemistry, Cambridge, **1989**.

94 E. H. Fischer , *Ber. Dtsch. Chem. Ges.* **1894**, 27, 2985.

95 J. N. Langley, *J. Physiol.* **1907**, 35, 33.

96 (a) H. Loewe, (ed.), Paul Ehrlich, *Schöpfer der Chemotherapie*. Stuttgart: Wissenschaftliche Verlagsgesellschaft m.b.H. **1950**, (b) E. Bäumler, (ed.), Paul Ehrlich, *Forscher für das Leben*. Frankfurt: Societ·ts-Verlag, **1979**.

97 P.Ehrlich, Croonian Lecture, *Proc. Roy. Soc.*, London, **1900**, 66, 424.

98 P. G. Waser, U. Lüthi, *Nature* **1956**, 178, 981, *Anaesthesist* **1957**, 6, 103, *Arch. Int. Pharmacodynam. Therap.* **1957**, 112, 272.

99 J. Büchi, (ed.) *Grundlagen der Artzneimittelforschung und der synthetischen Arzneimittel*. Basel: Birkhäuser-Verlag, **1963**.

100 D. J. Cram, R. H. Bauer, *J. Am. Chem. Soc.* **1959**, 81, 5971.

101 L. A. Singer, D. J. Cram, *J. Am. Chem. Soc.* **1963**, 85, 1080.

102 C. J. Pedersen, *J. Am. Chem. Soc.* **1967**, 89, 2495.

103 C. J. Pedersen, *J. Am. Chem. Soc.* **1967**, 89, 7017.

104 B. Dietrich, J.-M. Lehn, J.-P. Sauvage, *Tetrahedron Lett.* **1969**, 2885.

105 B. Dietrich, J.-M. Lehn, J.-P. Sauvage, *Tetrahedron Lett.* **1969**, 2889.

106 E. P. Kyba, R. C. Helgeson, K. Madan, G. W. Gokel, T. L. Tarnowski, S. S. Moore, D. J. Cram, *J. Am. Chem. Soc.* **1977**, 99, 2564.

107 M. Mascal, *Contemp. Org. Synth.* **1994**, 1, 31.

108 D. J. Cram, K. N. Trueblood, *Host-Guest Complex Chemistry Macrocycles*, [F. Vögtle, E. Weber, (ed.)], Berlin, Springer-Verlag, **1985**.

109 F. A. Walker, M. Benson, *J. Am. Chem. Soc.* **1980**, 102, 5530.

110 C. A. Hunter, J. K. M. Sanders, *J. Am. Chem. Soc.* **1990**, 112, 5525.

111 W. L. Koltun, *Biopolymers 3*, **1965**, 665.

112 D. J. Cram, G. M. Lein, *J. Am. Chem. Soc.* **1985**, 107, 3657.

113 D. J. Cram, K. N. Trueblood, *Top. Curr. Chem.* **1981**, 98, 43.

114 M. R. Truter, *Structure and Bonding*, **1993**, 16, 17.

115 J. D. Dunitz, M. Dobler, P. Seiler, R. P. Phizackerley, *Acta Cryst.* **1974**, B30, 2733. J. D. Dunitz, P. Seiler, *Acta Cryst.* **1974**, B30, 2739. M. Dobler, J. D. Dunitz, P. Seiler, *Acta Cryst.* **1974**, B30, 2741. P. Seiler, M. Dobler, J.

D.Dunitz, *Acta Cryst.* **1974**, B30, 2744. M. Dobler, R. P. Phizackerley, *Acta Cryst.* **1974**, B30, 2746. M. Dobler, R. P. Phizackerley, *Acta Cryst.* **1974**, B30, 2748.

116 Reviewed by N. K. Dalley, *Synthetic Multidentate Macrocyclic Compounds,* [R. M. Izatt, J. J. Christensen, (ed.)], New York, Academic Press, **1978**.

117 J. Dale, *Tetrahedron* **1974**, 30, 1683; *Israel J. Chem.* **1980**, 20, 3.

118 D. Live, S. I. Chan, *J. Am. Chem. Soc.* **1976**, 98, 3769.

119 K. T. Chapman, W. C. Still, *J. Am. Chem. Soc.* **1989**, 111, 3075.

120 J. Canceill, M. Cesario, A. Collet, J. Guilhem, L. Lacombe, B. Lozach, C. Pascard, *Angew. Chem. Int. Ed. Engl.* **1989**, 28, 1246.

121 W. Blokzijl, J. F. Engberts, *Angew. Chem. Int. Ed. Engl.* **1993**, 32, 1545.

122 M. S. Searle, D. H. Williams, *J. Am. Chem. Soc.* **1992**, 114, 10690; *ibid*, pp. 10697.

123 U. E. Spichiger-Keller, *Anal. Chim. Acta*, **1999**, 400, 65.

124 Y. Inoue, T. Hakushi, Y. Liu, *Cation Binding in Macrocycles*, Y. Inoue and G. W. Gokel (eds) Marcel Dekker, New York, Basel, **1990**.

125 J. Szejtli, *Cyclodextrins and their Inclusion Complexes*, Akadémiai Kiadó, Budapest, **1982**.

126 G. Wenz, *Angew. Chem. Int. Ed. Engl.* **1994**, 33, 803.

127 M. L. Bender, M. Komiyama, *Cyclodextrin Chemistry*, Springer-Verlag, Berlin, **1978**.

128 J. Szejtli, *Cyclodextrin Technology*, Kluwer, Dordrecht, **1988**.

129 G. W. Gokel, D. J. Cram, C. L. Liotta, H. P. Harris, F. L. Cook, *J. Org. Chem.* **1974**, 39, 2445.

130 G. W. Gokel, D. J. Cram, C. L. Liotta, H. P. Harris, F. L. Cook, *Org. Synth.* **1977**, 57, 30; *Org. Synth. Coll. Vol. VI*, **1988**, 301.

131 B. Dietrich, J. –M. Lehn, J. –P. Sauvage, *Tetrahedron. Lett.* **1969**, 2889; B. Dietrich, J. –M. Lehn, J. –P. Sauvage, *Tetrahedron. Lett.* **1973**, 29, 1647.

132 J. Cheney, J. –P. Kintzinger, J. –M. Lehn, *Nouv. J. Chim.* **1978**, 2, 411.

133 H. –J. Brügge, D. Carboo, K. von Deuten, A. Knöchel, J. Kopf, W. Dreissig, *J. Am. Chem. Soc.* **1986**, 108, 107.

134 K. N. Trueblood, C. B. Knobler, E. Maverick, R. C. Helgeson, S. B. Brown, D. J. Cram, *J. Am. Chem. Soc.* **1981**, 103, 5594.

135 D. J. Cram, M. P. deGrandpre, C. B. Knobler, K. N. Trueblood, *J. Am. Chem. Soc.* **1984**, 106, 3286.

136 H. Stetter, E. –E. Roos, *Chem. Ber.* **1955**, 88, 1390.

137 J. M. Timko, S. S. Moore, D. M. Walba, P. C. Hiberty, D. J. Cram, *J. Am. Chem. Soc.* **1977**, 99, 4207.

138 K. R. A. S. Sandanayake, I. O. Sutherland, *Tetrahedron Lett.* **1993**, 34, 3165.

139 M. Ciampolini, N. Nardi, B. Valtancoli, M. Micheloni, *Coord. Chem. Rev.* **1992**, 120, 223.

140 B. Dietrich, *Comprehensive Supramolecular Chemistry, Vol 1*, [G. W. Gokel, (ed.)], Oxford, Elsevier Science Ltd. **1996**.

141 C. D. Gutsche, *Calixarenes,* The Royal Society of Chemistry, Cambridge, England, **1989**.

142 F. Arnaud-Neu, S. Barboso, A. Casnati, A. Pinalli, M. J. Schwing-Weill, R. Ungaro, *New J. Chem.* **2000**, 24, 967.

143 M. Perrin, D. Oehler, Conformations of Calixarenes in the Crystalline State, p65-85 in *Calixarenes. A Versatile Class of Macrocyclic Compounds*, (Eds.: Vicens, J.; Böhmer, V.), Kluwer, Dordrecht, **1991**.

144 C. D. Gutsche, *Calixarenes, Monographs in Supramolecular Chemistry*, ed. Stoddart, J. F., The Royal Society of Chemistry, Cambridge, **1989**.

145 Y. Kubo, S. Hamaguchi, A. Niimi, K. Yoshida, S. Tohita, *J. Chem. Soc., Chem. Commun.* **1993**, 305.

146 Y. Kubo, S. Hamaguchi, K. Kotani, K. Yoshida, *Tetrahedron Lett.* **1991**, 32, 7419.

147 L. Prodi, F. Bolletta, M. Montalti, N. Zaccheroni, A. Casnati, F. Sansono, R. Ungaro, *New. J. Chem.* **2000**, 24, 155.

148 H. M. Chawla, K. Srinivas, *Tetrahedron Lett.* **1994**, 35, 2925.

149 H. M. Chawla, V. Singh, U. Hooda, *J. Chem. Soc., Chem. Commun.* **1993**, 305

150 C. Alfieri, E. Dradi, A. Pochini, R. Ungaro, G. D. Andreetti, *J. Chem. Soc. Chem. Commun.* **1983**, 1075.

151 A. Arduini, A. Pochini, S. Reverberi, R. Ungaro, *J. Chem. Soc. Chem. Commun.* **1984**, 981.

152 K. Iwamoto, K. Araki, H. Fujishima, S. Shinkai, *J. Chem. Soc. Perkin Trans.1*, **1992**, 1885.

153 C. Pérez-Jiménez, S. J. Harris, D. Diamond, *J. Chem. Soc. Chem Commun.* **1993**, 480.

154 I. Aoki, H. Kawabata, K. Nakashima, S. Shinkai, *J. Chem Soc. Chem Commun.* **1991**, 1771.

155 T. Jin, K. Ichikawa, T. Koyama, *J. Chem. Soc. Chem. Commun.* **1992**, 499.

156 R. Ungaro, A. Pochini, A. Arduini, in *"Inclusion Phenomena and Molecular Recognition"*, ed. J. L. Atwood, Plenum, New York, **1990**.

157 J. Vicens, A. E. Armah, S. Fujii, K.-I. Tomita, *J. Inclusion Phenom., Mol. Recognit. Chem.* **1990**, 19, 159.

158 R. Ungaro, A. Pochini, G. D. Andreetti, V. Sangermano, *J. Chem. Soc., Perkin Trans. 2*, **1984**, 1979.

159 A. Casnati, P. Jacopozzi, A. Pochini, F. Ugozzoli, R. Cacciapaglia, L. Mandolini, R. Ungaro, *Tetrahedron*, **1995**, 51, 591.

160 K. Iwamoto, A. Ikeda, K. Araki, T. Harada, S. Shinkai, *Tetrahedron*, **1993**, 49, 9937.

161 I. Aoki, T. Sakaki, S. Tsutsui, S. Shinkai, *Tetrahedron Lett.* **1992**, 33, 89.

162 G. Arena, A. Casnati, A. Contino, G. G. Lombardo, D. Sciotto, R. Ungaro, *Chem. Eur. J.* **1999**, 5, 738.

163 S. Shinkai, K. Araki, T. Matsuda, N. Nishiyama, H. Ikeda, L. Takasu, M. Iwamoto, *J. Am. Chem Soc.* **1990**, 112, 9053.

164 G. Arena, A. Casnati, A. Contino, D. Sciotto, R. Ungaro, *Tetrahedron Lett.* **1997**, 38, 4685.

165 G. Arena, A. Contino, F. G. Gulino, A. Magri, F. Sansone, D. Sciotto, R. Ungaro, *Tetrahedron Lett.* **1999**, 40, 1597.

166 R. Muthukrishnan, C. D. Gutsche, *J. Org. Chem.* **1979**, 44, 3962.

167 A. Ikeda, T. Nagasaki, S. Shinkai, *J. Phys. Org. Chem.* **1992**, 5, 699.

168 T. Arimura, H. Kawabata, T. Matsuda, T. Muramatsu, H. Satoh, K. Fujio, O. Manabe, S. Shinkai, *J. Org Chem.* **1991**, 56, 301.

169 C. D. Gutsche, K. C. Nam, *J. Am. Chem. Soc.* **1988**, 110, 6153.

170 M. Newcomb, J. L. Toner, R. C. Helgeson, D. J. Cram, *J. Am. Chem. Soc.* **1979**, 101, 4941.

171 F. Diederich, M. Hester, M. A. Uyeki, *Angew. Chem. Int. Ed. Engl.* **1988**, 27, 1705.

172 S. Anderson, U. Neidlein, V. Gramlich, F. Diederich, *Angew. Chem. Int. Ed. Engl.* **1995**, 34, 1596.

173 F. Garcia-Tellado, J. Albert, A. D. Hamilton, *J. Chem. Soc. Chem Commun.* **1991**, 1761.

174 E. Pinkhassik, I. Stibor, A. Casnati, R. Ungaro, *J. Org. Chem.* **1997**, 62, 8654.

175 Y. Kubo, S. Maeda, S. Tokita, M. Kubo, *Nature*, **1996**, 382, 522.

176 L. O. Healy, M. M. McEnery, D. G. McCarthy, S. J. Harris, J. D. Glennon, *Analytical Lett.* **1998**, 31, 1543.

177 J. D. Glennon, E. Horne, K. O'Connor, G. Kearney, S. J. Harris, M. A. McKervey, *Analytical Proceed.* **1994**, 31, 33.

178 K. Araki, K. Inada, S. Shinkai, *Angew. Chem. Int. Ed. Engl.* **1996**, 35, 72.

179 T. Grady, S. J. Harris, M. R. Smyth, D. Diamond, *Anal. Chem.* **1996**, 68, 3775.

180 T. Grady, T. Joyce, M. R. Smyth, S. J. Harris, D. Diamond, *Analytical Communications*, **1998**, 35, 123.

181 K. Jennings, D. Diamond, *Analyst,* **2001**, 126, 1063.

2 Synthesis of Fluorescent Calixarenes

2.1 Introduction

In designing any molecular sensor, two main issues must be addressed

- Recognition of the target species
- Transduction of the binding event

In this case we are targeting the discrimination of enantiomers of a series of chiral amines (see Figure 2-1). Both pairs of enantiomers are similar in that they have phenyl rings substituted with alkyl amino and alcohol groups, which contain chiral centres. The two amino alcohols differ in that the spacer group from the chiral centre to the phenyl ring is longer by a $-CH_2-$ linker in the case of phenylalaninol than in phenylglycinol. In order to recognise our target amines a calixarene host should be functionalised with chiral moieties that define a 3-D distribution of binding sites, complementary to that of the guest. These binding types include hydrogen-bonding sites, which, are represented in our series of amines by the $-NH_2$ and -OH functionalities.

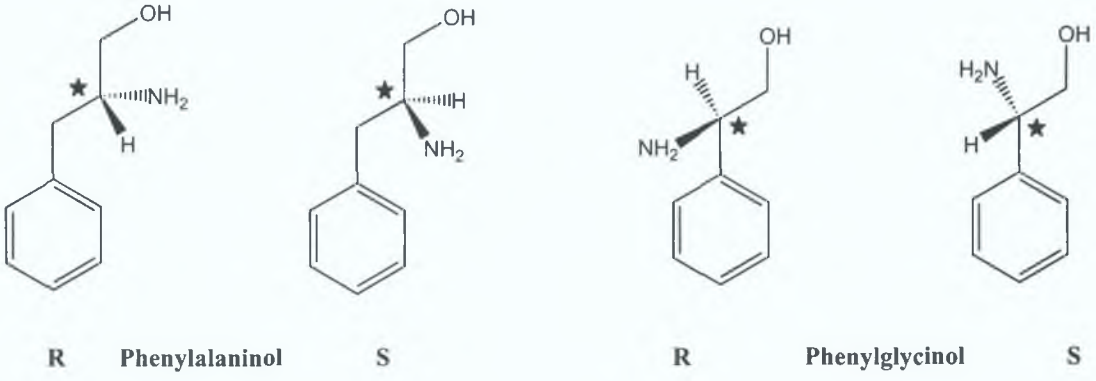

Figure 2-1: *Guest enantiomers of phenylalaninol and phenylglycinol (chiral centres are marked by the asterisk).*

Ultimately, the objective is to define a chiral space into which one enantiomer of the guest molecule preferentially fits and binds. The interaction of host and guest may be attributed to hydrogen bonding between the two molecules, with one enantiomer having more hydrogen bonding possibilities than the other. In order to observe this preferential binding a means for signaling that binding with the guest molecule has occurred is necessary. Fluorescence is an attractive option in this regard, given its

sensitivity and variety of measurement modes that can be employed (fluorescence emission, quenching, lifetime, phase angle) (see Chapter four).

For this reason our molecular sensor was designed to incorporate a fluorescent naphthyl moiety to provide a potential route to transduction of binding. Our calix[4]arene **L1** was specifically designed to discriminate between enantiomers of a chiral drug and therefore consists of pendant groups with chiral centres. Also incorporated in the design of this novel receptor was the combination of subgroups with certain desirable characteristics, such as a backbone for anchoring active groups, which is represented by the tetra phenyl cyclic framework of the calixarene. In addition ligating groups with binding capabilities are present in the calixarene, such as the hydroxy groups and lone pairs of electrons (-N-, -OH, $-CO_2$), fluorophores/ chromophores to signal guest arrival and finally, reactive groups capable of covalently immobilising the ligand, represented by the unsaturated allyl groups at the upper rim of the calixarene. These allylic sites are capable of being covalently incorporated into silica-based polymers/beads, which could be used in packing of columns for HPLC, GC or capillary electrophoresis.

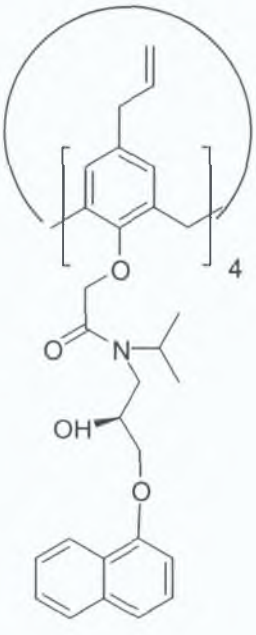

L1

After the successful synthesis and performance of calixarene **L1** (see chapters 3, 4 and 5), we decided to prepare a series of calixarene sensor molecules that possess similar properties to **L1**, but are prepared from inexpensive starting materials. For this reason amines such as 1-naphthylamine (**102**) and (S)-1-naphthylethylamine (**103**)

were chosen, naphthylamine for fluorescent ion recognition and naphthylethylamine for chiral recognition using fluorescence as the mode of signal transduction. Methyl tryptophanoate (**104**) which is an essential amino acid derivative, was also chosen as a building block since it can be easily and relatively inexpensively purchased and has the necessary properties for chiral recognition and fluorescence emission.

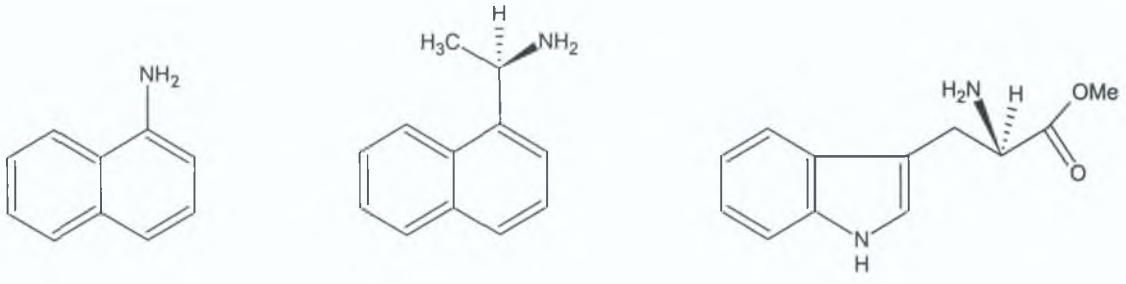

(**102**) (**103**) (**104**)

Figure 2-2: *Naphthylamine, S-naphthylethylamine and D-tryptophan methyl ester.*

2.2 *Results and Discussion*

2.2.1 Synthesis of calix[4]arene amides from acids via acid chlorides

Since cyclic tetramer formation is most greatly favoured when *t*-butyl phenol is used, the most commonly commercially available calixarenes possess *t*-butyl groups on the upper rim (**105**). It is necessary therefore to remove these groups to introduce the desired allyl groups into the upper rim. This has been previously achieved by treatment with $AlCl_3$ in the presence of phenol and toluene [**1**]. In general alkyl groups can be cleaved from aromatic rings by treatment with Lewis acids, with tertiary R-groups (i.e. the *t*-butyl group) most easily removed. This reaction as described by Gutsche yielded a white crystalline solid having a melting point of 314-318°C. The ^{1}H-NMR spectrum of this product displayed no signals for the *t*-butyl groups in the alkyl region (1.0 - 1.5 ppm) and therefore it was concluded that the de-alkylation to (**106**) had proceeded successfully, mp lit. 315-318°C [**1**].

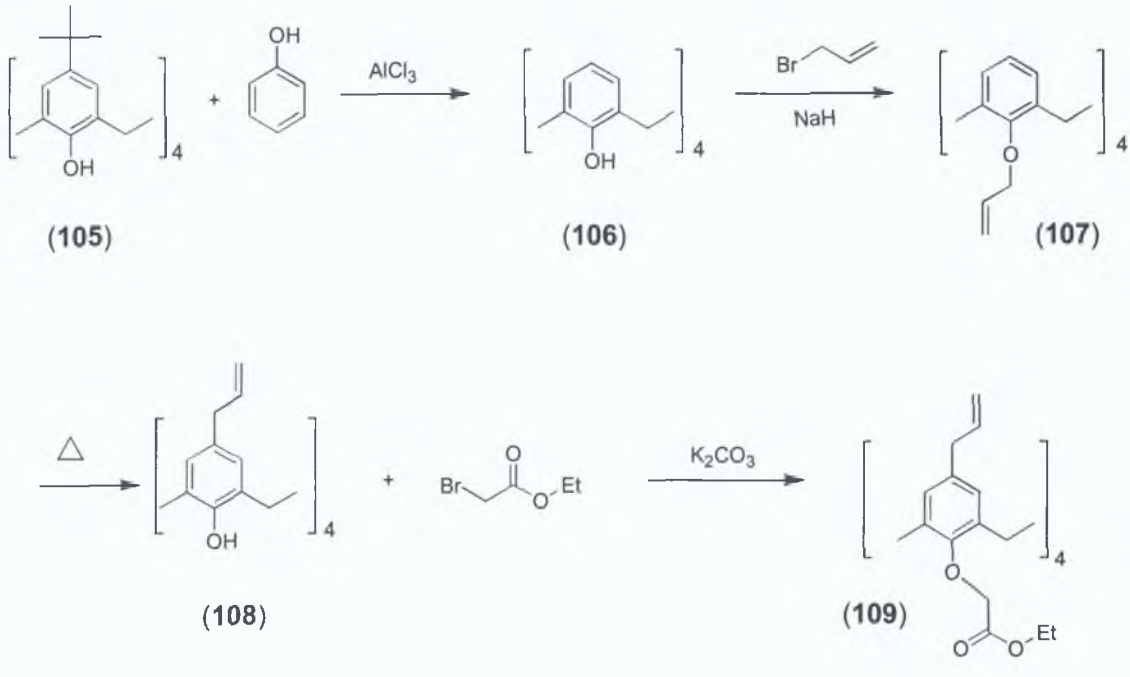

Figure 2-3: *Transalkylation of (**105**) followed by introduction of suitable functional groups on upper and lower rim.*

The allyl groups were introduced into the upper rim via a two-step sequence, by introducing an allylic system onto the lower rim of the calixarene (**107**) followed by a

Claisen rearrangement to afford (**108**). The first step involved refluxing (**106**) in DMF/ THF in the presence of NaH followed by the addition of allyl bromide. This afforded white needles mp 188°C. The IR spectrum of these needles did not display a stretch around 3157cm^{-1} corresponding to the phenolic hydroxy groups of the calixarene. The ^{1}H-NMR spectrum of this solid displayed a characteristic multiplet representing four allylic protons at 6.27ppm, and a multiplet corresponding to eight methylene protons of the allyl system at 5.1 - 5.2ppm. A doublet was located at 4.4ppm which represents the eight methylene ether protons in addition to the doublets at 3.1 and 4.3ppm for the methylene H_A and H_B protons between the aromatic rings. A multiplet at 6.5 - 6.6ppm represents the twelve aromatic protons. On the basis of this evidence this solid was identified as the tetra allyl ether (**107**) mp lit. 186-187°C [**2**].

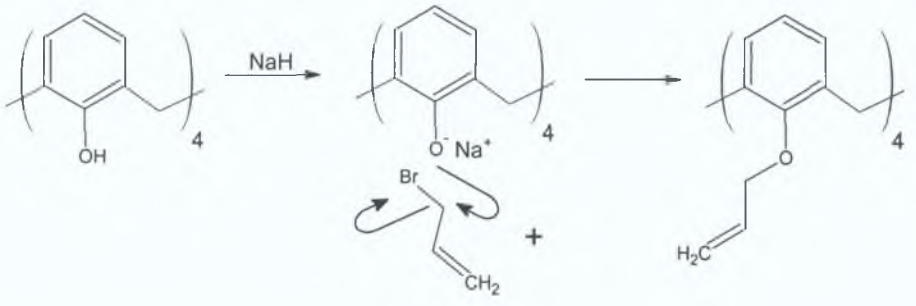

Figure 2-4: *Williamson ether synthesis of calix[4]arene.*

Heating (**107**) to 200-250 °C then effects Claisen rearrangement, which generally leads to the *o*-allyl phenol. If however, both ortho positions are filled as in the case of a calixarene molecule, then migration of the allyl groups to the para position ensues (see Figure 2-5). Refluxing the previous product in N,N,-diethylaniline followed by acidification with HCl resulted in an off-white solid having a melting point of 248 - 249°C. The IR spectrum of this solid displayed a stretch at 3157cm^{-1} corresponding to the phenolic hydroxy groups of the calixarene. The ^{1}H-NMR spectrum of this solid displayed a doublet at 3.2ppm corresponding to the eight alkyl protons of the allylic system, a multiplet at 5.1ppm which represents the eight $=CH_2$ protons and a multiplet observed at 5.91ppm representing four allylic protons (-CH=). A singlet was also observed at 6.88ppm representing eight aromatic protons and a singlet at 10.18ppm represents the four hydroxy protons. On the basis of this evidence this solid was identified as the *p*-allyl calix[4]arene (**108**) mp lit. 250.5 - 252°C [**3**].

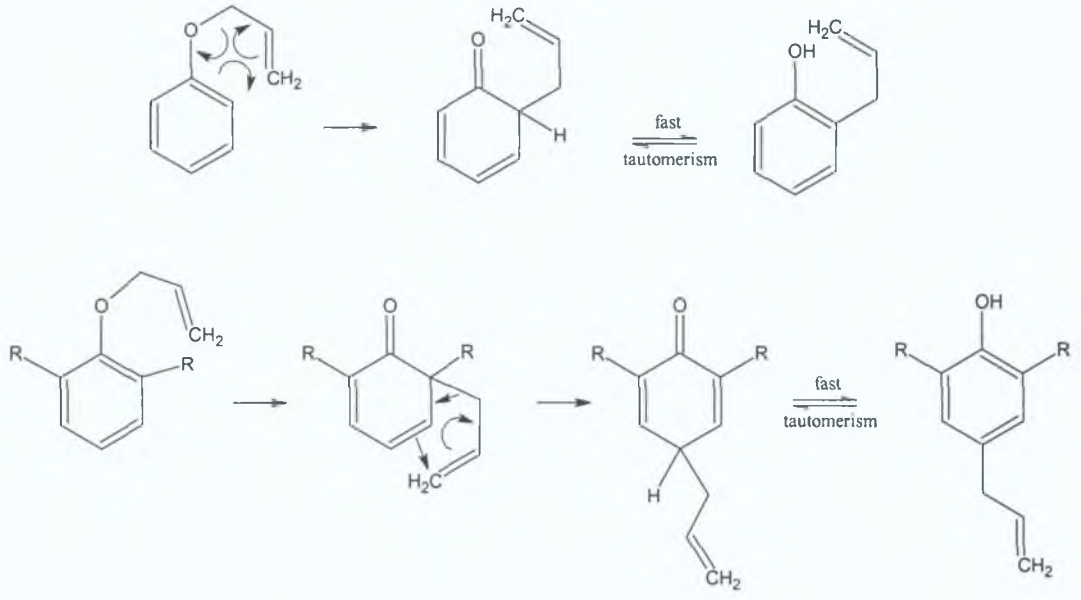

Figure 2-5: *Claisen rearrangement mechanism of the tetra-allyl ether calix[4]arene to the p-allyl calix[4]arene.*

Following the introduction of the allyl group on the upper rim, the phenolic hydroxy group is once more available for functionalisation. Keeping in mind that the desired end-product/ ligand should display properties which include hydrogen bonding, it was decided that an amide functionality would serve best in this regard. The establishment of amide moieties can be achieved by hydrolysis of esters to their corresponding carboxylic acids followed by conversion of the acid to its acid chloride derivative, which readily reacts with amines to form amides. Ester formation of the *p*-allyl calix[4]arene follows a similar mechanism as outlined in Figure 2-4. The *p*-allyl-calix[4]arene was refluxed in acetone in the presence of K_2CO_3 and ethyl bromoacetate which produced an oily substance that solidified on standing to form colourless crystals mp 98°C. In addition to the resonances listed for the previous product, the ^{1}H-NMR spectrum displayed a singlet at 4.65ppm corresponding to the two protons of the ether to carbonyl linkage and also a quartet at 4.1ppm and a triplet at 1.2ppm corresponding to two and three protons each, of the ester groups. The IR spectrum of this solid displayed a peak at 1750cm^{-1} which represents the carbonyl stretch of the ester group. On the basis of this evidence this solid was identified as the tetra ethyl ester (**109**).

We were interested in converting the upper rim allyl groups to alcohols, which could then be used to incorporate the calixarene onto silica surfaces. Ozonolysis followed by hydride reduction was attempted on (**109**). This reaction afforded white

micro crystals having a melting point of 68-70°C. The ^{1}H-NMR spectrum lacked the multiplet at 5.9ppm, which is characteristic of the allyl system, and also showed two triplets at 2.54ppm and 3.56 representing the two sets of methylene protons of the ethyl alcohol. On this basis the product was identified as the tetra-ethyl alcohol calix[4]arene tetra-ethyl ester (**110**).

Hydrolysis of the ester groups in (**110**) to form the corresponding tetra-acid was then necessary in order to form the amide, via the acid chloride. Refluxing this product (**111**) in basic ethanolic solution followed by acidification with aqueous H_2SO_4 afforded an off-white solid, which did not melt above 400°C. The ^{1}H-NMR spectrum of this solid was very difficult to interpret, and the solid was not very soluble in any of the usual organic solvents, therefore further use of this product was very limited. It was therefore decided that since the allyl groups are further capable of functionalisation, without the necessity of alcohol formation, these would be employed as the upper rim substituents and further work was carried out on the lower rim functionalisation instead.

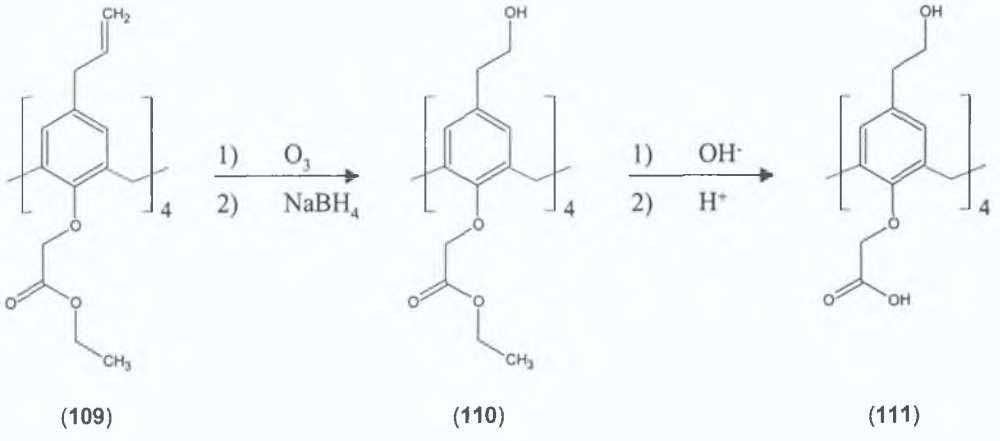

(109) (110) (111)

Figure 2-6: *Ozonolysis of (**109**), followed by reduction to the corresponding alcohol derivative (**110**), which was followed by hydrolysis of the ester groups to (**111**).*

The tetra-acid (**112**) was prepared by refluxing (**109**) in basic ethanolic solution followed by acidification with aqueous H_2SO_4 afforded a white solid which decomposed above 220°C. The ^{1}H-NMR spectrum of this white solid did not display the quartet and triplet of the ethyl ester protons. The IR spectrum of this solid displayed a peak at 1680cm^{-1} which represents the carbonyl stretch of the hydrolysed ester group, that is of the acid functionality. Mass spectral data of this solid showed a molecular ion with a mass of 839, which represented the molecular mass of the *p*-

allyl calix[4]arene tetra acid + sodium. On the basis of this evidence this solid was identified as (**112**).

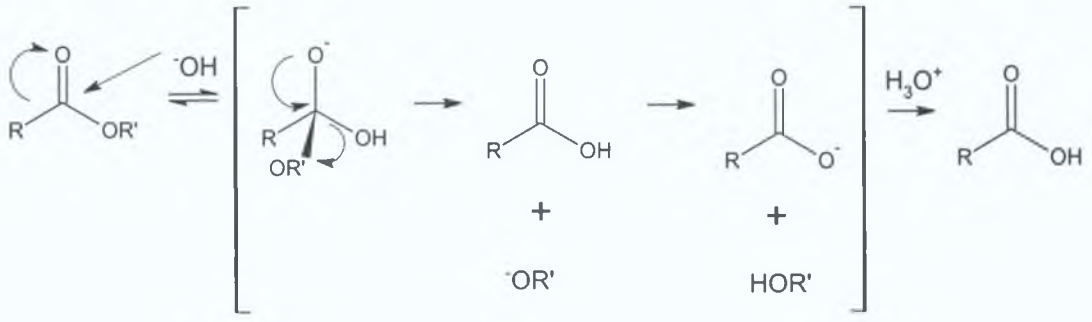

Figure 2-7: *Mechanism of base-induced ester hydrolysis, to produce a carboxylic acid and an alcohol.*

The conversion of acids to acid chlorides occurs by a nucleophilic substitution pathway, whereby the carboxylic acid is first converted into a reactive chlorosulfite intermediate, which is then attacked by the nucleophilic chloride ion. This was affected by refluxing the acid in thionyl chloride to afford an off-white solid (**113**) which was used immediately, and not fully characterised due to the ready reversibility of the reaction when the product is exposed to moisture from the air.

Acid chlorides react rapidly with amines to give amides in good yield. Both mono- and disubstituted amines can be used, with one equivalent of the amine reacting with the acid chloride and another equivalent reacting with the HCl by-product to form the corresponding amine-chloride salt. The tetra acid chloride was dissolved in THF and to this a solution of S-propranolol (**114**) and triethylamine in THF was added. This afforded a pale yellow solid, which decomposed above 190°C. The ^{1}H-NMR spectrum displayed double doublets at 1.13 and 1.37ppm, which represent the iso-propyl protons of the amide nitrogen, and two doublets at 6.62 and 6.8ppm representing protons of the naphthalene ring. A multiplet at 7.35ppm and two doublets at 7.66 and 8.19ppm represent the remaining protons of the naphthyl ring. Because of overlapping peaks and the complexity of this spectrum further identification of peaks was difficult. The IR spectrum of this solid displayed a peak at 1640cm^{-1} which represents the carbonyl stretch of the amide group. Mass spectral data of this solid showed a molecular ion with a mass of 1805, which represented the molecular mass of the *p*-allyl calix[4]arene tetra amide + sodium. On the basis of this evidence this solid was identified as **L1**, (**115**).

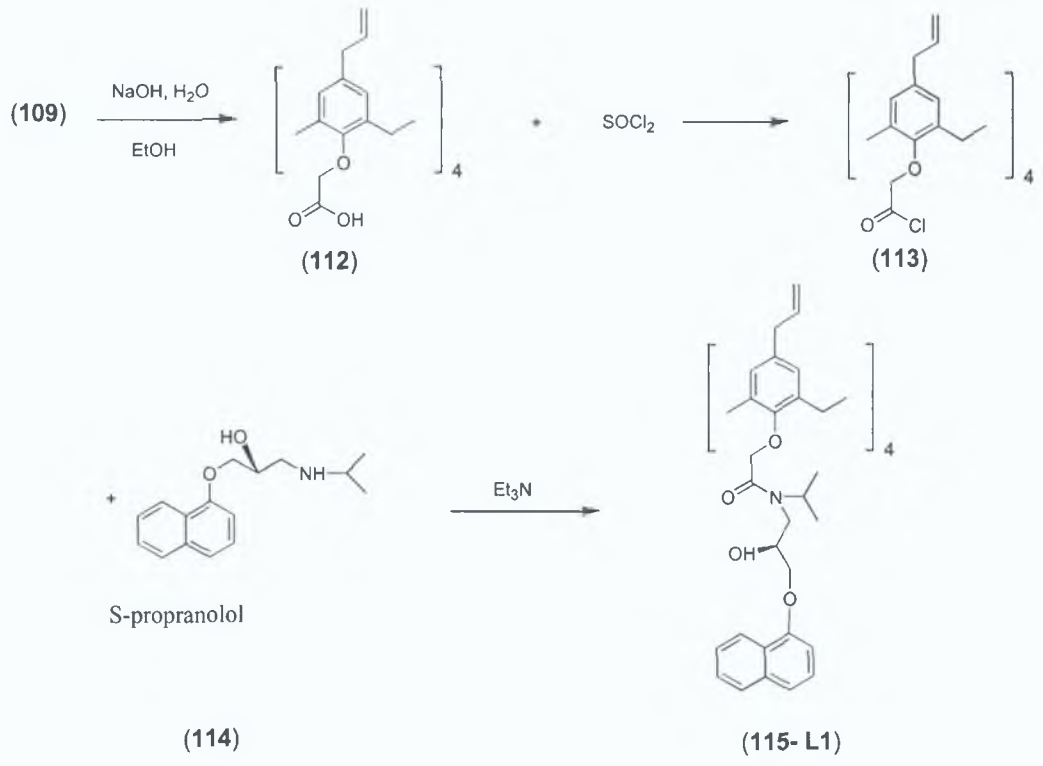

Figure 2-8: *Conversion of the calixarene tetra-acid into the amide, ligand **L1**.*

2.2.2 Synthesis of calix[4]arene amides directly from acids

An alternative strategy for the direct conversion of acids to amides involves using 1,3-dicyclohexylcarbodiimide (DCC), as a coupling agent (**116**). This would mean the amide could be formed in a one pot reaction, avoiding the acid chloride intermediate, and reducing the number of steps involved in the synthesis. The mode of action of DCC is outlined in Figure 2-9.

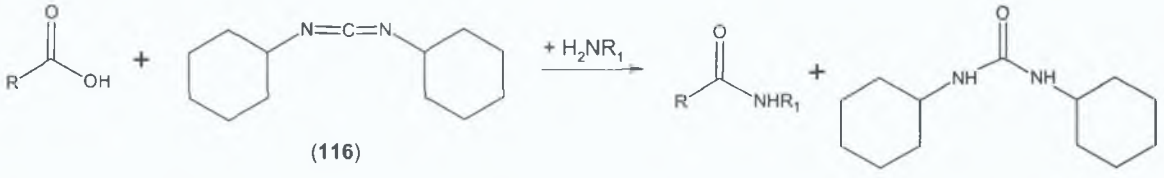

Figure 2-9: *Mode of action of coupling of amines with carboxylic acids using 1,3-dicyclohexylcarbodiimide.*

Considering this as an alternate route, the synthesis of the opposite enantiomer of *p*-allyl calix[4]arene propranolol tetra amide was undertaken employing the R-

propranolol isomer, the tetra acid (**112**) and 1,3-dicyclohexylcarbodiimide. This resulted in a pale yellow solid, the IR spectrum of which displayed carbonyl stretches at 1636 and 1654 cm^{-1} representing both the presence of amide and acid functions. Mass spectral data of this solid however showed that not all of the acid moieties had undergone reaction, resulting in a mixture of tri-acid/ mono-amide and di-acid/ di-amide substituted calix[4]arene (**117a, b**).

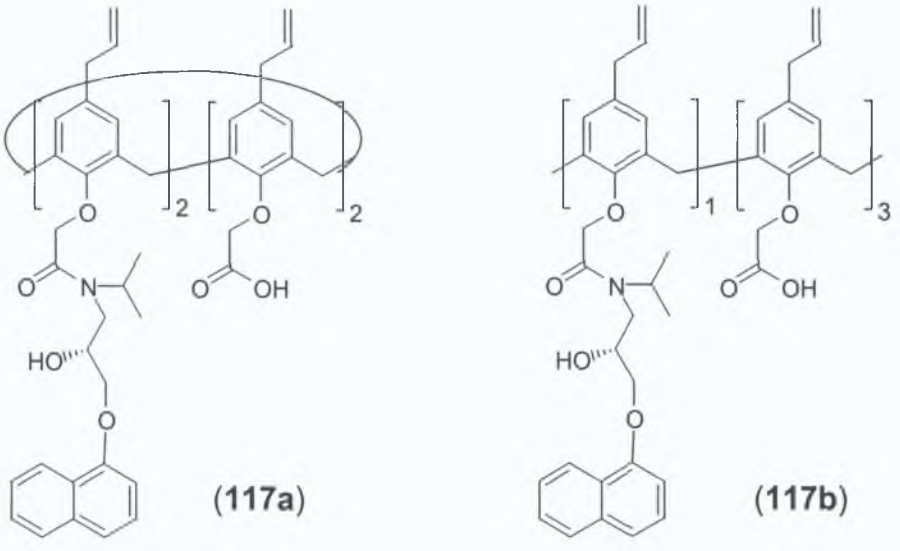

Figure 2-10: *Structures of DCC reaction mixture (**117**).*

The reasons for the partial substitution of the calixarene may include steric inaccessibility of DCC with the lower rim of the calix[4]arene. It is relatively easy to visualise how this may occur if one considers the bulky reaction intermediates involved in these coupling procedures. When it is considered that the four acid groups of the calix[4]arene are organised in a cyclic array, it is conceivable that steric hindrance may be one of the reasons responsible for the lack of full substitution of the calixarene acid functionalities. Further optimisation of this synthetic procedure was not undertaken due to the expense of the reactant, R-propranolol. This enantiomer is not as readily available as the S-isomer, and is four times more expensive than its S-form, thereby rendering it less attractive as a building block for a sensor molecule, which ideally should be relatively inexpensive and straightforward to synthesise.

2.2.3 Synthesis of novel calix[4]arene tetra-amides via acid chlorides

(**112**) was refluxed in thionyl chloride and following the removal by distillation of thionyl chloride, a solution of (**102**) and triethylamine in dry THF was added to calixarene (**113**). This was stirred at room temperature under N_2 for 24 hrs, and following work-up yielded merely a mixture of starting products. The reaction was repeated in chloroform as solvent however, again only a mixture of starting materials was recovered after the reaction. A possible reason for the lack of success of the reaction may be due to steric reasons, since there is not as much flexibility in the naphthylamine molecule as the propranolol label previously used in the case of **L1,** which may hinder the progress of the reaction. In the case of the tetra acid (**112**), the lower rim of the calixarene is quite crowded making the substitution immediately adjacent onto a naphthalene ring difficult from a steric point of view. Also the fact that naphthylamine is less nucleophilic than aliphatic amines may have prevented the reaction from occurring.

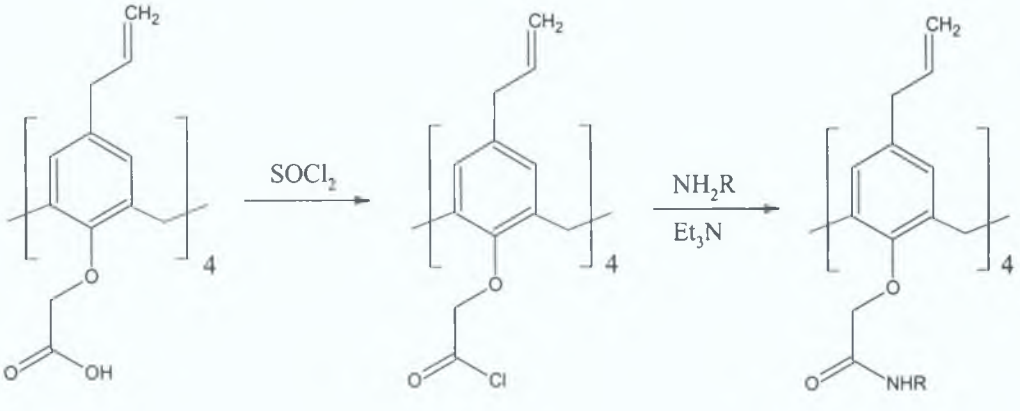

(**112**) (**113**)

Figure 2-11: *General formation of calixarene tetra-amides, where NH_2R is either (**102**) or (**104**).*

(**112**) was refluxed in thionyl chloride for 2 hours. Following the removal by distillation of thionyl chloride, a solution of (**104**) and triethylamine in dry THF was added to this calixarene tetra acid chloride. This was stirred at room temperature under N_2 for 24 hrs, and following work-up yielded merely a mixture of unidentifiable products, which did not have peaks in the ^{1}H-NMR that would represent amide formation with this amine. Mass spectral data of these solids showed molecular ions with masses, which were not consistent with full substitution of the acid groups or with any combination of partial substitution of the calixarene.

After several attempts at these two reactions an alternative synthetic route was pursued which involves formation of amide moieties separately which are then appended to the calix[4]arene (**108**) frame, which will be discussed in section 2.2.4.

2.2.4 Synthesis of calix[4]arene amides by appending pre-formed amides via phenol hydroxy groups

To endeavour to avoid such partial substitutions in derivatives of the *p*-allyl calix[4]arene an approach whereby the synthesis of single amide moieties, which can then be appended to the calix[4]arene via the hydroxy groups of the phenolic subunits was attempted. This can be achieved in two steps,

1. generation of the amide from a fluorescent amine with a molecule bearing both an acid group and a halogen component,
2. nucleophilic displacement of the halogen to form an ether connection between the calixarene annulus and the amide groups.

2.2.4.1 Synthesis of amides from fluorescent amines

Bromoacetic acid (**118**) was chosen as a suitable molecule, which incorporates both an acid group and the halogen necessary to facilitate attachment to the calixarene hydroxy group. As a test molecule, naphthylamine was chosen due to its ready availability and low cost. (**118**) was placed with (**104**) in dichloromethane solution under nitrogen, cooled to 0°C, followed by the addition of DCC. After thirty minutes at this temperature the reaction mixture was allowed to warm up to room temperature and proceed for 6 hours, which resulted in a pale purple solid with m.p. 148-150 °C. The IR spectrum of this solid displayed a peak at 1660cm^{-1} which represents the carbonyl stretch of the amide group. The ^{1}H-NMR spectrum displayed a singlet at 4.16ppm, which represents the two protons of the methylene group between the bromine and amide functions, in addition to the protons of the naphthalene. Mass spectral data of this solid showed two molecular ion peaks with a mass of 265 and 266 which were equal in intensity to each other, due to the 1:1 isotopic abundance of bromine, which represented the molecular mass of the amide + hydrogen. On the basis of this evidence the solid was identified as 2-bromo-*N*-1-naphthylacetamide (**119**).

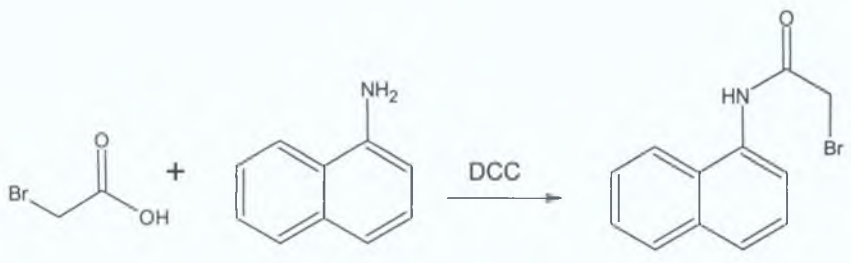

(118) (102) (119)

Figure 2-12: *Reaction between bromoacetic acid (**118**) and 1-naphthylamine (**102**) using activating agent 1,3-dicyclohexylcarbodiimide.*

In order to develop a sensor molecule that could function as a chiral sensor we decided to introduce a chiral fluorescent amine as a building block, which is why S-naphthylethylamine (**103**) was chosen as the amine for an alternative coupling reaction. (**118**) was placed in dichloromethane solution with (**103**) under nitrogen, cooled to 0°C, followed by the addition of DCC. After thirty minutes at this temperature the reaction mixture was allowed to warm up to room temperature and proceed for 6 hours, which resulted in pale orange needles with m.p. 130-131°C. The IR spectrum of this solid displayed a peak at 1650cm^{-1} which represents the carbonyl stretch of the amide group. The ^{1}H-NMR spectrum displayed two doublets at 3.82ppm and 3.87ppm (J=13.2Hz), which represent the two protons of the methylene group between the bromine and amide functions. On the basis of this evidence the solid was identified as 2-bromo-N-[1-(1-naphthyl)ethyl]-acetamide (**120**).

Tryptophan is an essential amino acid, which is both chiral in nature and has a delocalised π-system, which undergoes fluorescence. The methyl-ester derivative of this amine (**104**) is inexpensive and can be easily purchased, and would provide an interesting comparison to the previous chiral amine described. (**118**) and (**104**) were placed in dichloromethane solution under nitrogen, cooled to 0°C, followed by the addition of DCC. After thirty minutes at this temperature the reaction mixture was allowed to warm up to room temperature and to proceed for 6 hours, which resulted in a light brown solid, m.p. 140-141°C. The IR spectrum of this solid displayed peaks at 1672 and 1744 cm^{-1} which represents the carbonyl stretching of the amide and ester groups. The ^{1}H-NMR spectrum displayed a singlet at 3.98ppm, which represents the two protons of the methylene group between the bromine and amide

functions. The chiral hydrogen of the residue was shifted to 4.93ppm (from 3.87ppm in the starting material) and a single doublet at 3.8ppm represent the protons of the $-CH_2-$ between the chiral centre and indole group, which were represented in the starting material by two sets of double doublets. On the basis of this evidence the solid was identified as 2-bromo-*N*-acetamide methyl tryptophanoate (**121**) m.p. lit. 141-142°C. [**4**].

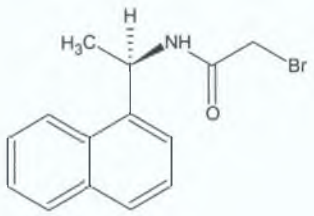

(**120**)

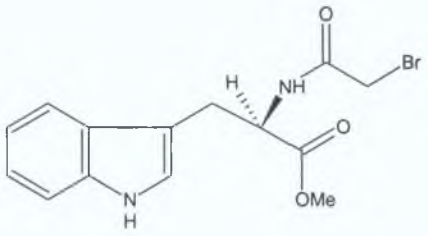

(**121**)

Having successfully formed the desired fluorescent amide subgroups it was then necessary to append these to the p-allyl calix[4]arene. This was attempted by a series of reactions employing calix[4]arene (**106**) and p-allyl calix[4]arene (**108**).

2.2.4.2 Synthesis of calixarene amides

Calix[4]arene (**106**) was refluxed in acetone with (**119**) and potassium carbonate for five days. This yielded a white solid that was identified as a mixture of products by thin layer chromatography (TLC). Purification by column chromatography isolated two products as white crystalline solids. The first product isolated had a m.p. 270-272°C, and the IR spectrum of this solid had peaks at 3388, 3289 and 1677cm^{-1} representing hydroxy, amine and carbonyl stretching correspondingly. The ^{1}H-NMR spectrum of this solid had two sets of doublets at 3.38 and 3.55ppm and at 4.05 and 4.29ppm representing the eight protons of the methylene bridges between the phenol units of the calixarene. A singlet was observed at 4.82ppm, which represents two protons of the ether to carbonyl methylene group. Mass spectral data of this solid showed a molecular ion with a mass of 630, which represented the molecular mass of the monoamide + sodium. On the basis of this evidence the solid was identified as mono-*N*-1-acetamide calix[4]arene (**122**).

The second product isolated had a m.p. 294-296°C, and peaks at 1686 and 3336cm^{-1} in its IR spectrum representing carbonyl and hydroxy stretching. The ^{1}H-NMR spectrum of this solid had two sets of doublets at 3.38 and 3.55ppm and at 4.05 and 4.29ppm representing the eight protons of the methylene bridges between the

phenol units of the calixarene. A singlet was observed at 4.82ppm which represents two protons of the ether to carbonyl methylene group. Mass spectral data of this solid showed a molecular ion with a mass of 813, which represents the molecular mass of the di-amide + sodium. On the basis of this evidence the solid was identified as 26, 28-di-*N*-1-acetamide calix[4]arene (**123**).

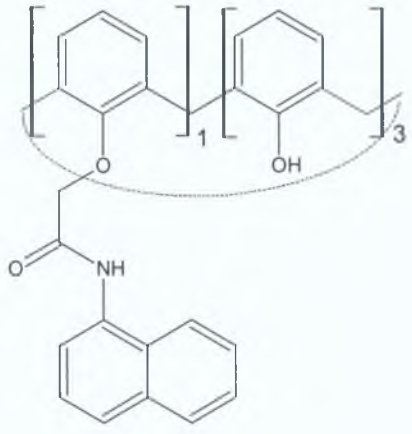

(**122**)

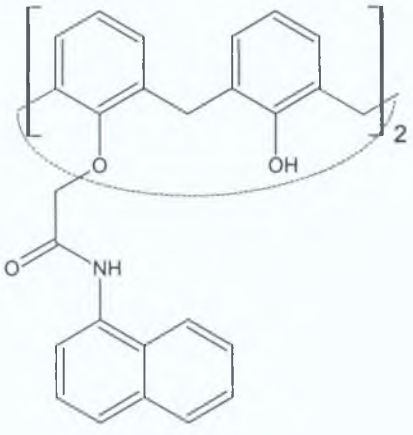

(**123**)

Tetra-*p*-allyl calix[4]arene (**108**) was refluxed in acetone with (**119**) and potassium carbonate for five days. This yielded a white solid, which was identified as a mixture of products by thin layer chromatography (TLC). Purification by column chromatography isolated two products. The first product had a m.p. 210-214°C, and carbonyl, amine and hydroxy stretching in its IR spectrum represented by peaks at 1696, 3312 and 3364cm^{-1}. The ^{1}H-NMR spectrum of this solid had two sets of doublets at 2.98 and 3.27ppm representing the eight alkyl protons of the allyl systems. A singlet was observed at 4.44ppm, which represents four protons of two ether to carbonyl methylene groups. Two multiplets, which are characteristic of the allylic proton were observed at 5.66 and 5.92ppm. Mass spectral data of this solid showed a molecular ion with a mass of 973, which represented the molecular mass of the *p*-allyl di-amide + sodium. On the basis of this evidence the solid was identified as 5, 11, 17, 23-tetraallyl-25, 27-di-*N*-1-acetamide calix[4]arene (**124**).

The second solid isolated from this reaction had a m.p. 130-134°C, and carbonyl and hydroxy stretching represented by peaks at 1677 and 3349cm^{-1} in its IR spectrum. The ^{1}H-NMR spectrum of this solid had three sets of doublets at 2.75, 2.91 and 3.24ppm, representing the eight alkyl protons of the allyl systems. Three multiplets, which are characteristic of the allylic proton, were observed at 5.50, 5.66 and 5.87ppm. Mass spectral data of this solid showed a molecular ion with a mass of 1156, which represented the molecular mass of the *p*-allyl tri-amide + sodium. On the

basis of this evidence the solid was identified as 5, 11, 17, 23-tetraallyl-25, 26, 27-tri-*N*-1-acetamide calix[4]arene (**125**).

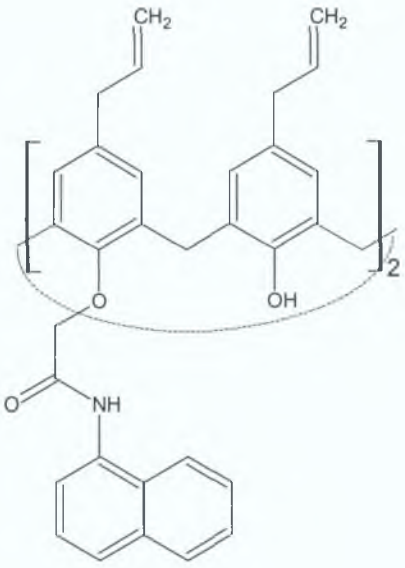

(**124**)

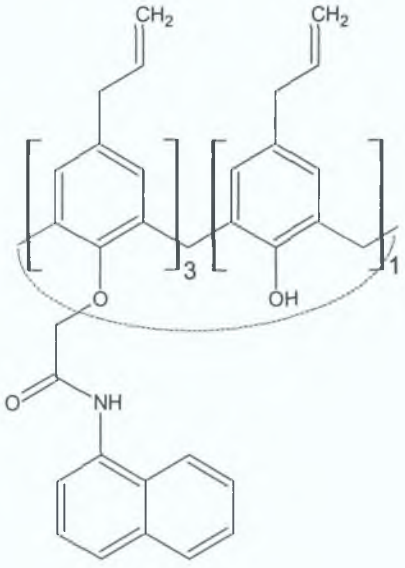

(**125**)

(**108**) was refluxed in acetone with (**120**) and potassium carbonate for five days. This yielded a light brown solid, which was identified as a mixture of products by thin layer chromatography (TLC). After column chromatography an off-white solid was obtained with m.p. 120-124°C, the IR spectrum of which had carbonyl-amide, hydroxy and amine stretching represented by peaks at 1675, 3323 and 3403cm^{-1} respectively. The ^{1}H-NMR spectrum of this solid had characteristic multiplets of the naphthalene rings between 7.12 and 7.48ppm, the two chiral hydrogens of the appended amides was represented by two multiplets at 6.02 and 5.64ppm, and the three methyl protons adjacent to the chiral centre were represented by two doublets at 1.89 and 1.32ppm. Mass spectral data of this solid showed a molecular ion with a mass of 1029, which represented the molecular mass of the *p*-allyl di-amide (**126**) + sodium. On the basis of this evidence the solid was identified as 5, 11, 17, 23-tetraallyl-25, 27-di-*N*-[1-(1-naphthyl)ethyl]-acetamide calix[4]arene (**126**).

(**108**) was refluxed in acetone with (**121**) and potassium carbonate for five days. This yielded a yellow solid, which was identified as a mixture of products by thin layer chromatography (TLC). After column chromatography an off-white solid was obtained with m.p. 100-104°C, the IR spectrum of which had carbonyl-amide and –ester, hydroxy and amine stretching represented by peaks at 1676, 1744, 3309 and 3504cm^{-1} respectively. The ^{1}H-NMR spectrum of this solid had a multiplet between 7.09 and 7.28ppm, representing the protons of the indole system. The chiral hydrogen of the tryptophan subunit was represented by a multiplet at 5.34ppm, and

the three methyl ester protons were represented by a singlet at 3.88ppm. Mass spectral data of this solid showed a molecular ion with a mass of 865, which represented the molecular mass of the *p*-allyl mono-amide (**127**) + sodium. On the basis of this evidence the solid was identified as 5, 11, 17, 23-tetraallyl-25-mono-*N*-acetamide methyl tryptophanoate calix[4]arene (**127**).

In order to prove whether the di-amides produced were substituted at adjacent or opposite hydroxy groups on the calix[4]arenes, it was necessary to prepare one of these isomers to compare with the products previously obtained. The synthesis of 1,3-dialkylated calix[4]arenes has undergone extensive study in our research and literature preparation have been much improved on by Wall [**5**]. This provides a relatively simple manner in which calix[4]arenes are stirred at room temperature in acetonitrile for four days, with two equivalents of the desired alkyating group and one equivalent of base, which yields a di-alkylated calix[4]arene with substitution occurring at opposite phenoxy groups. Subsequent purification by column chromatography produces the 1,3-di-alkylated calixarene in approximately 50% yield. The calix[4]arene (**123**) and *p*-allyl calix[4]arenes (**124**) and (**126**) were produced in this manner, and had spectroscopic data consistent with the products obtained by the reaction in refluxing acetone. This then proved what was already suggested by the corresponding ^{1}H-NMR spectra, that the di-alkylated products obtained by reaction in acetone were 1,3 in nature.

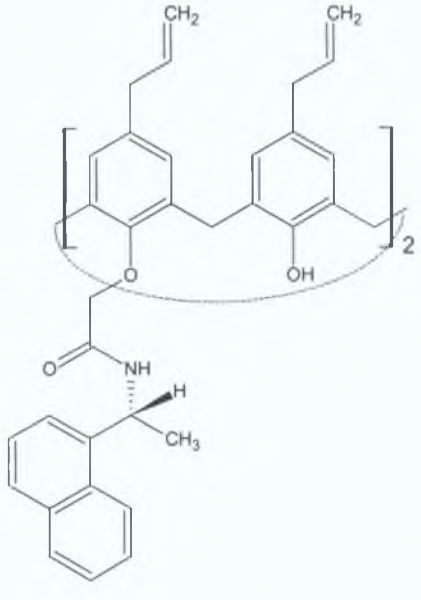

(**126**)

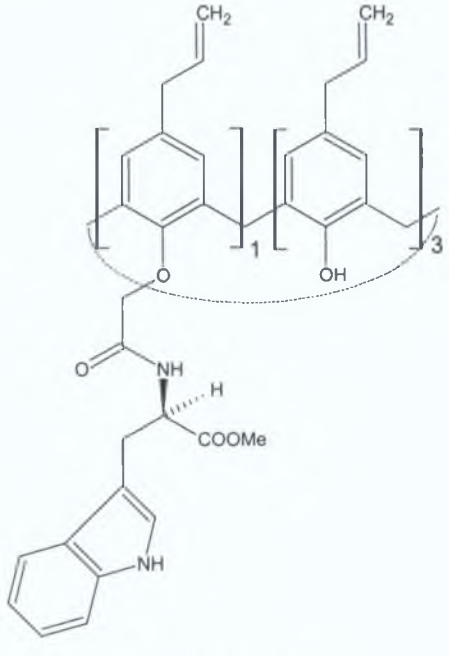

(**127**)

Since calix[4]arene esters and amides have such interesting and varying ion-binding and ion-selectivity properties, it was also considered how mixing these types of groups would change the host : guest characteristics of these molecules.

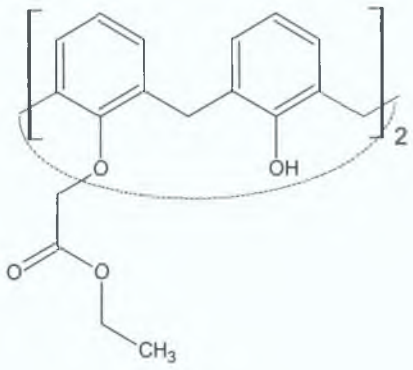

(**128**)

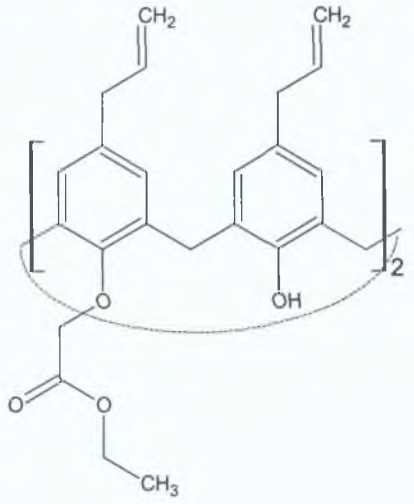

(**129**)

(**106**) was stirred in acetonitrile at room temperature followed by the addition of two equivalents of ethyl bromoacetate and one equivalent of potassium carbonate for four days under N_2. This yielded a white solid m.p. 172-174°C, the IR spectrum of which displayed a carbonyl stretch at 1753cm^{-1} and a hydroxy stretch at 3425cm^{-1}. The ^{1}H-NMR spectrum displayed a singlet at 4.77ppm representing the two protons of the ether linkage to the carbonyl group and a quartet and triplet at 4.37 and 1.39ppm representing two and three protons each of the ester group. Mass spectral data of this solid showed a molecular ion with a mass of 635, which represented the molecular mass of the di-alkylated calix[4]arene + potassium. On the basis of this evidence the solid was identified as 25, 27-diethylester calix[4]arene (**128**).

(**108**) was stirred in acetonitrile at room temperature followed by the addition of two equivalents of ethyl bromoacetate and one equivalent of base. This yielded a white solid m.p. 72°C, the IR spectrum of which displayed a carbonyl stretch at 1754cm^{-1}, a hydroxy stretch at 3422cm^{-1}, and a hydroxy stretch at 3364cm^{-1}. The ^{1}H-NMR spectrum displayed a singlet at 4.76ppm representing the two protons of the ether linkage to the carbonyl group and a quartet at 4.35ppm and a triplet at 1.38ppm representing two and three protons of the ester group respectively. Mass spectral data of this solid showed a molecular ion with a mass of 779, which represented the molecular mass of the di-alkylated calix[4]arene + sodium. On the basis of this evidence the solid was identified as 5, 11, 17, 23-tetraallyl-25, 27-diethylester calix[4]arene (**129**).

(**128**) was refluxed in acetone with (**119**) and potassium carbonate for five days. This yielded a white solid that was identified as a complex mixture of products by thin layer chromatography (TLC). However following several attempts at purification by liquid chromatography, only starting materials were isolated.

(**129**) was refluxed in acetone with (**119**) and potassium carbonate for five days. After purification by liquid chromatography an off-white solid was isolated with m.p. 86-88°C. The IR spectrum of this compound displayed a carbonyl stretch at 1757cm^{-1}, an amide stretch at 1637cm^{-1}, an amine stretch at 3327cm^{-1}, and a hydroxy stretch at 3344cm^{-1}. The ^{1}H-NMR spectrum of this solid was very complicated and requires further study for complete characterisation. Mass spectral data of this solid showed a molecular ion with a mass of 962, which represents the molecular mass of the *p*-allyl calix[4]arene di-ester mono-amide + sodium. On the basis of this evidence the solid was identified as 5, 11, 17, 23-tetraallyl-25, 27-diethylester-26-mono-*N*-naphthylacetamide calix[4]arene (**130**).

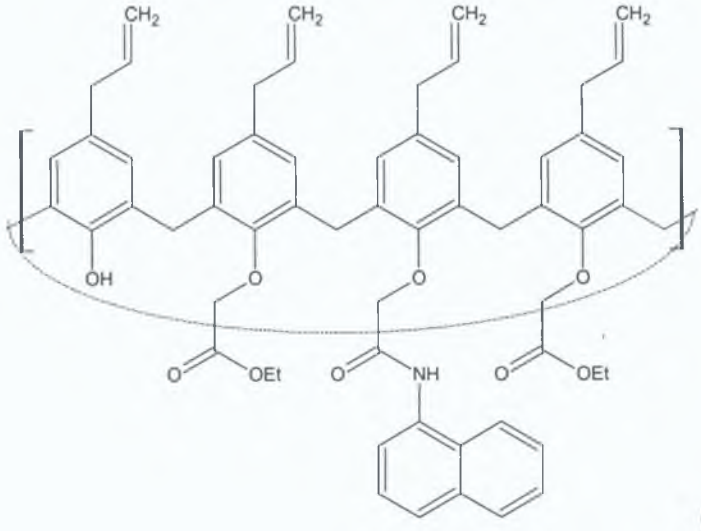

(130)

These results indicate that a five-fold excess of alkylating agent in conjunction with potassium carbonate as base are not suitable conditions for the full alkylation of calix[4]arenes.

2.3 Conclusion

The synthesis of **L1** was successful via the acid chloride route (section 2.2.1). This synthesis however is quite long, and therefore an attempt was made to shorten the number of reaction steps. Using DCC as a coupling agent to form amides directly from calixarene tetra-acids does not achieve tetra-substituted amides. It was necessary therefore to find an alternative route to produce tetra-amide substituted calixarenes. The cost of the appended ligand S-propranolol in **L1** was considered expensive as a building block for a sensor molecule. Bearing this mind 1-naphthylamine (**102**), S-naphthylethylamine (**103**) and tryptophan methyl ester (**104**) were chosen as appendages due to their low cost, ready availability and suitable fluorescent and hydrogen bonding properties.

The alternative route taken to produce calixarene tetra-amides involved two steps

1. formation of the amide moiety
2. attachment of amide moieties to calixarene backbone

The first of these two steps was carried out successfully and led to the formation of three amide units (**119**), (**120**) and (**121**). The second step however suffered from partial substitution, and resulted in a series of mono, di and tri substituted fluorescent calixarenes. A five-fold excess of the amide moiety was used which is not sufficient to complete the tetra-substitution. Potassium carbonate as base may not be strong enough to allow the reaction to go to completion. A stronger base with a greater excess of alkylating agent (amide) could possibly produce tetra-substituted amides.

2.4 *Experimental*

2.4.1 Procedure and Equipment

IR spectral analysis was carried out on a Nicolet Impact 410 FTIR. KBr was purchased from Sigma-Aldrich of puriss grade (99%).

^{1}H-NMR spectra were obtained using a Bruker Avance (400MHz) instrument. Measurements were generally carried out in $CDCl_3$ unless otherwise stated. Chemical shifts were recorded relative to TMS. The spectra were converted from their free induction decay (FID) profiles using XWIN-NMR software.

Mass spectral data was obtained using a Brucker/Hewlett-Packard Esquire LC-MS. Measurements were carried out using electrospray ionisation (ESI) after direct injection into the ESI source (positive mode) at a rate of 5μl min^{-1}. The nebulisation gas and drying gas were set to 15 psi and 4 l min^{-1} respectively and the source temperature maintained at 250 °C. The octupole voltage was 2.83 V, skimmer 1 voltage was 50 ± 5 V and the trap drive voltage was 57 ± 2 V. All samples were dissolved in acetonitrile at a concentration of approximately 0.1mg/ml.

TLC plates used were purchased from Fluka, and were silica gel TLC cards, 0.2mm layer thickness.

2.4.2 Synthetic Procedures

Calix[4]arene (106) [1]

A slurry of *p-t*-butyl calix[4]arene (**105**) (26.60g, 41.0mmol), phenol (18g, 190mmol) and aluminium chloride (28g, 210mmol) was stirred in dry Toluene (250cm^3) under nitrogen at room temperature for one hour. 500cm^3 of HCl (0.2M) was added to the reaction mixture in an ice bath. The two-phase system was separated and the organic layer was reduced *in vacuo* and treated with methanol which precipitated the pure white dealkylated tetramer in 74% yield, (12.80g).

m.p. 314-318°C. Lit.[**1**] 315-318°C.

I.R.υ_{max} (KBr) [cm^{-1}]: 3157 (OH str.)

^{1}H-NMR (400MHz) δ ($CDCl_3$) [ppm]: 3.55 (8H, d, broad, Ar-C$\underline{H}_A$-Ar), 4.25 (8H, d, broad, Ar-C$\underline{H}_B$-Ar), 6.73 - 7.08 (12H, m, ArH, 2, 3 and 4) 10.22 (4H, s, Ar-O$\underline{H}$).

25,26,27,28-Tetra-o-allyl-calix[4]arene (107) [2]

Calix[4]arene (**106**) (9.81, 23.3mmol) was added to a solution of sodium hydride (4.44g, 186mmol) in dry THF/DMF (4:1, 100cm^3) under N_2 and the reaction was refluxed with stirring for 30 minutes. The reaction was cooled and allyl bromide (22.50g, 186mmol) was added and the reaction mixture was maintained at reflux for 3 days. Excess sodium hydride was carefully destroyed by addition of water. The mixture was reduced *in vacuo* and the residue partitioned between dichloromethane and water. The organic layer was separated, dried over magnesium sulphate, the solvent was evaporated and the resulting residue was recrystallised from methanol/ dichloromethane to give white needles in 63% yield, (8.40g).

m.p. 188-188.5°C. Lit.[**2**] 186-187°C.

I.R.υ_{max} (KBr) [cm^{-1}]: 2815, 2922 (CH-aliphatic str.), 3005, 3112 (CH-aromatic str.)

^{1}H-NMR (400MHz) δ ($CDCl_3$) [ppm]: 3.07 (4H, d, J=13.6Hz, Ar-C$\underline{H}_A$-Ar), 4.34 (4H, d, J=13.6Hz, Ar-C$\underline{H}_B$-Ar), 4.39 (8H, d, J=6.4Hz, Ar-O-C$\underline{H}_2$-) 5.09-5.20 (8H, m, -CH=C$\underline{H}_2$(allyl)), 6.24-6.31 (4H, m, -C$\underline{H}$=CH_2(allyl)), 6.51 - 6.58 (12H, m, ArH, 2, 3 and 4).

5,11,17,23-Tetraallyl-calix[4]arene (108) [3]

Tetra-o-allyl-calix[4]arene (**107**), (6.30g, 10.8mmol) in N,N-diethylaniline (50cm^3) was refluxed for two hours under N_2. After acidification with conc. HCl and filtration, the crude product was recrystallised from isopropanol to give a cream coloured solid in 80% yield, (5.10 g).

m.p. 248-249°C. Lit.[**3**] 250.5-252°C.

I.R.υ_{max} (KBr) [cm^{-1}]: 3157 (OH str.)

^{1}H-NMR (400MHz) δ ($CDCl_3$) [ppm]: 3.22 (8H, d, J=6.8Hz, -C$\underline{H}_2$CH=CH$_2$) 3.48 (4H, d, J=13.6Hz, Ar-C$\underline{H}_A$-Ar), 4.24 (4H, d, J=13.6Hz, Ar-C$\underline{H}_B$-Ar), 5.05-5.10 (8H, m, -CH=C$\underline{H}_2$), 5.85-5.95 (4H, m, -C$\underline{H}$=CH$_2$), 6.88 (8H, s, ArH, 2 and 4) 10.18 (4H, s, -O$\underline{H}$).

5,11,17,23-Tetraallyl-25,26,27,28-tetra(ethoxycarbonylmethyl)calix[4]arene (109)

Tetra-(*p*-allyl)-calix[4]arene (**108**), (5.10g, 8.8mmol) was refluxed in dry acetone (60 cm^3) with anhydrous K_2CO_3 (7.80g, 52.8mmol) and ethyl bromoacetate (18.8cm^3, 74.8mmol) under N_2 for five days. The reaction mixture was filtered, concentrated and redissolved in $CHCl_3$, which was then washed, dried, filtered and concentrated, and the residue recrystallised from dichloromethane/ methanol to give a white crystalline solid in 50% yield, (4.06 g).

m.p. 97.5-98.5°C.

I.R.υ_{max} (KBr) [cm^{-1}]: 1757 (C=O str.)

^{1}H-NMR (400MHz) δ ($CDCl_3$) [ppm]: 1.20 (12H, t, -O-CH$_2$C$\underline{H}_3$) 2.98 (8H, d, J=6.8Hz, Ar-C$\underline{H}_2$-(allyl)) 3.08 (4H, d, J=13.6Hz, Ar-C$\underline{H}_A$-Ar), 4.09-4.17 (12H, Ar-C$\underline{H}_B$-Ar and -O-C$\underline{H}_2$CH$_3$ overlapping), 4.65 (8H, s, -O-C$\underline{H}_2$-CO-) 4.73-4.89 (8H, m, -CH=C$\underline{H}_2$(allyl)), 5.67-5.71 (4H, m, -C$\underline{H}$=CH$_2$(allyl)), 6.42 (8H, s, ArH, 2 and 4).

5,11,17,23-Tetra(2-hydroxyethyl)-25,26,27,28-tetra(ethoxycarbonylmethyl)-calix[4]arene (110) [3]

Tetra-(*p*-allyl)-tetra-ethyl ester (**109**) (2.25g, 3.5mmol) in dichloromethane/methanol (3:1, 40cm^3) was cooled in a dry ice/ acetone bath and treated with O_3 until ozone was present in excess. Nitrogen was then bubbled through the solution and sodium borohydride (1.65g, 43.5mmol) was added. This reaction mixture was stirred at room

temperature for 4 hours, poured onto an ice-cold dilute HCl solution and partitioned between dichloromethane and water to yield a crude sample as a white resin. Recrystallisation from 3:5 acetone: hexane produced white microcrystals in 50% yield, (1.65g).

m.p. 68-70°C.

I.R.υ_{max} (KBr) [cm^{-1}]: 1758 (C=O str.), 3414 (OH str.)

^{1}H-NMR (400MHz) δ ($CDCl_3$) [ppm]: 1.15 (12H, t, -COO-$CH_2\underline{CH_3}$) 2.57 (8H, t, Ar-$CH_2\underline{CH_2}$OH) 3.09 (4H, d, J=13.6Hz, Ar-$\underline{CH_A}$-Ar), 3.57 (8H, t, Ar-$CH_2\underline{CH_2}$OH) 4.01 (1H, s, broad, ArO$\underline{H}$) 4.21 (8H, q, -COO-$\underline{CH_2}CH_3$), 4.79 (8H, s, O-$\underline{CH_2}$-CO-), 4.85 (4H, d, J=13.6Hz, Ar-$\underline{CH_B}$-Ar), 6.62 (8H, s, ArH, 2 and 4).

5,11,17,23-Tetraallyl-25,26,27,28-tetra(carboxymethyl)calix[4]arene (112)

Tetra-(*p*-allyl)-tetra-ethyl ester (**109**) (2.03g, 2.2mmol) was hydrolysed to its carboxylic acid sodium salt by refluxing with NaOH (1.67g, 42.0mmol) in ethanol (50 cm^3), followed by acidification with 50% aqueous H_2SO_4 and filtration to give 87% of the corresponding acid, (1.55 g).

m.p. decomposed above 220°C.

I.R.υ_{max} (KBr) [cm^{-1}]: 1685 (C=O str.), 3433 (OH str.)

^{1}H-NMR (400MHz) δ ($CDCl_3$) [ppm]: 3.13 (8H, d, J=6.8Hz, Ar-$\underline{CH_2}$-(allyl)) 3.27 (4H, d, J=13.6Hz, Ar-$\underline{CH_A}$-Ar), 4.35 (12H, Ar-$\underline{CH_B}$-Ar and -O-$\underline{CH_2}$-CO- overlapping), 4.96-5.03 (8H, m, -CH=$C\underline{H_2}$(allyl)), 5.79-5.81 (4H, m, -$\underline{CH}$=CH_2(allyl)), 6.84 (8H, s, ArH, 2 and 4).

ESIMS (acetonitrile) m/e (rel intensity): 839 (MNa^+,100%).

5,11,17,23-Tetraallyl-25,26,27,28-tetra[(S-propranolol-amide)oxy]calix[4]arene (115) L1

Tetra-(*p*-allyl)-tetra-acid (**112**) (0.31g, 0.40mmol) was subsequently converted to the acid chloride by a 2 hour reflux in thionyl chloride (10cm^3), followed by removal of volatiles, which was used immediately. To the acid chloride (**113**) (0.30g, 0.40mmol) in dry THF (5cm^3), S-propranolol (0.44g, 1.6 mmol) and triethylamine (0.24cm^3, 1.6mmol) was added with stirring at room temperature for 24 hours. A pale yellow

product was isolated, and purified by column chromatography (silica, ethyl acetate / methanol). This yielded a yellow solid in 40% yield, (0.27g) (**115**, **L1**).

m.p. decomposes above 190°C

I.R.υ_{max} (KBr) [cm^{-1}]: 1654 (C=O str.(amide)), 3435 (OH str.)

^{1}H-NMR (400MHz) δ ($CDCl_3$) [ppm]: 1.13 and 1.37 (12H each, N-CH-($C\underline{H}_3$)$_2$), 3.09-3.15 (12H, Ar-$C\underline{H}_A$-Ar and Ar-$C\underline{H}_2$-(allyl) overlapping), 3.4-4.1 (20H, overlaping, N-$C\underline{H}_2$, N-C$\underline{H}$, $C\underline{H}_2$-O-Naphth), 4.2-4.7 (16H, overlapping, chiral C$\underline{H}$, Ar-$C\underline{H}_B$-Ar, Ar-O-$C\underline{H}_2$), 4.94 and 4.96 (d, 4H each, CH-$C\underline{H}_2$(allyl)), 5.8 (m, 4H, CH_2-C$\underline{H}$=CH_2), 6.62 (d, 4H, naphthyl), 6.8 (8H, s, phenolic benzene), 7.19 (d, 4H, naphthyl), 7.35 (m, 12H naphthyl), 7.66 (d, 4H, naphthyl), 8.19 (d, 4H, naphthyl).

ESIMS (acetonitrile) m/e (rel intensity): 1805 (MNa^+,100%).

5,11,17,23-Tetraallyl-mono[(R-propranolol-amide)oxy]calix[4]arene (117a)

5,11,17,23-Tetraallyl-di[(R-propranolol-amide)oxy]calix[4]arene (117b)

Tetra-(*p*-allyl)-tetra-acid (**113**) (0.12g, 0.14mmol) was dissolved in anhydrous dichloromethane (30cm^3) with R-propranolol (0.15g, 0.58mmol) and triethylamine (0.06g, 0.58mmol). The mixture was cooled to 0°C, and 1,3-dicyclohexylcarbodiimide (0.12g, 0.58mmol) added. After 30 minutes the solution was raised to room temperature and the reaction allowed to proceed for 24hr. The precipitated N,N-dicyclohexylurea was removed by filtration and the filtrate washed with dilute HCl solution and water and subsequently dried over magnesium sulphate. The solvent was evaporated in vacuo and the residue purified by column chromatography (silica, ethyl acetate / methanol). This yielded the title products, as a mixture of mono and di-substituted calix[4]arene as a yellow solid (0.103g, 40%).

m.p. decomposes above 200°C.

I.R.υ_{max} (KBr) [cm^{-1}]: 1619-1654 (broad, C=O str.(amide) and C=O str.(amide) overlapping), 3448 (broad, OH str.)

ESIMS (acetonitrile) m/e (rel intensity): 1097(monoamide), 1336.6(diamide) (MK^+,100%).

2-Bromo-*N*-1-naphthylacetamide (119)

Bromoacetic acid (**118**) (4.36g, 31.4mmol) was dissolved in anhydrous dichloromethane (50cm^3) with 1-naphthylamine (**102**) (4.50g, 31.4mmol). The mixture was cooled to 0°C, and 1,3-dicyclohexylcarbodiimide (6.48g, 31.4mmol) added. After 30 minutes the solution was raised to room temperature and the reaction allowed to proceed for 6hr. The precipitated N,N-dicyclohexylurea was removed by filtration and the filtrate washed with water and dried over magnesium sulphate. The solvent was evaporated in vacuo and recrystallisation from acetonitrile yielded the title product as an off-white solid in 48% yield, (3.98g).

m.p. 148-150°C.

I.R.υ_{max} (KBr) [cm^{-1}]: 1660 (C=O str.(amide)), 3255 (NH str.)

^{1}H-NMR (400MHz) δ ($CDCl_3$) [ppm]: 4.16 (2H, s, Br-C$\underline{H}_2$-CONH-), 7.46-7.57 (3H, m, naphthyl), 7.73 (1H, d, J=8Hz, naphthyl), 7.86-7.91 (3H, m, naphthyl), 8.72 (1H, s, broad, -N$\underline{H}$-).

ESIMS (acetonitrile) m/e (rel intensity): 265, 266 (MH^+,100%).

2-Bromo-N-[1-(1-naphthyl)ethyl]acetamide (120)

Bromoacetic acid (**118**) (2.18g, 15.7mmol) was dissolved in anhydrous dichloromethane (30cm^3) with S-naphthylethylamine (**103**) (2.69g, 15.7mmol). The mixture was cooled to 0°C, and 1,3-dicyclohexylcarbodiimide (3.24g, 15.7mmol) added. After 30 minutes the solution was raised to room temperature and the reaction allowed to proceed for 6hr. The precipitated N,N-dicyclohexylurea was removed by filtration and the filtrate washed with water and dried over magnesium sulphate. The solvent was evaporated in vacuo and recrystallisation from acetonitrile yielded the title product as an off-white solid in 52% yield, (2.38g).

m.p. 130-131°C.

I.R.υ_{max} (KBr) [cm^{-1}]: 1650 (C=O str.(amide)), 3269 (NH str.)

^{1}H-NMR (400MHz) δ ($CDCl_3$) [ppm]: 1.69 (3H, d, J=6.8Hz, -CH-C$\underline{H}_3$), 3.82 (1H, d, J=13.2Hz, Br-C$\underline{H}_2$-CONH-), 3.87 (1H, d, J=13.2Hz, Br-C$\underline{H}_2$-CONH-), 5.90 (1H, m, -C$\underline{H}$-CH_3), 6.94 (1H, d, broad, NH), 7.46-7.59 (3H, m, naphthyl), 7.83 (1H, d, J=8Hz, naphthyl), 7.90 (1H, d, J=8Hz, naphthyl), 8.05 (1H, d, J=8Hz, naphthyl).

2-bromo-*N*-acetamide methyl tryptophanoate (121)

Bromoacetic acid (**118**) (2.18g, 15.7mmol) was dissolved in anhydrous dichloromethane (30cm^3) with tryptophan methyl ester (**104**) (3.40g, 15.7mmol). The mixture was cooled to 0°C, and 1,3-dicyclohexylcarbodiimide (3.24g, 15.7mmol) added. After 30 minutes the solution was raised to room temperature and the reaction allowed to proceed for 6hr. The precipitated N,N-dicyclohexylurea was removed by filtration and the filtrate washed with water and dried over magnesium sulphate. The solvent was evaporated in vacuo and yielded the title product as a light brown solid in 47% yield (2.15g).

m.p. 140-141°C. Lit.[**4**] 141-142°C.

I.R.υ_{max} (KBr) [cm^{-1}]: 1672 (C=O str.(amide)), 1744 (C=O str.(ester)), 3400 (NH str.), 3478 (NH str.).

^{1}H-NMR (400MHz) δ ($CDCl_3$) [ppm]: 3.38 (2H, m, -C$\underline{H}_2$-CHNH$_2$), 3.70 (3H, s, -COOC$\underline{H}_3$), 3.98 (2H, s, Br-C$\underline{H}_2$-CONH-), 4.94 (1H, m, -CH$_2$-C$\underline{H}$NH$_2$), 6.99 (1H, s, broad -CON$\underline{H}$-), 7.14-7.23 (3H, m, indole), 7.35 (1H, d, J=8Hz, indole), 7.56 (1H, d, J=8Hz, indole), 8.72 (1H, s, broad, -NH(indole)).

28-mono-carboxymethyl-calix[4]arene-1-naphthylamide (122)

26, 28-di-carboxymethyl-calix[4]arene di(1-naphthylamide) (123)

Calix[4]arene (**106**), (0.2g, 0.47mmol) was refluxed in 30cm^3 of dry acetone with anhydrous K_2CO_3 (0.326g, 2.35mmol) and 2-bromo-N-1-naphthyl-acetamide (**119**) (0.62g, 2.35mmol) under N_2 for five days. The reaction mixture was filtered, the solvent was evaporated *in vacuo*, and the residue purified by column chromatography (silica, ethyl acetate / hexane, 4:1). This yielded two white solids in 30% yield (0.09g) (Rf: 0.16) (**122**) and 28% yield (0.11g) (Rf:0.13) (**123**).

Analysis for (**122**): m.p. 270-272°C.

I.R.υ_{max} (KBr) [cm^{-1}]: 1677 (C=O str.(amide)), 3289 (NH str.), 3388 (OH str.)

^{1}H-NMR (400MHz) δ ($CDCl_3$) [ppm]: 3.38 (2H, d, J=13.6Hz, Ar-C$\underline{H}_A$-Ar), 3.55 (2H, d, J=13.6Hz, Ar-C$\underline{H}_A$-Ar), 4.05 (2H, d, J=13.6Hz, Ar-C$\underline{H}_B$-Ar), 4.29 (2H, d, J=13.6Hz, Ar-C$\underline{H}_B$-Ar), 4.82 (4H, s, -O-C$\underline{H}_2$-CO-) 6.59-6.67 (3H, m, ArH, 2, 3 and 4), 6.84-6.91 (3H, m, ArH, 2, 3 and 4), 6.97-7.05 (6H, m, ArH, 2, 3 and 4), 7.46-7.55 (3H, m, naphthyl), 7.76-7.85 (3H, m, naphthyl), 8.14 (1H, d, J=8Hz, naphthyl), 9.12 (2H, s, OH), 9.49 (1H, s, OH), 10.62 (1H, s, NH),.

ESIMS (acetonitrile) m/e (rel intensity): 630 (MNa^+,100%).

Analysis for (**123**): m.p. 294-296°C.

I.R.υ_{max} (KBr) [cm^{-1}]: 1686 (C=O str.(amide)), 3336 (NH str.), 3400 (OH str.)

^{1}H-NMR (400MHz) δ ($CDCl_3$) [ppm]: 3.48 (4H, d, J=13.6Hz, Ar-C$\underline{H}_A$-Ar), 4.21 (4H, d, J=13.6Hz, Ar-C$\underline{H}_B$-Ar), 4.45 (4H, s, -O-C$\underline{H}_2$-CO-) 6.54 (2H, t, ArH, 3), 6.72 (4H, d, J=7.6Hz, ArH, 2 and 4), 6.78 (2H, t, ArH, 3), 7.04 (2H, t, naphthyl), 7.12 (4H, d, J=7.6Hz, ArH, 2 and 4), 7.26-7.33 (6H, m, naphthyl), 7.43 (2H, d, J=8Hz, naphthyl), 7.67 (2H, d, J=8Hz, naphthyl), 8.00 (2H, d, J=8Hz, naphthyl), 9.62 (2H, s, -NH).

ESIMS (acetonitrile) m/e (rel intensity): 813 (MNa^+,100%).

26, 28-di-carboxymethyl-calix[4]arene di(1-naphthylamide) (123) -[method by Wall-5]

Calix[4]arene (**106**), (2.5g, 5.88mmol) was stirred at room temperature in 30cm^3 of dry acetonitrile with anhydrous K_2CO_3 (0.81g, 5.88mmol) and 2-bromo-N-1-naphthyl-acetamide (**119**) (3.1g, 11.78mmol) under N_2 for four days. The reaction mixture was filtered, the solvent was evaporated *in vacuo*, and the residue purified by column chromatography (silica, ethyl acetate / hexane, 4:1). This yielded a white solid in 48% yield (2.23g).

m.p. 294-296°C.

I.R.υ_{max} (KBr) [cm^{-1}]: 1686 (C=O str.(amide)), 3336 (NH str.), 3400 (OH str.)

^{1}H-NMR (400MHz) δ ($CDCl_3$) [ppm]: 3.48 (4H, d, J=13.6Hz, Ar-C$\underline{H}_A$-Ar), 4.21 (4H, d, J=13.6Hz, Ar-C$\underline{H}_B$-Ar), 4.45 (4H, s, -O-C$\underline{H}_2$-CO-) 6.54 (2H, t, ArH, 3), 6.72 (4H, d, J=7.6Hz, ArH, 2 and 4), 6.78 (2H, t, ArH, 3), 7.04 (2H, t, naphthyl), 7.12 (4H, d, J=7.6Hz, ArH, 2 and 4), 7.26-7.33 (6H, m, naphthyl), 7.43 (2H, d, J=8Hz, naphthyl), 7.67 (2H, d, J=8Hz, naphthyl), 8.00 (2H, d, J=8Hz, naphthyl), 9.62 (2H, s, -NH).

ESIMS (acetonitrile) m/e (rel intensity): 813 (MNa^+,100%).

5,11,17,23-Tetraallyl-26, 28-di(carboxymethyl) calix[4]arene di(1-naphthylamide) (124)

5,11,17,23-Tetraallyl-25,26,27-tri(carboxymethyl) calix[4]arene tri(1-naphthylamide) (125)

Tetra-*p*-allyl calix[4]arene (**108**), (0.2g, 0.34mmol) was refluxed in 30cm^3 of dry acetone with anhydrous K_2CO_3 (0.237g, 1.7mmol) and 2-bromo-N-1-naphthyl-acetamide (**119**) (0.45g, 1.7mmol) under N_2 for five days. The reaction mixture was filtered, the solvent was evaporated *in vacuo*, and the residue purified by column chromatography (silica, ethyl acetate / hexane, 4:1). This yielded two white solids in 30% yield (0.10g) (Rf: 0.31) (**124**) and 33% yield (0.13g) (Rf: 0.17) (**125**).

Analysis for (**124**): m.p. 210-214°C.

I.R.υ_{max} (KBr) [cm^{-1}]: 1696 (C=O str.(amide)), 3312 (NH str.), 3364 (OH str.)

^{1}H-NMR (400MHz) δ ($CDCl_3$) [ppm]: 2.95 (4H, d, J=6.4Hz, Ar-C$\underline{H}_2$-(allyl)), 3.26 (4H, d, J=6.4Hz, Ar-C$\underline{H}_2$-(allyl)), 3.42 (4H, d, J=13.6Hz, Ar-C$\underline{H}_A$-Ar), 4.17 (4H, d, J=13.6Hz, Ar-C$\underline{H}_B$-Ar), 4.43 (4H, s, -O-C$\underline{H}_2$-CO-) 4.72-5.00 (8H, m, -CH=C$\underline{H}_2$(allyl)), 5.61-5.68 (2H, m, -C$\underline{H}$=CH$_2$(allyl)), 5.88-5.94 (2H, m, -C$\underline{H}$=CH$_2$(allyl)), 6.65 (4H, s, ArH, 2 and 4), 6.91 (4H, s, ArH, 2 and 4), 7.01-7.06 (4H, m, naphthyl), 7.26-7.31 (4H, m, naphthyl), 7.40 (2H, d, J=8Hz, naphthyl), 7.64 (2H, d, J=8Hz, naphthyl), 8.01 (2H, d, J=8Hz, naphthyl) 9.71 (2H, s, -N$\underline{H}$).

ESIMS (acetonitrile) m/e (rel intensity): 973 (MNa$^+$,100%).

Analysis for (**125**): m.p. 130-134°C.

I.R.υ_{max} (KBr) [cm^{-1}]: 1677 (C=O str.(amide)), 3349 (NH str.), 3449 (OH str.)

^{1}H-NMR (400MHz) δ ($CDCl_3$) [ppm]: 2.76 (2H, d, J=6.8Hz, Ar-C$\underline{H}_2$-(allyl)), 3.88-3.94 (4H, overlaid, Ar-C$\underline{H}_2$-(allyl)), 3.08 (1H, d, J=13.6Hz, Ar-C$\underline{H}_A$-Ar), 3.25 (4H, overlaid, 2H-Ar-C$\underline{H}_2$-(allyl) and 2H,-Ar-C$\underline{H}_A$-Ar), 3.67 (1H, d, J=13.6Hz, Ar-C$\underline{H}_A$-Ar), 3.87 (1H, d, J=13.6Hz, Ar-C$\underline{H}_B$-Ar), 3.98-4.07 (3H, m, 1H,-Ar-C$\underline{H}_B$-Ar and overlaid 2H,-O-C$\underline{H}_2$-CO-), 4.4 (1H, d, J=13.6Hz, Ar-C$\underline{H}_B$-Ar) 4.5 (1H, d, J=13.6Hz, Ar-C$\underline{H}_B$-Ar) 4.65-5.00 (8H, m, -CH=C$\underline{H}_2$(allyl) and overlaid 2H,-O-C$\underline{H}_2$-CO-), 5.48-5.50 (1H, m, -C$\underline{H}$=CH$_2$(allyl)), 5.65-5.67 (1H, m, -C$\underline{H}$=CH$_2$(allyl)), 5.85-5.92 (2H, m, -C$\underline{H}$=CH$_2$(allyl)), 6.49-6.73 (6H, m, ArH), 6.89-6.95 (6H, m, ArH), 7.05-7.45 (9H, m, naphthyl), 7.50-7.78 (8H, m, naphthyl), 7.90-8.01 (3H, m, naphthyl), 8.33-8.39 (1H, d, J=8Hz, naphthyl).

ESIMS (acetonitrile) m/e (rel intensity): 1156.5 (MNa$^+$,100%).

5,11,17,23-Tetraallyl-26, 28-di(carboxymethyl) calix[4]arene di(1-naphthylamide) (124) [method by Wall-5]

Tetra-*p*-allyl calix[4]arene (**108**), (1.30g, 2.22mmol) was stirred at room temperature in 30 cm^3 of dry acetonitrile with anhydrous K_2CO_3 (0.31g, 2.22mmol) and 2-bromo-1-N-naphthyl-acetamide (**119**) (1.17g, 4.44mmol) under N_2 for four days. The reaction mixture was filtered, the solvent was evaporated *in vacuo*, and the residue purified by column chromatography (silica, ethyl acetate / hexane, 4:1). This yielded a white solid in 50% yield (1.06g).

m.p. 210-214°C.

I.R.υ_{max} (KBr) [cm^{-1}]: 1696 (C=O str.(amide)), 3312 (NH str.), 3364 (OH str.)

^{1}H-NMR (400MHz) δ ($CDCl_3$) [ppm]: 2.95 (4H, d, J=6.4Hz, Ar-C$\underline{H}_2$-(allyl)), 3.26 (4H, d, J=6.4Hz, Ar-C$\underline{H}_2$-(allyl)), 3.42 (4H, d, J=13.6Hz, Ar-C$\underline{H}_A$-Ar), 4.17 (4H, d, J=13.6Hz, Ar-C$\underline{H}_B$-Ar), 4.43 (4H, s, -O-C$\underline{H}_2$-CO-) 4.72-5.00 (8H, m, -CH=C$\underline{H}_2$(allyl)), 5.61-5.68 (2H, m, -C$\underline{H}$=CH_2(allyl)), 5.88-5.94 (2H, m, -C$\underline{H}$=CH_2(allyl)), 6.65 (4H, s, ArH, 2 and 4), 6.91 (4H, s, ArH, 2 and 4), 7.01-7.06 (4H, m, naphthyl), 7.26-7.31 (4H, m, naphthyl), 7.40 (2H, d, J=8Hz, naphthyl), 7.64 (2H, d, J=8Hz, naphthyl), 8.01 (2H, d, J=8Hz, naphthyl) 9.71 (2H, s, -N$\underline{H}$).

ESIMS (acetonitrile) m/e (rel intensity): 973 (MNa^+,100%).

5,11,17,23-Tetraallyl-26, 28-di(carboxymethyl) calix[4]arene di(1-naphthylethylamide (126)

Tetra-*p*-allyl calix[4]arene (**108**), (0.20g, 0.34mmol) was refluxed in 30cm^3 of dry acetone with anhydrous K_2CO_3 (0.24g, 1.7mmol) and (**120**) (0.50g, 1.7mmol) under N_2 for five days. The reaction mixture was filtered, the solvent was evaporated *in vacuo*, and the residue purified by column chromatography (silica, ethyl acetate / hexane, 4:1). This yielded a white solid in 31% yield (0.11g).

m.p. 120-124°C.

I.R.υ_{max} (KBr) [cm^{-1}]: 1675 (C=O str.(amide)), 3323 (OH str.), 3403 (NH str.)

^{1}H-NMR (400MHz) δ ($CDCl_3$) [ppm]: 2.64 (1H, d, J=13.6Hz, Ar-C$\underline{H}_A$-Ar), 2.82 (2H, d, J=6.8Hz, Ar-C$\underline{H}_2$-(allyl)), 2.86 (2H, d, J=6.8Hz, Ar-C$\underline{H}_2$-(allyl)), 2.95 (1H, d, J=13.6Hz, Ar-C$\underline{H}_A$-Ar), 3.14 (2H, d, J=6.8Hz, Ar-C$\underline{H}_2$-(allyl)), 3.22-3.27 (3H, 2d overlapping, Ar-C$\underline{H}_2$-(allyl) and Ar-C$\underline{H}_A$-Ar) 3.33 (1H, d, J=13.6Hz, Ar-C$\underline{H}_A$-Ar), 3.52-3.63 (3H, 3d overlapping, Ar-C$\underline{H}_B$-Ar), 4.06, (2H, d, J=15.2Hz, -O-C$\underline{H}_2$-CO-), 4.29 (2H, 2d,

J=15.2Hz, -O-C$\underline{H}_2$-CO-), 4.72-5.01 (8H, m, -CH=C$\underline{H}_2$(allyl)), 5.52-5.63 (3H, m, -C$\underline{H}$=CH$_2$(allyl) and chiral H), 5.84-5.91 (2H, m, -C$\underline{H}$=CH$_2$(allyl)), 6.02-6.09 (1H, m, chiral H) 6.45-6.52 (4H, m, ArH), 6.55 (1H, s, ArH), 6.61 (2H, d, J=2.0Hz, ArH), 6.63 (2H, d, J=2.0Hz, ArH), 6.84(1H, s, ArH), 7.12-7.16 (2H, m, naphthyl), 7.19-7.40 (9H, m, naphthyl), 7.47(1H, d, J=6.8Hz, naphthyl), 7.57 (1H, d, J=8Hz, naphthyl), 7.63 (1H, d, J=8Hz, naphthyl), 8.89 (1H, d, J=7.6 Hz, NH) 9.38 (1H, d, J=7.2Hz, NH)

ESIMS (acetonitrile) m/e (rel intensity): 1029.5 (MNa^+,100%).

5,11,17,23-Tetraallyl-26, 28-di(carboxymethyl) calix[4]arene di(1-naphthylethylamide (126) [method by Wall-5]

Tetra-*p*-allyl calix[4]arene (**108**), (0.20g, 0.34mmol) was stirred at room temperature in 30 cm^3 of dry acetonitrile with anhydrous K_2CO_3 (0.05g, 0.34mmol) and (**120**) (0.20g, 0.68mmol) under N_2 for four days. The reaction mixture was filtered, the solvent was evaporated *in vacuo*, and the residue purified by column chromatography (silica, ethyl acetate / hexane, 4:1). This yielded a white solid in 50% yield (0.17g).

m.p. 120-124°C.

I.R.υ_{max} (KBr) [cm^{-1}]: 1675 (C=O str.(amide)), 3323 (OH str.), 3403 (NH str.)

^{1}H-NMR (400MHz) δ ($CDCl_3$) [ppm]: 2.64 (1H, d, J=13.6Hz, Ar-C$\underline{H}_A$-Ar), 2.82 (2H, d, J=6.8Hz, Ar-C$\underline{H}_2$-(allyl)), 2.86 (2H, d, J=6.8Hz, Ar-C$\underline{H}_2$-(allyl)), 2.95 (1H, d, J=13.6Hz, Ar-C$\underline{H}_A$-Ar), 3.14 (2H, d, J=6.8Hz, Ar-C$\underline{H}_2$-(allyl)), 3.22-3.27 (3H, 2d overlapping, Ar-C$\underline{H}_2$-(allyl) and Ar-C$\underline{H}_A$-Ar) 3.33 (1H, d, J=13.6Hz, Ar-C$\underline{H}_A$-Ar), 3.52-3.63 (3H, 3d overlapping, Ar-C$\underline{H}_B$-Ar), 4.06, (2H, d, J=15.2Hz, -O-C$\underline{H}_2$-CO-), 4.29 (2H, 2d, J=15.2Hz, -O-C$\underline{H}_2$-CO-), 4.72-5.01 (8H, m, -CH=C$\underline{H}_2$(allyl)), 5.52-5.63 (3H, m, -C$\underline{H}$=CH$_2$(allyl) and chiral H), 5.84-5.91 (2H, m, -C$\underline{H}$=CH$_2$(allyl)), 6.02-6.09 (1H, m, chiral H) 6.45-6.52 (4H, m, ArH), 6.55 (1H, s, ArH), 6.61 (2H, d, J=2.0Hz, ArH), 6.63 (2H, d, J=2.0Hz, ArH), 6.84(1H, s, ArH), 7.12-7.16 (2H, m, naphthyl), 7.19-7.40 (9H, m, naphthyl), 7.47(1H, d, J=6.8Hz, naphthyl), 7.57 (1H, d, J=8Hz, naphthyl), 7.63 (1H, d, J=8Hz, naphthyl), 8.89 (1H, d, J=7.6 Hz, NH) 9.38 (1H, d, J=7.2Hz, NH)

ESIMS (acetonitrile) m/e (rel intensity): 1029.5 (MNa^+,100%).

5,11,17,23-Tetraallyl -28-mono-carboxymethyl- calix[4]arene *N*-acetamide methyl tryptophanoate (127)

Tetra-*p*-allyl calix[4]arene (**108**), (0.2g, 0.34mmol) was refluxed in 30cm^3 of dry acetone with anhydrous K_2CO_3 (0.237g, 1.7mmol) and (**121**) (0.46g, 1.7mmol) under N_2 for five days. The reaction mixture was filtered, the solvent was evaporated *in vacuo*, and the residue purified by column chromatography (silica, ethyl acetate / hexane, 4:1). This yielded a white solid in 30% yield (0.09g).

m.p. 100-104°C.

I.R.υ_{max} (KBr) [cm^{-1}]: 1676 (C=O str.(amide)), 1744 (C=O str.(ester)), 3309 (OH str.), 3504 (NH str.).

^{1}H-NMR (400MHz) δ ($CDCl_3$) [ppm]: 3.18-3.23 (5H, overlaid, Ar-C$\underline{H}_2$-(allyl) and Ar-C$\underline{H}_A$-Ar), 3.27-3.21 (4H, m, Ar-C$\underline{H}_2$-(allyl)), 3.41-3.60 (5H, overlaid, Ar-C$\underline{H}_A$-Ar, CH-C$\underline{H}_2$-indole), 3.99 (2H, d, J=13.6Hz, Ar-C$\underline{H}_B$-Ar), 4.10 (2H, d, J=13.6Hz, Ar-C$\underline{H}_B$-Ar) 4.41 (1H, d, J=14.8Hz, -O-C$\underline{H}_2$-CO-), 4.67 (1H, d, J=14.8Hz, -O-C$\underline{H}_2$-CO-), 5.05-5.16 (8H, m, -CH=C$\underline{H}_2$(allyl) 5.30-5.36 (1H, m, chiral H), 5.80-6.04 (4H, m, -C$\underline{H}$=CH$_2$(allyl)), 6.86-6.92 (8H, m, ArH), 7.09-7.28 (4H, m, indole), 6.67 (1H, d, J=7.6Hz indole), 8.01 (1H, s, broad, NH-indole), 8.90 (1H, s, OH), 9.34 (2H, m, overlapping OH and NH), 9.53 (1H, s, OH)

ESIMS (acetonitrile) m/e (rel intensity): 865 (MNa$^+$,100%).

25,27-di-ethoxycarbonylmethyl calix[4]arene (128)

Calix[4]arene (**106**), (2.0g, 4.70mmol) was stirred at room temperature in 30cm^3 of dry acetonitrile with anhydrous K_2CO_3 (0.65g, 4.70mmol) and ethylbromoacetate ((1.57g, 9.40mmol) under N_2 for four days. The reaction mixture was filtered, the solvent was evaporated *in vacuo*, and the residue purified by column chromatography (silica, ethyl acetate / hexane, 4:1). This yielded a white solid in 55% yield, (1.54g).

m.p. 172-174°C.

I.R.υ_{max} (KBr) [cm^{-1}]: 1753 (C=O str.(ester)), 3425 (OH str.)

^{1}H-NMR (400MHz) δ ($CDCl_3$) [ppm]: 1.39 (12H, t, OCH$_2$C$\underline{H}_3$), 3.44 (4H, d, J=13.2Hz, Ar-C$\underline{H}_A$-Ar), 4.37 (8H, q, OC$\underline{H}_2$CH$_3$), 4.53 (4H, d, J=13.2Hz, Ar-C$\underline{H}_B$-Ar), 4.77 (4H, s, -O-C$\underline{H}_2$-CO-) 6.70 (2H, t, J=7.2Hz, ArH, 3), 6.77 (2H, t, J=7.6Hz, ArH, 3), 6.94 (4H, d, J=7.6Hz, ArH, 2 and 4), 7.10 (4H, d, J=7.2Hz, ArH, 2 and 4), 7.68 (2H, s, -OH).

ESIMS (acetonitrile) m/e (rel intensity): 635 (MK^+,100%).

5,11,17,23-Tetraallyl-25,27-di- ethoxycarbonylmethyl calix[4]arene (129)

Tetra-*p*-allyl-calix[4]arene (**108**), (2.0g, 3.40mmol) was stirred at room temperature in 30 cm^3 of dry acetonitrile with anhydrous K_2CO_3 (0.47g, 3.40mmol) and ethylbromoacetate (1.14g, 6.80mmol) under N_2 for four days. The reaction mixture was filtered, the solvent was evaporated *in vacuo*, and the residue purified by column chromatography (silica, ethyl acetate / hexane, 4:1). This yielded a white solid in 58% yield, (1.49g).

m.p. 72°C.

I.R.υ_{max} (KBr) [cm^{-1}]: 1754 (C=O str.(ester)), 3422 (OH str.)

^{1}H-NMR (400MHz) δ ($CDCl_3$) [ppm]: 1.39 (12H, t, $OCH_2C\underline{H}_3$), 3.13 (4H, d, J=6.8Hz, Ar-$C\underline{H}_2$-(allyl)), 3.26 (4H, d, J=6.8Hz, Ar-$C\underline{H}_2$-(allyl)), 3.35 (4H, d, J=13.2Hz, Ar-$C\underline{H}_A$-Ar), 4.35(8H, q, $OC\underline{H}_2CH_3$), 4.48 (4H, d, J=13.2Hz, Ar-$C\underline{H}_B$-Ar), 4.76 (4H, s, -O-$C\underline{H}_2$-CO-) 4.93-5.08 (8H, m, -CH=$C\underline{H}_2$(allyl)), 5.79-5.86 (2H, m, -$C\underline{H}$=CH_2(allyl)), 5.92-5.99 (2H, m, -$C\underline{H}$=CH_2(allyl)), 6.78 (4H, s, ArH, 2 and 4), 6.85 (4H, s, ArH, 2 and 4), 7.72 (2H, s, -$O\underline{H}$).

ESIMS (acetonitrile) m/e (rel intensity): 779 (MNa^+,100%).

5,11,17,23-Tetraallyl-25,27-di- ethoxycarbonylmethyl -26-mono-carboxymethyl-calix[4]arene 1-naphthylamide (130)

Tetra-*p*-allyl calix[4]arene 1,3-di ethyl ester (**127**) (0.2g, 0.26mmol) was refluxed in acetone with (**119**) (0.14g, 0.53mmol) and potassium carbonate (0.07g, 0.53mmol) for five days. This yielded a white solid which was identified as a complex mixture of products by thin layer chromatography (TLC). After liquid chromatography (SiO_2, hexane/ethyl acetate, 8:2) the title product was isolated as an off-white solid (0.06g, 25%).

m.p. 86-88°C.

I.R.υ_{max} (KBr) [cm^{-1}]: 1757 (C=O str.(ester)), 1685, 1636 (C=O str.(amide)), 3327 (NH str.), 3434 (OH str.)

ESIMS (acetonitrile) m/e (rel intensity): 962 (MNa^+,100%).

2.5 *References*

1 C.D. Gutsche, J.A. Levine, *J. Am. Chem. Soc.* **1982**, 104, 2652.

2 C.D. Gutsche, B. Dhawan, J.A. Levine, K. Hyun No, L.J. Bauer, *Tetrahedron*, **1983**, 39, 409.

3 C.D. Gutsche, J.A. Levine, P.K. Sujeeth, *J. Org. Chem.*, **1985**, 50, 26, 5802.

4 A. L. Beck, M.Mascal, C. J. Moody, A. M. Z. Slawin, D. J. Williams, W. J. Coates, *J. Chem. Soc. Perkin Trans. 1*, 1992, 797.

5 G. McMahon, R. Wall, K. Nolan, D. Diamond, *Talanta*, **2002**, 57, 1119.

3 Molecular Recognition and Enantiomeric Discrimination based on Fluorescence Quenching of Chiral Calixarene L1

3.1 *Fluorescence Introduction*

Luminescence is generally defined as cold emitted light, and it was first in 1852 that Sir G. G. Stokes provided a scientific explanation for fluorescence. A substance must absorb light in order to fluoresce, and luminescence is described as the emission of light from any substance, which occurs from electronically excited states. Electronic transitions in molecular systems, especially in biological molecules, start from the singlet ground state in which the closed shell electrons are paired. In excited singlet states, the electron in the excited orbital is paired to the second electron in the ground-state orbital, whereby return to the ground state occurs rapidly (10^8 s^{-1}) by the emission of a photon of light and is spin allowed.

Fluorescence typically occurs from aromatic molecules, particularly where there is extended conjugation, with the excitation wavelength generally increasing with the degree of conjugation, for examples see Figure 3-1. In contrast to aromatic organic molecules atoms are generally non-fluorescent in condensed phases, exceptions to this are the lanthanides. Fluorescence spectral data is generally presented as emission spectra, which consists of a plot of fluorescence intensity versus wavelength (nm) / wavenumbers (cm^{-1}). Emission spectra are widely variable and depend on the chemical structure of the fluorophore and also the nature of solvent employed. The processes occurring, between the absorption and emission of light, are usually illustrated by a Jablonski diagram (see Figure 3-2).

S_0 represents the ground singlet state and S_1, S_2, the first and second excited electronic states respectively. At each electronic level the fluorophore can exist in a number of vibrational levels, 0, 1 and 2 etc. Transitions typically occur in about 10^{-15} seconds, which is too short to cause significant displacement of the nuclei (Franck Condon Principle). Absorption typically occurs from molecules with the lowest vibrational energy. The energy difference between S_0 and S_1, excited states is too large for thermal population (at R.T.) of S_1, therefore light and not heat is used to induce fluorescence. Emission from fluorophores usually occurs at longer wavelengths than those at which absorption takes place. This loss of energy is due to a variety of dynamic processes which occur following light absorption.

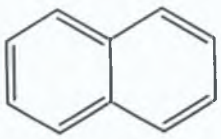

Naphthalene

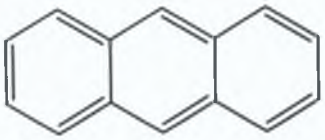

Anthracene

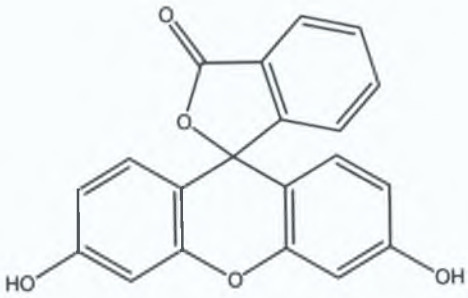

Fluorescein

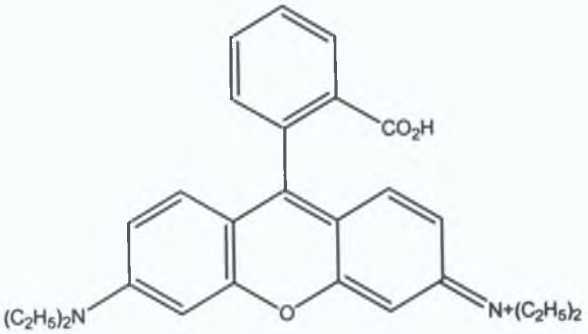

Rhodamine B

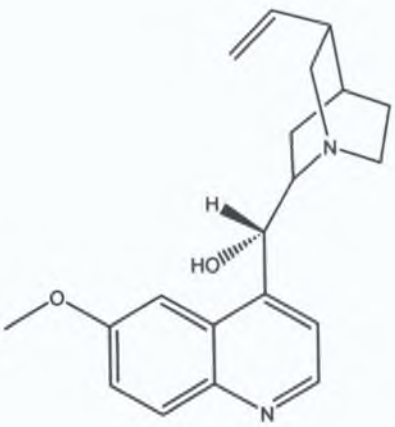

Quinine

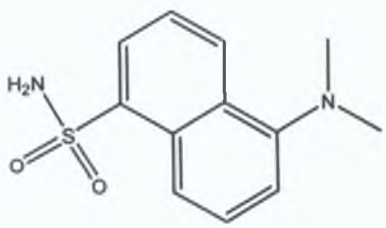

Dansyl chloride

Figure 3-1: *Structures of typical fluorescent molecules*

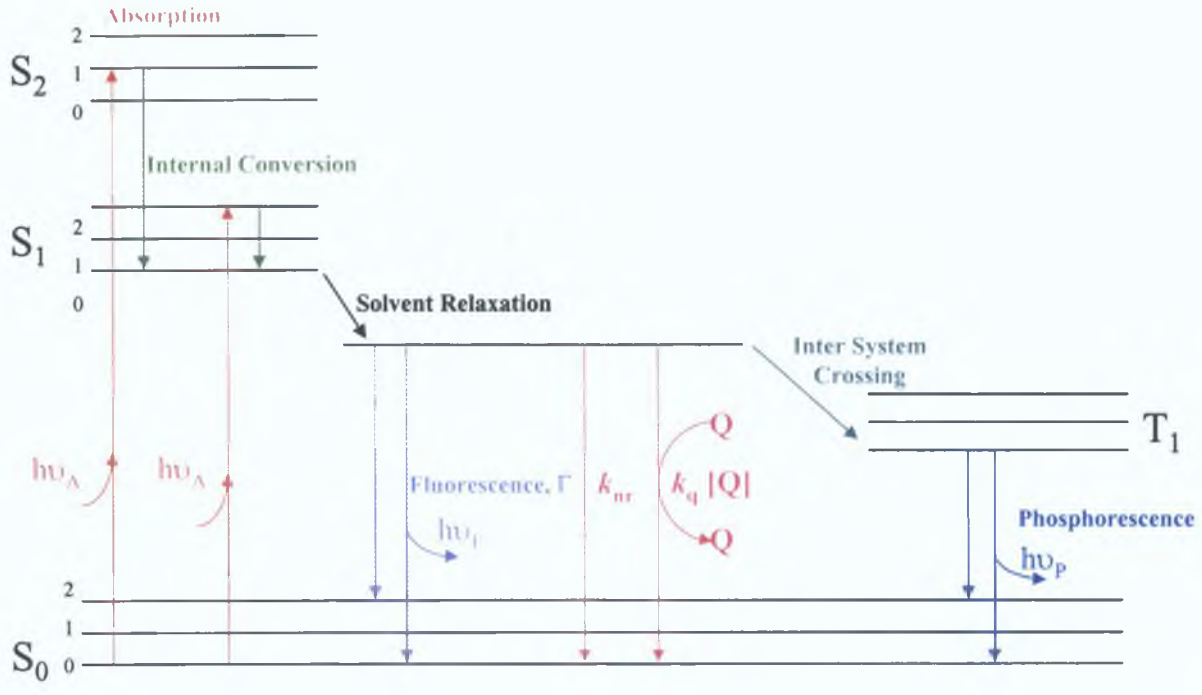

Figure 3-2: *Jablonski diagram illustrating various molecular processes which can occur in excited states, υ = wavelength, Γ = emissive rate of fluorophore, k_{nr} = rate of non-radiative decay to S_0, k_q = bimolecular quenching constant, and Q represents the quencher .*

A fluorophore is usually excited to a higher vibrational level of either S_1 or S_2 and in most cases molecules in the condensed phase relax rapidly to the lowest vibrational level of S_1. This is called internal conversion and generally occurs in 10^{-12} s, and is followed by fluorescence emission from this thermally equilibrated excited state (10^{-8} s). The excess vibrational energy is rapidly lost to the solvent. Return to the ground state typically occurs to a higher excited vibrational ground-state level, which then quickly reaches thermal equilibrium. A consequence of emission to a higher vibrational ground states is that the emission spectrum is typically a mirror image of the absorption spectrum of the $S_0 \rightarrow S_1$ transition. This similarity occurs because electronic excitation does not greatly alter the nuclear geometry, therefore the spacing of the vibrational energy levels of the excited states is similar to that of the ground state.

Solvent effects shift the emission to still lower energy due to stabilisation of the excited state by polar solvent molecules. The fluorophore has typically a larger dipole moment in the excited state (μ_E) than in the ground state (μ_G). Following excitation,

the solvent dipoles can reorient or relax around μ_E, which lowers the energy of the excited state. As the solvent polarity increases, this effect becomes larger, resulting in emission at lower energies or lower wavelengths. In general, only fluorophores which are themselves polar in nature will display a large sensitivity to solvent polarity, with non-polar molecules such as hydrocarbons, showing much less sensitivity to solvent polarity. Molecules in the S_1 state can undergo a spin conversion to the first triplet state, T_1. Emission from T_1 is termed phosphorescence and is generally shifted to longer wavelengths relative to the fluorescence. Conversion of S_1 to T_1 is called intersystem crossing.

Within its lifetime, the singlet excited state can interact with other entities present in solution. A molecule may be non-fluorescent as a result of a fast rate of internal conversion or a slow rate of emission. Fluorescence parameters sense the changes that occur in the fluorophores' environment within the excited state, and the nett result of these interactions is typically a decrease in fluorescence emission intensity, called quenching, which can occur by several mechanisms.

- Collisional quenching occurs when the excited-state fluorophore is deactivated upon contact with some other molecule (called quencher) in solution. The molecules are not chemically altered in the process; the fluorophore is returned to the ground state during a diffusive encounter with the quencher.

- Static quenching is however, due to the formation of a non-fluorescent ground state complex between the fluorophore and quencher. This process occurs in the ground state and is not diffusion controlled.

Quenching can also occur by a variety of trivial (nonmolecular mechanisms), such as attenuation of the incident light by the fluorophore or other absorbing species. The efficiency of the quenching processes between the fluorophore (calixarene in this case), and the quenching species (guest enantiomer), follows the Stern-Volmer relationship provided that no self-quenching results i.e. both are present in the appropriate concentrations. The Stern-Volmer equation can be derived by consideration of the fluorescence intensities observed in the absence and presence

of quencher. The fluorescence intensity observed for a fluorophore id proportional to its concentration in the excited state [F*]. Under continuous illumination, a constant population of excited fluorophores is established, and therefore *d*[F*]/*dt* = 0. In the absence of quencher, the differential equation describing [F*] is

$$\frac{d[F^*]}{dt} = f(t) - \gamma[F^*]_0 = 0 \qquad \textbf{Equation 3-1}$$

and in the presence of quencher

$$\frac{d[F^*]}{dt} = f(t) - (\gamma + k_q[Q])[F^*] = 0 \qquad \textbf{Equation 3-2}$$

where *f(t)* is the constant excitation function, and $\gamma = \tau_0^{-1}$ is the decay rate of the fluorophore in the absence of quencher. In the absence of quenching, the excited-state population decays with a rate $\gamma = (\Gamma + k_{nr})$, where Γ is the radiative decay rate and k_{nr} is the non-radiative decay rate. In the presence of quencher there is an additional decay rate, $k_q[Q]$. With continuous excitation, the excited-state population is constant, so the derivative can be eliminated from the equations above. Division of Eq.3.2 by Eq.3.1 yields

$$\frac{F_0}{F} = \frac{\gamma + k_q[Q]}{\gamma} \qquad \textbf{Equation 3-3}$$

which is the Stern-Volmer equation.

$$\frac{I_0}{I} = 1 + K_{SV}[Q] \qquad \textbf{Equation 3-4:}$$

where

I_o	=	Fluorescence of the fluorophore in the absence of quencher
I	=	Fluorescence of the fluorophore in the presence of quencher
[Q]	=	Concentration of the quenching species
K_{SV}	=	Stern-Volmer constant

If the concentrations are in the correct range (i.e. no self-quenching occurs) and the system obeys the Stern-Volmer relationship, then a plot of I_0/I versus [Q] will yield a straight line, the slope of which gives the Stern-Volmer constant (K_{sv}) and whose

intercept is 1. The greater the K_{sv} value the greater the quenching efficiency of the guest molecule. Therefore the guest with the greater Stern-Volmer constant has the greatest interaction with the host calix[4]arene.

3.2 Importance of chirality

Determination of enantiomeric purity has in recent years become more important than ever, due to increasing restrictions on the marketing of, and administering as mixtures, therapeutic agents which are chiral in nature (that is combinations of isomeric substances whose biological activity may well reside predominantly in one optical form). In drug disposition, enantiomeric discrimination depends on the mechanism of the process under consideration. Absorption, distribution and excretion are generally passive processes, which do not differentiate between enantiomers, but enzymic metabolism and protein binding, to plasma or tissue proteins, can show a high degree of stereoselectivity. Chiral discrimination occurs at both substrate and product levels in terms of metabolism, and as a result the metabolic and pharmacokinetic profiles of enantiomers after administration of racemic drugs can vary greatly; so much so that the exposure to the two enantiomers may be very different. The net result of the interaction of the two stereoselectivities of these various processes can obscure the fact that one (or more) shows a marked stereoselectivity. This is particularly the case for metabolism: while the ratios of the total plasma clearance of the enantiomers of a wide range of drugs never exceed 2, individual metabolic pathways often show much greater stereoselectivity.

The interaction of the enantiomers of a chiral drug molecule with a chiral macromolecule, such as an enzyme, results in the formation of a pair of diastereoisomeric complexes, which differ energetically. In the absence of an external chiral influence, enantiomers have identical chemical properties except towards optically active reagents, and identical physical properties except for the direction of rotation of the plane of polarised light. It is from these numerous similarities that the difficulty in enantiomeric discrimination arises. The single difference between these isomers is the spatial orientation of their groups, making the task of separation an arduous one. It is however, desirable to separate enantiomers of a chiral drug, due to the different effects that they may exhibit, for example:

1. all of the particular pharmacological action may reside in just one of the isomers
2. because of different binding at active receptor sites the enantiomers may have different pharmacological actions
3. enantiomers may have different rates of reaction within the body
4. the enantiomers may have different toxicities because of the difference in binding at asymmetric sites
5. one enantiomer may react at an active site to produce synergism or antagonism of the action of the other enantiomers

Examples of these include a drug used to treat morning sickness in pregnant women, which is associated with the Thalidomide babies of the 1960's. R-Thalidomide acts as a sedative whereas the S-enantiomer is teratogenic and caused the phocomelia tragedy [1]. These two enantiomers also racemise after ingestion. Another example is the heart drug propranolol, the R-enantiomer of which was introduced in the 1960's as a β-blocker in the treatment of heart disease with the S-form exhibiting contraceptive properties. A third example comes from the newly developed family of drugs called glitazones used in the treatment of Type II diabetes. Troglitazone (manufactured by Parke Davis) has 2 chiral centres, one (with a ready enolisable proton, prone to racemisation) at the C-5 position of the 1,3-thiazolidine-2-4-dione ring and an additional one at the 2-position of the chromane ring system, a tertiary centre which is essentially inert to racemisation. This drug causes potentially fatal liver damage in a small percentage of patients and it is not clear which of the four possible stereoisomers is responsible [1].

These striking differences in the behaviour of enantiomers of chiral drugs make it necessary for analysts in the pharmaceutical industry to assess the stereoisomeric composition of potential drugs. The characterisation of drugs for enantiomeric purity is required subsequent to their synthesis and also during *in vivo* and *in vitro* studies for determining the possible interactions of a chiral molecule and its metabolites within the body. Several methods commonly employed in the pharmaceutical industry to determine enantiomeric purity include specific rotation, circular dichroism, separation techniques such as liquid and gas chromatography, and capillary electrophoresis. In particular HPLC and GC have been used extensively to perform

chiral separations. There are predominantly three methods for resolving enantiomers by HPLC, which include

1. exploitation of conventional column technology by the formation of diasteromeric derivatives
2. exploitation of conventional column technology by the use of chiral mobile phase additives
3. the use of chiral stationary phases

In the case of the third technique, chiral host molecules are covalently attached to a silica support, which generally form inclusion complexes with enantiomers. These chiral hosts complex enantiomers of the same molecule to differing degrees, thereby rendering enantiomeric separation possible. It is necessary to transmit information about these host-guest recognition events to the outside world, since they occur on a scale too small to be detected by the human eye. Fluorescence is an attractive option in this regard, given its sensitivity and variety of measurement modes that can be employed (fluorescence emission, quenching, lifetime, phase angle). When fluorophores are covalently attached to appropriate sites on calixarenes and cyclodextrins, changes can occur in fluorescence intensity when these hosts come into contact with certain guests. Guest enantiomers induce different fluorescence intensity changes in the hosts' spectrum rendering discrimination of the enantiomers possible.

3.2.1 Chiral discrimination in fluorescence quenching

It can be difficult to theoretically predict the host-guest properties of receptors, as the overall selectivity observed might be the sum of many subtle interactions, which may be interdependent. Several publications dealing with steric influence upon fluorescence quenching rates have dealt with measuring the quenching rate as a function of substitution on the quenchers or the excited molecules [**2**, **3**, **4**, **5**, **6**]. However, with the introduction of substituents comes the implication of electronic as well as steric changes, which can affect the role of a charge-transfer interaction in the excited state [**7**]. Froehlich and Morrison [**4**] showed how variation in chain length of straight chain aromatic hydrocarbons affects their quenching by cis-piperylene.

However in examining pure steric effects on quenching without the disturbances of electronic factors, Irie and co-workers [8] used chiral compounds as excited molecules and quenchers, since enantiomers have inherently the same electronic nature, i.e. oxidation-reduction potential. They demonstrated during early work, that specific geometry is required for the fluorescence quenching of 1,1'-binaphthyl by N,N-dimethyl-α-phenyl ethylamine. Photo excited 1,1'-binaphthyl gives a fluorescence maximum around 360nm, the fluorescence of which can be quenched by adding N,N-dimethyl-α-phenyl ethylamine. No difference was discerned in the quenching rate of Stern-Volmer plots of a fluorescence quenching of racemic mixture of 1,1'-binapthyl by enantiomers, (S)-(-)- and (R)-(+)-N,N-dimethyl-α-phenethylamines in *n*-hexane. However a significant difference in the rates was observed for the quenching of (R)-(-)-1,1'-binapthyl fluorescence by these enantiomers, the greatest interaction being observed for the (S)-(-)-enantiomer.

As an extension to the previous study, Irie and co-workers investigated the effect on the quenching rate and the ratio of the quenching rates of the two enantiomers k_q (R-S)/k_q (R-R) of quenchers bearing bulky substituents [9]. Significant differences were observed in the quenching rates of (S)-(-) and (R)-(+)- N,N-dimethyl-1-phenylethylamines, N,N-dimethyl-α-phenyl-2-methylpropylamines and N,N-dimethyl-α-phenyl-2,2-dimethylpropylamines with respect to the fluorescence of (R)-(-)-1,1'-binaphthyl, while no difference for the fluorescence quenching of a racemic mixture of 1,1'-binaphthyl was discerned. The ratios of the quenching rates were found to increase as the bulkiness of the amine increased, and were found to be 1.9, 2.7 and 4.0 respectively. Such a large difference in the quenching rates of each enantiomers reinforces the supposition that specific orientation is required in the quenching process between chiral 1,1'-binaphthyl and chiral amines.

James et al. demonstrated that chiral recognition of saccharides could be achieved and signalled by fluorescence, by employing a ligand incorporating a chiral tertiary amine (which provided the potential for chiral discrimination) and a binaphthyl group (to transduce the host-guest interaction into a fluorescent signal) [10]. In the absence of the guest, efficient photoelectron transfer (PET) from the amine to the binaphthyl moiety occurred, which served as an effective mechanism for fluorescence quenching, providing that the nitrogen atom was suitably oriented. To ensure the desired position of the nitrogen, boronic acid groups were sited near the chiral amine

group, and upon binding with the target saccharides a strong Lewis acid interaction occurred between the boronic acid and the amine, which hampered the ability of the latter to quench the binaphthyl fluorescence.

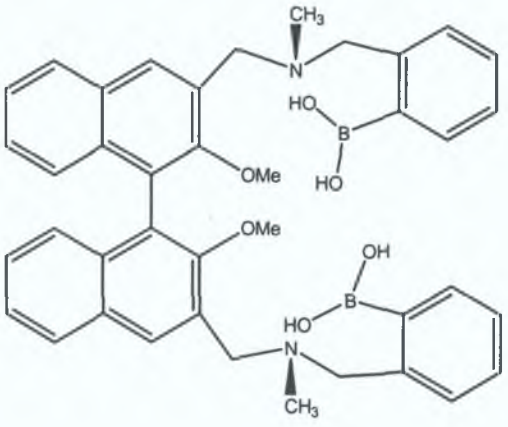

Figure 3-3: *Chiral diboronic acid*

Concerning the (R)- form of this ligand (Figure 3-3) the 1:1 host-guest complex stabilities of D- fructose, glucose and mannose are greater than those of L- fructose, glucose and mannose. With regard to the (S)-ligand the reverse trend is expected and indeed observed, complexing L- fructose and glucose to a greater extent than D-fructose and glucose. The PET quenching efficiency on saccharide binding follows exactly the same trends with respect to the (R)- and (S)- ligands. This work elegantly established that chiral discrimination and signal transduction could be achieved, by placing groups with the required functionalities in a suitable conformation.

Recently Yan and Myrick [**11**] showed how the total complexation by α-acid glycoprotein (AGP) could discriminate between enantiomers of dansyl-D,L-phenylalanine. The centrality of chiral recognition in biology inspired the use of biomolecules, in this case bovine α-acid glycoprotein (AGP), as receptors for a fluorescence-based determination of enantiomeric purity.

Bearing in mind the importance of chirality and the difficulties in distinguishing between enantiomers of the same molecule, the aim of this project is to develop a molecular sensor, which has the ability to perform such a task. Development of successful materials for sensors is particularly challenging, as the host-guest properties of receptors are theoretically difficult to predict accurately, since the overall

observed selectivity is the sum of many subtle interactions, which may or may not be interdependent.

In designing any molecular sensor, the main issues to be addressed are;

1. Recognition of the target species
2. Transduction of the binding event
3. Immobilisation or controlled localisation

However broad predictions can be made about the type of features, which should be present if a ligand is to possess the ability of performing the required task. In order to achieve the goal of chiral recognition of molecular guests, the calixarene host must be functionalised with chiral moieties that define a 3-D chiral distribution of binding sites complementary to that of the guest. The structure of the host calix[4]arene (**L1**) is given below (for synthesis see Chapter 2). The molecular design components necessary can be summarized as follows;

- A calix[4]arene backbone (4-repeat units in the macrocycle) which acts as a scaffold to anchor ligating groups
- A 3-D distribution of hydrogen bonding sites defined by carbonyl oxygen, amide nitrogen and hydroxy groups at each pendent group
- A chiral centre (indicated by red star) located in the vicinity of the hydrogen bonding sites, which is complementary to the guest.
- Naphthyl groups sited at the bottom of the pendent groups to provide a fluorescence signaling capability.
- Allyl groups positioned at the opposite end of the calix[4]arene to the chiral binding sites (the upper rim) in order to facilitate immobilisation on a polymer substrate with minimal effect on the host-guest characteristics and fluorescence properties.

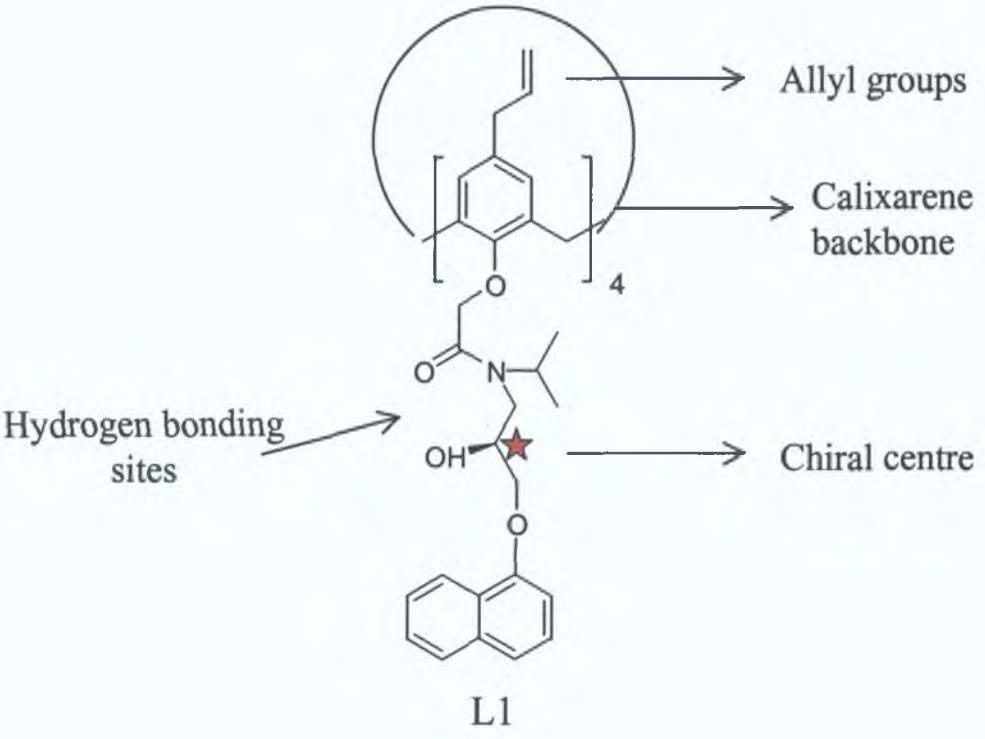

L1

Figure 3-4: *Calixarene L1, with allyl groups on upper rim for immobilisation, calixarene backbone to anchor ligating groups, various groups capable of hydrogen bonding, chiral centre denoted by red star and naphthalene moieties for signal transduction.*

With these guidelines in mind, a study was implemented to determine whether a calixarene macrocycle, which in principle satisfy the above criteria, could be used as sensor molecules in chiral recognition.

3.3 Experimental Section

3.3.1 Equipment and Materials

All fluorescence emission and quenching experiments were performed using a Perkin-Elmer Luminescence Spectrometer LS 50B (Beaconsfield, Buckinghamshire, UK), interfaced with a Pentium PC which employs fluorescence data management software, FLWinlab. Post-run data processing was performed using Microsoft Excel '97 and 2000 after importing the spectra as ascii files.

All fluorescence lifetime measurements were performed using an Edinburgh Analytical Instruments Single Photon Counter in a T-setting, which employs a nanosecond deuterium flash-lamp nF900, with photo-multiplier detector, model S300 (-20°C to -30°C). Post-run data processing was performed using a Pentium PC, F900 data correlation program, version 3.13 and Microsoft Excel 2000 after importing the spectra as ascii files.

All UV measurements were carried out using a Perkin-Elmer Lambda 900 UV/VIS/NIR spectrometer. The instrument was controlled via UV WinLab software and post-run data processing was performed using Microsoft Excel '97 and 2000 after importing the spectra as ascii files.

Both enantiomers of phenylalaninol, (R)-(+)-phenylalaninol and (S)-(-)-phenylalaninol, both enantiomers of phenylglycinol, (R)-(-)-2-phenylglycinol and (S)-(+)-2-phenylglycinol and both enantiomers of phenylethylamine were of puriss grade (98% pure, the other 2% consisting of the other enantiomeric form), obtained from Fluka Biochemika (Gillingham, Dorset, UK). In addition as a control, the three aforementioned chiral amines were obtained of puriss grade from Sigma-Aldrich. The solvents used (methanol- HPLC grade) was obtained from Labscan (Stillorgan, Co. Dublin). The synthesis of calixarene L1 has been described in Chapter Three.

3.3.2 Procedure for Fluorescence Measurements

Solutions giving concentrations of the propranolol amide calix[4]arene **L1** (0.7 μmol dm^{-3}) and phenylalaninol in the range 1 – 25 mmol dm^{-3} in methanol were prepared as follows. A 0.1 mmol dm^{-3} stock solution of calixarene **L1** was prepared by dissolving 8.9 mg in 50mL of methanol. A 0.25 mol dm^{-3} stock solution of phenylalaninol was prepared by dissolving the required combination of the two

enantiomers, totalling 0.945 g, in 25 mL of methanol. Test solutions were prepared by taking 70 μL of the calixarene stock solution in a 10 mL volumetric flask, adding 0.2, 0.4, 0.6, 0.8, and 1.0 mL of phenylalaninol stock solution, and making up to the volume with methanol. Measurements were repeated a minimum of three times for each addition. The fluorescence intensities of the solutions were measured at an excitation wavelength of 227nm. The fluorescent intensity readings were compared to that of a solution containing 0.7 μmol dm^{-3} calixarene **L1** and no phenylalaninol.

Similar solutions to those described above were employed for the three-dimensional fluorescence experiments. These were scanned at excitation wavelength's from 200-340nm in increments of 4nm, and each spectrum was observed at emission wavelengths from 300nm – 460nm.

Solutions giving concentrations of phenylglycinol in the range 1 – 15 mmol dm^{-3} in methanol were prepared in a similar manner as described for phenylalaninol above. For the preparation of solutions containing phenylethylamine in the concentration range 1 – 8 mmol dm^{-3} in methanol, the same general procedure was followed. Measurements were repeated in both cases a minimum of three times for each addition. The concentration of calixarene in all cases was 0.7 μmol dm^{-3}.

3.3.3 Preparation of solutions for Fluorescence Lifetime Measurements

Solutions giving absorbance readings of 0.474 of the propranolol amide calix[4]arene **L1** and therefore a concentration of 56.1 μmol dm^{-3} in methanol were prepared. Extinction coefficient (ε_{300nm}) of **L1** is 8449 dm3 mol^{-1} cm^{-1}. Each sample was spiked with the R-enantiomer of phenylalaninol and the consequent fluorescence lifeitme was observed. The concentration range of R-phenylalaninol examined after an addition of 10, 20, 30 and and 40μL of the 1.0 mol dm^{-3} stock solution of R-phenylalaninol was 4-16 mmol dm^{-3}. Solutions giving absorbance readings of 0.453 of the propranolol amide calix[4]arene **L1** and therefore a concentration of 53.6 μmol dm^{-3} in methanol were prepared, and were spiked with the S-enantiomer of phenylalaninol in the same general procedure as in the case of the R-enantiomer.

3.3.4 Procedure for Fluorescence Measurements of Propranolol label

Solutions giving concentrations of the propranolol label (2.8 μmol dm^{-3}) in methanol were prepared as follows. A 1.0 mmol dm^{-3} stock solution of the propranolol label was prepared by dissolving 12.9 mg in 50mL of methanol. A 0.1 mmol dm^{-3} stock solution of the propranolol label was prepared by making a one in ten dilution of the former stock solution. Test solutions were prepared by taking 70 μL and 280 μL of the 0.1 mmol dm^{-3} stock solution in a 10 mL volumetric flask, and making up to the volume with methanol. The fluorescence intensities of the solutions were measured at an excitation wavelength of 227nm and an emission wavelength of 336nm. Data was collected at an interval of 0.02 minutes over a period of 10 minutes. After approximately 30 seconds each sample was spiked with the appropriate enantiomer of phenylalaninol and the decrease in fluorescence intensity was observed. The concentration range of phenylalaninol examined after an addition of 10, 20 and 30 μL of the 0.25 mol dm^{-3} stock solution of phenylalaninol was 1-3 mmol dm^{-3}. Measurements were repeated a minimum of three times for each addition. Solutions with calixarene **L1** were prepared and spiking experiments were carried out in a similar manner as described above.

3.3.5 Procedure for Fluorescence Measurements of di-functionalised R-propranolol amide calix[4]arene

Solutions giving concentrations of the R-propranolol diamide calix[4]arene **L2** (0.7 μmol dm^{-3}) and phenylalaninol in the range 1 – 20 mmol dm^{-3} in methanol were prepared as follows. A 0.1 mmol dm^{-3} stock solution of calixarene **L1** and 0.25 mol dm^{-3} stock solutions of enantiomers of phenylalaninol were prepared as previously described. Test solutions were prepared by taking 70 μL of the calixarene stock solution in a 10 mL volumetric flask, adding 0.08 - 0.8 mL of phenylalaninol stock solution, and making up to the volume with methanol. Measurements were repeated a minimum of three times for each addition. The fluorescence intensities of the solutions were measured at an excitation wavelength of 227nm. The fluorescence intensity readings were compared to that of a solution containing 0.7 μmol dm^{-3} calixarene **L1** and no phenylalaninol.

3.4 Results and Discussion

3.4.1 Excitation and Emission Spectra

The excitation and emission spectra of the p-allyl-S-propranolol tetra amide calix[4]arene (**L1**) at a concentration of 0.7 μmol dm^{-3} in methanol are shown in Figure 3-6. The maximum of the excitation spectrum is at 227 nm (Figure 3-6a), and the maximum of the emission spectrum obtained using an excitation wavelength of 227 nm is at 338 nm (Figure 3-6b). Considering that the guest species (see Figure 3-5) exhibit modest absorbance in these regions, 227nm is a suitable excitation wavelength for the following experiments.

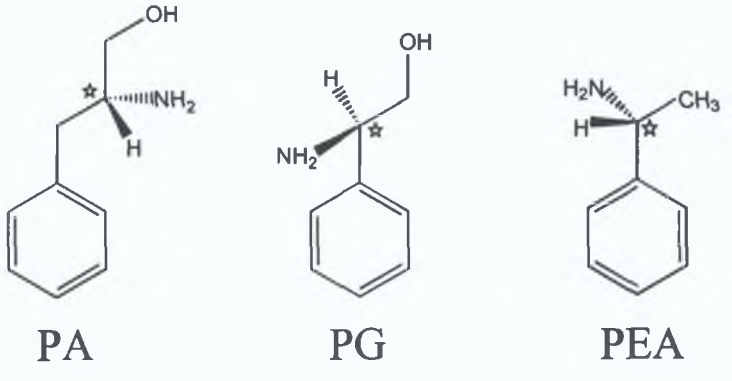

Figure 3-5: *Structures of guest phenylamines; phenylalaninol (R-PA), phenylglycinol (R-PG) and phenylethylamine (R-PEA), (chiral centres denoted by stars).*

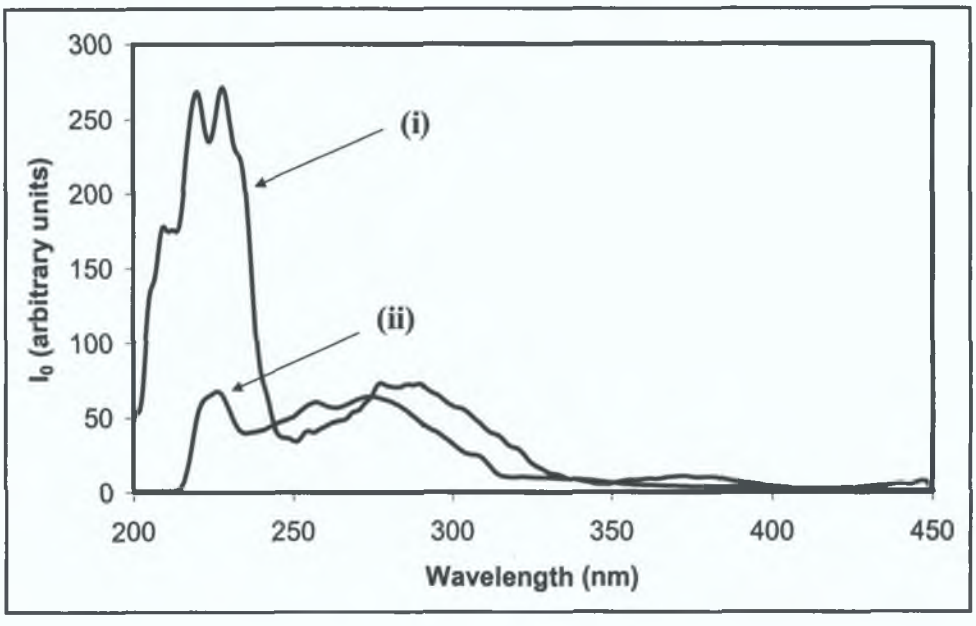

(a)

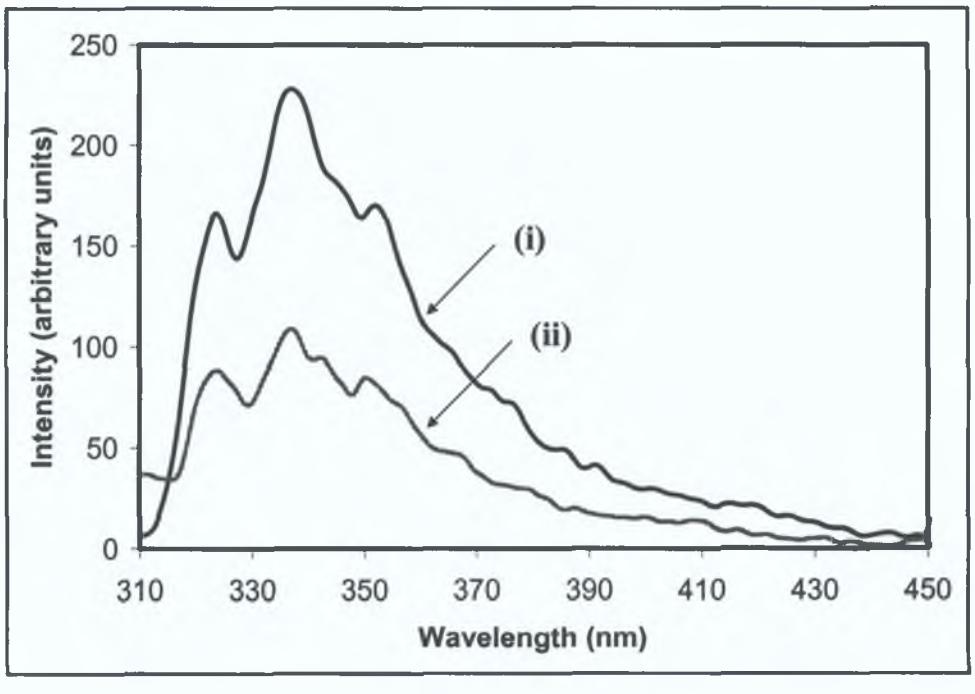

(b)

Figure 3-6: *Excitation and emission spectra of p-allyl-S-propranolol tetra amide calix[4]arene at a concentration of 0.7 μmol dm^{-3} in methanol. (a) Excitation spectrum of the calixarene in the absence (i) and presence (ii) of 25 mmol dm^{-3} phenylalaninol at an emission wavelength of 340nm. (b) Emission spectra of the calixarene in the absence (i) and presence (ii) of 25 mmol dm^{-3} phenylalaninol at an excitation wavelength of 227nm .*

3.4.2 Linear Response range

The linear response range of fluorescence intensity to concentration of calixarene **L1** in methanol was determined to be between 0.1 and 0.7μmol dm^{-3} as shown in Figure 3-7. It is important to use a concentration of the calixarene within the linear range in order to ensure that no self-quenching occurs and therefore that no alternative self-quenching mechanisms are present. A concentration of 0.7 μmol dm^{-3} was chosen for subsequent experiments to examine the effects of phenylalaninol (PA), phenylglycinol (PG) and phenylethylamine (PEA) and hence any quenching observed can be related to the effect of the target species on the ligand.

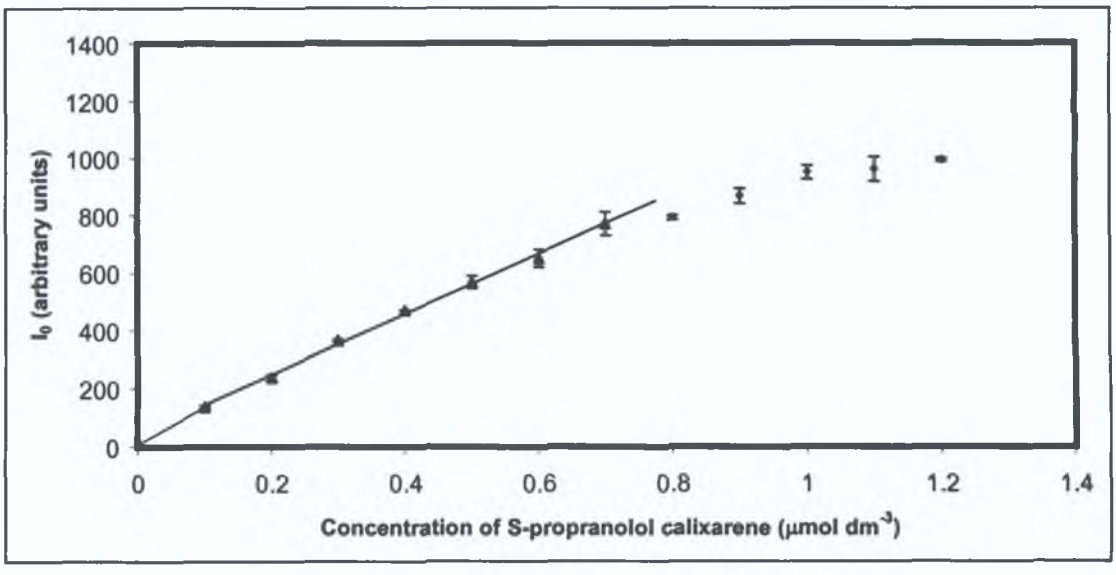

Figure 3-7: *Linear fluorescence response of p-allyl-S-propranolol calixarene in methanol, measured using an excitation wavelength of 227nm and at an emission wavelength of 338nm, data points represent the mean of three replicate measurements (n=3), with error bars representing ± standard deviation.*

3.4.3 Linear range of Stern-Volmer plot.

The Stern-Volmer plot was found to be linear over a range of 0-25 mmol dm^{-3} of racemic phenylalaninol. The Stern-Volmer plot for the same calixarene in the presence of racemic phenylglycinol was found to be linear over the measured range of 0-15 mmol dm^{-3}, and linear over the measured range of 0-8 mmol dm^{-3} of racemic phenyl ethylamine.

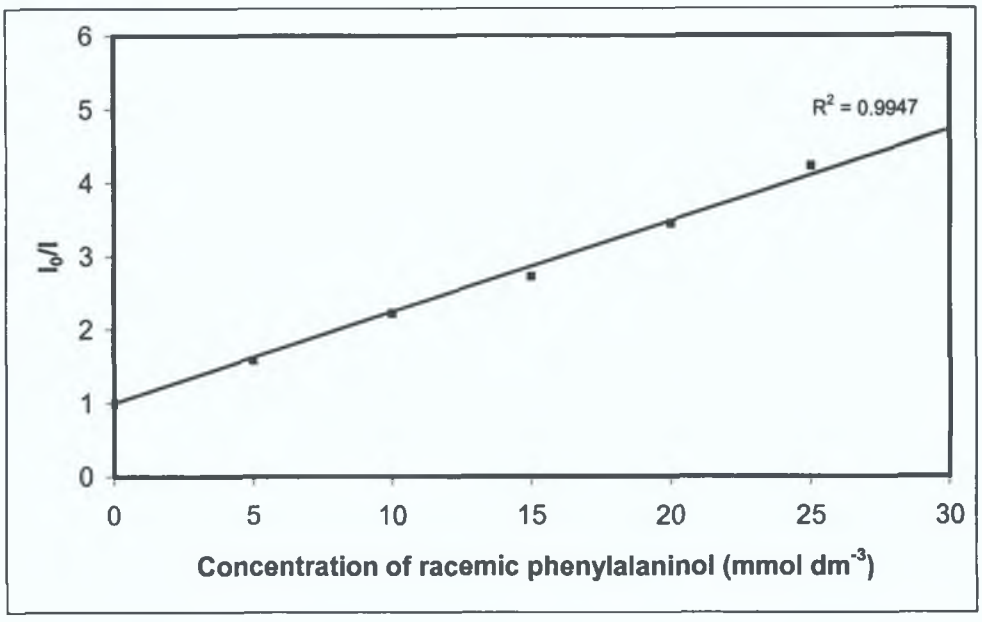

Figure 3-8: *Stern-Volmer plot of S-propranolol calixarene in methanol, measured using an excitation wavelength of 227nm and at an emission wavelength of 338nm, data points represent the mean of three replicate measurements (n=3), with error bars representing ± standard deviation (error bars may be masked by symbols).*

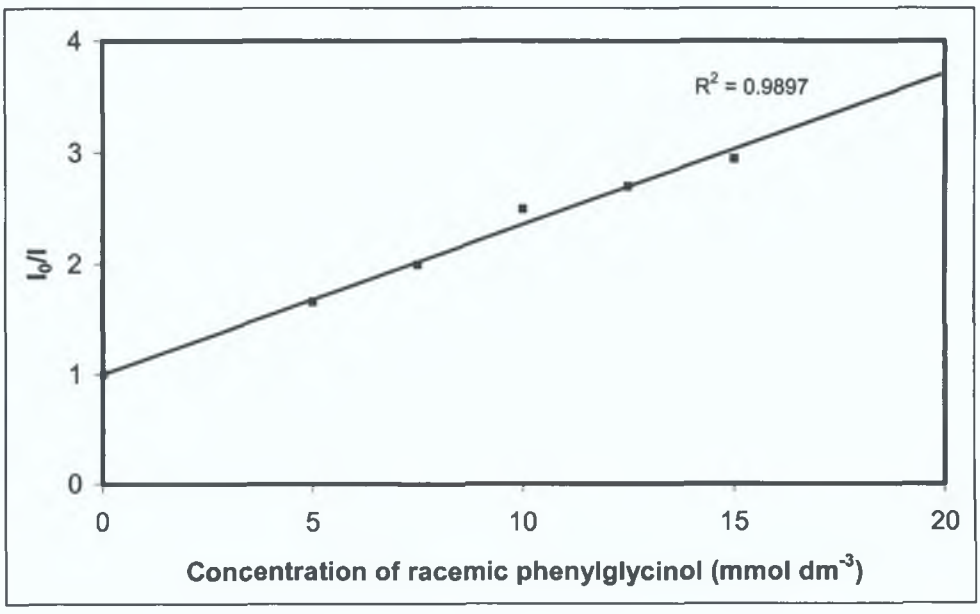

Figure 3-9: *Stern-Volmer plot of S-propranolol calixarene in methanol (experimental conditions described in the caption for Figure 3-8), mean of three replicate measurements (n=3), with error bars representing ± standard deviation (error bars may be masked by symbols).*

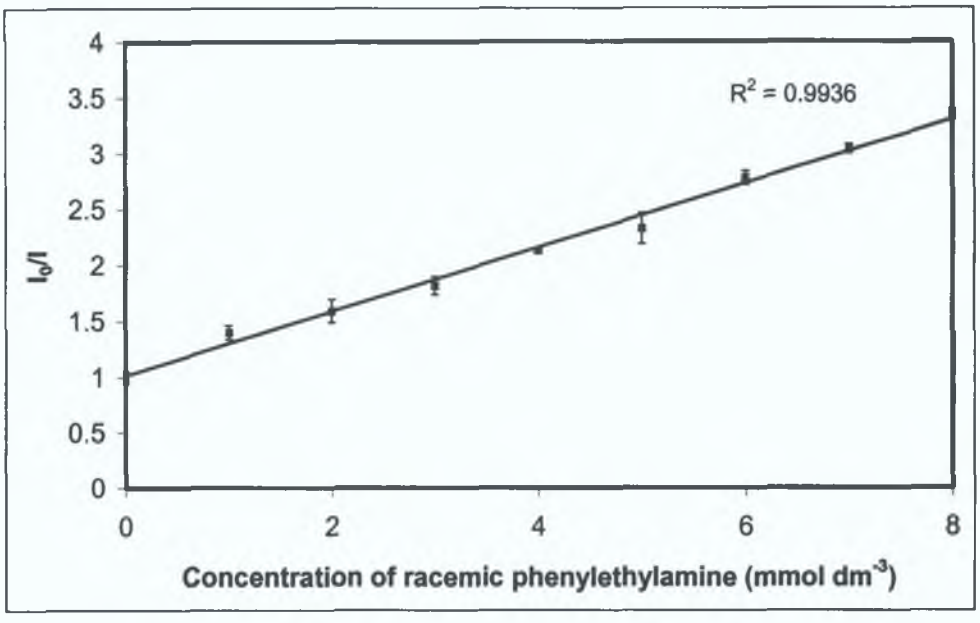

Figure 3-10: *Stern-Volmer plot of S-propranolol calixarene in methanol (experimental conditions described in the caption for Figure 3-8) mean of three replicate measurements (n=3), with error bars representing ± standard deviation (error bars may be masked by symbols).*

3.4.4 Variation of Stern-Volmer plot with enantiomeric composition

The Stern-Volmer plot of **L1** was found to be linear over the range 0-25 mmol dm^{-3} of racemic phenylalaninol. Figure 3-11 illustrates the Stern-Volmer plots for the quenching of the fluorescence of calixarene **L1**, upon addition of 0, 50 and 100% (S)-phenylalaninol respectively, at a concentration range of 0 – 25mmol dm^{-3}. The Stern-Volmer constant K_{SV}, is a measure of the quenching efficiency and a large value for this parameter indicates a sensitive response. The values for the Stern-Volmer constants (K_{SV}) are 0.17, 0.12 and 0.09 after the addition of 0, 50 and 100% (S)-phenylalaninol respectively, and the (K_{SV}) ratio [100% (R)/100% (S)] is 1.9. Because the Stern-Volmer plots show such a large difference in the K_{SV} values of each enantiomer, it can be concluded that the propranolol amide derivative of p-allyl-calix[4]arene exhibits significant ability to discriminate between the enantiomers of phenylalaninol.

Figure 3-12 illustrates the Stern-Volmer plots for the quenching of the fluorescence of calixarene **L1**, upon addition of 100% (S) (a) and 100% (R)-phenylglycinol (b) at a concentration range of 0 – 15mmol dm^{-3}. The values for the Stern-Volmer constants

(K_{SV}) are 0.16 for both the addition of 0, and 100% (S)-phenylglycinol respectively, and the (K_{SV}) ratio [100% (R)/100% (S)] is ~1. It is evident from the Stern-Volmer plot of phenylglycinol, that virtually no difference is observed between the K_{sv} values for the R- and S-enantiomers. It can therefore be concluded that approximately equal interactions takes place between the propranolol amide derivative of p-allyl-calix[4]arene **L1** and both enantiomers of phenylglycinol. Chiral discrimination of phenylglycinol is therefore not possible with this calix[4]arene.

Figure 3-13 illustrates the Stern-Volmer plots for the quenching of the fluorescence of calixarene **L1**, upon addition of 100% (R) and 100% (S)-phenyl ethylamine at a concentration range of 0 – 6.25 mmol dm^{-3}. The values for the Stern-Volmer constants (K_{SV}) are 0.38 and 0.36 after the addition of 100% (R), and 100% (S)-phenyl ethylamine respectively, and the (K_{SV}) ratio [100% (R)/100% (S)] is ~1. It is clear that virtually no difference is observed between the K_{sv} values for the R- and S-enantiomers of phenyl ethylamine with this calixarene, therefore it can be concluded, similar to the case for phenylglycinol, that more or less equal interactions take place between **L1** and both enantiomers of phenyl ethylamine. Chiral discrimination of this chiral amine is consequently not possible with this calix[4]arene.

Although the observation of linear Stern-Volmer plots usually indicates that collisional (or dynamic) quenching has occurred, static quenching can also result in a linear Stern-Volmer plot. In general, static and dynamic quenching can be distinguished by their differing dependence on temperature and viscosity, or preferably by lifetime measurements. An additional method to distinguish static and dynamic quenching is by careful examination of the absorption spectra of the fluorophore. Collisional quenching only affects the fluorophores' excited states and therefore no changes in their absorption spectra are predicted. Ground state complex formation (which results in static quenching) however, will frequently result in perturbation of the absorption spectra of fluorophores. Preliminary studies of the absorption spectra of ligand L1 (see Figure 3-6 (a)) would seem to indicate a static quenching mechanism occurs between the calixarene host and phenylalaninol guest, due to the presence of changes in the absorption spectrum in the presence of a guest molecule. This would lead one to believe that quenching occurs as a result of the formation of a non-fluorescent complex between the fluorophore (calixarene host) and quencher (phenylalaninol guest).

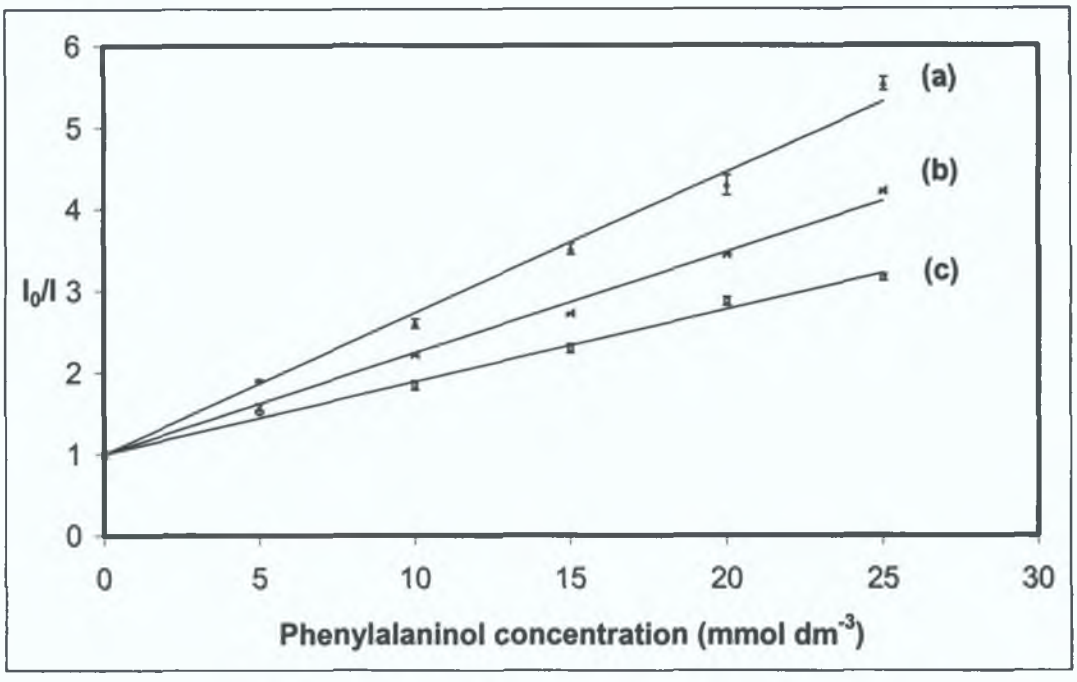

Figure 3-11: *Stern-Volmer plots for the quenching of S-propranolol calixarene upon addition of 0 (a), 50 (b) and 100% (c) (S)-phenylalaninol in methanol. Standard deviations are shown as error bars (n=3), which may be masked by symbols.*

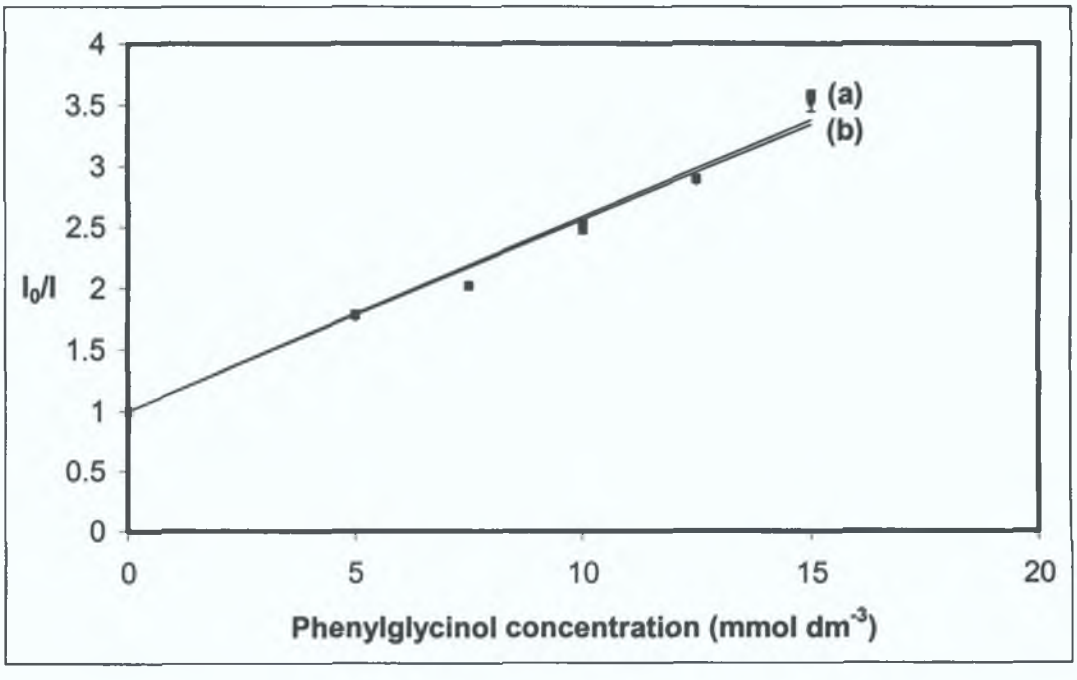

Figure 3-12: *Stern-Volmer plots for the quenching of S-propranolol calixarene upon addition of 100% (a) and 0% (b) (S)-phenylglycinol in methanol. Standard deviations are shown as error bars (n=3), which may be masked by symbols*

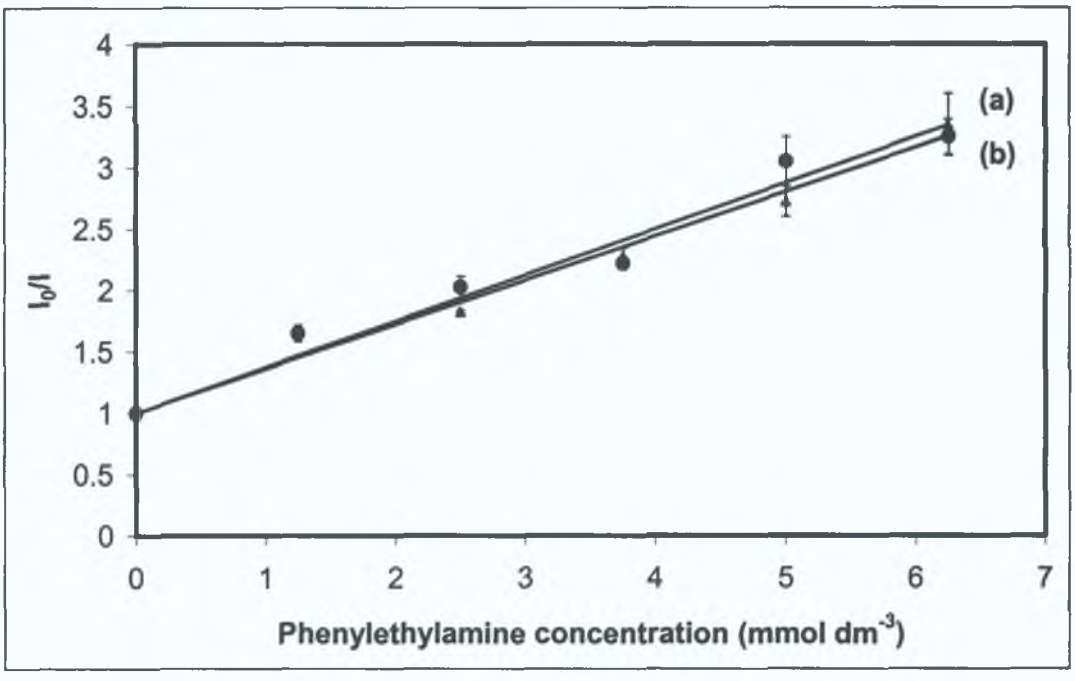

Figure 3-13: *Stern-Volmer plots for the quenching of S-propranolol calixarene upon addition of 100% (a) and 0% (b) (R)-phenyl ethylamine in methanol. Standard deviations are shown as error bars (n=3), which may be masked by symbols.*

Guest	*Composition*	K_{SV}	*St. Dev.*
PA	100%R, 0%S	0.17 (0.9930)	0.08
	0%R, 100%S	0.09 (0.9939)	0.04
PG	100%R, 0%S	0.16 (0.9845)	0.07
	0%R, 100%S	0.16 (0.9801)	0.04
PEA	100%R, 0%S	0.38 (0.9685)	0.14
	0%R, 100%S	0.36 (0.9791)	0.25

Table 3-1: *Stern-Volmer slopes, correlation coefficients and standard deviations for curves in Figure 3-11, Figure 3-12 and Figure 3-13 respectively.*

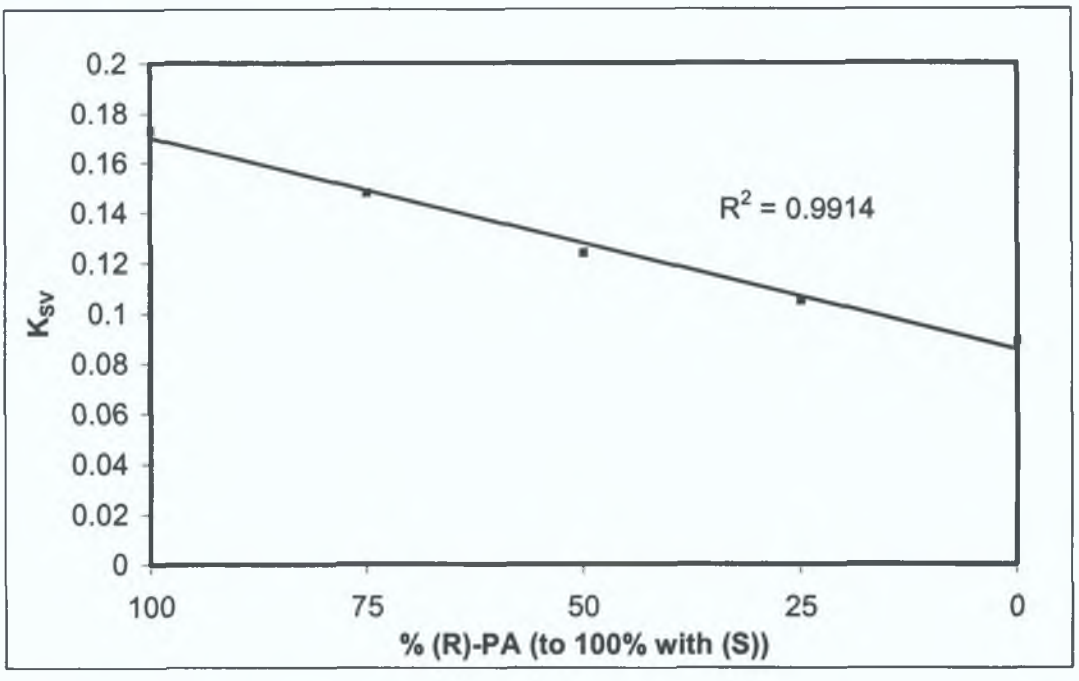

Figure 3-14: *The variation of the Stern-Volmer constant for the quenching of the fluorescence of S-propranolol calixarene with enantiomeric composition of phenylalaninol, data points represent the mean of three replicate measurements (n=3), with error bars representing ± standard deviation (error bars may be masked by symbols).*

The data obtained from the Stern-Volmer plots for the quenching of the fluorescence of calixarene **L1**, upon addition of varying amounts of phenylalaninol show that the quenching efficiency varies linearly with increasing proportion of one enantiomer. That is, in a mixture of both enantiomers of phenylalaninol, each enantiomer will make a contribution to the over-all quenching efficiency proportional to its fraction of the total amount of amino alcohol present. This is a faster and less tedious method than determining the slope of individual Stern-Volmer plots, since it employs a single fluorescence measurement if the total PA concentration is known. This linear relationship between the efficiency of quenching measured and enantiomeric composition could be used as a method for the determination of the enantiomeric purity of a solution of phenylalaninol in methanol. For these measurements, a total concentration of 25 mmol dm^{-3} of phenylalaninol was chosen as this gives the maximum discrimination in the Stern-Volmer plots (see Figure 3-11). The measurement will be optimum for the highest concentration of PA which still obeys the Stern-Volmer plot since it will provide the greatest distribution in the fluorescence measurements.

Figure 3-14 shows the linear relationship between fluorescence intensity and enantiomeric composition at a total PA composition of 25 mmol dm^{-3}. Previous work in this field has led to the enantiomeric discrimination of 1-phenylethylamine [**12**]. The authors report a K_{SV} ratio of 1.14, which they state is outside the range of measurement error, claiming that the gradients were significantly different when compared using a t-test. The ability of calixarene **L1** to discriminate between the enantiomers of phenylalaninol is clearly evident, returning a K_{SV} ratio 1.7 times that reported by Parker and Townshend with regard to phenylethylamine. Since there is no overlap in the standard deviations with respect to the response from **L1** to R- and S-phenylalninol, t-tests are not needed to prove the difference in quenching achieved.

3.4.5 Variation of two-dimensional emission intensity contour plots with enantiomeric composition

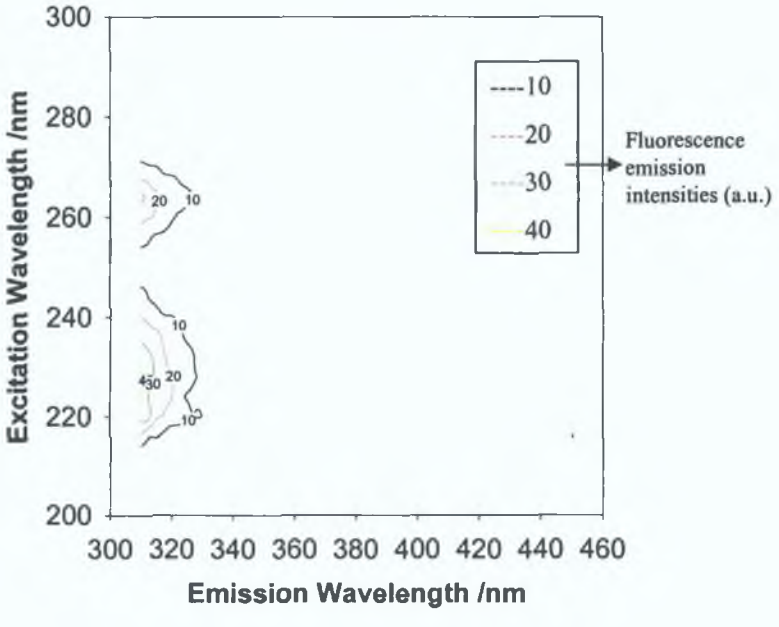

Figure 3-15: *Two-dimensional fluorescence spectrum of guest phenylalaninol in methanol, with the numbers on contour lines representing fluorescence emission intensity units.*

Both enantiomers of phenylalaninol exhibit two-dimensional spectra with maxima at $\lambda_{ex}/\lambda_{em}$ = 230/310nm and 265/310nm (see Figure 3-15). When however the

enantiomers of this amino-alcohol are present in solution with the S-propranolol-tetra-amide calix[4]arene interesting changes are observed in the two-dimensional spectra of the corresponding solutions. A notable difference in the contours of the spectra for the enantiomers alone and the enantiomer/calixarene complex is observed. In the case of the (R)-enantiomer of phenylalaninol/calixarene complex (Figure 3-16), it can be seen that new emission bands as far as wavelengths of 360nm are observed for excitation wavelengths between 220 and 240nm inclusively. There are also new emission bands present in the areas between $\lambda_{ex}/\lambda_{em}$ = 265/320nm and 300/370nm. If the corresponding two-dimensional spectrum for the (S)-phenylalaninol enantiomer/calixarene complex is examined, it is evident that the contours of these regions, $\lambda_{ex}/\lambda_{em}$ = 220/320nm - 240/380nm and $\lambda_{ex}/\lambda_{em}$ = 265/320nm - 300/370nm exhibit different levels of intensity (demonstrated by the proximity of the contour lines, see Figure 3-17). Due to the fact that the R-enantiomer quenches the fluorescence of the calixarene to the greatest extent the 2-D emission intensity plot for this enantiomer/calixarene pair in solution has somewhat fewer contour lines of consequently lower intensity (see Figure 3-16) than the S-enantiomer/calixarene pair, however it is not immediately obvious which guest enantiomer is in the presence of the calixarene by the contour variations alone.

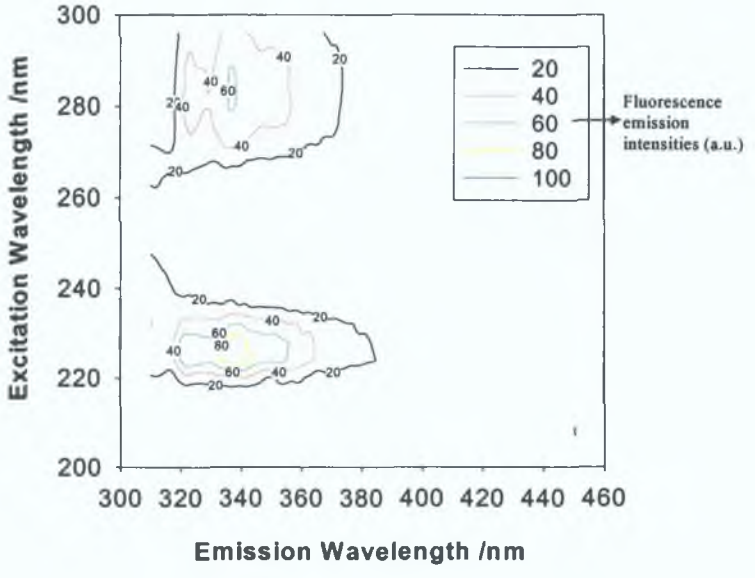

Figure 3-16: *Two-dimensional emission intensity contour plot of p-allyl-tetra-S-propranolol amide calix[4]arene in the presence of guest molecule, R-phenylalaninol in methanol.*

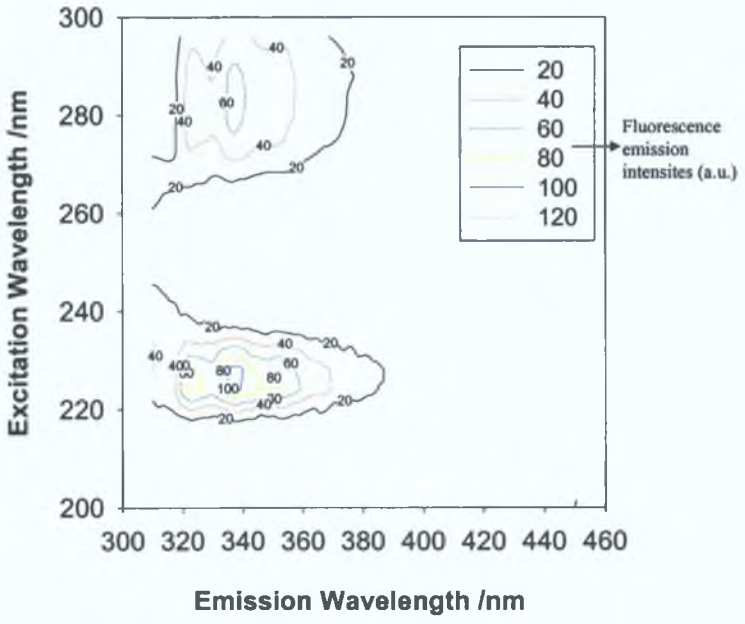

Figure 3-17: *Two-dimensional emission intensity contour plot of p-allyl-tetra-S-propranolol amide calix[4]arene in the presence of guest S-phenylalaninol in methanol.*

Upon observation of the contours produced by solutions of each enantiomer/calixarene pair it is evident that a wide range of emission data is obtainable from these associations. However, it is not immediately obvious from these plots which enantiomer is present in solution with the calixarene **L1**. Employing an excitation wavelength of 227nm appears to provide the most complete or extensive fluorescence emission information. It is therefore prudent to use such an excitation wavelength when examining the effects of the association of this calixarene with the enantiomers of phenylalaninol. In order to clearly differentiate between which enantiomer is present in solution, it is necessary to measure fluorescence intensities at the maximum emission wavelength, 336nm in this case.

3.4.6 Variation of fluorescence lifetimes with enantiomeric composition

Quenching that results from diffusive encounters between the fluorophore and quencher during the lifetime of the excited state, is a time dependent process and is termed "dynamic quenching". Quenching can also occur as a result of the formation of a non-fluorescent complex between the fluorophore and the quencher ("static quenching"), which subsequent to the absorption of light, returns immediately to the ground state without the emission of a photon. The fluorescence intensity decrease is linearly dependent on the concentration of the quencher, a case that is identical for both static and dynamic quenching. Unless additional information is supplied, either a dynamic or a static process can explain quenching.

The measurement of fluorescence lifetimes is the most definitive method to distinguish between static and dynamic quenching. Static quenching removes a fraction of the fluorophores from observation. The complexed fluorophores are non-fluorescent, and the only observed fluorescence is from the uncomplexed fluorophores. The uncomplexed fraction is unperturbed by other molecules or diffusional processes in solution, and hence the lifetime is τ_0. Therefore for static quenching $\tau_0/\tau = 1$. During the process of dynamic quenching, the quencher must diffuse to the fluorophore during the lifetime of its excited state, thereby decreasing the lifetime of the excited state fluorophore. Therefore the higher the concentration of quencher present in solution, the lower the lifetime of the fluorescent excited state will be, so for dynamic quenching $\tau_0/\tau = F_0/F$, which is in contrast to static quenching.

The lifetime of the excited state is defined by the average time the molecule spends in the excited state prior to return to the ground state. The fluorescence lifetime is important in that it determines the time available for the fluorophore to interact with or diffuse in its environment, and hence the information available from its emission. Figure 3-18 shows the decay profile of calixarene **L1** in methanol.

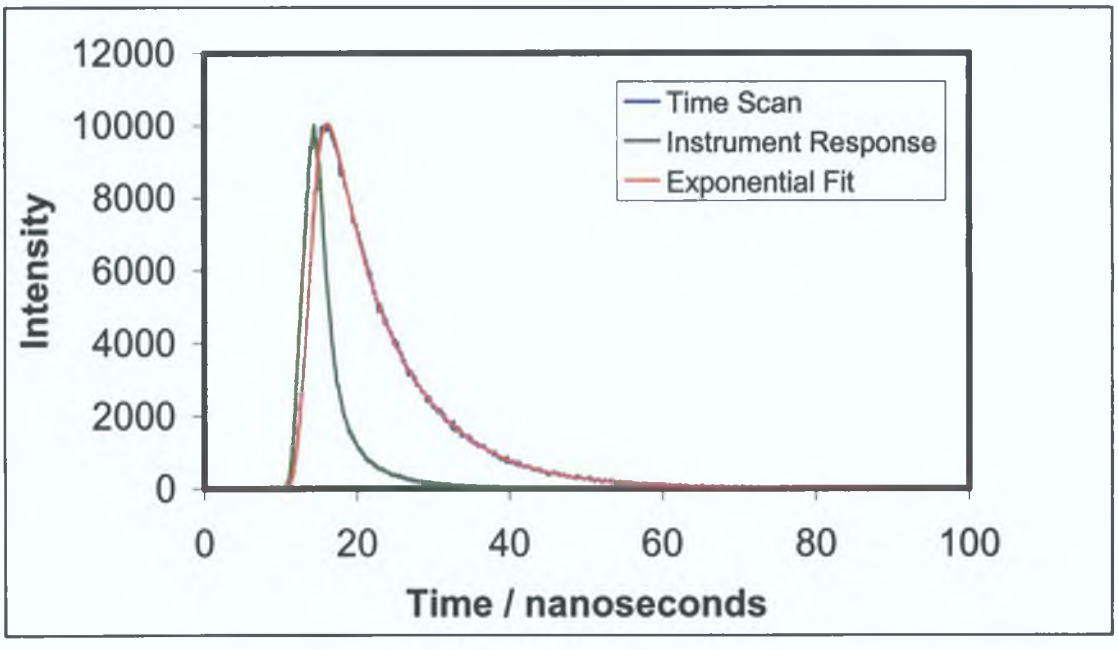

(a)

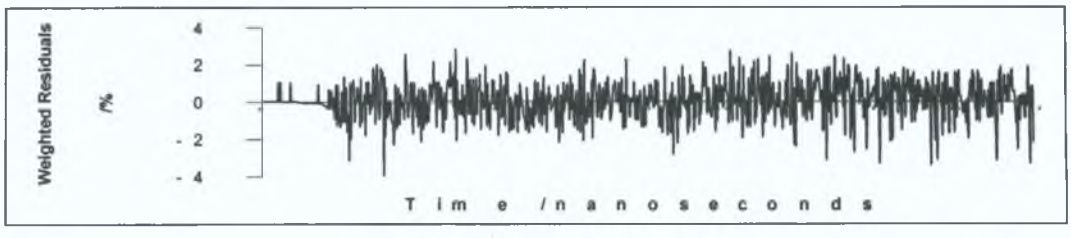

(b)

Figure 3-18: *Fluorescence lifetime decay spectrum of p-allyl-tetra-S-propranolol amide calix[4]arene in methanol, in comparison to the instrument response and the exponential model fit* ***(a)****. Residual plot of exponential fit* ***(b)****.*

$$y_n = A_0 + A_1 e^{-\left(\frac{x_n}{t_1}\right)} + A_2 e^{-\left(\frac{x_n}{t_2}\right)}$$

Equation 3-5: *Exponential fit equation used to calculate the fluorescence lifetime*

(Where A_0, A_1 and A_2 are constants, y_n = intensity data, x_n = time (ns) and t_1 and t_2, are time constants of the 1st and 2nd exponential component respectively.)

The decay time of the fluorescence of organic molecules is generally of the order of several nanoseconds, and techniques for its measurement include the stroboscopic

(pulsed-flash) technique and the phase-shift technique, the former of which uses a nanosecond spectral source containing either a nitrogen or a deuterium flash-lamp. When measuring the lifetime of any fluorescent species it is important that the response of the instrument used is quantitatively smaller than the signal produced by the fluorescing moiety, in order to allow distinction of the signal from the lamp and therefore accurate calculation of the lifetime. Using the above bi-exponential equation (Equation 3-5), the lifetime exponential decay can be modelled to yield the fluorescence lifetime of the excited state of calixarene **L1**. Using an excitation wavelength of 307nm and scanning at an emission wavelength of 340nm, two values of 9.4 and 4.6 ns were measured for the lifetime of **L1** in methanol. This would suggest that two fluorescing species are present in solution. Since spectroscopic grade solvents were used and the calixarene was pure, the second value was not attributed to an impurity. This could instead be due to different conformations of the calixarene, as the array of naphthalene groups may be differently positioned in one conformer over the other, possibly altering the electronic state of the molecule. It is interesting to note that this and any following lifetime measurements were obtained in both degassed and non-degassed solutions, and no difference was discerned between the values acquired. This would seem to indicate that molecular oxygen has no effect on the fluorescence spectra of these solutions, failing to contribute to the quenching process in any way. It is also important that a χ^2 value close to 1 is obtained after fitting the data measured to Equation 3-5, since this means that the values of the lifetimes returned by this equation are within the 95% confidence interval.

Figure 3-19 shows how the solutions used for lifetime measurements relate to the emission and quenching studies previously carried out. A solution of **L1** in methanol (Figure 3-19(i)) was spiked with aliquots of a 1.0M R-phenylalaninol in methanol (Figure 3-19(ii), (iii) and (iv)). The fluorescence emission spectra and lifetime decays were then measured and the results can be seen in Figure 3-19 and Table 3-2. It is evident from the data acquired that the lifetime measurements do not exhibit a concentration dependence on the quencher, unlike the emission spectra and also that $\tau_0/\tau \neq F_0/F$. This infers that $\tau_0/\tau \sim 1$, and therefore the mechanism of quenching of **L1** by R-phenylalaninol is confirmed to be static, in agreement with the absorbance spectral data discussed previously (section 3.4.4).

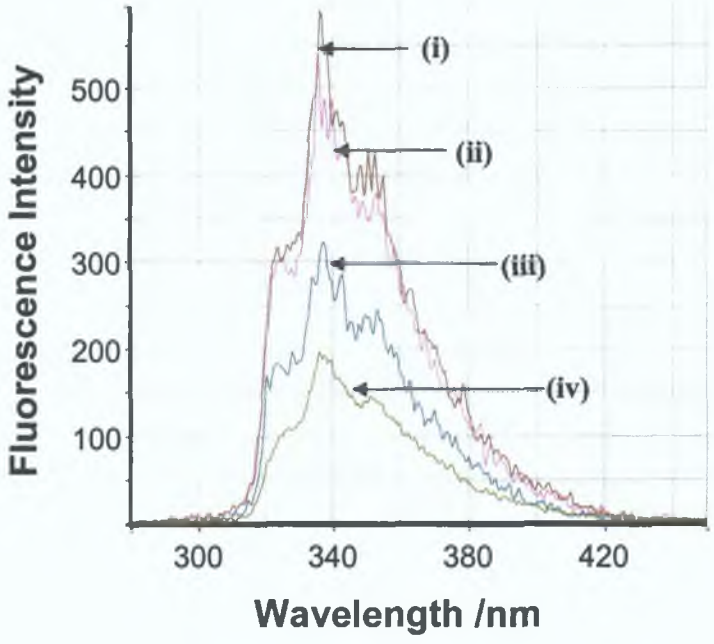

Figure 3-19: Fluorescence intensity spectrum of calixarene (56.1 μmol dm^{-3}), in the absence **(i)** and presence of R-phenylalaninol, (4 mmol dm^{-3} **(ii), 12 mmol dm^{-3} (iii), 16 mmol dm^{-3} (iv)**).

Solution	*τ_1 and τ_2 / Nanoseconds*	*χ^2*
Calixarene alone	9.44, 4.63	1.02
L1 + 4 mmol dm^{-3}	9.48, 4.43	1.06
L1 + 8 mmol dm^{-3}	9.39, 4.72	1.02
L1 + 12 mmol dm^{-3}	9.43, 4.53	1.03
L1 + 16 mmol dm^{-3}	9.37, 4.62	1.10

Table 3-2: *Fluorescence lifetimes of calixarene in the absence and presence of R-phenylalaninol.*

The lifetime of the excited state **L1** was also measured in the presence of the S-enantiomer of phenylalaninol. The results can be seen in Table 3-3, which illustrate that the presence of this guest enantiomer in solution does not perturb the excited state lifetime of the calixarene, confirming that both enantiomers of phenylalaninol form ground state complexes with calixarene **L1** in methanol solution, but as confirmed by the emission quenching data, by clearly different degrees.

Solution	τ_1 *and* τ_2 */ Nanoseconds*	χ^2
Calixarene alone	9.26, 4.43	0.98
L1 + 4 mmol dm^{-3}	9.12, 4.69	0.98
L1 + 8 mmol dm^{-3}	9.25, 4.45	0.91
L1 + 12 mmol dm^{-3}	9.06, 4.56	0.96
L1 + 16 mmol dm^{-3}	9.11, 4.73	0.99

Table 3-3: *Fluorescence lifetimes of calixarene in the absence and presence of R-phenylalaninol.*

3.4.7 Variation of Stern-Volmer plot of propranolol label with enantiomeric composition

In order to ensure that enantiomeric discrimination is due to the calixarene and not simply caused by the presence of the propranolol label, fluorescence-quenching studies were carried out on the label alone in the presence of enantiomers of phenylalaninol. These studies were carried out over a period of minutes and as phenylalaninol enantiomers were spiked into the solution, the fluorescence intensity was monitored at an emission wavelength of 336nm. These spiked solutions were then scanned over a range of wavelengths to see the full effect on the label's spectrum.

It is evident from Figure 3-20 that quenching of the label does occur after the addition of the amino alcohol enantiomers are added to solution. However selectivity in quenching is not achieved, that is both enantiomers quench the label's fluorescence to the same degree, thereby proving that enantiomeric discrimination of phenylalaninol is not possible with this label alone. Figure 3-21 shows the full spectra of the label after addition of 1, 2, and 3-mmol dm^{-3} of both enantiomers of phenylalaninol. These spectra further prove that selective quenching of this label by one enantiomer does not occur.

Comparison studies were carried out on the calixarene with phenylalaninol enantiomers, both over time and across a full spectrum. Figure 3-22 shows how the addition of the (S)-enantiomer of phenylalaninol quenches the fluorescence of calixarene **L1**, but not to the same degree as the (R)-enantiomer (as already shown in the Stern-Volmer plots- see Figure 3-11). Further proof of enantiomeric discrimination by this calixarene ligand is obtained from the emission spectra after the spiked solutions were scanned from 310-400 nm (see Figure 3-23). These results suggest that the chiral recognition exhibited by L1 with phenylalaninol is not an inherent characteristic of the label itself, but rather an effect of the 3-d distribution of groups within the calixarene.

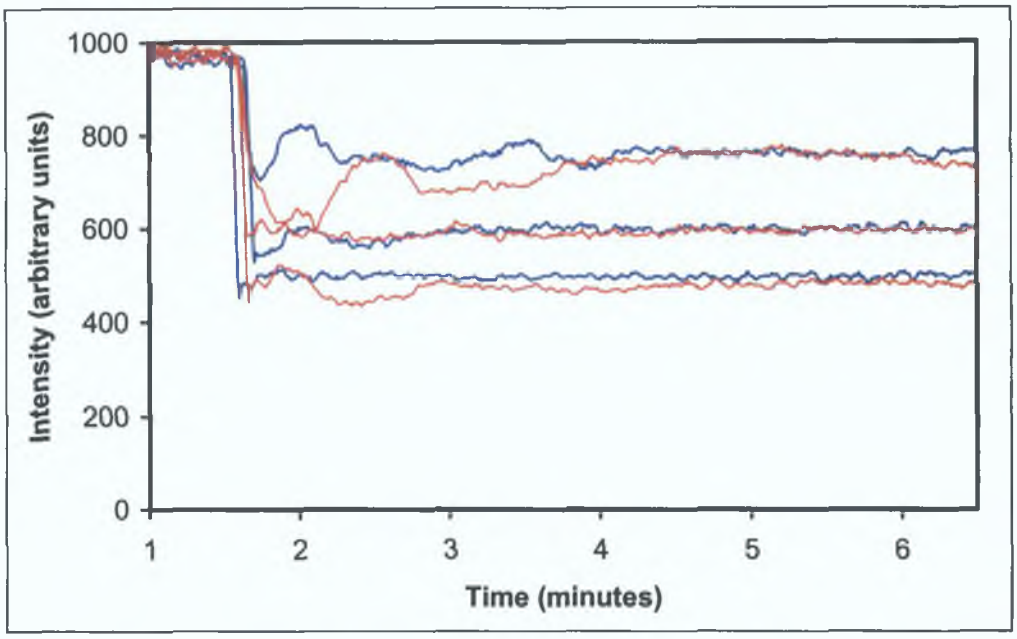

Figure 3-20: *Fluorescence intensity changes of S-propranolol label (2.8 μmol dm^{-3} in methanol) over time, after the addition of (S)-phenylalaninol (blue) and (R)-phenylalaninol (red) in aliquots of 1 (upper), 2 (middle) and 3 mmol dm^{-3} (lower), monitored at an emission wavelength of 338nm.*

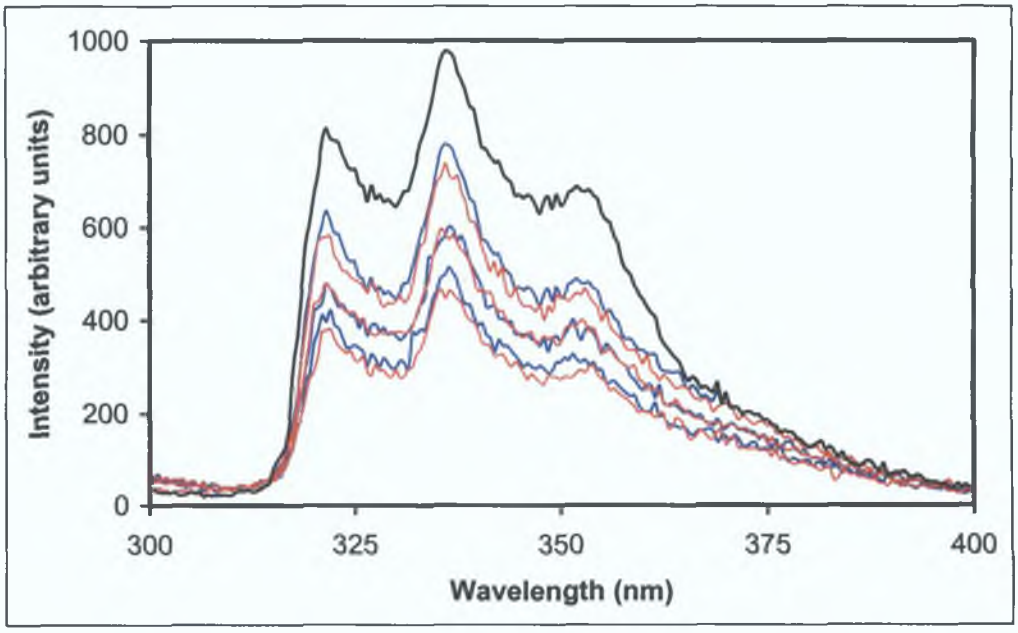

Figure 3-21: *Fluorescence emission spectra of S-propranolol label (spectrum in black (2.8 μmol dm^{-3} in methanol)) after the addition of (S)- and (R)-phenylalaninol (blue and red spectra respectively), in aliquots of 1 (upper), 2 (middle) and 3 mmol dm^{-3} (lower), monitored after a time of 7 minutes.*

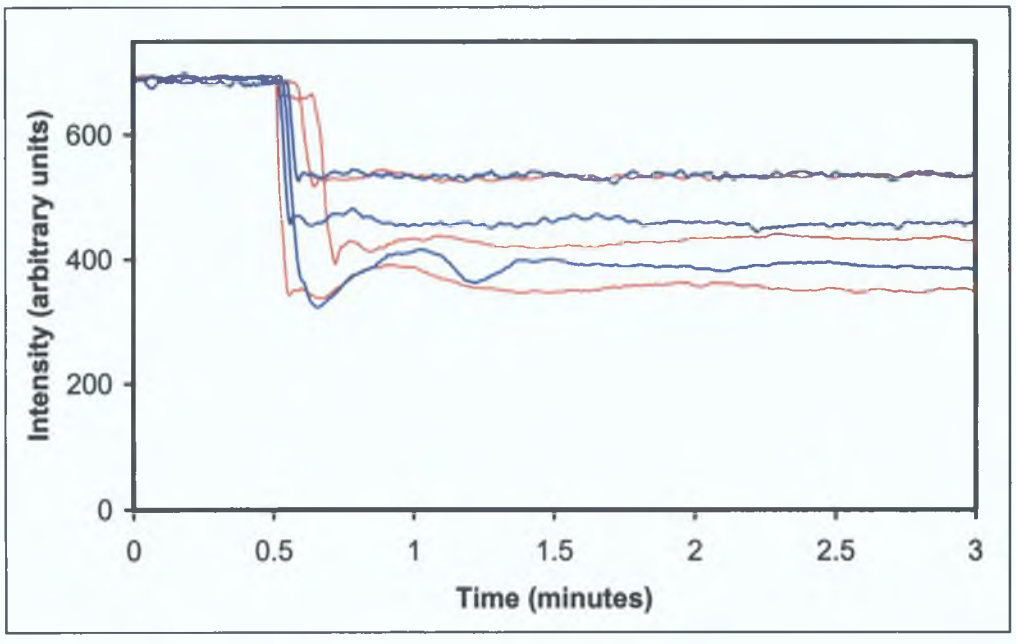

Figure 3-22: *Fluorescence intensity changes of calixarene **L1** (0.7 μmol dm^{-3} in methanol) over time, after the addition of (S)-phenylalaninol (blue) and (R)-phenylalaninol (red) in aliquots of 1 (upper), 2 (middle) and 3 mmol dm^{-3} (lower), monitored at an emission wavelength of 338nm.*

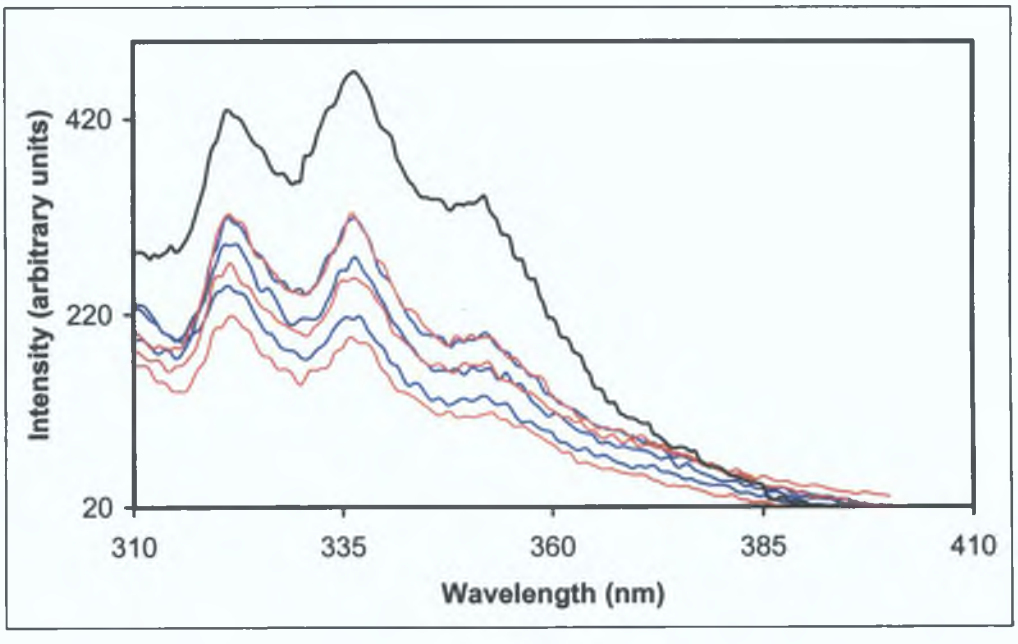

Figure 3-23: *Fluorescence emission spectra of calixarene **L1** (0.7 μmol dm^{-3} in methanol) after the addition of 1 (upper), 2 (middle) and 3 mmol dm^{-3} (lower), (S)- and (R)-phenylalaninol (blue and red spectra respectively) after a time of 7 minutes (calixarene alone in black).*

3.4.8 Variation of Stern-Volmer plot of a partially functionalised calix[4]arene with enantiomeric composition

As another control study to ensure that enantiomeric discrimination is due to the three-dimensional cavity of the lower calixarene rim and not simply caused by the presence of the propranolol label, fluorescence-quenching studies were carried out on the p-allyl calix[4]arene-mono- and di-R-propranolol amide mixture (see Chapter 3 (**117**)) in the presence of both enantiomers of phenylalaninol. These studies were carried out at an excitation wavelength of 227nm, as phenylalaninol enantiomers were spiked into the calixarene solution, while the fluorescence intensity was monitored at an emission wavelength of 336nm.

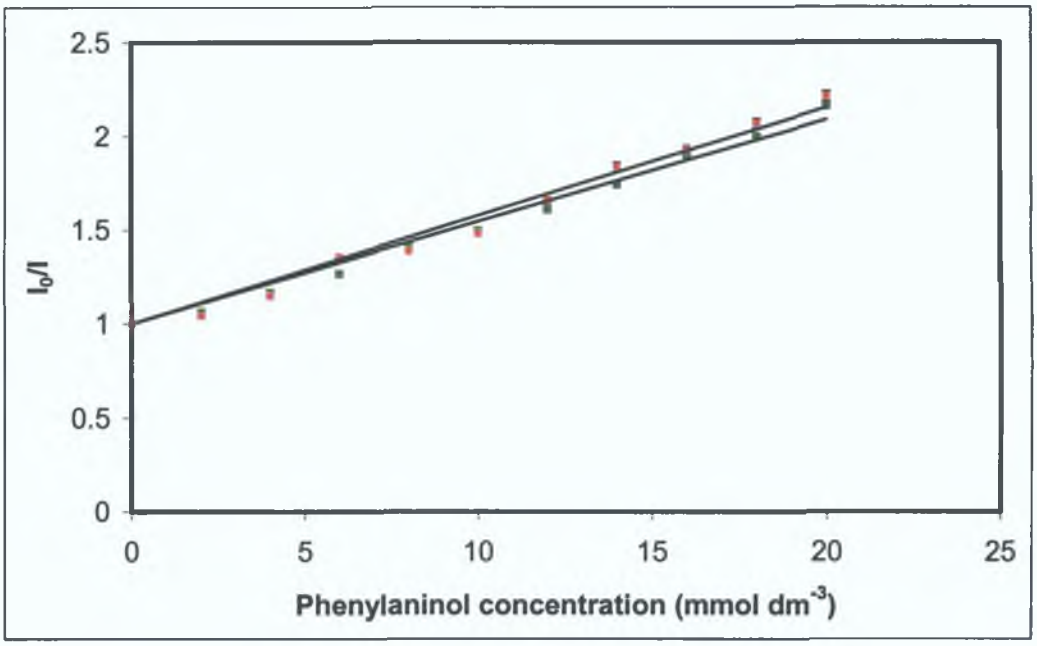

Figure 3-24: *Stern-Volmer plots for the quenching of di-R-propranolol calixarene (0.7 μmol dm^{-3} in methanol) upon addition of 100% (red) and 0% (green) (R)-phenyl alaninol in methanol. Standard deviations are shown as error bars (n=3), which may be masked by symbols.*

As can be seen from Figure 3-24 practically no difference is discerned in the slopes, and in some cases the error bars for each series overlap. Consequently there is no difference in the K_{SV} constants of the plot of each enantiomer of phenylalaninol in the presence of the mono-/di-substituted calixarene. This therefore signifies that the partially substituted equivalents of the aforementioned propranolol calixarene **L1** do not possess the ability to discriminate between the enantiomers of phenylalaninol,

and as suggested previously that discrimination is achieved due to an effect of the 3-D distribution of groups within the calixarene.

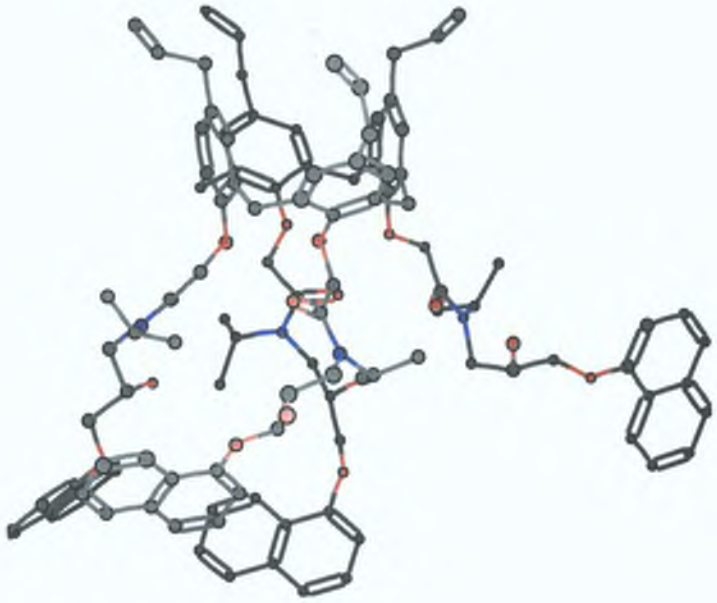

Figure 3-25: *Energy minimised structure of* ***L1*** *(experimental details in Chapter 4, files were incorporated into CS Chem 3D Pro for viewing after calculations were carried out using Spartan).*

The interpretation of these results is as follows: **L1** possesses a relatively well-defined 3-D chiral space in the calixarene cavity (see Figure 3-25). It is almost certain that the guest amines approach from the more open end of the molecule (i.e. that defined by the fluorescent naphthyl groups), and hydrogen bond with appropriate groups within the cavity of the host molecules. Association between the aryl groups of the guest and the naphthyl groups on the host could be the source of the quenching effect, and this will be most efficient if;

1. Hydrogen bonding is favoured (depends on the host, guest and the solvent)
2. Distance from the hydrogen bonding sites to the aromatic groups corresponds (depends on presence or absence of appropriate spacer groups in the host and guest).
3. The orientation the guest during hydrogen bonding is such that the aryl group interacts with the naphthyl group of the host.

The absence of selective quenching of **L1** by the enantiomers of phenylglycinol and phenylethylamine is most likely due to inadequate distances between the appropriate hydrogen bonding sites and the aromatic ring systems in the guest molecules. If the

distances between the chiral centres (and adjacent amine groups) and the aryl rings of the host and guest molecules are compared, it is clear that in the case of the aforementioned guest molecules they are too short to effectively bind with the host calixarene and simultaneously align the aromatic groups with the naphthyl moieties to quench the calixarene fluorescence (see Figure 3-26). If the aromatic rings of the guest assemble alongside the naphthyl rings of the host a lack of favourable hydrogen bonding exists, which is necessary to form a non-fluorescent ground state complex.

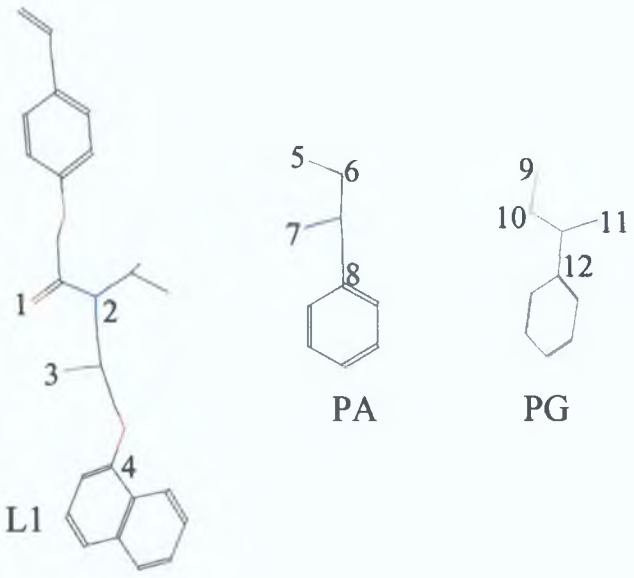

Figure 3-26: *Distances from hydrogen bonding sites to aromatic groups within molecules (modelled and measured using CS Chem 3D Pro).*

	Distance /Å	*Distance /Å*	*Distance /Å*
L1	6.29 ((**1-4**) C=**O**– C_{aryl})	6.01 ((**2-4**) **HN**– C_{aryl})	3.68 ((**3-4**) **HO**–C_{aryl})
PA	4.36 ((**5-8**) **HO**– C_{aryl})	3.88 ((**6-8**) HO–**C**– C_{aryl})	2.92 ((**7-8**) **HN**– C_{aryl})
PG	3.75 ((**9-12**) **HO** – C_{aryl})	2.50 ((**10-12**) HO-**C** – C_{aryl})	2.48 ((**11-12**) **HN**– C_{aryl})

Table 3-4: *Intramolecular distances of the molecules in* ***Figure 3-26****.*

The fact that the calixarene fluorescence is however quenched, could be due to dynamic or collisional quenching. With respect however, to the phenylalaninol guest molecules, both enantiomers have the correct spacing between the hydrogen bonding groups and the aryl group, facilitating both hydrogen-bonding opportunities and quenching incidences concurrently. The (R)-enantiomer of phenylalaninol is

favoured over the (S)-isomer under the conditions cited in (1) (2) and (3), above, and (R)-phenylalaninol thereby selectively forms a ground state complex with the calixarene which is non-fluorescent. This results in a reduction of the excited state population of the calixarene, causing quenching of the signal, namely a decrease in the fluorescence intensity. The fact that a ground state non-fluorescent complex is formed by phenylalaninol guests in the presence of **L1** is confirmed by excited state fluorescence lifetime measurements in the absence and presence of the guest. It is clear that no change in lifetime is observed when the calixarene is present in solution with the guest, establishing that the mechanism of quenching between this host : guest pair is static.

As the tetra-derivatised host molecule **L1** is in itself chiral in nature, bearing an (S)-amide substituent, the (R)-enantiomers in each case should be better predisposed to interact than the (S)-enantiomers. This would lead to a more favourable interaction with the host and the guest and therefore a greater slope for the Stern-Volmer plot. This is observed experimentally in the case of phenylalaninol, where the (R)-enantiomer displays the larger quenching effect, with greater K_{sv} values than the corresponding (S)-enantiomer. The importance of the spacing between the hydrogen boding sites and the aromatic groups of the guest is also clearly demonstrated in this study. The fact that **L1** cannot differentiate between the 'shorter' guest enantiomers, e.g. phenylglycinol and phenyl ethylamine, demonstrates the important molecular recognition capabilities of this host. **L1** is very specific in its interactions with guest molecules and as well as discriminating between mirror image forms, can successfully recognise such a small difference in guest molecules as a methylene spacer.

The energy minimized structure in Figure 3-27 shows a possible position of the guest molecule, phenylalaninol in the calixarene cavity, and gives an indication of the number of hydrogen bonding possibilities between the host and guest. There appear to be several possibilities for the $-NH_2$ of the guest amino alcohol to interact with one of the carbonyl groups of the calixarene, and for the -OH of the guest to interact with the carbonyl of the same pendant leg [**13**]. Further examination of Figure 3-27 shows how the –OH of the guest seems to interact with the chiral hydroxy group of another pendant group of the calixarene, leaving the aryl ring of the guest sandwiched amid

two of the calixarene pendant naphthyl rings, which may facilitate a π-stacking interaction

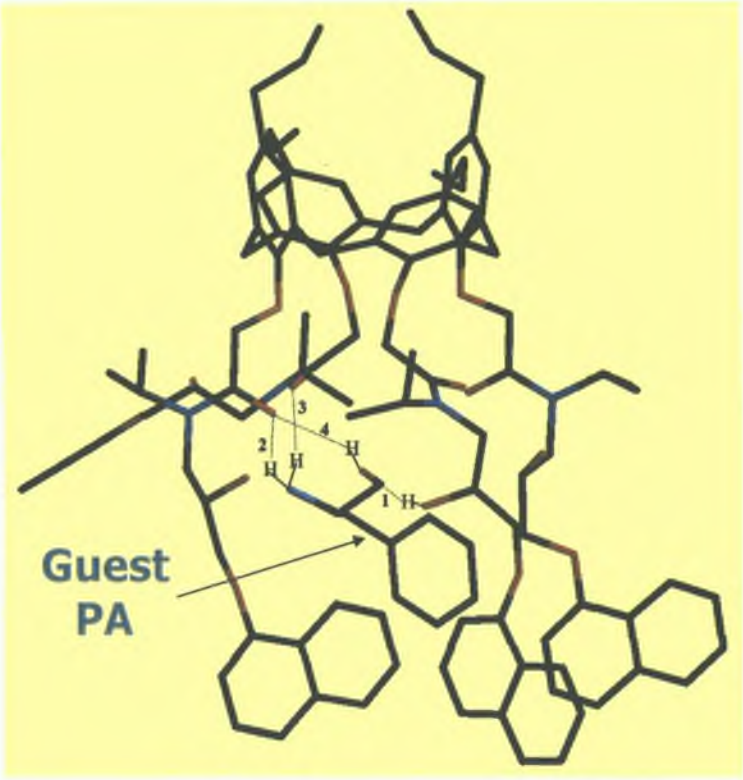

Figure 3-27: *Energy-minimized structure of the p-allyl (S-) propranolol tetra amide calix[4]arene with guest molecule phenylalaninol (PA) [**13**].*

If one compares simple molecular models of the pendent legs of the calixarene, it can be seen how the interactions of one enantiomer may be favoured over the other. In the case of (R)-phenylalaninol (see Figure 3-28), the amino group would appear to be in a favourable position to hydrogen bond to the hydroxy group adjacent to the chiral centre, which may then allow further hydrogen bonding of the guest hydroxyl moiety to either the carbonyl oxygen or nitrogen of the calixarene amide functionality. In the case of the (S)-guest however (see Figure 3-29), the amino group being on the other side of the molecule does not appear to favour such hydrogen bonding.

In the case of the free label, it is quite certain that the (R)-enantiomer of phenylalaninol interacts a similar manner to the (S)-isomer both displaying equal abilities to deactivate the excited state of the free label. Whether or not the quenching mechanism is static or dynamic in nature is not of great importance in this study, due to the fact that no discrimination by the free label is achieved. Also the results of the

mono-/di-amide-functionalised R-propranolol calixarene prove that the label alone is not responsible for enantiomeric discrimination, and that a 3-D distribution of binding sites is necessary for selective associations to occur. In the case of the tetra S-propranolol calixarene an additional chiral 3-D space seems to be created by the association of the propranolol pendent legs on the lower rim of the annulus, which favours the insertion of the (R)-enantiomer over the (S)-isomer.

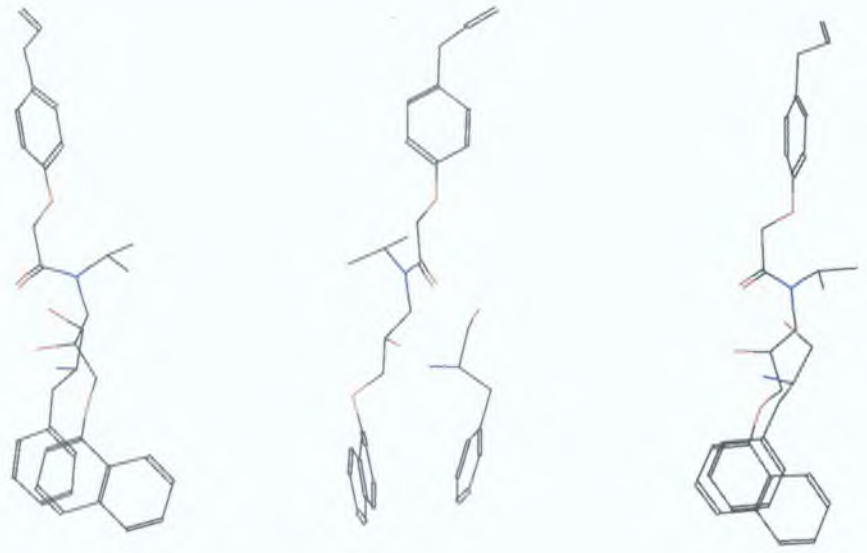

Figure 3-28: *possible orientations of host **L1** with guest R-phenylalaninol.*

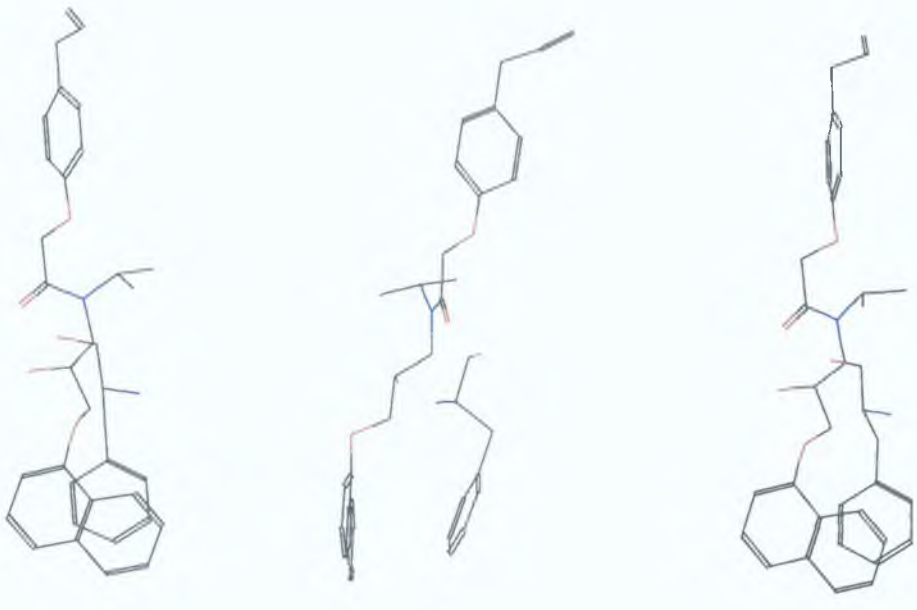

Figure 3-29: *possible orientations of host **L1** with guest S-phenylalaninol.*

Structures above were modelled using CS Chem 3D Pro version 6.0, MM2 force field. The models shown correspond to the conformer with the lowest energy.

3.5 Conclusion

Ligand **L1** was designed with a methylene spacer between the chiral centre and fluorescent naphthyl moiety. This ligand was found to successfully discriminate between the amino alcohol, phenylalaninol, with a methylene spacer between its aromatic moiety and chiral centre. However, discrimination between two pairs of shorter chain amino alcohol enantiomers (R- and S- phenylglycinol and phenyl ethylamine) was not observed with this calixarene. The fact that **L1** cannot differentiate between the 'shorter' guest enantiomers, e.g. phenylglycinol and phenyl ethylamine, demonstrates the important molecular recognition capabilities of this host. **L1** is very specific in its interactions with guest molecules and as well as discriminating between mirror image forms, can successfully recognise such a small difference in guest molecules as a methylene spacer.

In this study there are relatively well-defined, 3-D chiral spaces in the cavity of the calixarene **L1** through which the enantiomers must pass in order to facilitate quenching. This infers that since the host molecule is itself chiral in nature, bearing an (S)-amide substituent, that the (R)-enantiomer should be better predisposed to interact with the calixarene than the (S)-enantiomer. This would in turn lead to a more efficient energy transfer from the naphthalene of the (S)-propranolol group to the guest and therefore a greater slope for the Stern-Volmer plot. What is observed experimentally is that the R-enantiomer is in fact the preferred guest molecule with regard to Ligand **L1**, with greater interaction and selectivity being observed in its fluorescence plots than in the case of the S-enantiomer.

The fact that the excitation spectrum of calixarene **L1** undergoes changes in the presence of a phenylalaninol guest molecule indicates that the process of quenching is probably static, that is, the guest molecule forms a non-fluorescent ground state complex with the calixarene host. With the aid of fluorescence lifetime studies further information on the mechanism of quenching was obtained, and it was established that since the lifetime of the excited state of **L1** was independent of the concentration of the guest molecule, that static quenching was the cause of the decrease in fluorescence intensity of **L1** in the presence of phenylalaninol.

3.6 References

1 T. Eriksson, S. Björkman, B. Roth, Å. Fyge, P. Höglund, *Chirality*, **1995**, 7, 44.

2 D. A. Labianca, G. N. Taylor, G. S. Hammond, *J. Am. Chem. Soc.* **1972**, 94, 3679.

3 G. N. Taylor, G. S. Hammond, *J. Am. Chem. Soc.* **1972**, 94, 3684.

4 P. M. Froehlich, H. A. Morrison, *J. Am. Chem. Soc.* **1974**, 96, 332.

5 G. N. Taylor, E. A. Chandross, A. H. Schiebel, *J. Am. Chem. Soc.* **1974**, 96, 2693.

6 C. C. Warnser, R. T. Medary, I. E. Kochevar, N. J. Turro, P. H. Chang, *J. Am. Chem. Soc.* **1975**, 97, 4864.

7 P. Froehlich, E. L. Wehry, *Modern Fluorescence Spectroscopy 2*, E. L. Wehry, (Ed.,) Plenum Press, New York & London, **1976**, Chapter 8.

8 M. Irie, T. Yorozu, K. Hayashi, *J. Am. Chem Soc.*, **1978**, 100, 2236.

9 T. Yorozu, K. Hayashi, M. Irie, *J. Am. Chem Soc.* **1981**, 103, 5480.

10 T. D. James, K. R. A. S. Sandanayake, S. Shinkai, *Nature*, **1995**, 374, 345.

11 Y. Yan, M. L. Myrick *Anal. Chem.* **1999**, 71, 1958.

12 K. S. Parker, A. Townshend, S. J. Bale, *Anal. Proc. Anal. Commun.* **1995**, 32, 329.

13 D. Fayne, *Ph.D Thesis*, **2001**.

4 Host-Guest Behaviour of Ion-Complexes of Calix[4]arene Host L1

4.1 *Introduction -Fluorescent cyclodextrins as host molecules*

Cyclodextrins (CD's), are macrocyclic oligosaccharides, produced by the enzymatic catabolism of starch consisting of 6(α), 7(β) or 8(γ) α-D-glucopyranose units connected by 1,4-glycosidic bonds. It is known from crystal structure and spectroscopic analyses that CD's exist in an approximately round conical shape (see below), in solution as well as in the solid state [**1**]. They are inherently chiral and form inclusion complexes with a variety of organic compounds in aqueous solution, accommodating a guest molecule in their central cavity [**2**, **3**, **4**]. Cyclodextrins, which are spectroscopically inert, can be converted into fluorescent CD's by modification with one or more fluorophores (e.g. naphthalene, pyrene or dansyl moieties). Such labelled CD hosts may exhibit changes in fluorescence emission intensities upon addition of guest compounds.

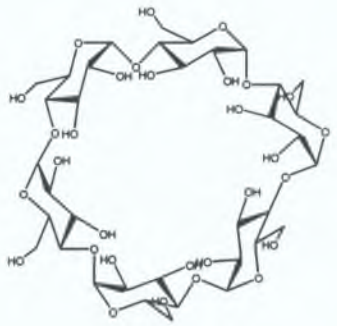

***Alpha*-cyclodextrin**

On this basis fluorescent CD's were used as fluorescent chemosensors for molecular recognition. The driving force in the formation of CD inclusion complexes with organic guests is considered to be the hydrophobic interaction between the CD framework and the guest molecule. Dye-modified CD's have been used as colour-change indicators for molecules [**5**, **6**, **7**, **8**]. The finding that pyrene-modified γ-CD forms an association dimer (see Figure 4-1) and exhibits excimer emission around 470nm, was the inspiration for using fluorophore-attached CD's as sensors [**9**, **10**]. The fluorescence change (decrease in excimer emission and increase in monomer emission at 397nm) induced by the association dimer to 1:1 host-guest complexes was confirmed on examination of the guest-induced circular dichroism spectra and absorption variations. Since guest-induced fluorescence variation is greatly affected by the size and shape of guest species, this proved possible as a sensory system for molecular recognition of organic compounds [**11**].

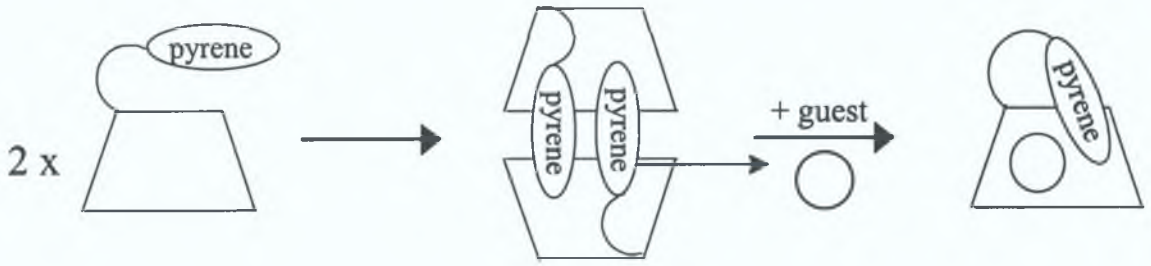

Figure 4-1: *γ-CD's modified with mono-pyrene moieties need to form to dimers to facilitate a change in spectrum when the guest is complexed.*

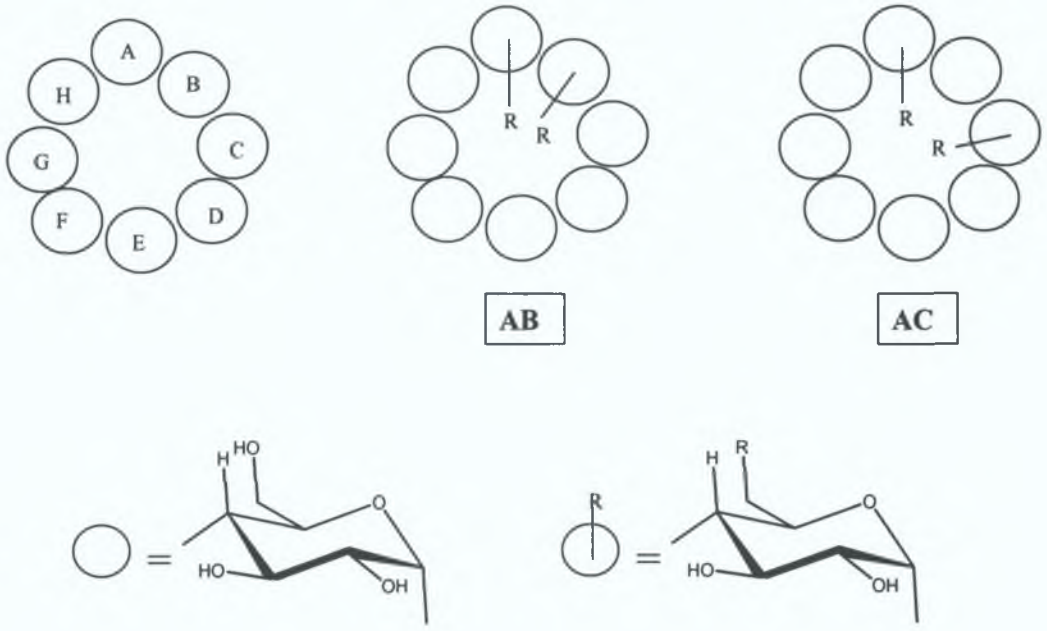

Figure 4-2: *di-substituted γ-CD's eliminate the need for dimer formation, since different positional isomers exhibit different fluorescence changes in the presence of a guest molecule.*

This work further inspired synthesis of γ-CD's bearing two pyrene units, since they change their fluorescence spectra without the necessity of dimer formation. If a γ-CD is prepared with two naphthalene moieties, then four isomers are possible, AB, AC, AD, AE, with A, B, C, D, E, etc. denoting the juxtaposed glucose units of the CD circle (see Figure 4-2). Different geometrical isomers of the CD's bearing two pyrene moieties may have different guest-responsive properties. All isomers exhibit predominant excimer emission around 520nm and intensities increased upon addition of (-)-borneol (**128**), whereas in the case of two of the isomers the addition of

lithocholic acid caused a decrease in intensity. Thereby confirming that spectral variation is dependent on the two species, both host and guest.

The same approach was used with two naphthalene-modified (R = 2-naphthyl-sulphnoyl) β- and γ-CD's for detecting molecules [**12**, **13**, **14**]. Three geometrical isomers are possible in the case of the β-CD's bearing two substituents. It is noted that in the case of β-CD derivatives, the excimer formation is not possible without accommodation of guest species in the CD cavity, because one naphthyl group is included in the cavity, while another is located outside in the absence of a guest (see below). Remarkable differences have also been found between the two series of β- and γ-CD derivatives [**14**].

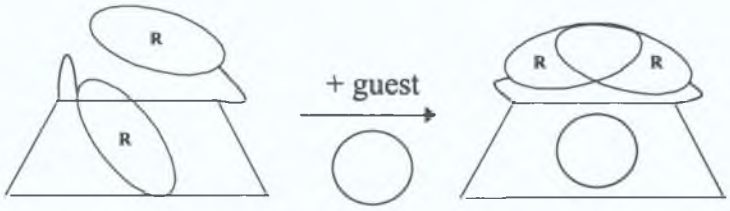

Figure 4-3: *in contrast to γ-CD's, di-substituted β-CD's only exhibit excimer emission in the presence of a guest molecule, since in its absence one of the naphthyl-sulphonyl (***R***) moieties is located inside the CD-cavity.*

Large guest molecules such as urso- and cheno-deoxycholic acid (**129** - isomers) exhibit high responsitivity for γ-CD derivatives, whereas tricyclic and bicyclic ball-like guests such as adamantanol (**130**) and (-)-borneol (**128**) exhibit high sensitivities for β-CD derivatives and smaller guests such as cyclohexanol display a negligible effect.

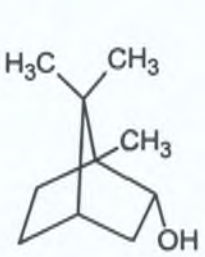

128

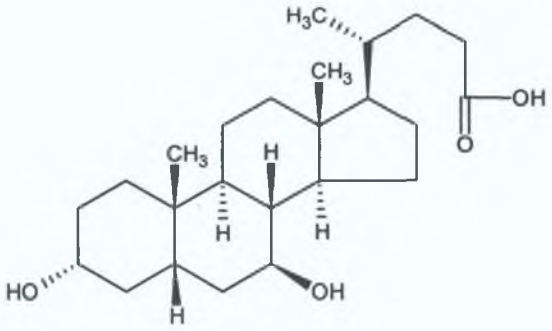

129

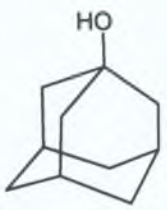

130

Both enantiomers of dansylglycine- and dansylleucine-modified CD's (see below, a and b respectively) were prepared [**15**, **16**, **17**] since dansyl is known as a probe

which exhibits a strong fluorescence in a hydrophobic environment, but a weak one in bulk water solution. β-CD derivatives of the aforementioned series form self-inclusion complexes, in which, the appended dansyl chromophore is included in its own cavity and exhibits strong emission. Upon guest addition these β-CD derivatives decrease their fluorescence intensities around 535nm, by excluding the dansyl unit from the cavity into bulk water solution. After addition of larger guest species to solutions of similar γ-CD derivatives a decrease in fluorescence intensity is observed, but the intensity increases upon addition of smaller species due to co-inclusion of the fluorophore and a guest molecule in the large γ-CD cavity.

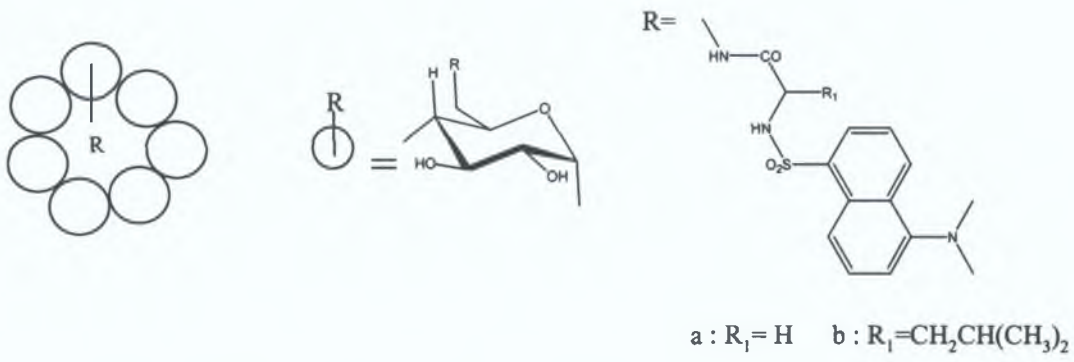

Figure 4-4: *β-CD's modified with dansylglycine (a) and dansylleucine (b), since dansyl is known as a strong fluorescing agent in a hydrophobic environment.*

In the case of β-CD derivatives, dansyl-L-leucine-β-CD gives larger binding constants than its D-isomer, while both show improved binding abilities over dansylglycine-modified β-CD. Conversely, the binding constants for 1-adamantanol (**130**) and dansyl-L-leucine-γ –CD, dansyl-D-leucine-γ –CD and dansylglycine-γ –CD are 116, 370 M^{-1} and negligible respectively, reversing the chirality preference and exhibiting much smaller binding constants than those of β-CD derivatives [**18**].

Monensin is known as an antibacterial compound capable of binding Na^+ ions and mediates transport of the ions through biomembranes. Consequently dansyl-monensin-β-CD was synthesised, in which monensin was covalently bound to the ω-amino group of a lysine unit via an amide linkage [**19**]. When this compound was compared with the binding ability of dansylglycine-modified β-CD, it was demonstrated that the monensin system enhances binding abilities for various guests, with the presence of a Na^+ ion further enhancing binding abilities [**19**]. These

results were found for the guest's nerol and geraniol, as shown by 64- and 92-fold improved binding abilities respectively, which are further enhanced by the presence of a Na^+ ion. The authors report that this enhancement may be due to the rearrangement of the monensin acyclic chain to form a macrocyclic one, in the centre of which is the bound sodium ion.

In conclusion fluorescent cyclodextrins (CD's) can be used for detecting molecules in respect to molecular recognition. Improved sensing and binding abilities of these compounds can be achieved by the incorporation of other functional moieties such as an amino acid with a hydrophobic side chain or monensin and proteins. The results described indicate that induced-fit types of conformational change are essential for these sensors.

Since it is well known that calixarenes with ester, amide and acid functionalities form metal ion complexes **[20]**, the effect of metal ion complexation on the S-propranolol tetra amide calix[4]arene **L1** was investigated. When a calixarene complexes with metal ions there is frequently a change in the conformation of the complexed calixarene when compared to the free ligand. The cyclodextrin results which indicate that conformational change is necessary for such molecules to be considered suitable as sensors for guests, suggest it might be interesting to investigate whether these conformational changes which accompany metal ion complexation will have a significant effect on the fluorescence behaviour of **L1** in the presence of guest molecules. In view of the fact that Ikeda and Ueno established improved guest binding abilities of a monensin appended cyclodextrin-sodium complex, the effect of metal ion complexes of our fluorescent calixarene **L1** in the presence of guest molecule phenylalaninol was investigated.

4.2 *Experimental Section*

4.2.1 Equipment and Materials

^{1}H-NMR spectra were obtained using a Bruker Avance (400MHz) instrument. Measurements were carried out in $CDCl_3$. Chemical shifts were recorded relative to TMS. The spectra were converted from their free induction decay profiles using XWIN-NMR software.

The modelling calculations were carried out using *Spartan* [**21**] SGI Version 5.1.1. The simulations were run on a Silicon Graphics O2 workstation with a MIPS R10000 Rev. 2.7, 195 MHz CPU running an IRIX operating system, Release 6.3. Monte Carlo conformational searches were carried out on the sodium complex. Each conformer found was geometry optimised *in vacuo* with molecular mechanics using the Merck Molecular Force Field (MMFF) [**22**]. The models shown correspond to the conformer found with the lowest energy. The model shown for the free ligand and the potassium complex were obtained in an identical manner.

All fluorescence emission and quenching experiments were performed using a Perkin-Elmer Luminescence Spectrometer LS 50B (Beaconsfield, Buckinghamshire, UK), interfaced with a Pentium PC employing fluorescence data management software, FLWinlab. Post-run data processing was performed using Microsoft Excel '97 and 2000 after importing the spectra as ascii files.

(R)-(+)-phenylalaninol and (S)-(-)-phenylalaninol, were of puriss grade (98% pure, the 2% represents the other enantiomer), sodium iodide, sodium perchlorate, potassium iodide and potassium perchlorate were of puriss grade (99% pure) and obtained from Fluka Biochemika (Gillingham, Dorset, UK). For comparison, phenylalaninol was also obtained of puriss grade from Sigma-Aldrich. The solvents used (methanol- HPLC grade) was obtained from Labscan (Stillorgan, Co. Dublin). The ^{1}H-NMR solvents used ($CDCl_3$ –0.03%TMS, >98.8 atom %D) was obtained from Apollo Scientific Ltd. (Whaley Bridge, Derbyshire, UK).

4.2.2 Procedure for Fluorescence Measurements

Test solutions for the sodium complexes of calixarene **L1** and PA were prepared in a manner identical to that of **L1** and PA in Chapter Three followed by an addition of sodium iodide and sodium perchlorate respectively, (10-fold excess was used to ensure complexation). Test solutions for the potassium complexes of **L1** and PA were prepared in an identical manner to that of the sodium complexes.

4.3 Effect of Ion-Complexation on Chiral Discrimination by L1

It is known that calixarene tetra-esters and tetra-amides complex metal ions [**20**], and therefore the effect of metal ion complexation on ligand **L1** was investigated. Since calix[4]arenes possess such well-known ion-binding properties, will ion-complexes have different host-guest behaviour compared to the free calix[4]arene host? In tetra-O-alkylated calix[4]arenes, the cone conformation may not necessarily be stabilized due to the absence of intramolecular hydrogen-bonding interactions [**23**, **24**, **25**, **26**, **27**, **28**, **29**, **30**, **31**, **32**, **33**, **34**, **35**]. This can lead to different conformations of calixarenes in solution, in particular in the absence of bulky substituents to crowd the upper or lower rim, forcing it into a locked position. However a more rigid conformation may be achieved upon complexation with metal ions.

The series of peaks in the region 5.3 – 6.2ppm of the ^{1}H-NMR's in Figure 4-6(a) represent the allyl protons of the calixarene **L1**. The presence of two peaks in the free ligand would indicate that the calixarene does not exist in a symmetrical cone conformation but as a distorted cone in solution. After the addition of sodium iodide to the $CDCl_3$ solution of this calixarene, the ^{1}H-NMR spectrum (Figure 4-6(a)) of this solution showed a single multiplet for these allylic protons. This would suggest binding of the sodium ion by the calixarene, which forces the molecule into a more rigid form and the presence of one peak representing the four allylic protons would indicate a more symmetrical conformation. The same trend was also observed upon addition of potassium iodide to a solution of the calixarene in $CDCl_3$ (Figure 4-6(a)), also indicating binding of the potassium ion.

The two sets of peaks at 1.25 and 1.46ppm represent the isopropyl protons of the calixarene **L1**. After the addition of sodium ions to the NMR solution the intensity of the peak at 1.25 decreases and the double doublet moves from 1.46 to 1.55ppm (Figure 4-6(b)). Upon addition of potassium ions to a $CDCl_3$ solution of L1 (Figure 4-6(b)) a change in intensity of the peak at 1.25ppm is again observed and the double doublet is now positioned at 1.53ppm. The reduction in intensity of the peak located at 1.25ppm after addition of the metal ions, resulting in just two sets of doublets located at ~1.5ppm (representing the isopropyl protons), suggests that the equilibrium of the conformation of the calixarene has changed and the molecules are forced into a more symmetrical cone conformation. The metal ions in solution complex with most of the calixarene molecules and the new peaks observed after the

addition of metal ions are due to the newly enforced conformation. The induced symmetry of the molecule causes one set of ^{1}H-NMR peaks to appear for each unit of the macrocycle. In calix[4]aryl tetra-esters and tetra-amides the four carbonyls are turned outwards to reduce electrostatic repulsion among carbonyl oxygens, whereas bound Na^+ induces the carbonyls to point inward in order to bind the Na^+ ion **[36]**. These changes in the positions of the isopropyl proton peaks would suggest that the carbonyl oxygens are indeed binding the Na^+ ion.

Further studies involving molecular modelling confirm this theory that the free ligand does not exist as a perfect cone, but rather as a distorted cone with 2-fold symmetry. Figure 4-7 shows the results of molecular modelling studies with the free ligand (a), the Na^+ complex (b) and the K^+ complex (c), respectively. It is evident from the pictures and from the distances between opposite phenolic units (see Table 4-1) that the free ligand and the two complexes have different conformations, the two complexes existing in a square; symmetrical cone conformation. The angles between the opposing phenolic units also suggest that the two adjacent phenolic units be at approximately right angles to each other, which is consistent with the distorted cone image (see Figure 4-7). In contrast the two calixarene-metal complexes have very similar angles between opposing phenolic units, which implies a more symmetrical cone conformation.

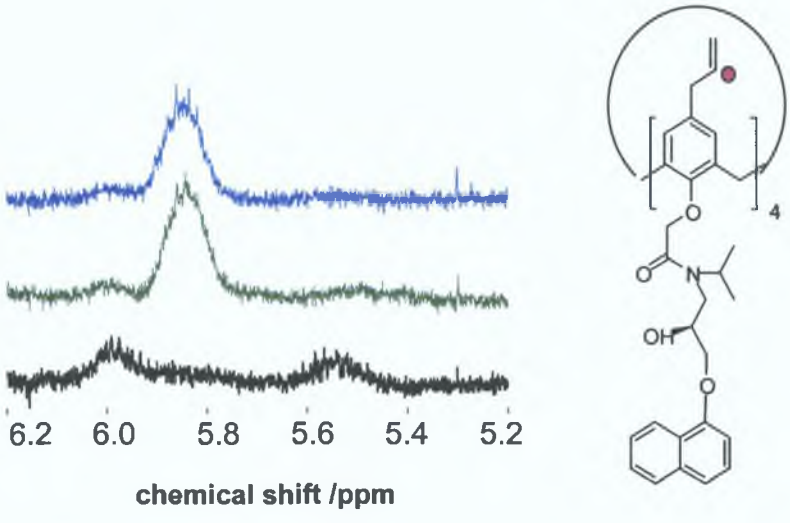

Figure 4-5 (a): *^{1}H-NMR spectra of L1 (black), L1-Na^+ (green) and L1-K^+ (blue) complex in $CDCl_3$. (a):allylic proton and (b): isopropyl proton signals.*

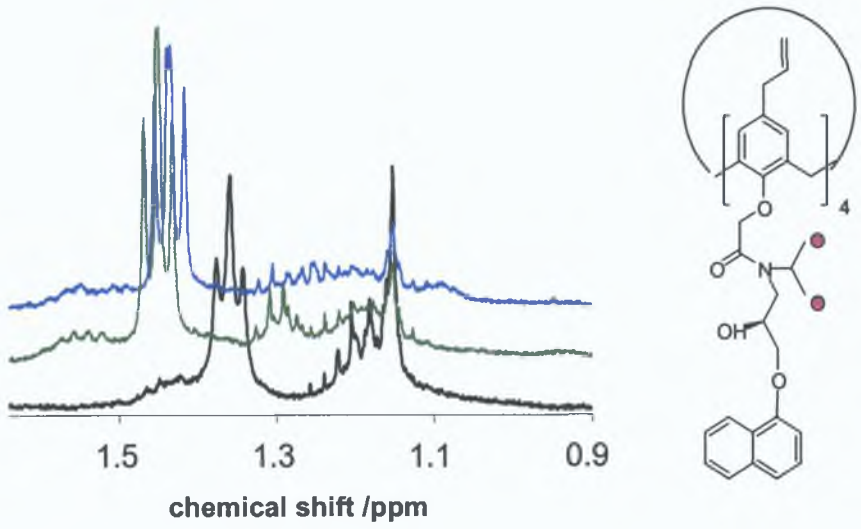

Figure 4-6 (b): *^{1}H-NMR spectra of **L1** (black), **L1**-Na^+ (green) and **L1**-K^+ (blue) complex in $CDCl_3$. **(a)**:allylic proton and **(b)**: isopropyl proton signals.*

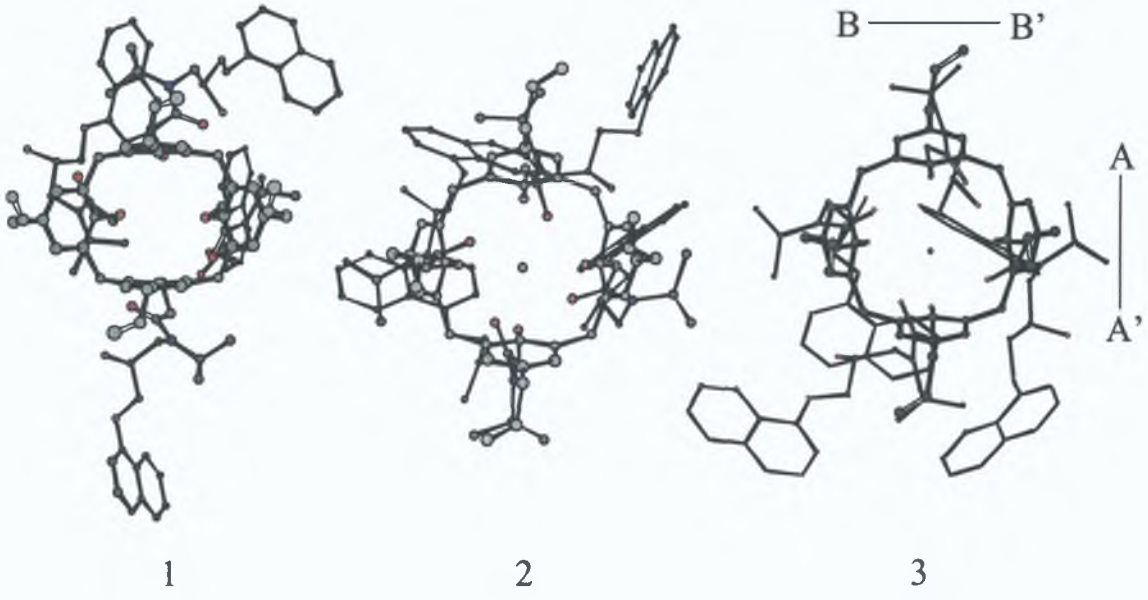

Figure 4-7: *Energy optimised structures of (1) the free ligand **L1**, (2) the **L1**-Na^+ complex (3), the **L1**-K^+ complex.*

		Free Ligand	Na^+ Complex	K^+ Complex
Distance between opposite phenyl rings /Å	A--A'	5.957	7.762	7.776
	B--B'	9.561	8.116	7.996
Distance between opposite phenolic oxygens / Å	A--A'	5.341	4.625	4.759
	B--B'	3.692	4.599	4.771
Angles made by planes /°	A--A'	11.2	56.1	52.7
	B--B'	87.4	49.9	49

Table 4-1: *Summary data extracted from energy-minimised structures. A-A' and B-B' are shown in Figure 4-7. (See section 4.2.2 for modelling experimental details)*

4.4 Results and Discussion

4.4.1 Linear Response range

It should be noted that the presence of a metal ion at a concentration ten times the concentration of the calixarene, causes no appreciable change in the fluorescence spectrum of the free ligand. The binding site of the metal ion is thought to be in the region of the phenyl ether oxygens and the carbonyl oxygens of the amide functionality. This area is clearly far removed form the source of fluorescence, that is the naphthalene moiety, and it is therefore only in the presence of guest molecules, that the effect of metal ion complexation with regards to fluorescence is observed. To further illustrate this point the linear ranges of the calixarene complexed with both sodium and potassium are shown in Figure 4-8 and Figure 4-9 respectively. The fluorescence intensities are comparable to that of the free calixarene in Chapter 3 (Figure 3-22) and are not quenched by the presence of a ten-fold excess of either metal ion (Na^+, K^+) in solution. This again verifies that the metal ion is bound to the calixarene and not merely present in solution, in a case similar to that of the guest.

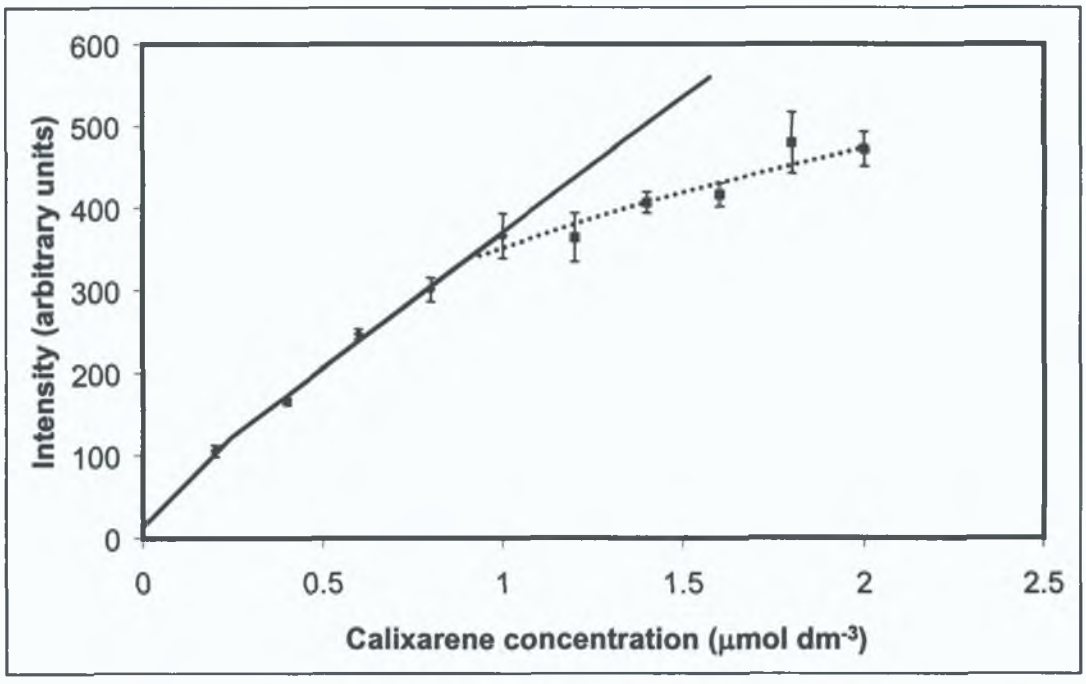

(a)

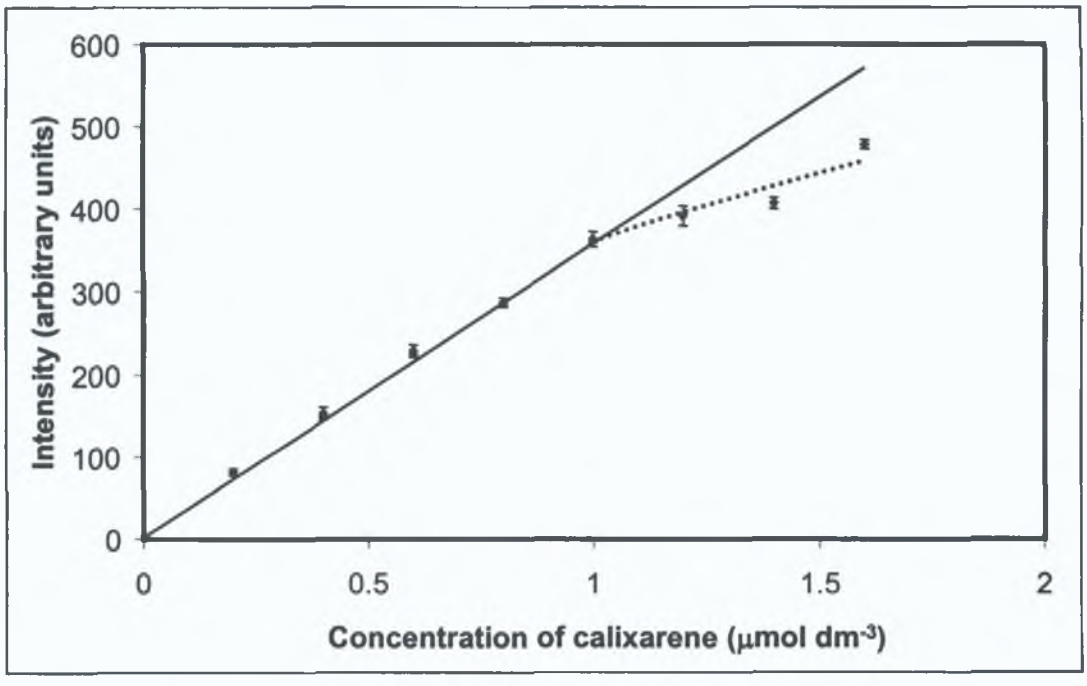

(b)

Figure 4-8: *Linearity of calixarene.Na^+ complex in methanol,* ***(a)*** *iodide as anion and* ***(b)*** *perchlorate as anion, points represent the mean of three replicate measurements (n=3) with error bars representing ± standard deviation.*

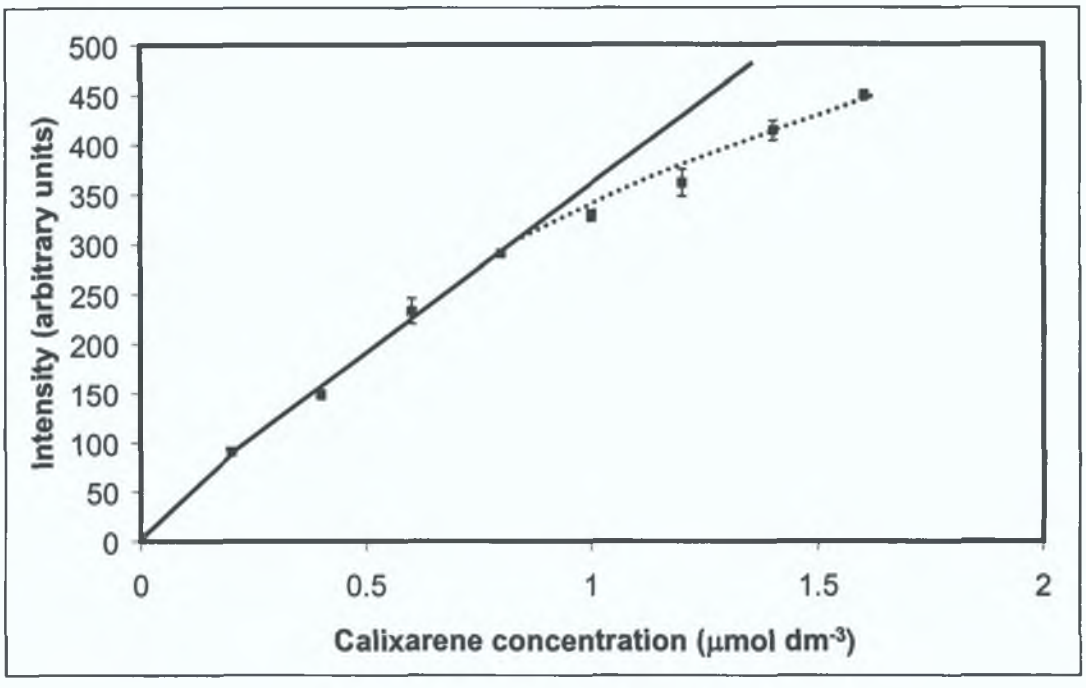

(a)

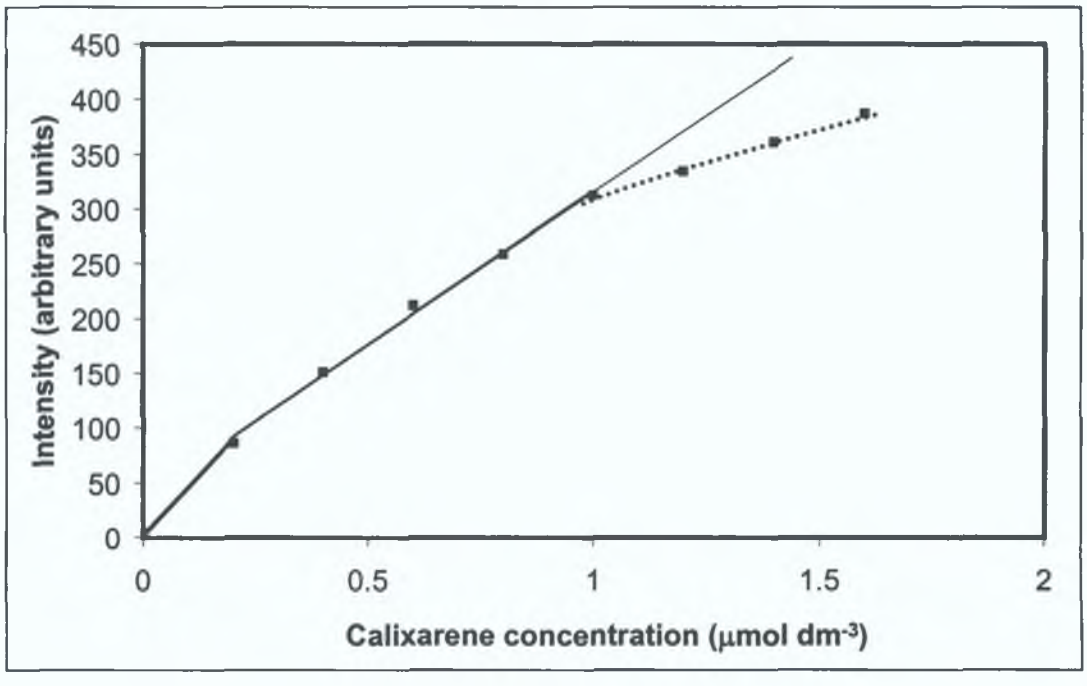

(b)

Figure 4-9: *Linearity of calixarene.K^+ complex in methanol,* ***(a)*** *iodide as anion and* ***(b)*** *perchlorate as anion, points represent the mean of three replicate measurements (n=3) with error bars representing ± standard deviation.*

4.4.2 Variation of Stern-Volmer plot with enantiomeric composition

When the initial Stern-Volmer plots of fluorescence quenching of the sodium and potassium complexes of ligand L1 in the presence of phenylalaninol are examined (Figure 4-10 and Figure 4-11 respectively), it can be seen that in the case of the R-enantiomer of phenylalaninol, they seem to deviate from linearity towards the y-axis. In many instances a fluorophore can be quenched both by collisions and by complex formation by the same quencher, Q. The characteristic feature of the Stern-Volmer plots in such circumstances is an upward curvature, concave toward the y-axis. The fractional fluorescence then remaining is given by the product of the fraction not complexed (f) and the fraction not quenched by collisional encounters, therefore:

$$\frac{F}{F_0} = f\left(\frac{\gamma}{\gamma + k_q[Q]}\right) \qquad \textbf{Equation 4-1}$$

(where F and F_0 are the fluorescence intensities of the fluorophore in the presence and absence of quencher respectively

- γ is the decay rate in the absence of quencher

-and $\gamma + k_q[Q]$ is the total decay rate in the presence of quencher

-k_q is the bimolecular quenching constant, [Q] is the concentration of quencher)

Considering however that $$\frac{F_0}{F} = \frac{\gamma + k_q[Q]}{\gamma} = 1 + k_q\tau_0[Q] \qquad \textbf{Equation 4-2}$$

(where τ_0 is the lifetime of the fluorophore in the absence of quencher)

And $$f^{-1} = 1 + K_S[Q] \qquad \textbf{Equation 4-3}$$

And $$k_q\tau_0 = K_D \qquad \textbf{Equation 4-4}$$

(where K_S is the Stern-Volmer constant (association constant) for a static quenching process and K_D is the Stern-Volmer constant when the process of quenching is dynamic)

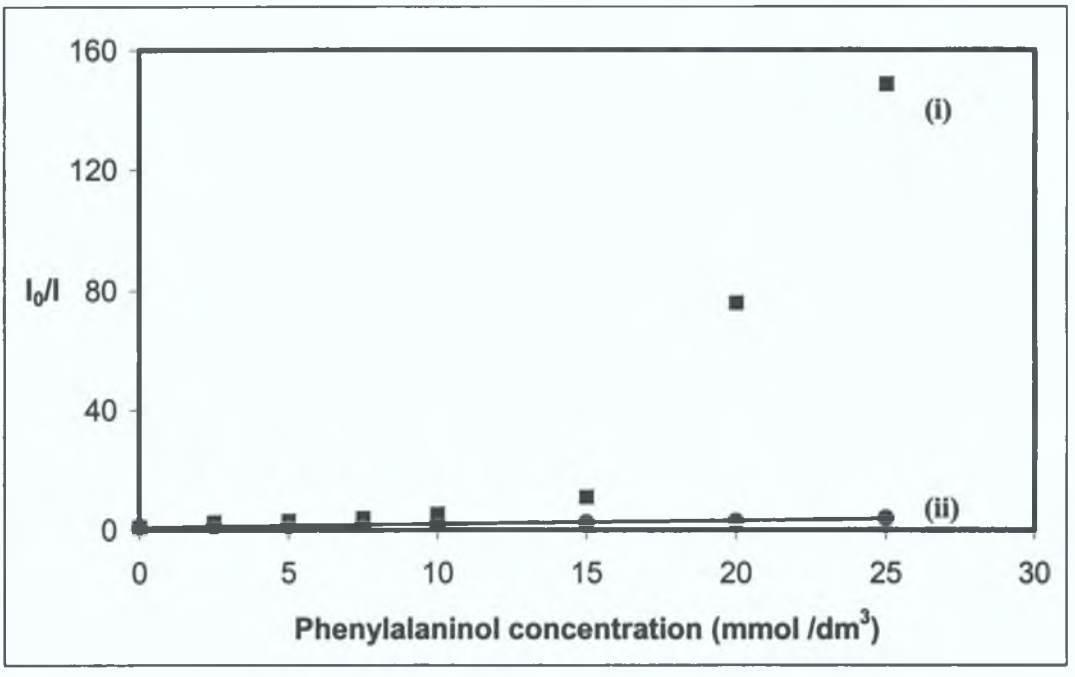

(a)

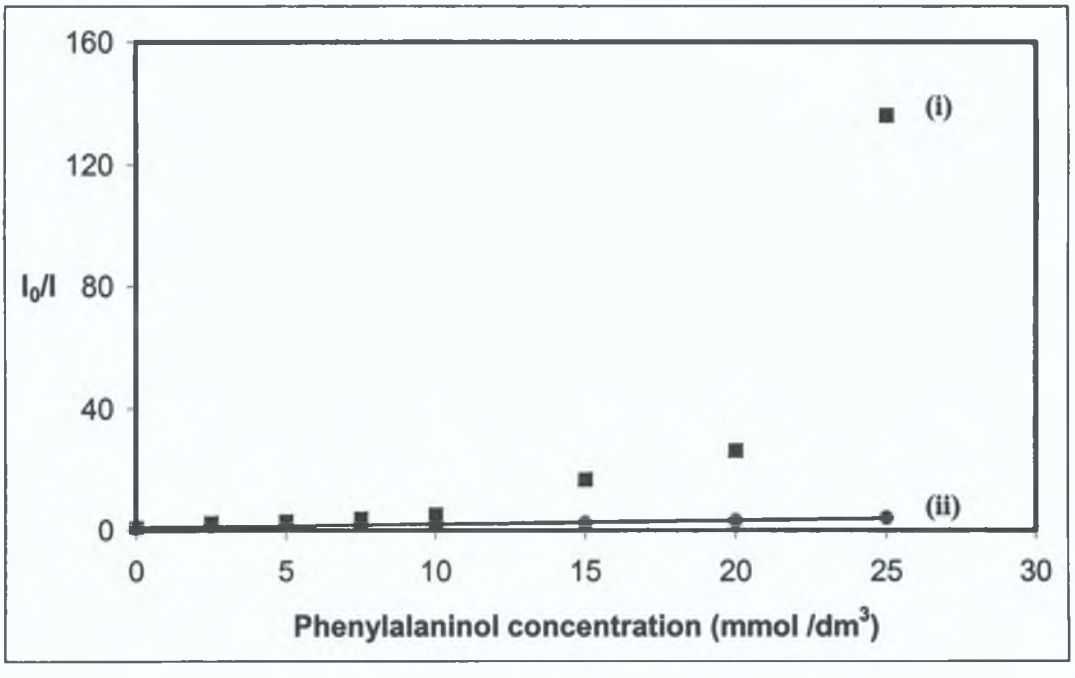

(b)

Figure 4-10: *Initial Stern-Volmer plots for the quenching of the fluorescence of calixarene* ***L1-Na***$^+$ *(0.7 μmol dm*$^{-3}$ *in methanol) upon addition of 0* ***(i)*** *and 100%* ***(ii)*** *S-Phenylalaninol.* ***(a)*** *Plot of sodium iodide complex,* ***(b)*** *Plot of sodium perchlorate complex, points represent the mean of three replicate measurements (n=3) with error bars representing ± standard deviation (error bars may be masked by symbols).*

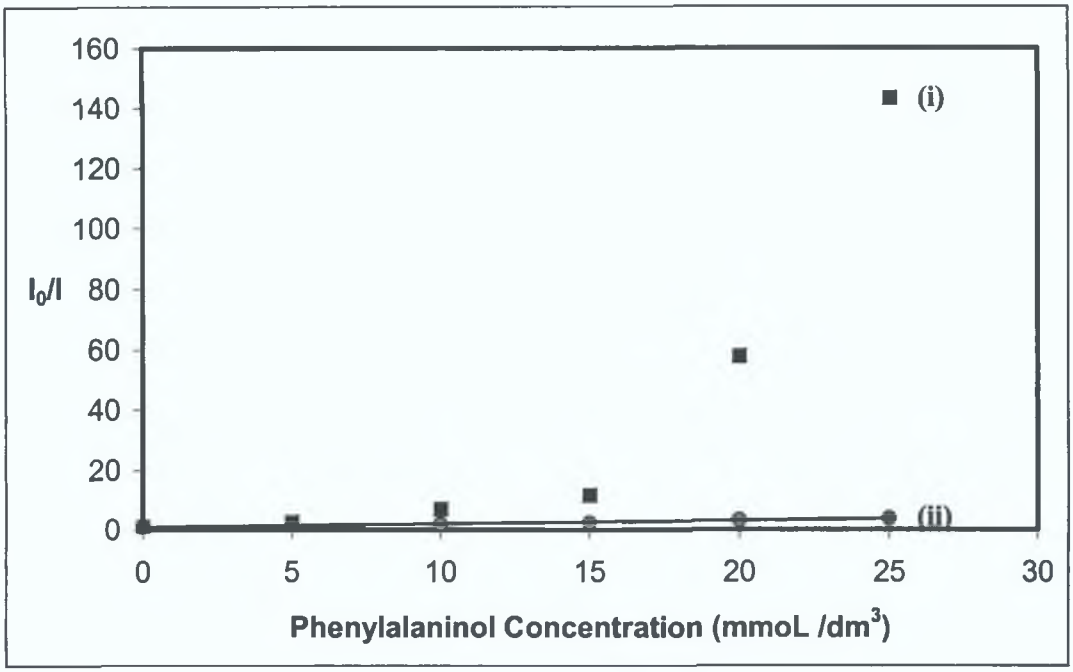

(a)

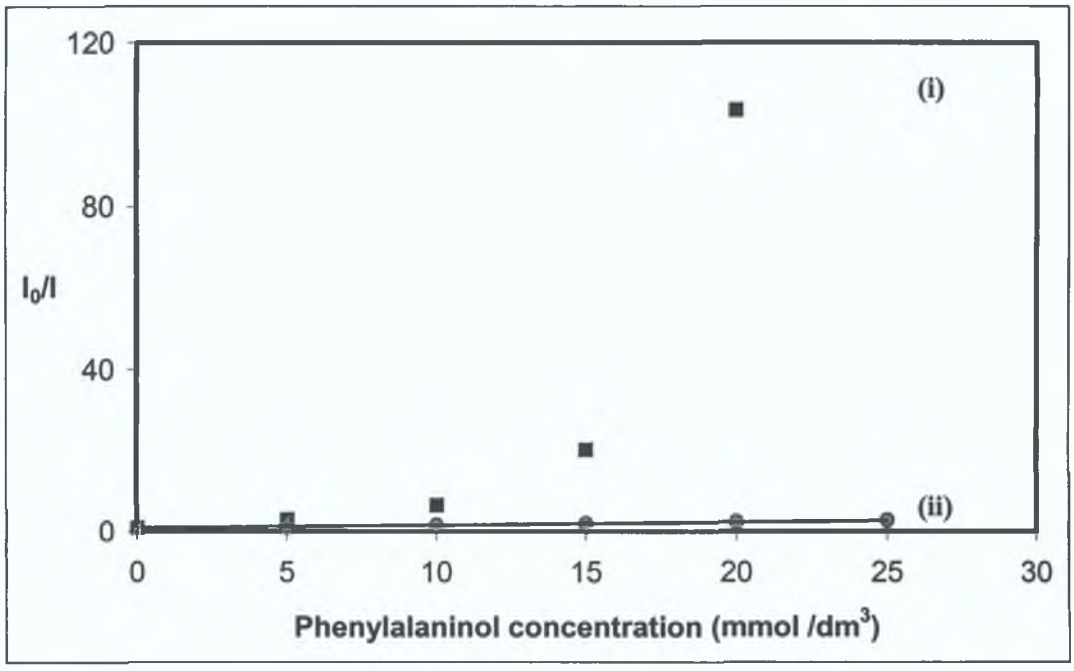

(b)

Figure 4-11: *Initial Stern-Volmer plots for the quenching of the fluorescence of calixarene **L1-K**$^+$ (0.7 μmol dm^{-3} in methanol) upon addition of 0 **(i)** and 100% **(ii)** S-Phenylalaninol. **(a)** Plot of potassium perchlorate complex, **(b)** Plot of potassium iodide complex, points represent the mean of three replicate measurements (n=3) with error bars representing ± standard deviation (error bars may be masked by symbols).*

4.4.3 Variation of K_{app} with R-phenylalaninol concentration

Theoretically this equation (equation 4-5) can be modified to allow graphical separation of K_S and K_D, [37] e.g.

$$\Rightarrow \quad \frac{F_0}{F} = (1 + K_D[Q])(1 + K_S[Q]) \qquad \textbf{Equation 4-5}$$

$$\frac{F_0}{F} = 1 + (K_D + K_S[Q]) + K_D K_S[Q]^2 \qquad \textbf{Equation 4-6}$$

$$= 1 + K_{app}[Q] \qquad \textbf{Equation 4-7}$$

The apparent quenching constant can then be calculated at each quencher concentration, and a plot of K_{app} versus [Q] should yield a straight line with an intercept of K_D+ K_S and a slope of K_D K_S. This would then allow solution of a quadratic equation and the dynamic and static components could thereby be calculated. When however K_{app} for the calixarene-metal ion complexes is plotted against the varying quencher (phenylalaninol) concentration it is clearly evident that a straight line is not the result (see Figure 4-12 and Figure 4-13 below).

Quencher concentration (mmol dm^{-3})	K_{app} Calix-NaI complex	K_{app} Calix-$NaClO_4$ complex	K_{app} Calix-KI complex	K_{app} Calix-$KClO_4$ complex
5	0.39	0.47	0.33	0.39
10	0.43	0.84	0.59	0.55
15	0.67	1.35	0.71	1.28
20	3.76	1.16	2.84	5.12
25	5.92	5.39	5.69	-

Table 4-2: *Comparison of K_{app} for both **L1**-Na^+ and **L1**-K^+ (0.7 μmol dm^{-3} in methanol) at varying quencher concentrations (i.e. (R)-phenylalaninol). Kapp for potassium perchlorate complex of L1 at a quencher concentration of 25 mmol dm^{-3} could not be measured due to total quenching of the emission signal.*

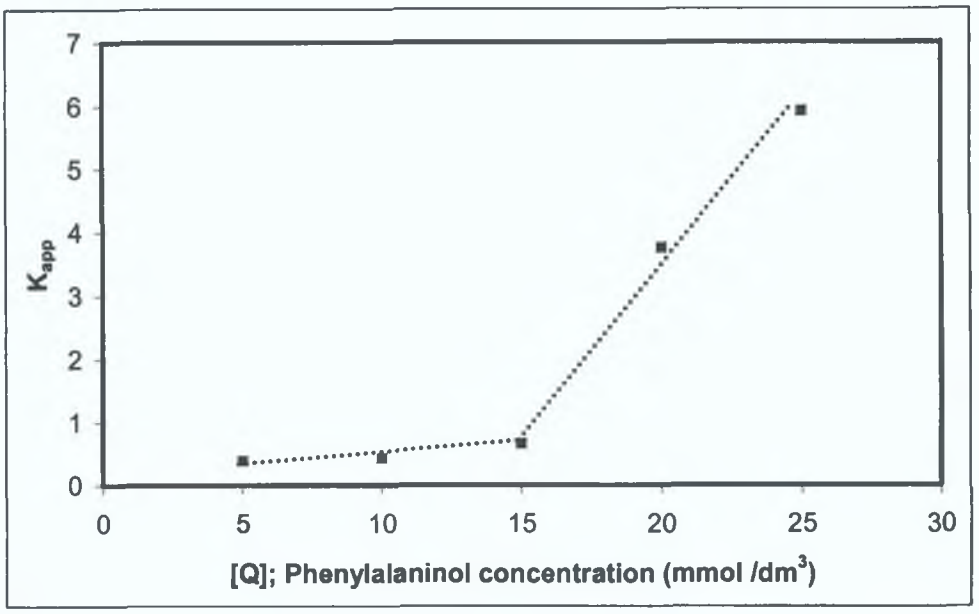

(a)

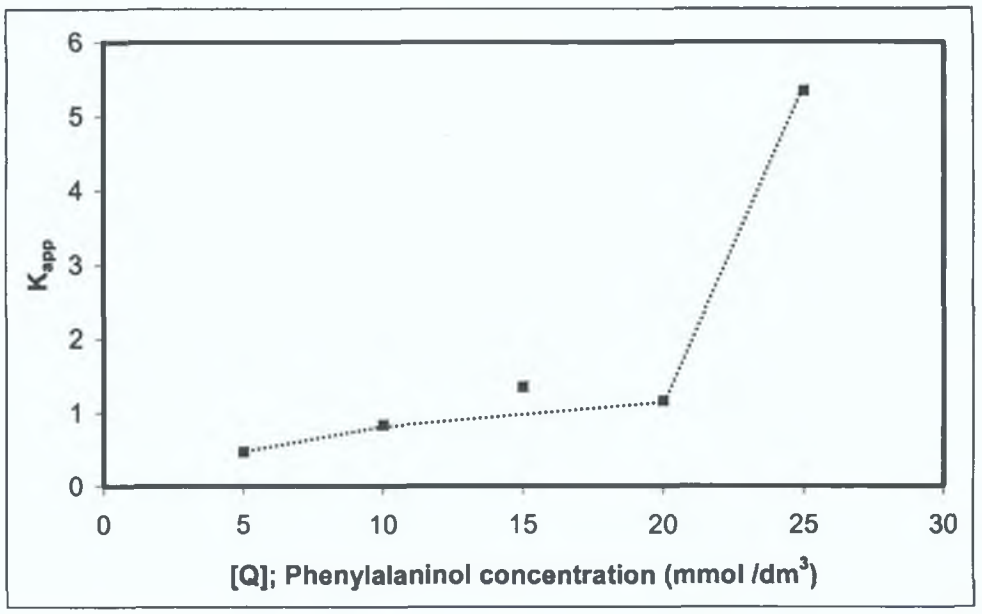

(b)

Figure 4-12: *Plot of the apparent quenching constant, K_{app}, at each quencher concentration ((R)-phenylalaninol as quencher),* ***(a)*** *Plot of sodium iodide complex,* ***(b)*** *Plot of sodium perchlorate complex, (0.7 μmol dm^{-3} in methanol for* ***(a)*** *and* ***(b)****). Points represent the mean of three replicate measurements (n=3) with error bars representing ± standard deviation (error bars may be masked by symbols).*

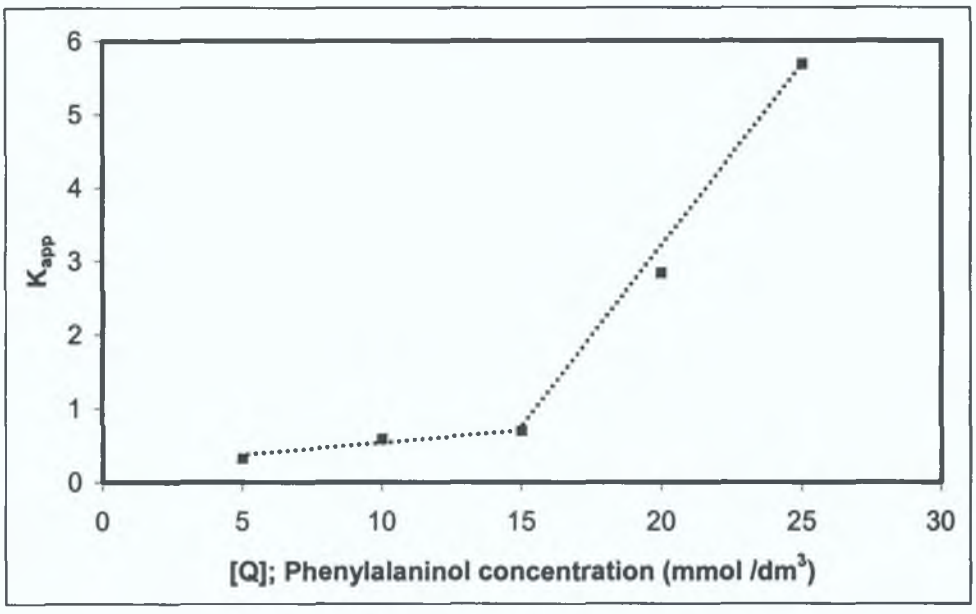

(a)

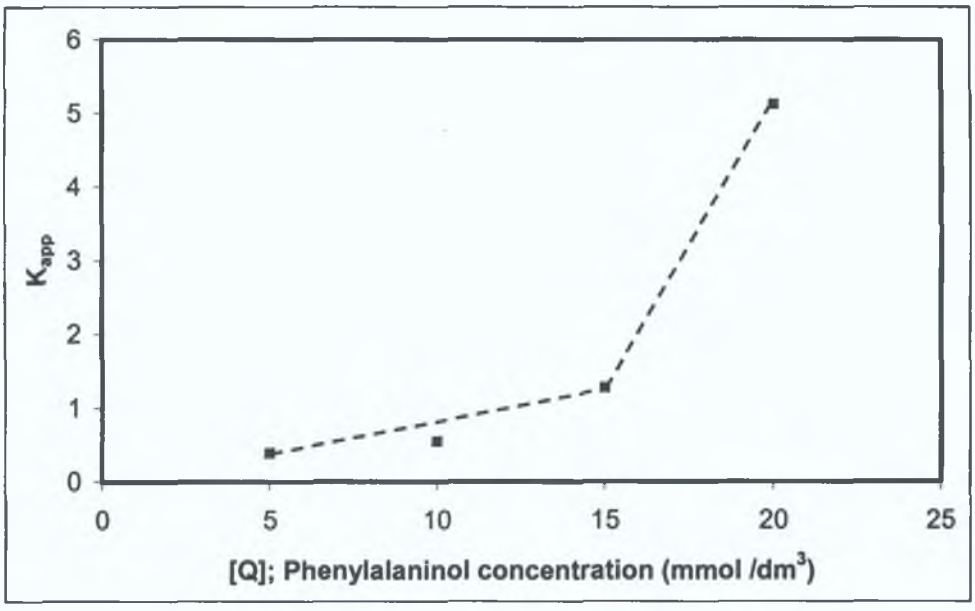

(b)

Figure 4-13: *Plot of the apparent quenching constant K_{app}, at each quencher concentration ((R)-phenylalaninol as quencher),* ***(a)*** *Plot of potassium iodide complex,* ***(b)*** *Plot of potassium perchlorate complex, (0.7 μmol dm^{-3} in methanol for* ***(a)*** *and* ***(b)****). Points represent the mean of three replicate measurements (n=3) with error bars representing ± standard deviation (error bars may be masked by symbols).*

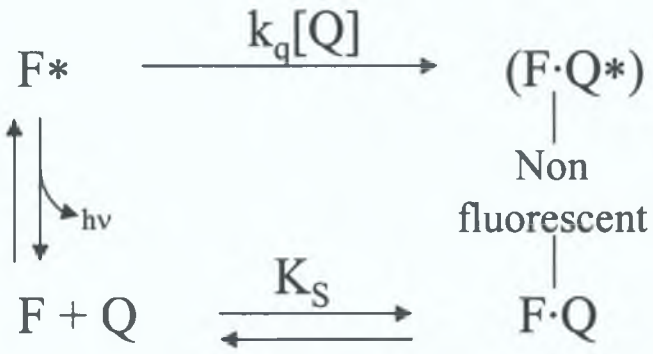

Figure 4-14: *processes involving dynamic and static quenching of the same population of fluorophores (where F = Fluorophore and Q = Quencher, in the ground state and * indicates the excited state, K_q is the bimolecular quenching constant and K_S is the static quenching association constant for complex formation).*

It is interesting to note how the effect of the anion is sensed only when the plots of K_{app} versus [Q] are examined. By observing Stern-Volmer plots alone it was thought that the metal ion effects were independent of the anion used in solution, however when iodide is employed as counter-anion, the slopes of the second of the two distinct linear portions (after 15mmol dm^{-3} R-PA) of the Stern-Volmer plots are noticeably different from those in the case of the perchlorate counter-anion. In the case of both metal complexes and both counter ions examined, it is apparent from Figure 4-12 and Figure 4-13 that a dramatic change is observed in the slope of the plots of K_{app} versus [Q] upon addition of R-phenylalaninol at concentrations greater than 15mmol dm^{-3}. This could be due to the fact that a different (or additional) quenching mechanism is responsible for the decrease in fluorescence intensity, due to the non-linear nature of degree of quenching with increasing guest concentration.

If the linear portion of these graphs is consulted then the Stern-Volmer constants for the sodium and potassium complexes can be examined (Figure 4-15 and Figure 4-16 respectively). It is then apparent that the complexes do discriminate between the enantiomers of phenylalaninol, while exhibiting a much greater selectivity for the R-enantiomer than the free calixarene ligand.

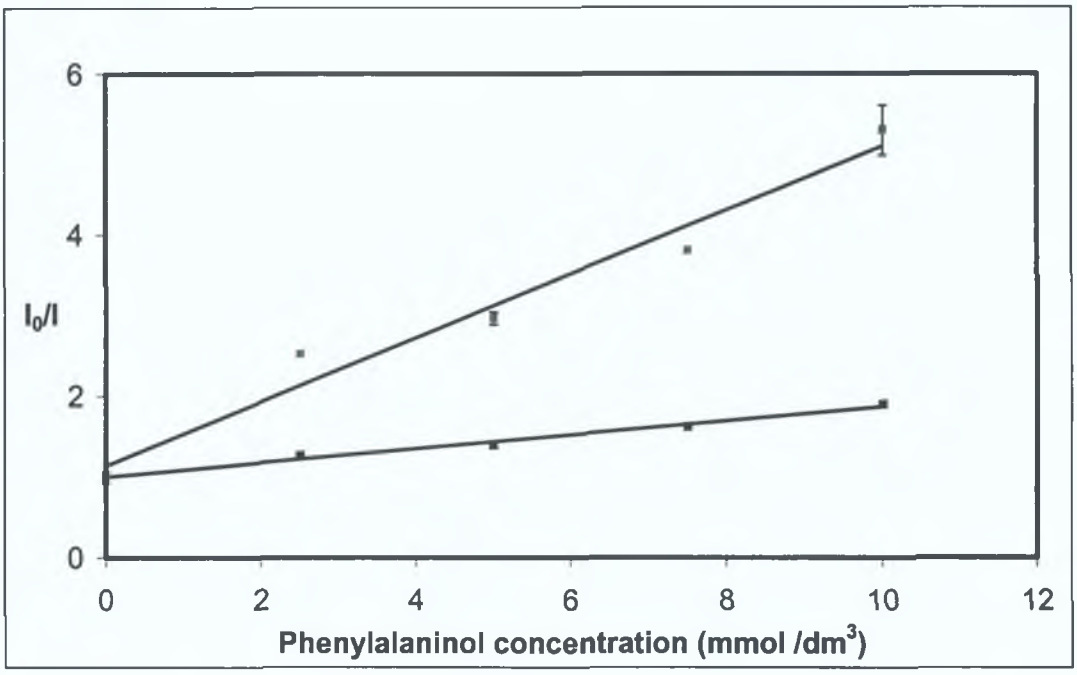

(a)

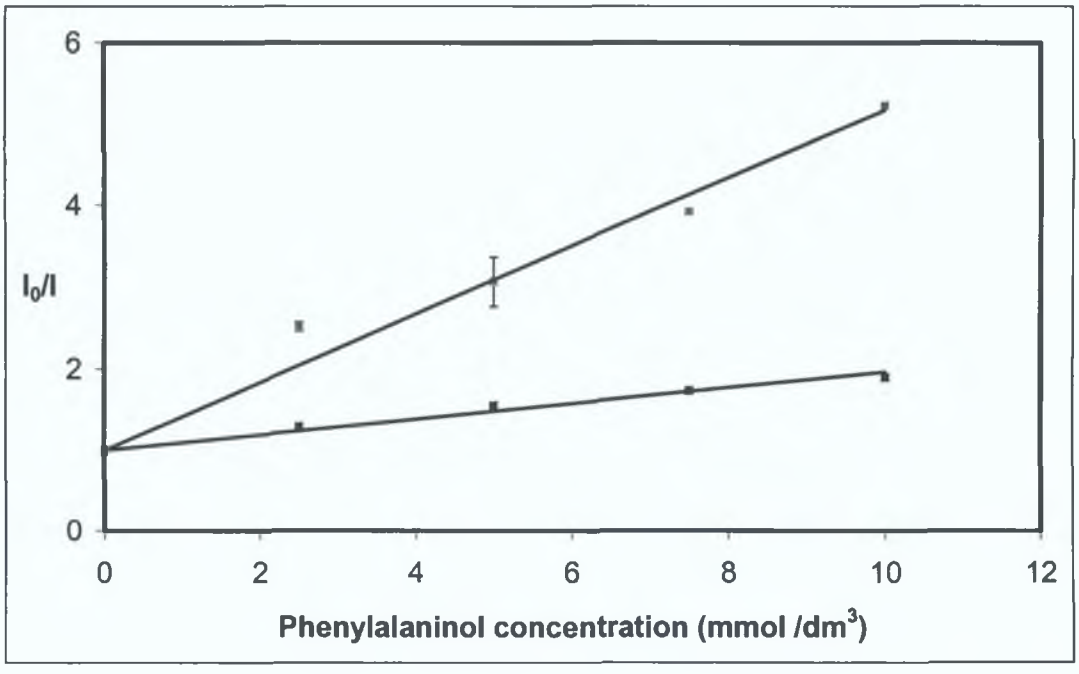

(b)

Figure 4-15: *Linear ranges of Stern-Volmer plots for the quenching of **L1**-Na^+ (0.7 μmol dm^{-3} in methanol) upon addition of 100% R- (green series) and 100% S-Phenylalaninol (black series) in methanol. Standard deviations are shown as error bars (n=3). **(a)** Plot of sodium iodide complex, **(b)** Plot of sodium perchlorate complex.*

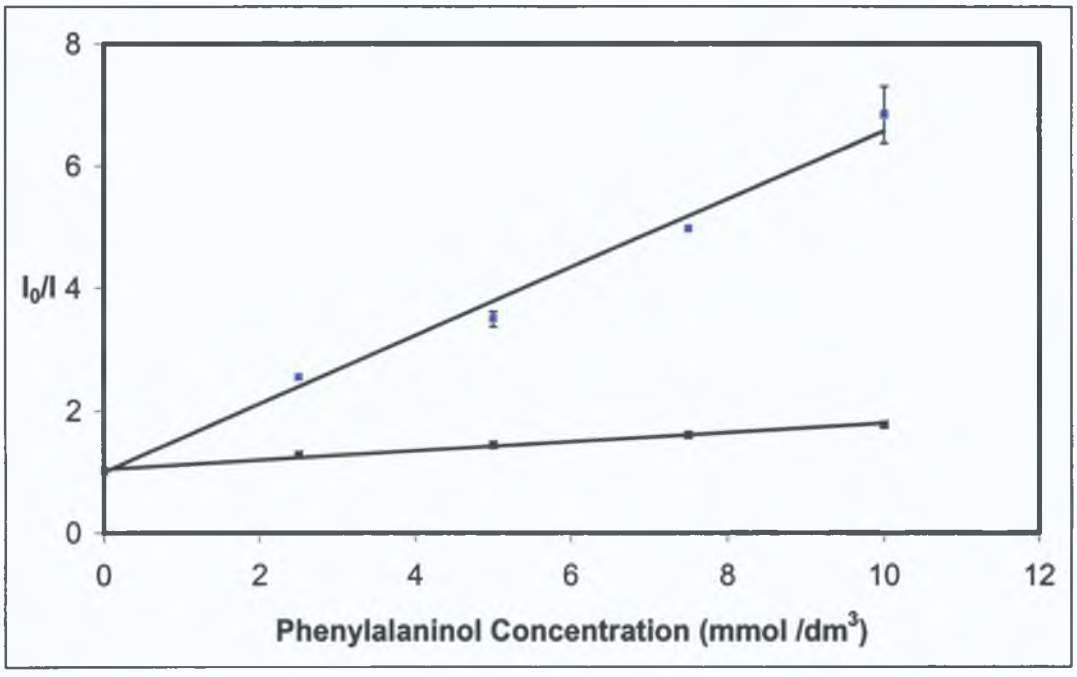

(a)

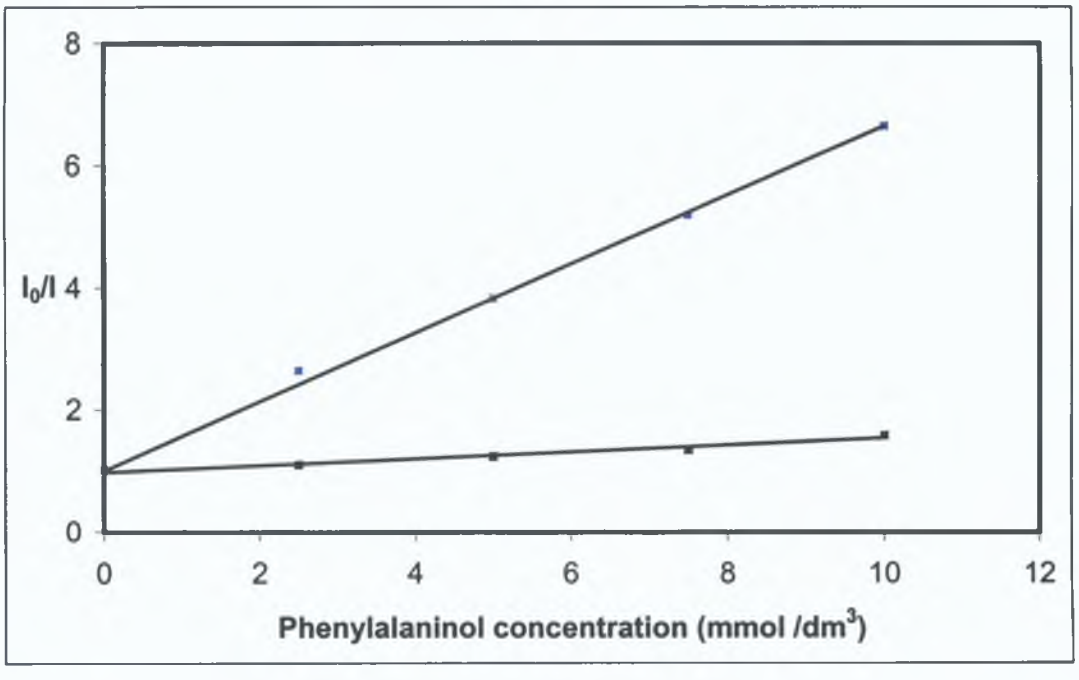

(b)

Figure 4-16: *Linear ranges of Stern-Volmer plots for the quenching of **L1**-K^+ (0.7 μmol dm^{-3} in methanol) upon addition of 100% R- (blue series) and 100% S-Phenylalaninol (black series) in methanol. Standard deviations are shown as error bars (n=3). (a) Plot of potassium iodide complex, (b) Plot of potassium perchlorate complex.*

Calixarene	*Composition of PA*	K_{SV}	K_{SV} *ratio*
NaI-complex	100%R, 0%S	0.40 (0.9674)	4.6
	0%R, 100%S	0.09 (0.9884)	
$NaClO_4$-complex	100%R, 0%S	0.42 (0.9723)	4.3
	0%R, 100%S	0.10 (0.9737)	
KI-complex	100%R, 0%S	0.56 (0.9887)	7.4
	0%R, 100%S	0.08 (0.9853)	
$KClO_4$-complex	100%R, 0%S	0.56 (0.9974)	10.1
	0%R, 100%S	0.06 (0.9743)	

Table 4-3: *Stern-Volmer slopes, correlation coefficients and K_{SV} ratios for series in Figure 4-15 and Figure 4-16 respectively.*

Figure 4-17 represents graphically the comparison in response of the free calixarene ligand and the potassium complex of **L1** to both enantiomers of phenylalaninol. Comparing the difference between the response of the free ligand (Figure 4-17(ii)) and the potassium complex of **L1** to the R-enantiomer of PA (Figure 4-17(i)), and then to the S-enantiomer (Figure 4-17(iii)), illustrates the magnitude in difference of slope and therefore response to R-PA, of the free ligand and the potassium complex of **L1**. It is clear from this comparison that the potassium complex of **L1** has a much more sensitive response to R-phenylalaninol than the calixarene without a metal ion. In the case of free **L1** 25mmol dm^{-3} of R-phenylalaninol was required to achieve a notable difference in response to the S-enantiomer. In the case of the potassium complex of **L1** however, there is no fluorescence emission at this concentration, signifying total quenching of the fluorescence signal at this large concentration of R-PA, and making detection of R-PA possible at much lower concentrations.

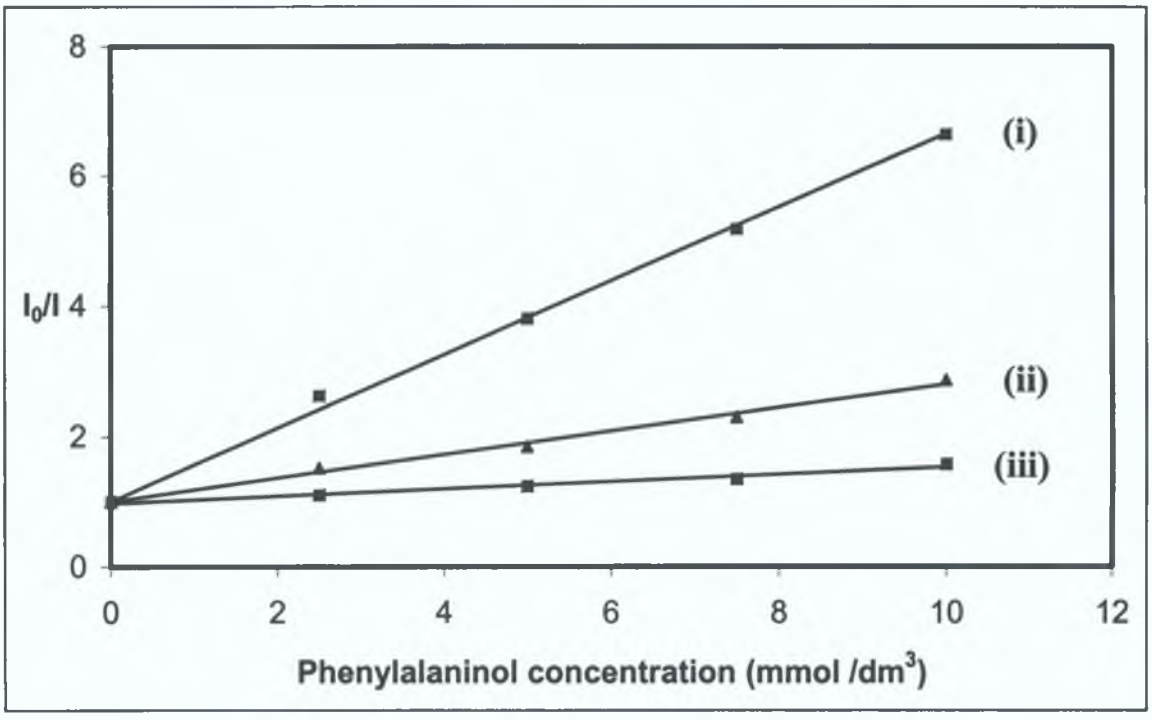

Figure 4-17: *Comparison of Stern-Volmer plots for the quenching of free calixarene-**L1** upon addition of 100% R-PA **(ii)**, **L1**-K^+ upon addition of 100% R-PA **(i)** and free **L1** and **L1**-K^+ upon addition of 100% S-Phenylalaninol **(iii)**. (Concentrations of **L1**, **L1**-Na^+ and **L1**-K^+ used were 0.7 μmol dm^{-3} in methanol)*

The K_{SV} ratio of the free ligand is calculated to be 1.9, whereas the sodium iodide and perchlorate complexes of **L1** return K_{SV} ratios of 4.6 and 4.3 respectively. This indicates a huge increase in selectivity of the sodium complexes and also that the counter-anion has little effect on fluorescence quenching. When the equivalent plots are examined for the potassium complexes of **L1** it can be seen that the K_{SV} ratios amount to 7.4 and a remarkable 10.1 for the potassium iodide and perchlorate complexes, respectively (see Table 4-3). We believe that the reason for this dramatic increase in enantiomeric selectivity lies in the well-known tendency of calix[4]arenes to adopt a more regular C_{4V} symmetry, in which the pendent groups are held in a much more rigid conformation compared to the free ligand. In a calix[4]arene like **L1**, the metal ion will be positioned between the planes defined by the carbonyl and phenoxy oxygen atoms of the calixarene macrocycle. The main electrostatic interaction is with the carbonyl oxygen atoms, and the ion therefore tends to lie nearer these than the phenoxy oxygen atoms [38]. This enforced cone conformation, and very well defined cavity (see Figure 4-19 and Figure 4-20) seem to allow for far greater interaction with the R-enantiomer of phenylalaninol, than in the case of the

(S)-enantiomer. In contrast, the free ligand **L1** is dependent solely on hydrogen bonding to define the lower cavity, and this will therefore be less rigid, with a greater tendency to open and accommodate various guests but with corresponding loss of chiral and molecular selectivities (see Figure 4-18).

The complexation trend observed in the case of **L1** is similar to that of the dansyl-monensin-β- cyclodextrin synthesised by Ikeda et al [19]. When this compound was compared with the binding ability of dansylglycine-modified β-CD, it was demonstrated that the monensin system enhances binding abilities for various guests with respect to the glycine system, with the presence of a sodium ion further enhancing binding abilities. These results were found for the guests nerol and geraniol, with binding abilities being further improved by the presence of a Na^+ ion. The authors report that this enhancement may be due to the rearrangement of the monensin acyclic chain to form a macrocyclic one, in the centre of which is the bound sodium ion. In the case of calixarene **L1** the change in conformation upon binding of sodium and potassium ions, generates a more rigid and square, symmetrical molecule which appears to greatly enhance the affinity of the ligand towards the R-enantiomer of the guest phenylalaninol.

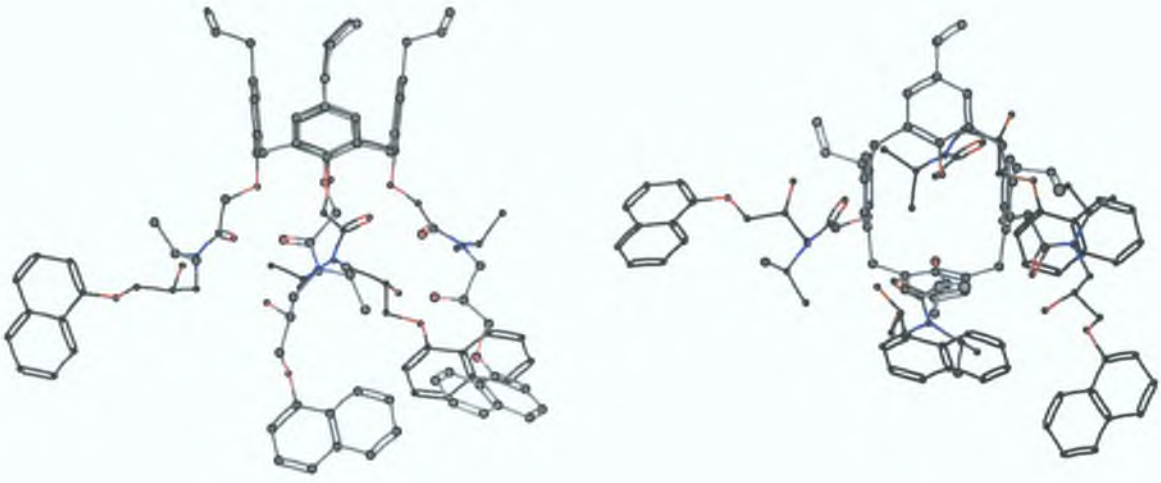

(a) (b)

Figure 4-18: *Energy optimised structures of the free ligand, **L1**, **(a)** from the side and **(b)** through the annulus.*

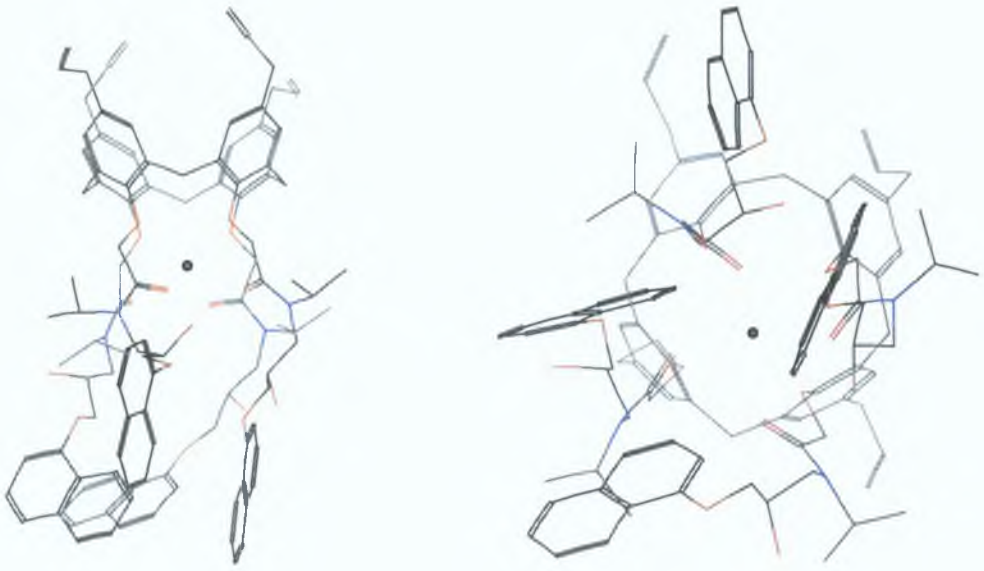

(a) (b)

Figure 4-19: *Energy optimised structures of the sodium complex of **L1**, **(a)** from the side and **(b)** through the annulus.*

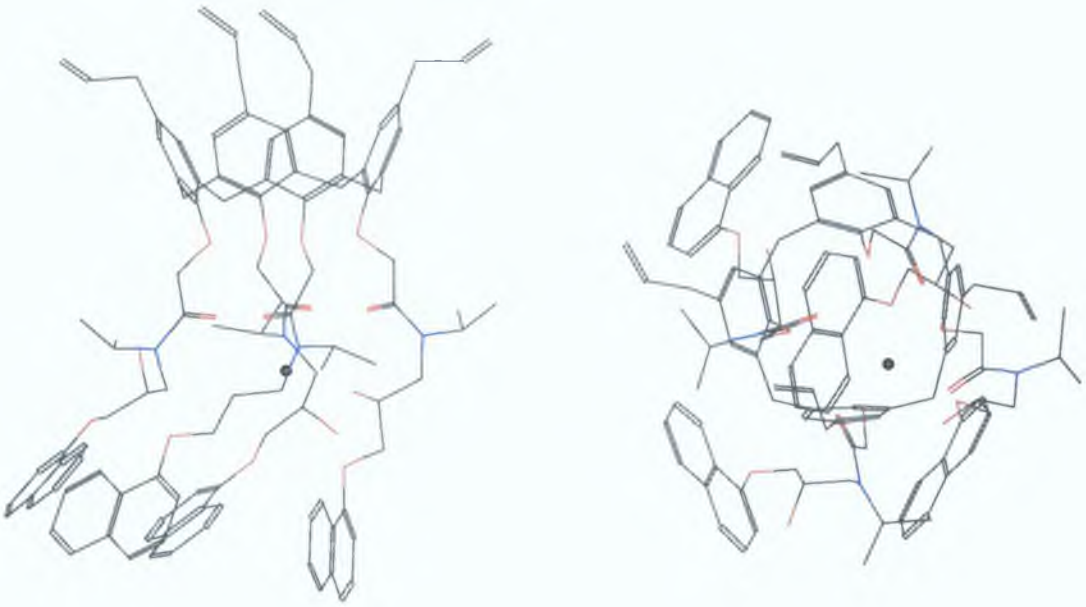

(a) (b)

Figure 4-20: *Energy optimised structures of the potassium complex of **L1**, **(a)** from the side and **(b)** through the annulus.*

In an analytical sense these results suggest there is potential to achieve very rapid and precise enantiomeric discrimination. The fact that the K_{SV} ratios are improved by up to 500% in the calixarene metal complexes compared to the free calixarene ligand renders the discrimination of the enantiomers of phenylalaninol enormously easy with this ligand, since there is such an obvious difference in the Stern-Volmer constants for the guest enantiomers. This is pictorially evident from Figure 4-21, and can also be determined without the necessity of statistical tests.

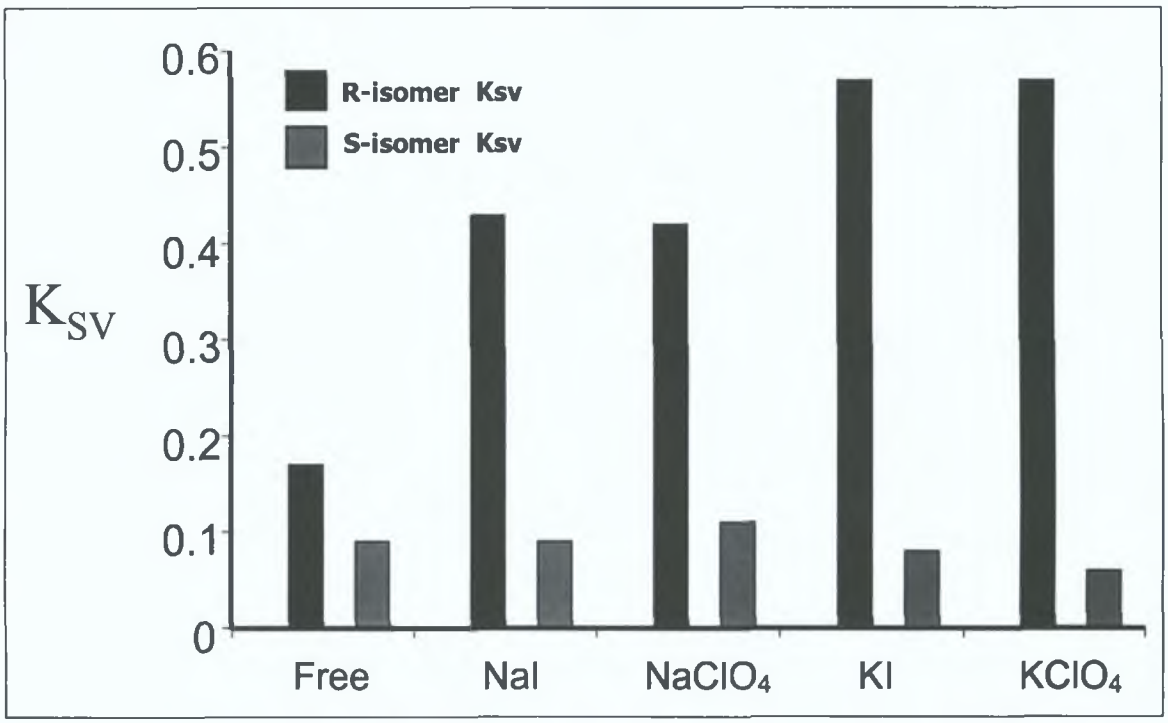

Figure 4-21: *Histogram comparing Stern-Volmer constants of phenylalaninol in methanol with free calixarene **L1** and the **L1**-Na^+ and **L1**-K^+ complexes (0.7 μmol dm^{-3} in methanol) (in the case of the calixarene complexes only the linear portions of these plots were consulted, with the data used taken from the linear regions between 0-15 mmol dm^{-3} of phenylalaninol).*

4.5 Conclusion

The molecular modelling data in conjunction with the fluorescence quenching results would seem to suggest that greatly enhanced enantiomeric discrimination is achieved when the calixarene exists in a highly structured symmetrical cone conformation, which is in this case induced by metal-ion complexation. A five-fold increase in association constant was obtained for the potassium complex of **L1** with respect to the free ligand regarding the association of the R-enantiomer of phenylalaninol.

Fluoresence lifetime measurements may be able to separate the static quenching component from the dynamic quenching processes in these metal-complex host-guest associations to give a clearer indication of the exact processes taking place in solution with the phenylalaninol guests and the metal ion complexes. However if this ligand **L1** is to be employed as an analytical sensing agent, then it is clear that the metal ion complexes, in particular that of potassium perchlorate are the most advantageous sensor molecules when it comes to the enantiomeric discrimination of phenylalaninol, due to a greater sensitivity of the ligand to the guest and the huge selectivities obtained.

4.6 References

1 J. Szejtli, *Cyclodextrins and their Inclusion Complexes*, Akadémiai Kiadó, Budapest, **1982**.

2 G. Wenz, *Angew. Chem. Int. Ed. Engl.* **1994**, 33, 803.

3 M. L. Bender, M. Komiyama, *Cyclodextrin Chemistry*, Springer-Verlag, Berlin, **1978**.

4 J. Szejtli, *Cyclodextrin Technology*, Kluwer, Dordrecht, **1988**.

5 A. Ueno, T. Kuwabara, A. Nakamura, F. Toda, *Nature*, **1992**, 356, 13.

6 A. Ueno, *Adv. Mater.* **1993**, 5, 132.

7 T. Kuwabara, A. Matsushita, A. Nakamura, A. Ueno, F. Toda, *Chem Lett.* **1993**, 2081.

8 T. Kuwabara, A. Nakamura, A. Ueno, F. Toda, *J. Phys. Chem.* **1994**, 98, 6297.

9 A. Ueno, I. Suzuki, T. Osa, *Chem. Lett.* **1989**, 1059.

10 A. Ueno, I. Suzuki, T. Osa, *J. Am. Chem. Soc.* **1989**, 111, 6391.

11 A. Ueno, I. Suzuki, T. Osa, *Anal. Chem.* **1990**, 62, 2461.

12 S. Minato, T. Osa, A. Ueno, *J. Am. Chem. Soc. Chem. Commun.* **1991**, 107.

13 F. Moriwaki, H. Kaneko, A. Ueno, T. Osa, F. Hamada, K. Murai, *Bull. Chem. Soc. Jpn.* **1987**, 60, 3619.

14 S. Minato, T. Osa, M. Morita, A. Nakamura, H. Ikeda, F. Toda, A. Ueno, *Photochem. Photobiol.* **1991**, 54, 593.

15 A. Ueno, S. Minato, I. Suzuki, M. Fukushima, M. Ohkubo, T. Osa, F. Hamada, K. Murai, *Chem. Lett.* **1990**, 605.

16 Y. Wang, T. Ikeda, A. Ueno, F. Toda, *Chem. Lett.* **1992**, 863.

17 F. Hamada, Y. Kondo, K. Ishikawa, H. Ito, I. Suzuki, T. Osa, A. Ueno, *J. Inclusion Phenom.* **1993**, 15, 273.

18 A. Ueno, *Supramol Sci.* **1996**, 3, 31.

19 M. Nakamura, A. Ikeda, N. Ise, T. Ikeda, H. Ikeda, F. Toda, A. Ueno, *J. Chem. Soc. Chem. Commun.* **1995**, 721.

20 A. Ikeda, S. Shinkai, *Chem. Rev.* **1997**, 97, 1713.

21. Spartan, Wavefunction Inc., 18401 Von Karman Ave., Suite 370, Irvine, CA 92612, U.S.A. http://www.wavefun.com/.

22. T. Halgren, *J. Am. Chem. Soc.* **1992**, 114, 7827-7843.

23 C. D. Gutsche, *Calixarenes*, Royal Society of Chemistry, Cambridge, **1989**.

24 J. Vicens, V. Böhmer, (Eds.) *Calixarenes*, Kluwer Academic Press, Dordrecht, **1991**.

25 S. Shinkai, *Bioorg. Chem. Front.* **1990**, 1, 161.

26 S. Shinkai, *Tetrahedron* **1993**, 49, 8933.

27 H. Ohtsuka, S. Shinkai, *Supramol. Sci.* **1996**, 3, 189.

28 J. L. Atwood, G. W. Orr, K. D. Robinson, F. Hamada, *Supramol. Chem.* **1993**, 2, 309.

29 V. Böhmer, *Angew. Chem., Int. Ed. Engl.* **1995**, 34, 713.

30 S. Shinkai, K. Fujimoto, T. Otsuka, H. L. Ammon, *J. Org. Chem.* **1992**, 57, 1516.

31 K. Iwamoto, S. Shinkai, *J. Org. Chem.* **1992**, 57, 7066.

32 C. D. Gutsche, P. A. Reddy, *J. Org. Chem.* **1991**, 56, 4783.

33 K. A. See, F. R. Fronczek, W. H. Watson, R. P. Kashyap, C. D. Gutsche, *J. Org. Chem.* **1991**, 56, 7256.

34 M. Iqbal, T. Mangiafico, C. D. Gutsche, *Tetrahedron* **1987**, 43, 4917.

35 W. Verboom, S. Datta, Z. Asfari, S. Harkema, D. N. Reinhoudt, *J. Org. Chem.* **1992**, 57, 5394.

36 A. Ikeda, S. Shinkai, *Chem. Rev.* **1997**, 97, 1713-1734.

37 P. Froehlich, E. L. Wehry, *Modern Fluorescence Spectroscopy* 2, E. L. Wehry, (Ed.,) Plenum Press, New York & London, **1976**.

38 P. Kane, D. Fayne, D. Diamond M. A. McKervey, *J. Mol. Mod.* **2000**, 6, 272.

5 Solvent effects on Enantiomeric Discrimination of Chiral Calixarene L1

5.1 Solvent effects on Electronic Spectra

Most electronic spectroscopy is practiced in fluid solutions involving solvents, many of which are highly polar or capable of hydrogen bonding with the absorbing or emitting molecules. The interactions of solute molecules with polar or hydrogen bonding solvents are capable of profoundly altering the electronic properties of the states from which absorption and emission occur, thereby leading to significant effects on the emission spectra of fluorophores. These effects are the origin of the Stokes' shift, which is one of the earliest observations in fluorescence. Solvent interactions with solute molecules are predominantly electrostatic and may be of the induced dipole-induced dipole, dipole-induced dipole, dipole-dipole or hydrogen bonding types [1]. In addition, hydrogen bonding usually accompanies dipole-dipole interaction as a mode of solvation.

A solvent which has positively polarized hydrogen atoms which can engage in hydrogen bonding is said to be a hydrogen bond donor solvent. A solvent, which has atoms bearing lone, or non-bonding electron pairs is said to be a hydrogen bond acceptor solvent. Qualitatively, a hydrogen bond donor behaves as a very weak Bronsted acid, partially donating a proton to a basic site on the solute molecule. A hydrogen bond acceptor behaves as a very weak Bronsted base, partially accepting a proton from the solute molecule. Because of the involvement of nonbonding and lone pairs in $n \rightarrow \pi^*$ and intramolecular charge transfer transitions, hydrogen bonding solvents have the greatest effect on the positions of these types of spectra. Because of the large dipole moment changes accompanying electronic reorganisation in $\pi \rightarrow \pi^*$ and intramolecular charge transfer transitions; these types of spectra are most affected by solvent polarity.

In the ground state of a polar molecule capable of hydrogen bonding, in a solvent of high polarity (dielectric strength) and having both hydrogen bond donor and acceptor properties (e.g. water), the molecule will have a solvent cage in which the positive ends of the solvent dipoles will be oriented about the negative ends of the solute dipole and the negative ends of the solvent dipoles will be oriented about the positive ends of the solute dipole. Positively polarised hydrogen atoms of the solvent may be oriented toward lone pairs on the solute and acidic hydrogen atoms of the solute may be oriented toward lone pairs on the solvent. The solvent cage is in thermal

equilibrium with the ground state electronic distribution of the solute. The light absorption process alters the electronic distribution of the solute so that the electronic dipole moment of the excited molecule is different from that of the ground state molecule. However the process of absorption is so rapid that it terminates with the excited molecule still in the ground state equilibrium solvent cage (i.e. in a Franck-Condon excited state). If the solute molecule becomes more polar in the excited state, there will be greater electrostatic stabilisation of the excited state, relative to the ground state, by interaction with the polar solvent. The greater the polarity of the solvent, the lower the energy of the Franck-Condon excited state (see Figure 5-1(a)). This type of behaviour is characteristic of most $\pi \rightarrow \pi^*$ and intramolecular charge-transfer transitions and is seen as a λ_{max} shift to longer wavelengths with increasing solvent polarity. When the electronic dipole moment is lower in the Franck-Condon excited state than in the ground state, increasing solvent polarity stabilises the ground state to a greater degree than the excited state and the absorption spectrum will shift to shorter wavelengths with increasing solvent polarity (see Figure 5-1(b)).

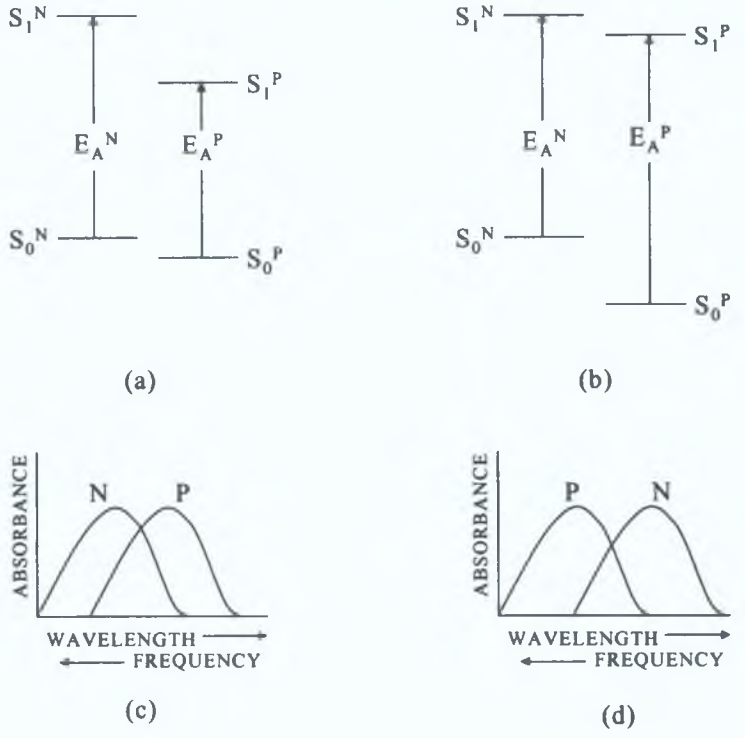

Figure 5-1: *The effect of going from a non-polar solvent (N) to a polar solvent (P), upon the energy (E_A) of and absorptive transition (a) when the excited singlet state to which absorption occurs (S_1) is more polar than the ground state (S_0), (b) when the excited singlet state to which absorption occurs is less polar than the ground state, (c) and (d) represent the way the spectral bands corresponding to the transitions in (a) and (b), respectively, might appear.*

In fluorescent molecules, subsequent to excitation to the Franck-Condon excited state, the ground state solvent cage reorients itself to conform to the new electronic distribution of the excited molecule. This solvent relaxation process involves reorientation of solute dipoles about new centres of positive and negative charge in the excited molecule, and possibly the strengthening, weakening, breaking and making of hydrogen bonds. Because nuclei motions are involved, solvent relaxation is contemporaneous with vibrational relaxation, taking about 10^{-14} – 10^{-12} seconds, and is rapid by comparison with the lifetime of the lowest excited singlet state (~10^{-8} seconds). Consequently, fluorescence originates from the excited solute molecule in a thermally equilibrated solvent cage configuration which is lower in energy than the Franck-Condon excited state, and generally even somewhat lower than the vibrationally relaxed unsolvated or weakly solvated excited molecule.

When fluorescence occurs, it terminates in the ground electronic state of the solute molecule, but because of the rapidity of the electronic transition, the molecule is still in the excited state equilibrium solvent cage (which is higher in energy than the thermally relaxed ground state). Rapid solvent relaxation then occurs (10^{-12} – 10^{-14} seconds), and the solute molecule ultimately returns to the ground state equilibrium solvent cage. Because the solvent relaxed excited state is lower in energy than the Franck-Condon excited state, and the Franck-Condon ground state is higher in energy than the solvent relaxed ground state, fluorescence often occurs at considerably longer wavelengths than would be anticipated purely on the basis of vibrational relaxation. It is for this reason that the 0 – 0 bands of fluorescence and absorption often do not coincide.

5.2 *Experimental Section*

5.2.1 Equipment and Materials

All fluorescence emission and quenching experiments were performed using a Perkin-Elmer Luminescence Spectrometer LS 50B (Beaconsfield, Buckinghamshire, UK), interfaced with a Pentium PC which employs fluorescence data management software, FLWinlab. Post-run data processing was performed using Microsoft Excel '97 and 2000 after importing the spectra as ASCII files.

All fluorescence lifetime measurements were performed using an Edinburgh Analytical Instruments Single Photon Counter in a T-setting, which employs an nF900 nanosecond nitrogen flash lamp, with photo-multiplier detector, model S300 (-20°C to -30°C). Post-run data processing was performed using F900 data correlation software, version 3.13 and Microsoft Excel 2000 after importing the spectra as ASCII files.

All UV measurements were carried out using a Perkin-Elmer Lambda 900 UV/VIS/NIR spectrometer. The instrument was controlled via UV WinLab software and post-run data processing was performed using Microsoft Excel '97 and 2000 after importing the spectra as ascii files.

Both enantiomers of phenylalaninol, (R)-(+)-phenylalaninol and (S)-(-)-phenylalaninol, both enantiomers of phenylglycinol, (R)-(-)-2-phenylglycinol and (S)-(+)-2-phenylglycinol and both enantiomers of phenylethylamine were of puriss grade (98% pure, the other 2% consisting of the other enantiomeric form), obtained from Fluka Biochemika (Gillingham, Dorset, UK). In addition as a control, the three aforementioned chiral amines were obtained of puriss grade from Sigma-Aldrich. The solvents used (acetonitrile and chloroform- HPLC grade (fluorescence emission) and Spectrometric grade (lifetime measurements)) were obtained from Labscan (Stillorgan, Co. Dublin).

5.2.2 Procedure for Fluorescence Measurements in Acetonitrile

Solutions giving concentrations of the propranolol amide calix[4]arene L1 (3.0 μmol dm^{-3}) and phenylalaninol in the range 1 – 20 mmol dm^{-3} in acetonitrile were prepared as follows. A 0.1 mmol dm^{-3} stock solution of calixarene L1 was prepared by

dissolving 8.9 mg in 50mL of methanol. A 0.25 mol dm^{-3} stock solution of phenylalaninol was prepared by dissolving the required combination of the two enantiomers, totalling 0.945 g, in 25 mL of methanol. Test solutions were then prepared by the general method followed in Chapters four and five, and making up to the volume with acetonitrile. Measurements were repeated a minimum of three times for each addition. The fluorescence intensities of the solutions were measured at an excitation wavelength of 285nm. The fluorescent intensity readings were compared to that of a solution containing 3.0 μmol dm^{-3} calixarene L1 and no phenylalaninol in acetonitrile.

5.2.3 Procedure for Fluorescence Measurements in Chloroform

Solutions giving concentrations of the propranolol amide calix[4]arene L1 (5.0 μmol dm^{-3}) and phenylalaninol in the range 1 – 44 mmol dm^{-3} in chloroform were prepared as described for experiments in acetonitrile. The fluorescence intensities of the solutions were measured at an excitation wavelength of 285nm. The fluorescence intensity readings were compared to that of a solution containing 5.0 μmol dm^{-3} calixarene L1 and no phenylalaninol in chloroform.

5.2.4 Procedure for Fluorescence Lifetime Measurements in Chloroform

Solutions giving absorbance readings of 0.57 of L1 and therefore a concentration of 44.9μmol dm^{-3} in chloroform were prepared. Each sample was spiked with the R-enantiomer of phenylalaninol and the consequent fluorescence lifetime was observed. The concentration range of phenylalaninol examined after an addition of 100-500, and 1000 μL of a 1.0mol dm^{-3} stock solution of R-phenylalaninol was 40-400mmol dm^{-3}. Solutions of L1 spiked with S-phenylalaninol were prepared in the same general manner as in the case of the R-enantiomer of PA.

5.3 *Fluorescence studies in Acetonitrile*

5.3.1 Excitation and Emission Spectra

The excitation and emission spectra of the p-allyl-S-propranolol tetra amide calix[4]arene at a concentration of 3.0 μmol dm^{-3} in acetonitrile are shown in Figure 5-3. There are maxima in the excitation spectrum at 220nm, 235nm and 285nm (Figure 5-3a), and the maximum of the emission spectrum obtained using an excitation wavelength of 285nm is at 339 nm (Figure 5-3b). Considering that the guest species do not absorb in the region of the spectrum higher than 280nm (Figure 5-2), 285nm is a suitable excitation wavelength for the following experiments.

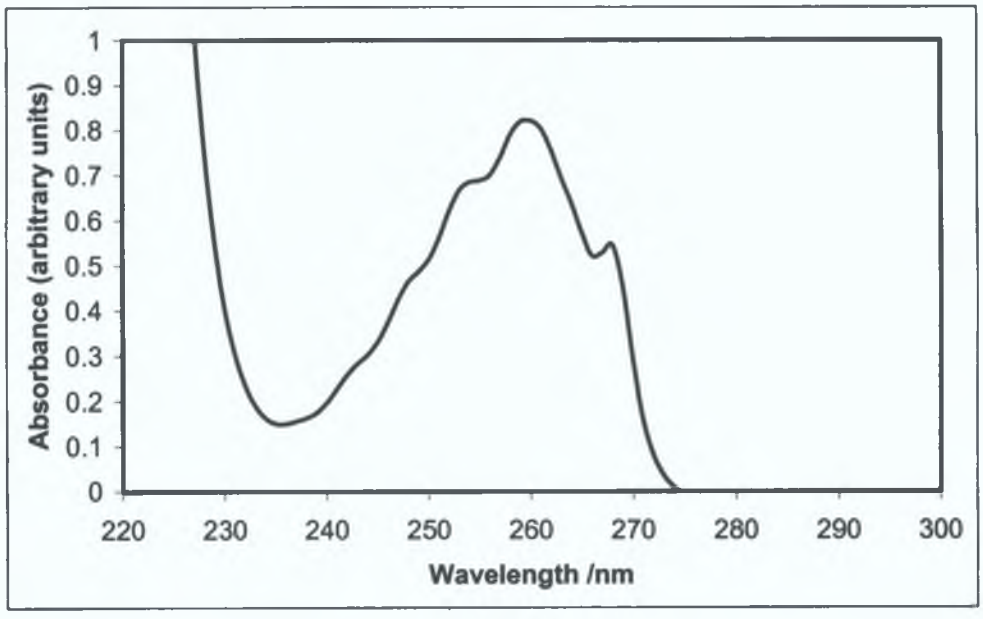

Figure 5-2: *Absorbance spectrum of phenylalaninol (PA) guest at a concentration of 4mmol dm^{-3} in acetonitrile.*

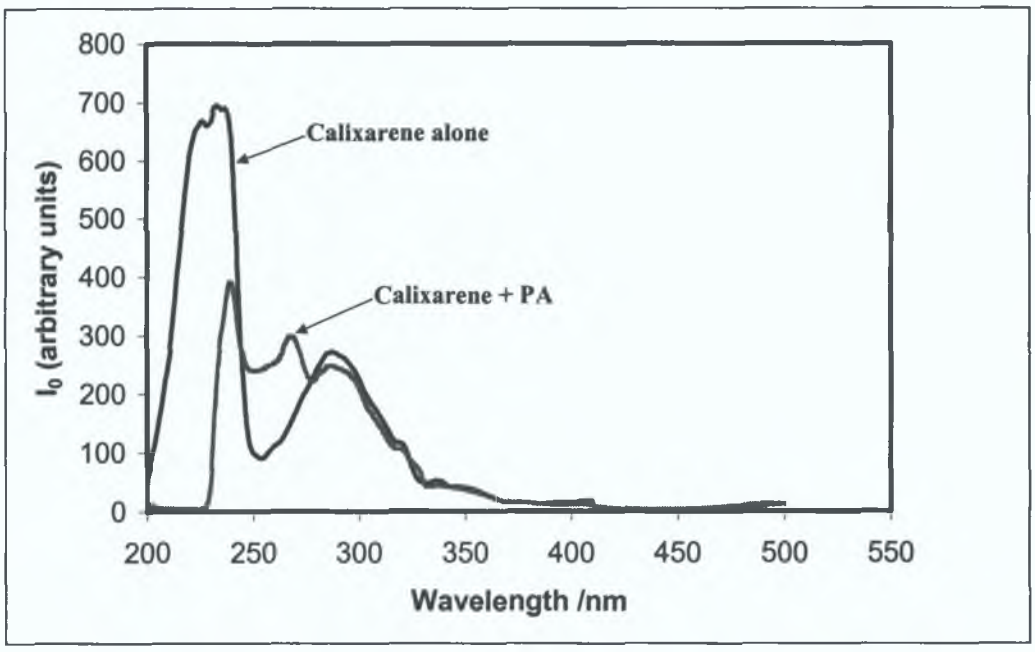

(a)

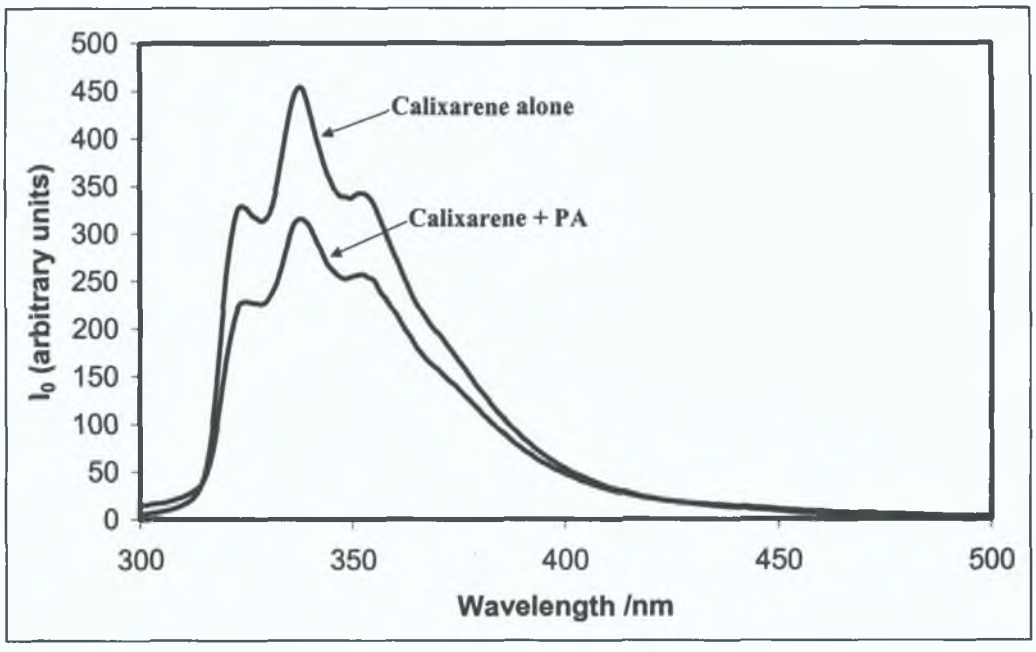

(b)

Figure 5-3: *Excitation and emission spectra of p-allyl-S-propranolol tetra amide calix[4]arene at a concentration of 3.0 μmol dm^{-3} in acetonitrile. (a) Excitation spectrum of the calixarene in the absence and presence of phenylalaninol (PA) (20 mmol dm^{-3}) at an emission wavelength of 340nm. (b) Emission spectra of the calixarene in the absence and presence of phenylalaninol at an excitation wavelength of 285nm .*

5.3.2 Linear Response range in Acetonitrile

The linear response range of fluorescence intensity to concentration of calixarene **L1** in acetonitrile was determined to be between 0.1 and 4.0μmol dm^{-3} as shown in Figure 5-4. It is important to use a concentration of the calixarene within the linear range in order to ensure that no self-quenching occurs and therefore that no alternative self-quenching mechanisms are present. A concentration of 3.0 μmol dm^{-3} was chosen for subsequent experiments to examine the effects of phenylalaninol (PA) and hence any quenching observed can be related to the effect of the target species on the ligand.

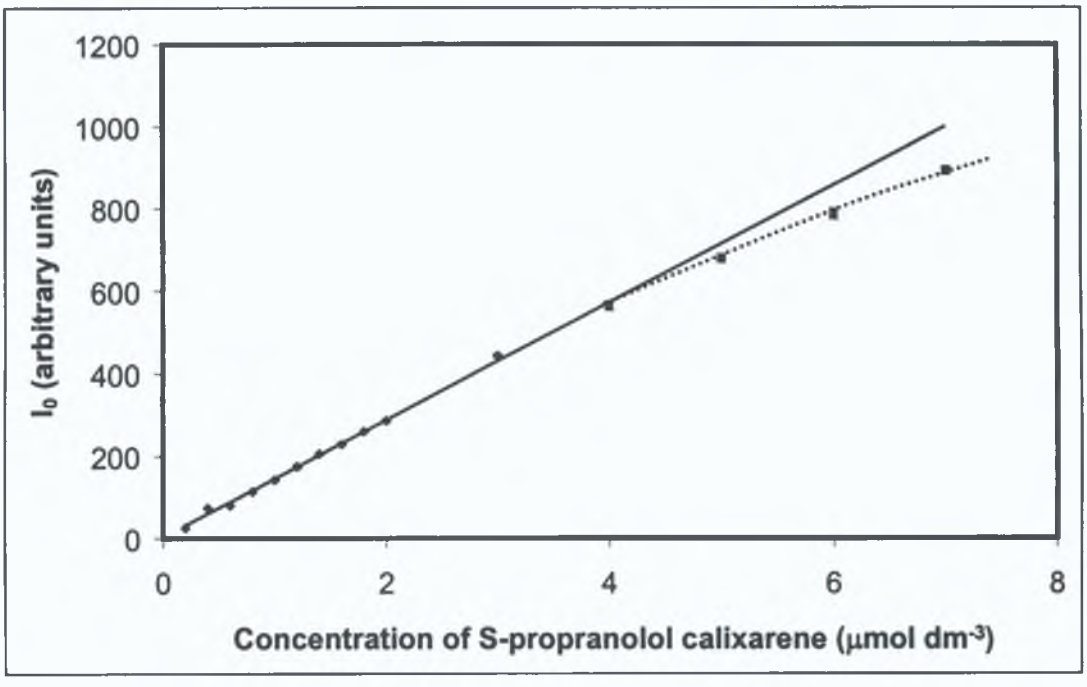

Figure 5-4: *Linear fluorescence response of p-allyl-S-propranolol calixarene in acetonitrile, measured using an excitation wavelength of 285nm and at an emission wavelength of 339nm, points represent the mean of three replicate measurements (n=3), with the error bars representing ± standard deviation (error bars may be masked by symbols).*

5.3.3 Linear range of Stern-Volmer plot.

The Stern-Volmer plot was tested for linearity over a series of concentration ranges, which include;

- 0 - 0.5 mmol dm^{-3} of racemic phenylalaninol (Figure 5-5).
- 0 - 4 mmol dm^{-3} of racemic phenylalaninol (Figure 5-6).
- 0 - 20 mmol dm^{-3} of racemic phenylalaninol (Figure 5-7).

Since quenching is described by the Stern-Volmer equation, quenching data is frequently presented as a plot of I_0/I versus [Q], because I_0/I is expected to be linearly dependent upon the concentration of the quencher. As can be seen from the following graphs, the Stern-Volmer plots are not linear over any of the concentration ranges tested and do not strictly obey the Stern-Volmer equation (that is the intercept of the linear region does not pass through one). There appears to be quite a sharp initial increase in the I_0/I values for the calixarene, after the addition of racemic phenylalaninol in acetonitrile as solvent, which then tailors off to a steady linear plot.

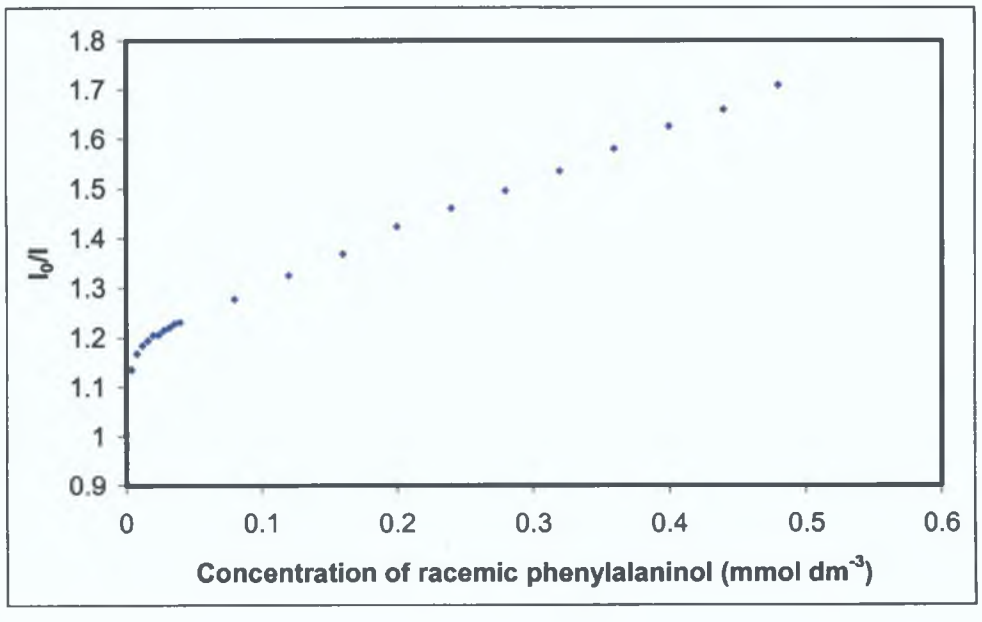

Figure 5-5: *Stern-Volmer plot of S-propranolol calixarene (3.0 μmol dm^{-3}) over the range 0 - 0.5 mmol dm^{-3} of racemic phenylalaninol in acetonitrile, measured using an excitation wavelength of 285nm and at an emission wavelength of 339nm, points represent the mean of three replicate measurements (n=3), with the error bars representing ± standard deviation (error bars may be masked by symbols).*

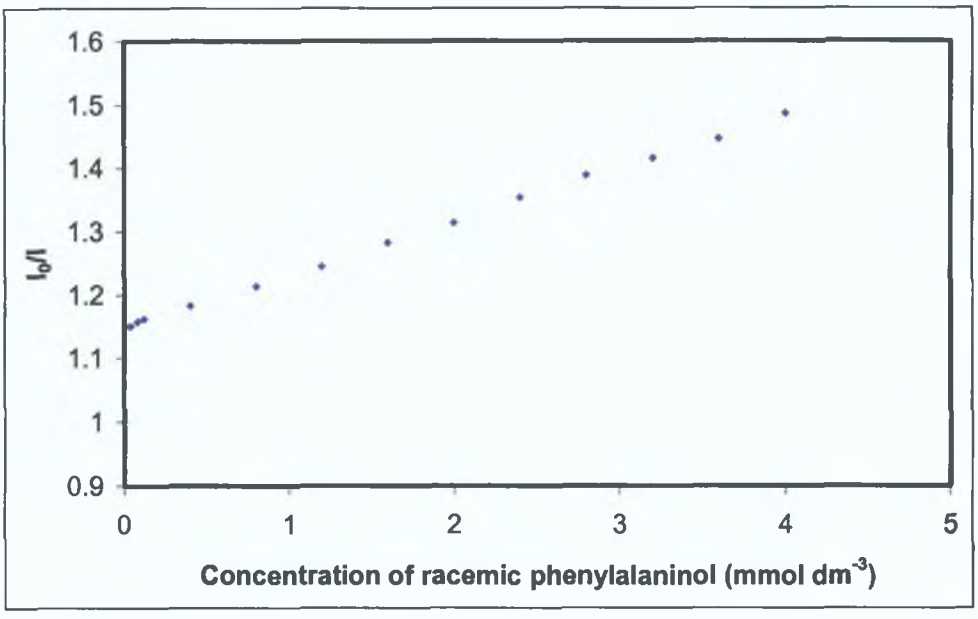

Figure 5-6: *Stern-Volmer plot of S-propranolol calixarene (3.0 μmol dm^{-3}) over the range 0 - 4 mmol dm^{-3} of racemic phenylalaninol in acetonitrile.*

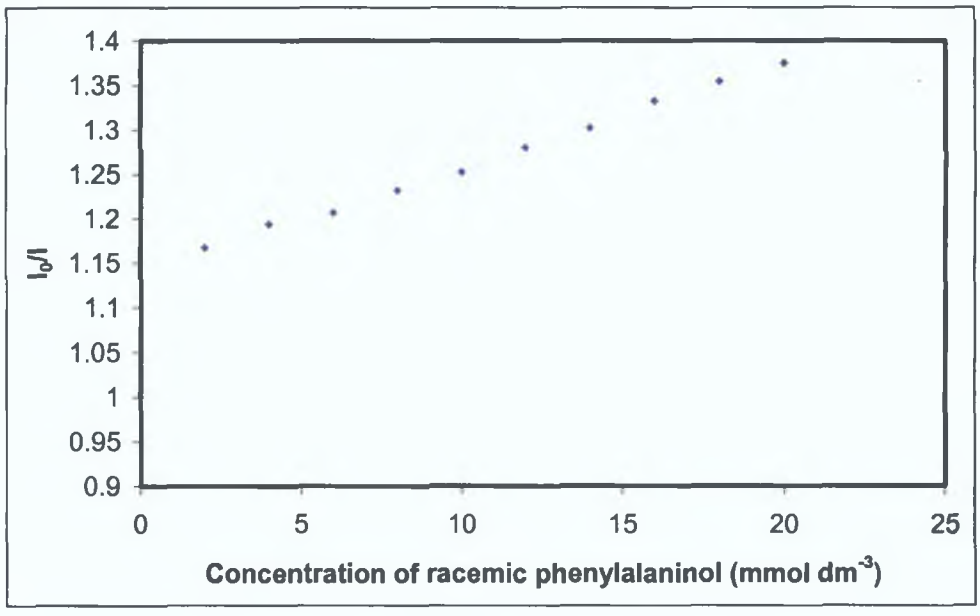

Figure 5-7: *Stern-Volmer plot of S-propranolol calixarene (3.0 μmol dm^{-3}) over the range 0 - 20 mmol dm^{-3} of racemic phenylalaninol in acetonitrile.*

For Figure 5-6 and Figure 5-7 data was measured using an excitation wavelength of 285nm and at an emission wavelength of 339nm, points represent the mean of three replicate measurements (n=3), with the error bars representing ± standard deviation (error bars may be masked by symbols).

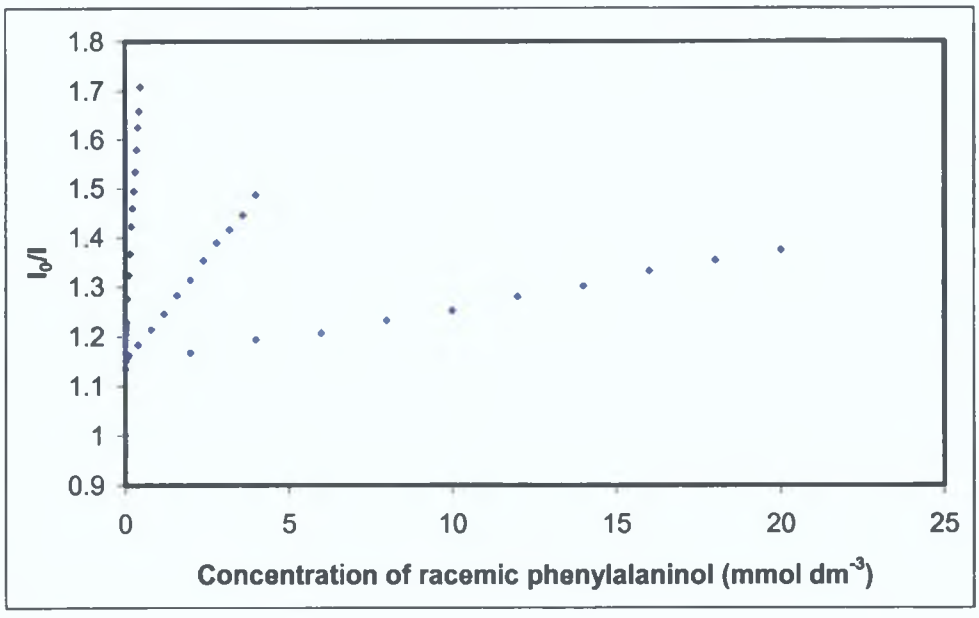

Figure 5-8: *Comparison of Stern-Volmer plots of S-propranolol calixarene in acetonitrile, combination of plots in Figure 5-5, Figure 5-6 and Figure 5-7.*

Figure 5-8 compares the values for I_0/I over the three concentration ranges of quencher tested, namely 0 - 0.5, 0 – 4 and 0 - 20 mmol dm^{-3}. The concentration range used does not seem to greatly affect the trend of calixarene quenching, since there appears to be a significant initial quenching process with considerably less prominent effects following subsequent addition of the guest (see Figure 5-10). Since the there is a significant initial quenching which does not change substantially upon further addition of quencher this would seem to imply that a 1:1 association between the calixarene host and guest quencher occurs.

5.3.4 Variation of Stern-Volmer plot with enantiomeric composition

Even though the Stern-Volmer plot of **L1** was not found to be linear over the range 0-20 mmol dm^{-3} of racemic phenylalaninol, the effects of both enantiomer of phenylalaninol on the fluorescence of **L1** in acetonitrile were investigated. Figure 5-9 illustrates the Stern-Volmer plots for the quenching of the fluorescence of calixarene **L1**, upon addition of 100% (R)- and 100% (S)-phenylalaninol respectively, at a concentration range of 0 – 40mmol dm^{-3}. Because the Stern-Volmer plots show such similarities in the behaviour of each enantiomer, and the fact that the quenching data does not strictly follow the Stern-Volmer equation, it can be concluded that in

acetonitrile, the propranolol amide derivative of p-allyl-calix[4]arene does not exhibit significant ability to discriminate between the enantiomers of phenylalaninol.

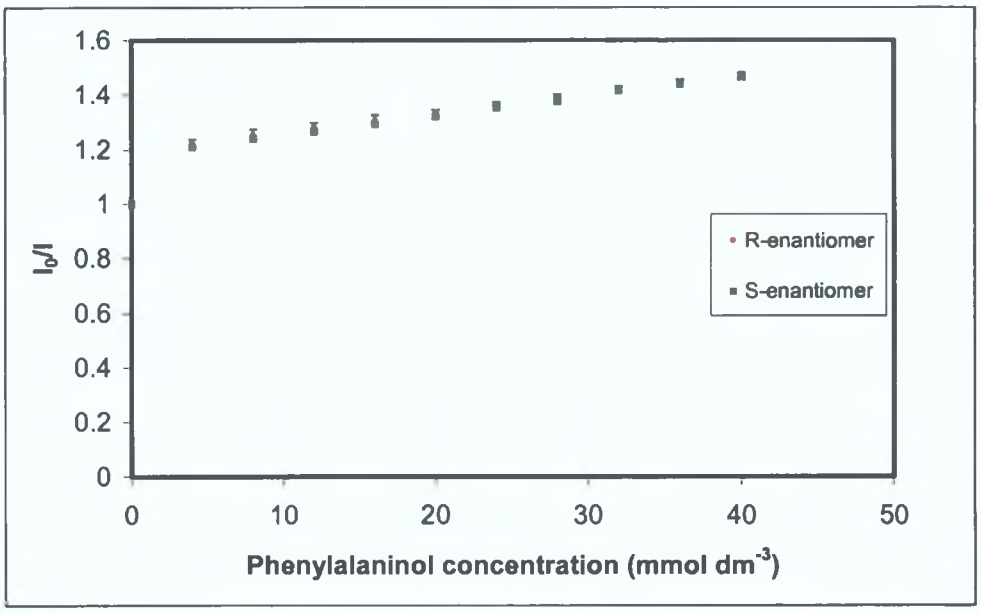

Figure 5-9: *Stern-Volmer plots for the quenching of S-propranolol calixarene (3.0 μmol dm^{-3}) measured using an excitation wavelength of 285nm and at an emission wavelength of 339nm, upon addition of 0 (red) and 100% (S)-phenylalaninol (green) in acetonitrile. Standard deviations are shown as error bars (n=3), which may be masked by symbols.*

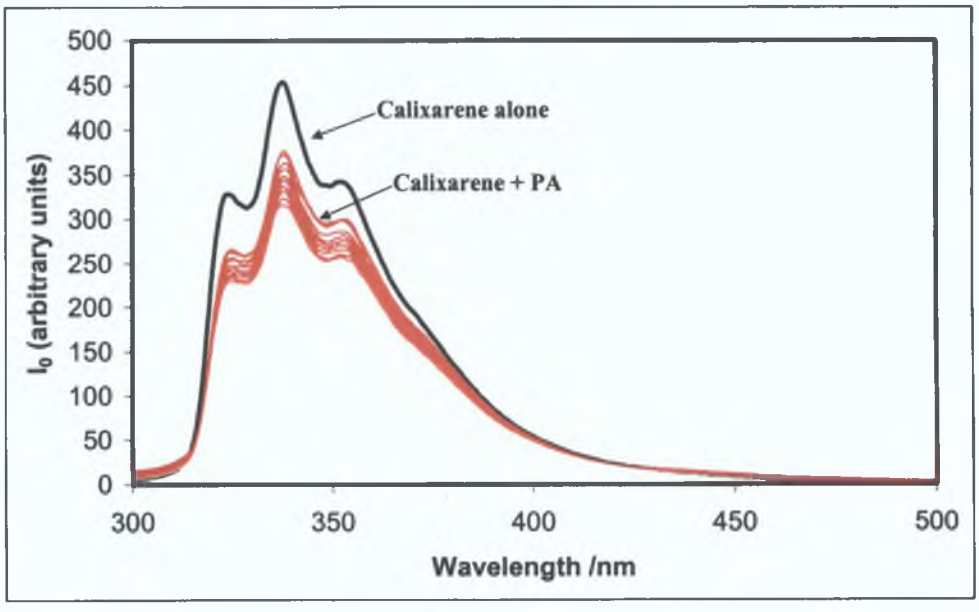

Figure 5-10: *Fluorescence emission spectra of calixarene alone (3.0 μmol dm^{-3}) in acetonitrile (black) and in the presence of varying amounts of R-phenylalaninol (PA) (0 – 20 mmol dm^{-3} –uppermost-lowest red spectra respectively).*

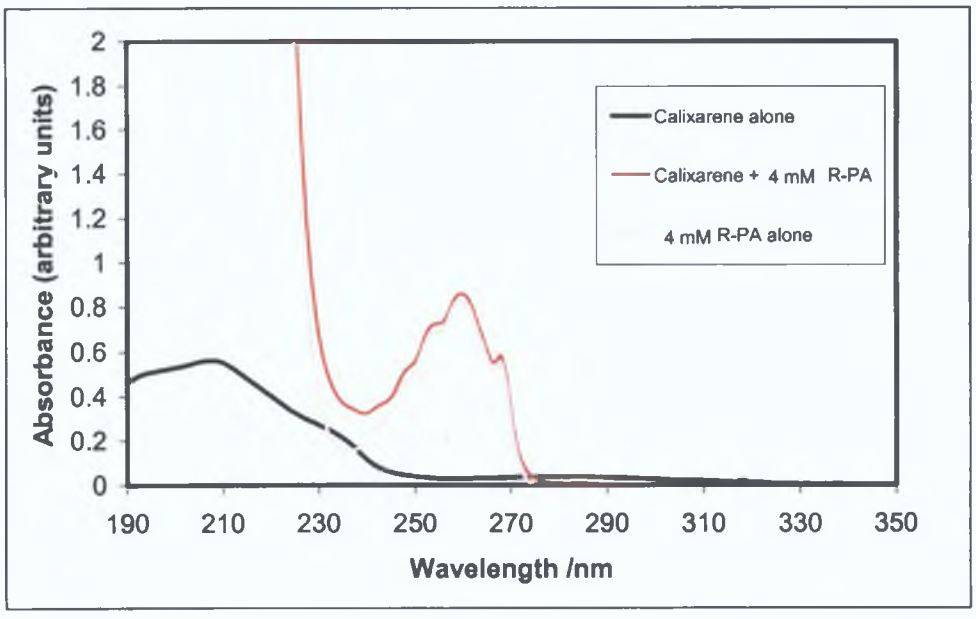

Figure 5-11: *UV-spectra in acetonitrile of calixarene alone (3.0 μmol dm^{-3}) (black), phenylalaninol guest alone (dotted red), and calixarene in the presence of 4 mmol dm^{-3} phenylalaninol guest (red).*

Preliminary studies of the absorption spectra of ligand **L1** in acetonitrile (Figure 5-11) make it difficult to ascertain whether changes occur in the calixarene spectrum after the addition of guest phenylalaninol. However the excitation spectrum (Figure 5-3 (a)) would seem to indicate a change in the absorption spectrum of the calixarene **L1** in the presence of a guest molecule in acetonitrile. For this reason it is possible that a static quenching mechanism is responsible for the decrease in fluorescence emission intensity of **L1**. This would lead one to believe that quenching occurs as a result of the formation of a non-fluorescent complex between the fluorophore (calixarene host) and quencher (phenylalaninol guest). This theory is further supported by the initial large decrease in fluorescence intensity in the calixarene spectrum after the addition of the phenylalaninol guest, which is followed by only minor changes subsequent to further aliquots of the guest being added (see Figure 5-10). This would imply that an immediate association with the guest phenylalaninol is formed when the guest is introduced to the solution. Considering that even at the lowest concentration ranges of guest, this is still 1000 times in excess of the calixarene **L1** concentration. If a 1:1 complex is formed between the host and guest then it will do so immediately, on the first addition of guest since the guest concentration is far in excess of the host, making the effect of further guest addition negligible, which is what is seen experimentally.

When this case is examined with regard to the host guest interactions in acetonitrile as solvent, it must be kept in mind that since acetonitrile is polar, non-protic in nature, it does not therefore engage in hydrogen bonding with solute molecules. This implies that the guest molecules do not need to disrupt any pre-existing hydrogen bonding between the calixarene host and the solvent. This suggests that the host is free to engage in direct bonding/association with the guest, and as soon as the first aliquot of guest is introduced to the host solution, a host: guest association immediately occurs. This is not extraordinary considering that the guest concentration is far in excess of that of the host, and unlike in the previously discussed case of methanol as solvent, the guest molecules are not required to be in excess, to force an association away from the solvent molecules and towards the guest species.

5.4 Fluorescence studies in Chloroform.

5.4.1 Excitation and Emission Spectra

The excitation and emission spectra of the p-allyl-S-propranolol tetra-amide calix[4]arene at a concentration of 5.0 μmol dm^{-3} in chloroform are shown in Figure 5-13. The maxima of the excitation spectrum are at 285 and 338 nm (Figure 5-13a), and the maximum of the emission spectrum obtained using an excitation wavelength of 285 nm is at 338 nm (Figure 5-13b). Considering that the guest species do not absorb in this region, 285nm is a suitable excitation wavelength for the following experiments.

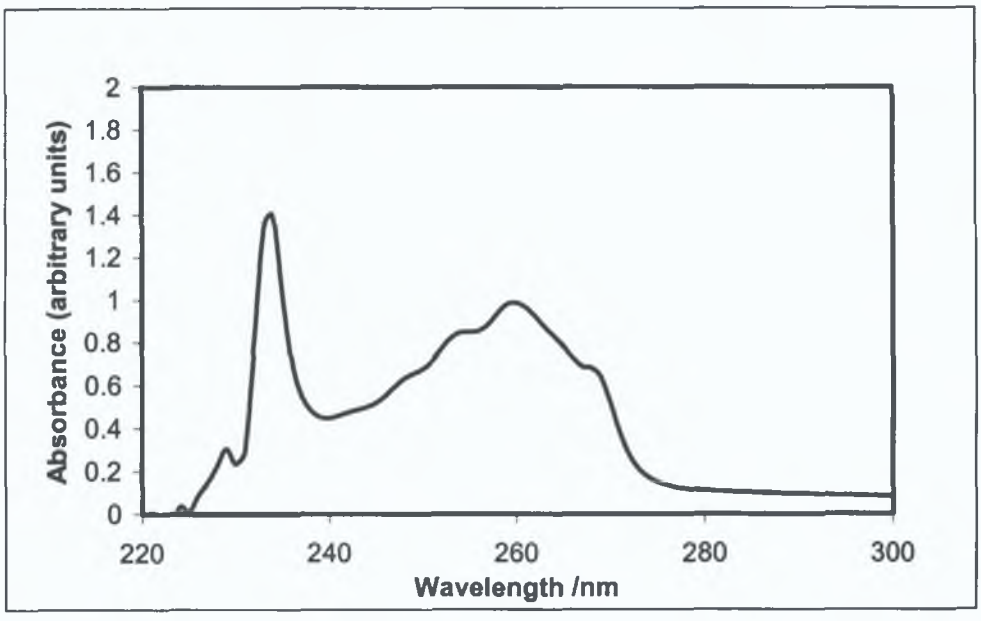

Figure 5-12: *Absorbtion spectrum of phenylalaninol (PA) guest at a concentration of 4mmol dm^{-3} in chloroform.*

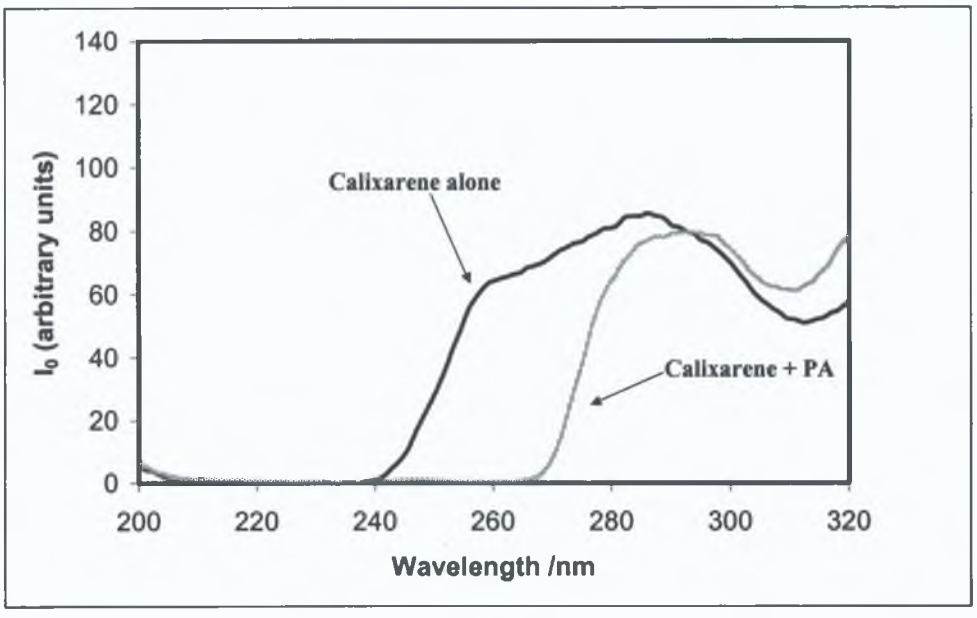

(a)

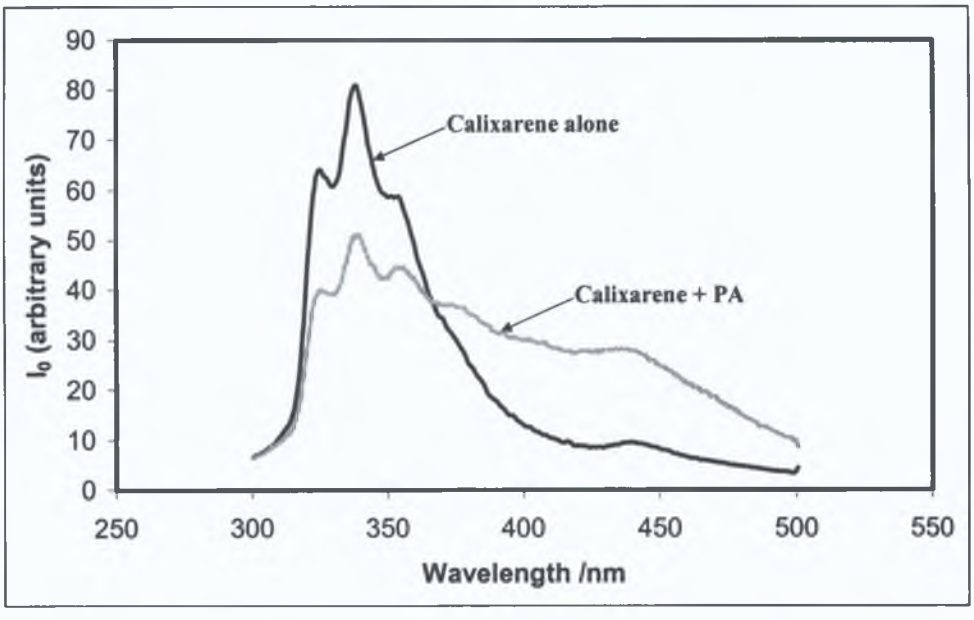

(b)

Figure 5-13: *Excitation and emission spectra of p-allyl-S-propranolol tetra amide calix[4]arene at a concentration of 5.0 μmol dm^{-3} in chloroform. (a) Excitation spectrum of the calixarene in the absence and presence of phenylalaninol (PA) (20 mmol dm^{-3}) at an emission wavelength of 340nm. (b) Emission spectra of the calixarene in the absence and presence of phenylalaninol (20 mmol dm^{-3}) at an excitation wavelength of 285nm.*

5.4.2 Linear response range in Chloroform

The linear response range of fluorescence intensity to concentration of calixarene **L1** in chloroform was determined to be between 0.1 and 6.0μmol dm^{-3} as shown in Figure 5-4. It is important to use a concentration of the calixarene within the linear range in order to ensure that no self-quenching occurs and therefore that no alternative self-quenching mechanisms are present. A concentration of 5.0 μmol dm^{-3} was chosen for subsequent experiments to examine the effects of phenylalaninol (PA) and hence any quenching observed can be related to the effect of the target species on the ligand.

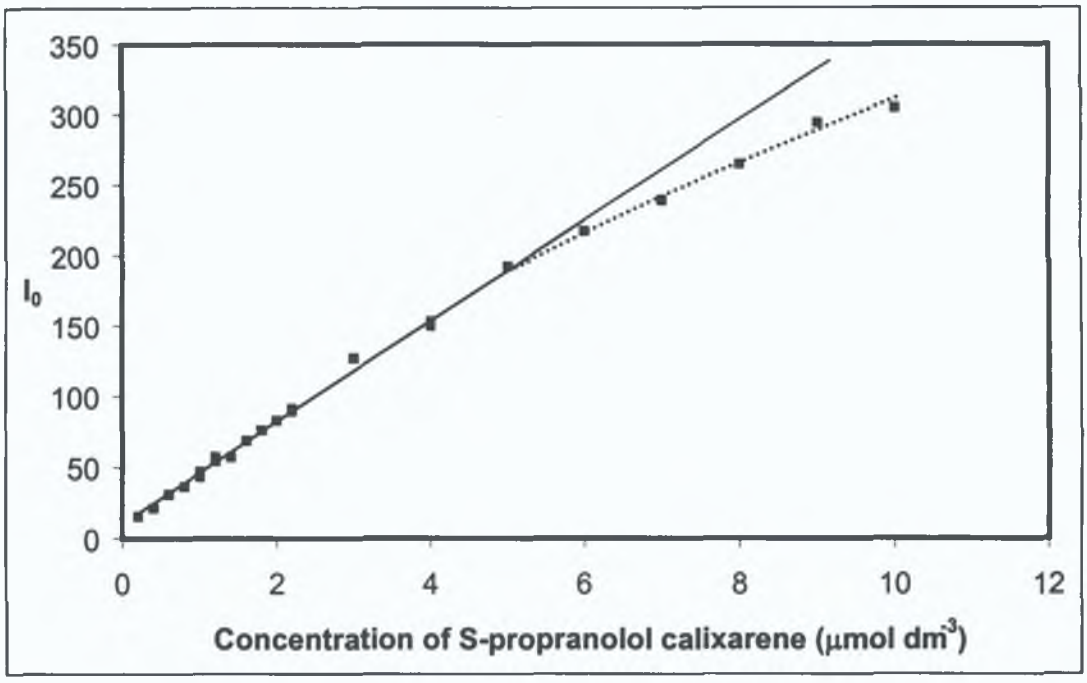

Figure 5-14: *Linear fluorescence response of p-allyl-S-propranolol calixarene in chloroform, points represent the mean of three replicate measurements (n=3), with the error bars representing ± standard deviation (error bars may be masked by symbols).*

5.4.3 Linear range of Stern-Volmer plot.

The Stern-Volmer plot when measured in chloroform was found to be linear over a range of 0-44 mmol dm^{-3} of racemic phenylalaninol.

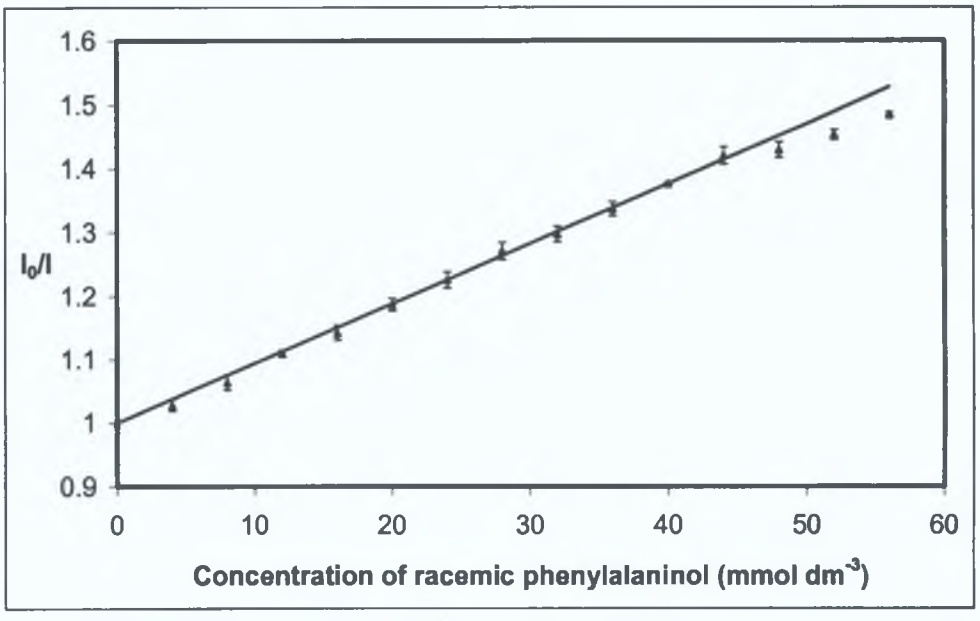

Figure 5-15: *Stern-Volmer plot of S-propranolol calixarene (5.0 μmol dm^{-3}) over the range 0 – 56 mmol dm^{-3} of racemic phenylalaninol in chloroform, points represent the mean of three replicate measurements (n=3), with the error bars representing ± standard deviation (error bars may be masked by symbols).*

5.4.4 Variation of Stern-Volmer plot with enantiomeric composition

The Stern-Volmer plot of **L1** was found to be linear over the range 0 - 40 mmol dm^{-3} of racemic phenylalaninol in chloroform. Figure 5-16 illustrates the Stern-Volmer plots for the quenching of the fluorescence of calixarene **L1** at an emission wavelength of 340nm, upon the addition of 100% R- (red data points) and 100% (S)-phenylalaninol (green data points), at a concentration range of 0 – 40 mmol dm^{-3}. These Stern-Volmer plots yield K_{SV} values of 0.014 and 0.011 for the R- and S-enantiomers of phenylalaninol respectively. These Stern-Volmer constants return a K_{SV} ratio of 1.25, and although the slopes for each enantiomer in the presence of **L1** are statistically different, these results taken at an emission wavelength of 340nm show great similarities in the behaviour of each enantiomer in the presence of **L1**, when compared to the metal-ion complexes previously discussed (Chapter 4). It can be concluded therefore that in chloroform when measuring at an emission wavelength of 340nm, the propranolol amide derivative of *p*-allyl-calix[4]arene does not exhibit the considerable ability to discriminate between the enantiomers of phenylalaninol as the metal ion complexes previously discussed (Chapter 4).

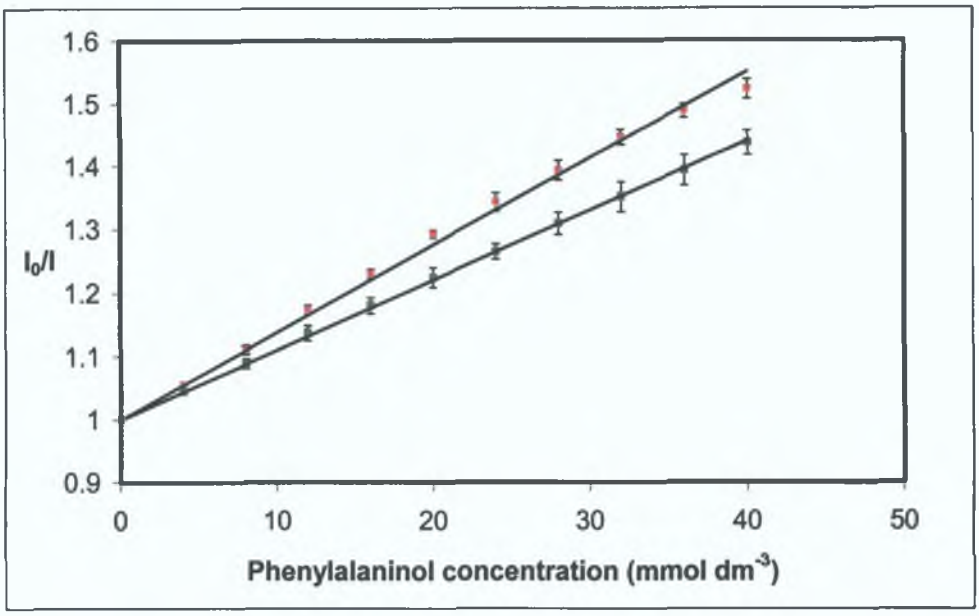

Figure 5-16: *Stern-Volmer plots for the quenching of S-propranolol calixarene (5.0 μmol dm^{-3}) upon addition of 0% (red) and 100% (S)-phenylalaninol (green) in chloroform at an excitation wavelength of 285nm and an emission wavelength of 340nm. Standard deviations are shown as error bars (n=3), which may be masked by symbols.*

Preliminary studies of the absorption spectra of ligand **L1** in chloroform (Figure 5-17) show that the addition of guest phenylalaninol produces a simple additive effect to the calixarene absorption spectrum. However when the excitation spectrum of **L1** is examined in the absence and presence of phenylalaninol (Figure 5-13a), differences are noted. When the full emission spectrum of calixarene **L1** in chloroform is examined in the presence of R- and S-phenylalaninol these differences can be clearly seen (see Figure 5-18a and b). In the presence of guest R-phenylalaninol the weak emission band of **L1** at 430nm is greatly enhanced. This enhancement is not however observed for **L1** in the presence of the S-enantiomer of phenylalaninol.

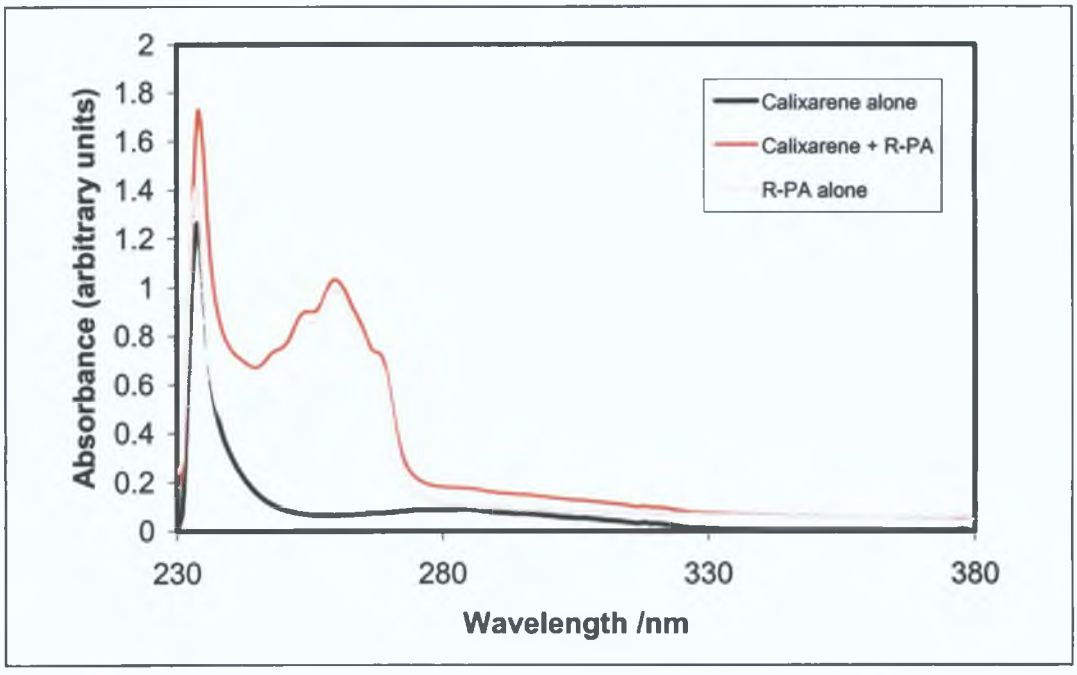

Figure 5-17: *UV-spectra in chloroform of calixarene alone (5.0 μmol dm^{-3}) (black), phenylalaninol guest alone (4 mmol dm^{-3}) (dotted red), and calixarene in the presence of phenylalaninol guest (5.0 μmol dm^{-3} and 4 mmol dm^{-3} respectively) (solid red).*

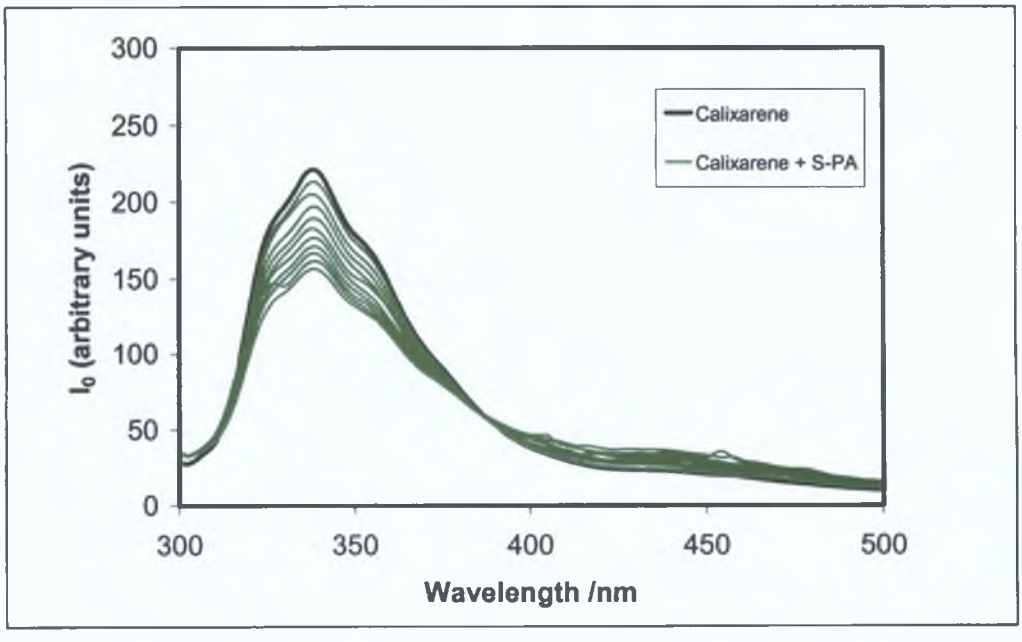

(a)

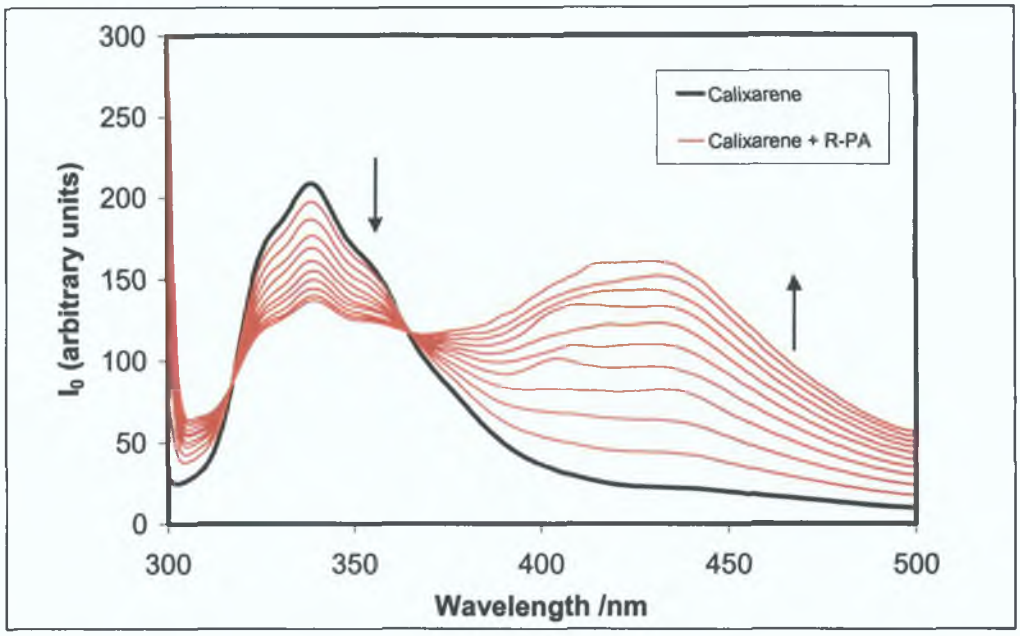

(b)

Figure 5-18: *Fluorescence emission spectra of calixarene **L1** (5.0 μmol dm^{-3}) in chloroform measured at an excitation wavelength of 285nm in the absence (black) and in the presence of varying amounts of S-phenylalaninol ((a) green spectra) and R-phenylalaninol ((b) red spectra). Phenylalaninol concentration in the range 4-40 mmol dm^{-3}, for both (a) and (b) concentration increases as fluorescence intensity decreases.*

The graph below (Figure 5-19) shows that by monitoring the fluorescence intensity of **L1** in the presence of each enantiomer of phenylalaninol at an emission wavelength of 430nm, a clear distinction between the effect of the R- and S-isomers of phenylalaninol can be observed from an increase in fluorescence, which is in contrast to the results previously obtained. When methanol is employed as solvent, the enantiomeric discrimination can be observed as a decrease in the fluorescence intensity with a corresponding increase in guest concentration. In the case of chloroform as solvent, if the fluorescence intensity is monitored at a wavelength of 430nm the enantiomeric discrimination can be observed as an increase in the fluorescence intensity with a corresponding increase in guest concentration. By monitoring at this wavelength (430nm) it can be clearly discerned which enantiomer is in solution with calixarene **L1**.

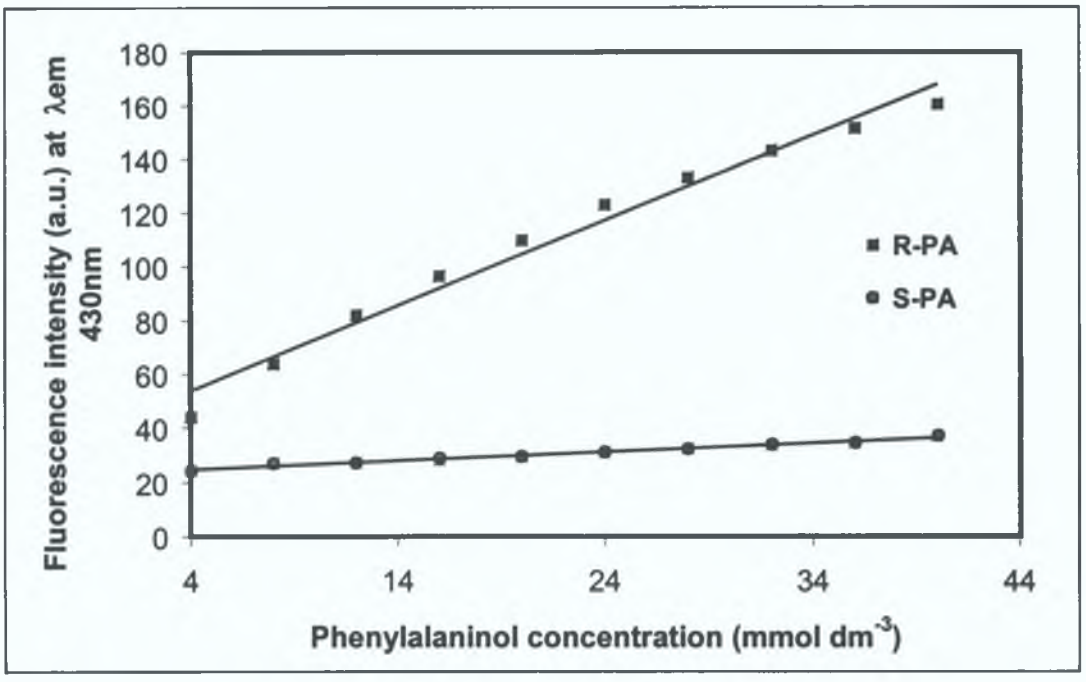

Figure 5-19: *Fluorescence intensity of exciplex band at λ-emission = 430nm with increasing phenylalaninol concentration, calixarene concentration 5.0 μmol dm^{-3} in the case of each enantiomer .*

An explanation for this increase in intensity of the emission band at 430nm is attributed to the presence of two emitting species in solution, which we have assigned as two different conformations of the calixarene **L1**. If one consults the energy minimised molecular modelling pictures in Chapter 4 it can be seen quite clearly how flexible the appended chains of this ligand can be. This in conjunction with the ^{1}H-NMR spectrum, which suggests that the calixarene does not exist as a symmetrical cone in $CDCl_3$ solution, but rather a distorted cone, would strengthen the argument that two conformations of the calixarene are present in chloroform solution. Upon addition of the guest molecule R-phenylalaninol, the conformation of the calixarene changes to accommodate and associate with the guest, thereby changing the equilibrium of conformations present in solution, which seems to generate more of the conformer which emits at 430nm, and less of the form whose emission is observed at 340nm. This would explain the intensity enhancement of the band at 430nm. The fact that the band at 340nm decreases in the presence of the S-enantiomer of phenylalaninol may be attributed to a weak complex formation between the S-enantiomer and **L1**.

However the enhancement of this new band in the presence of R-PA, could also be due to the formation of an excited state complex between the calixarene host and the phenylalaninol guest, whereby the excited state fluorophore accepts an electron from the amine. In non-polar solvents, fluorescence from the excited state charge transfer complex (exciplex) is frequently observed. It is well known that the fluorescence emission of hydrocarbons is quenched by electron transfer from amines **[2, 3]**. In order to determine which of these two processes is actually occurring in solution (exciplex formation or a change in equilibrium of conformations) the fluorescence lifetime of the calixarene in the absence and presence of phenylalaninol was measured. If an exciplex is formed, then the lifetime of the calixarene should change in the presence of the guest PA.

5.4.5 Variation of fluorescence lifetimes with enantiomeric composition

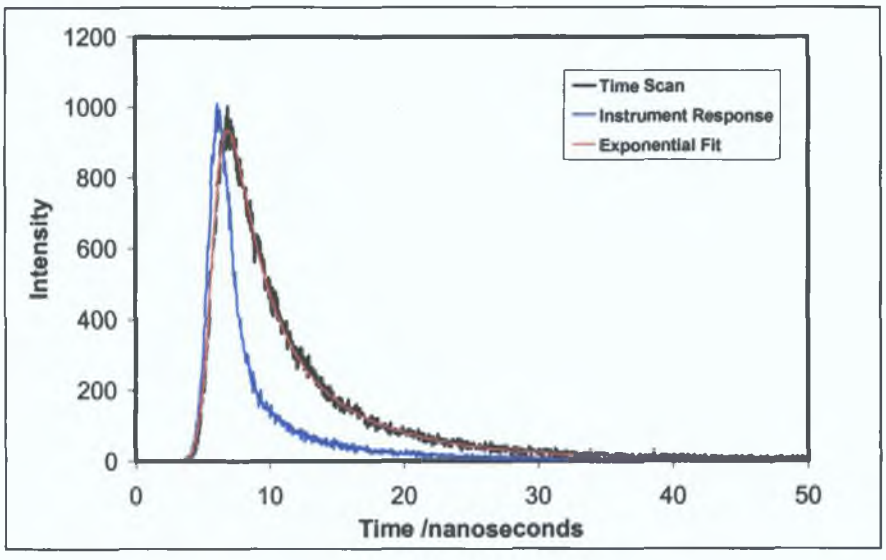

(a)

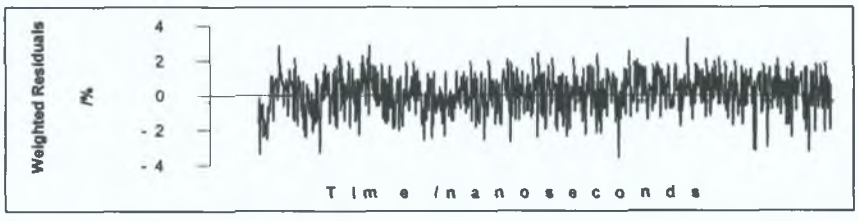

(b)

Figure 5-20: *Fluorescence lifetime decay spectrum of p-allyl-tetra-S-propranolol amide calix[4]arene in chloroform, in comparison to the instrument response and the exponential model fit* ***(a)****. Residual data not fitted to exponential model* ***(b)****.*

Figure 5-20 shows the decay profile of calixarene **L1** in chloroform Using the bi-exponential equation (equation 3-2), the lifetime exponential decay can be modelled to yield the fluorescence lifetime of the excited state of calixarene **L1** Using an excitation wavelength of 337nm and scanning at an emission wavelength of 520nm, two values of 6 6 and 1 6 ns were measured for the lifetime of **L1** in chloroform This would suggest that two fluorescing species are present in solution Since spectroscopic grade solvents were used and the calixarene was pure, the second value was not attributed to an impurity This could instead be due to different conformations of the calixarene, as the array of naphthalene groups may be differently positioned in one conformer over the other, possibly altering the electronic state of the molecule

A solution of **L1** in chloroform was spiked with aliquots of a 1 0M R-phenylalaninol in chloroform The fluorescence emission lifetime decays were then measured and the results can be seen in Table 5-1 It is evident from the data acquired that the lifetime measurements do not exhibit a concentration dependence on the quencher, unlike the emission spectra and also that $\tau_0/\tau \neq F_0/F$ This infers that $\tau_0/\tau \sim 1$, and therefore the mechanism of quenching of **L1** by R-phenylalaninol is determined to be static This implies that an excited state complex between the fluorophore and amine is not responsible for the increase in intensity of the emission band at 440nm

Solution	***τ_1 and τ_2 / Nanoseconds (St Dev)***	***χ^2***
Calixarene alone	6 7, 1 6 (±0 1)	1 11
L1 + 100 µL , 1 0 M R-PA	7 0, 1 8 (±0 2)	1 05
L1 + 200 µL, 1 0 M R-PA	6 6, 1 6 (±0 1)	1 14
L1 + 300 µL, 1 0 M R-PA	6 7, 1 6 (±0 1)	1 15
L1 + 500 µL, 1 0 M R-PA	6 3, 1 2 (±0 1)	1 28
L1 + 1000 µL, 1 0 M R-PA	6 2, 1 8 (±0 3)	1 13
L1 + 1500 µL, 1 0 M R-PA	6 7, 1 4 (±0 2)	1 05

Table 5-1 *Fluorescence lifetimes of calixarene in the absence and presence of R-phenylalaninol*

The lifetime of the excited state **L1** was also measured in the presence of the S-enantiomer of phenylalaninol The results can be seen in **Table 5-2**, which illustrate that the presence of this guest enantiomer in solution does not perturb the excited state lifetime of the calixarene, confirming that both enantiomers of phenylalaninol form ground state complexes with calixarene **L1** in chloroform solution

Solution	τ_1 ***and*** τ_2 ***/ Nanoseconds (St Dev)***	χ^2
Calixarene alone	6 7, 1 6 (±0 1)	1 11
L1 + 100 μL , 1 0 M S-PA	6 5, 1 7 (±0 2)	1 08
L1 + 200 μL, 1 0 M S-PA	6 6, 1 6 (±0 1)	1 14
L1 + 500 μL, 1 0 M S-PA	6 4, 1 6 (±0 4)	1 14
L1 + 1000 μL, 1 0 M S-PA	6 6, 1 6 (±0 1)	1 18

Table 5-2 *Fluorescence lifetimes of calixarene in the absence and presence of S-phenylalaninol*

The fluorescence lifetime data obtained in chloroform, confirms that the mechanism of quenching of the fluorescence of **L1** by each enantiomer of phenylalaninol is static and therefore that an excited state complex is not accountable for the increase in intensity of the emission band at 440nm This reinforces the argument that there is a change in equilibrium of two calixarene conformations in the presence of R-phenylalaninol in chloroform solution At present we cannot distinguish which conformation or rotamer is responsible for the emission bands at 340nm and 440nm Fluorescence emission and lifetime measurements of metal complexes of **L1** in chloroform may help to discern whether a more rigid cone conformation induced by metal ion complexation is responsible for one of the emission bands It is clear however, that enantiomeric discrimination is possible with calixarene **L1** in chloroform solution if the emission intensity is monitored at 440nm Since the intensity of **L1** in chloroform changes very little when in solution of S-PA (Figure 5-19), and undergoes a four-fold increase when in the presence of R-PA (highest concentration) it is immediately obvious which enantiomer one has in solution with this calixarene

5.5 Conclusion

Chiral discrimination of phenylalaninol is not possible with **L1** in acetonitrile There appears to be a 1 1 host guest association with **L1** and PA in this solvent Since acetonitrile is a polar non-protic solvent this may be due to the lack of hydrogen bonding from the solvent to the calixarene This implies that the guest PA does not need to disrupt any host-solvent associations when spiked into the calixarene in solution and therefore immediately associates with the host

In chloroform as solvent a very different behaviour is seen Chiral discrimination is statistically possible with **L1** and PA in chloroform, but while monitoring the emission at 340nm the extent of discrimination is not comparable to that of the metal-ion complexes discussed in the previous chapter When the emission intensity of this ligand is monitored at 440nm in the presence of PA, huge differences in the fluorescence intensities are seen with respect to the two enantiomers In the case of S-PA practically no change is observed at 440nm when this enantiomer is present in solution with **L1** However a dramatic increase in fluorescence intensity is observed at 440nm when R-PA is added to a solution of **L1** in chloroform

Fluorescence lifetime measurements verify that a static quenching mechanism is responsible for the changes in the emission intensities of **L1** in the presence of both enantiomers of PA This rules out the possibility of exciplex formation between **L1** and R-PA Lifetime measurements also confirm that two fluorescing species exist in solution, which have been attributed to two different calixarene conformations in chloroform This theory is supported by the ^{1}H-NMR spectra in chapter 4, and when one consults the energy minimised structures of **L1** in chapter 4 it is clear that the free ligand is quite flexible and may exist as conformations other than a rigid cone, when in solution

5 6 References

1 N S Bayliss, E G McRae, *J Phys Chem* **1954**, 58, 1002

2 T R Evans, *J Am Chem Soc* **1971**, 93, 8, 2081

3 J V Goodpaster, V L McGuffin, *Anal Chem* **2000**, 72, 1072

6 Conclusion and Future Work

6 1 Conclusions

The synthesis of **L1** was successful via the acid chloride route (section 2 2 1) Attempts at reducing the length of the synthesis with coupling agent DCC was not successful, since using DCC as a coupling agent to form amides directly from calixarene tetra-acids did not achieve tetra-substituted amides An alternative route to produce tetra-amide substituted calixarenes from less expensive building blocks, with however similar properties to L1 was attempted The alternative route taken involved two steps

1 formation of the amide moiety

2 attachment of amide moieties to calixarene backbone

The first of these two steps led to the formation of three amide units (**119**), (**120**) and (**121**) The second step however suffered from partial substitution, and resulted in a series of mono, di and tri substituted fluorescent calixarenes A five-fold excess of the amide moiety was used which is not sufficient to complete the tetra-substitution Potassium carbonate as base may not be strong enough to allow the reaction to go to completion A stronger base with a greater excess of alkylating agent (amide) could possibly produce tetra-substituted amides The partially substituted calixarenes could however prove useful in future studies as molecular receptors in chiral or anion recognition

Ligand **L1** was designed with a methylene spacer between the chiral centre and fluorescent naphthyl moiety and was found to successfully discriminate between the amino alcohol, phenylalaninol, with a methylene spacer between its aromatic moiety and chiral centre However, discrimination between two pairs of shorter chain amino alcohol enantiomers (R- and S- phenylglycinol and phenylethylamine) was not observed with this calixarene **L1** is therefore very specific in its interactions with guest molecules and as well as discriminating between mirror image forms, can successfully recognise such a small difference in guest molecules as a methylene spacer

In this study there are relatively well-defined, 3-D chiral spaces in the cavity of the calixarene **L1** through which the enantiomers must pass in order to facilitate

quenching. This infers that since the host molecule is itself chiral in nature, bearing an (S)-amide substituent, that the (R)-enantiomer should be better predisposed to interact with the calixarene than the (S)-enantiomer. The fact that the (R)-enantiomer is in fact the preferred guest molecule with greater interaction and selectivity observed for this enantiomer than in the case of the (S)-enantiomer was confirmed by fluorescence emission studies.

Preliminary studies on the absorption spectrum of calixarene **L1** showed changes in the presence of a phenylalaninol guest molecule. This would indicate that the process of quenching is probably static, that is, the guest molecule forms a non-fluorescent ground state complex with the calixarene host. With the aid of fluorescence lifetime studies it was established that since the lifetime of the excited state of **L1** was independent of the concentration of the guest molecule, that static quenching was the cause of the decrease in fluorescence intensity of **L1** in the presence of phenylalaninol. The lifetime measurements revealed that there were two fluorescing species in solution, which could be due to two different conformations of **L1** in solution.

The fluorescence behaviour of sodium and potassium complexes of **L1** was examined, which resulted in a five-fold increase in association constant (with respect to the R-enantiomer of phenylalaninol) for the potassium complex of **L1** with respect to the free ligand. The molecular modelling data in conjunction with the fluorescence quenching results would seem to suggest that greatly enhanced enantiomeric discrimination is achieved when the calixarene exists in a highly structured symmetrical cone conformation, which is in this case induced by metal-ion complexation. If ligand **L1** is to be employed as an analytical sensing agent, then it is clear that the metal ion complexes, in particular that of potassium perchlorate are the most advantageous sensor molecules when it comes to the enantiomeric discrimination of phenylalaninol, due to a greater sensitivity of the ligand to the guest and the huge selectivities obtained.

Chiral discrimination of phenylalaninol is however not possible with **L1** in acetonitrile. There appears to be a 1:1 host:guest association with **L1** and PA in this solvent. Since acetonitrile is a polar non-protic solvent this may be due to the lack of hydrogen bonding from the solvent to the calixarene. This implies that the guest PA

does not need to disrupt any host-solvent associations when spiked into the calixarene in solution and therefore immediately associates with the host

In chloroform as solvent a very different behaviour is seen Chiral discrimination is statistically possible with **L1** and PA in chloroform, but while monitoring the emission at 340nm the extent of discrimination is not comparable to that of the metal-ion complexes discussed in the previous chapter When the emission intensity of this ligand is monitored at 440nm in the presence of PA, huge differences in the fluorescence intensities are seen with respect to the two enantiomers In the case of S-PA practically no change is observed at 440nm when this enantiomer is present in solution with **L1** However a dramatic increase in fluorescence intensity is observed at 440nm when R-PA is added to a solution of **L1** in chloroform

Fluorescence lifetime measurements verify that the quenching mechanism responsible for the changes in the emission intensities of **L1** in the presence of both enantiomers of PA is static This rules out the possibility of exciplex formation between **L1** and R-PA Lifetime measurements also confirm that two fluorescing species exist in solution, which have been attributed to two different calixarene conformations in chloroform This theory is supported by the ^{1}H-NMR spectra in chapter 4, and when one consults the energy minimised structures of **L1** in chapter 4 it is clear that the free ligand is quite flexible and may exist as conformations other than a rigid cone, when in solution

6 2 *Future Work*

The formation of a fully completed series of mono- di- and tri-substituted calixarenes from (**119**), (**120**) and (**121**) could be produced from a series of reactions by varying the stoichiometry of calixarene, alkylating agent and base This would result in an interesting series of calixarene molecular receptors which could possibly be employed as chiral or anion receptors, with the possibility of fluorescence detection provided by the appended fluorophores

A five-fold excess of the amide moiety was used which was not sufficient to complete the tetra-substitution A stronger base therefore, with a greater excess of alkylating agent (amide) could possibly produce tetra-substituted amides A study could also be carried out with respect to the effect of solvent on the reaction for tetramer formation Since the conformations of calixarenes vary greatly depending (in part) on the upper rim substituents, varying the *p*-substituent may help to provide an insight into the effect of conformation on the binding of target molecules

Further research into the ion-binding properties of **L1** using ion selective electrodes is continuing, whereby the selectivity of this calixarene could be tested against a wide range of metal ions Metal ion complexation could also be verified by the conventional picrate extraction method

Fluorescence lifetime measurements of the calixarene-metal complexes may help to distinguish the two apparent quenching processes observed in the emission studies This data may provide a more exact insight into the processes occurring when a concentration of R-phenylalaninol higher than 15 mmol dm^3 is added to **L1** in methanol The host-guest behaviour of **L1** in acetonitrile with phenylalaninol at the same concentration should be investigated, to verify whether a 1 1 association is actually occurring This may be studied by ^{1}H-NMR spectra of the host, guest and host guest association in a 1 1 ratio in a solution of deuterated acetonitrile, or by measuring the fluorescence emission spectra of these solutions

Appendix A

Anal. Chem. **2002,** *74,* 59–66

Tuning and Enhancing Enantioselective Quenching of Calixarene Hosts by Chiral Guest Amines

Carol Lynam,[†] Karen Jennings,[†] Kieran Nolan,[†] Paddy Kane,[†] M. Anthony McKervey,[‡] and Dermot Diamond*[,†]

National Centre for Sensor Research (NCSR), School of Chemical Sciences, Dublin City University, Dublin 9, Ireland, and School of Chemistry, The Queen's University, Belfast BT9 5AG, N. Ireland

The synthesis of a propranolol amide derivative of *p*-allylcalix[4]arene is described, which has been designed to behave as a molecular sensor capable of distinguishing chiral amines on the basis of their shape and chirality. This molecule can discriminate between the enantiomers of phenylalaninol through the quenching of the fluorescence emission in methanol in contrast to an (*S*)-dinaphthylprolinol calix[4]arene derivative, which can discriminate between the enantiomers of phenylglycinol, but not phenylalaninol. The separation between the naphthyl fluorophores and the hydrogen-bonding sites within the chiral cavity can be tuned to recognize guest amines with similar separation between aryl groups and hydrogen-bonding sites. The formation of metal ion complexes of the *p*-allylcalix[4]arene propranolol amide derivative is shown to induce a more regular and rigid cone conformation in the calix[4]arene macrocycle, which generates a significant enhancement in the observed enantiomeric discrimination.

Approximately 50% of synthetic drugs currently used therapeutically are chiral in nature[1] with increasing numbers being supplied as a pure enantiomer, since the right-handed and left-handed forms can often have different pharmacological effects when administered to the body.[2] In the absence of an external chiral influence, enantiomers have identical chemical properties except toward optically active reagents and identical physical properties except for the direction of rotation of the plane of polarized light. Because of these similarities, analytical discrimination of enantiomers is very challenging and is usually based on chromatographic separations using chiral stationary phases.[3–6]

Much of the analytical interest in calixarenes derives from their potential as selective and useful complexation agents, with the main area of interest to date being their use as molecular sensors.[7] This depends in part on the presence of appropriately sized cavities; however, for the more sophisticated recognition mechanisms, it is also necessary that appropriate functional groups are present in a spatial arrangement that is complementary to binding sites in the guest molecule (i.e., shape-based recognition rather than size-based).

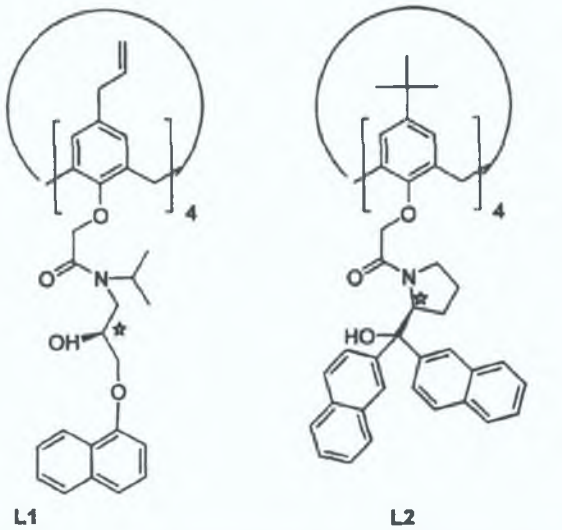

L1 L2

Figure 1. Propranolol amide derivative of *p*-allylcalix[4]arene **L1** and (*S*)-2-dinaphthylprolinol calix[4]arene derivative **L2** (chiral centers indicated by stars).

In designing any molecular sensor, the main issues to be addressed are as follows: (1) recognition of the target species; (2) transduction of the binding event; (3) immobilization or controlled localization.

To achieve our goal of chiral recognition of molecular guests, the calixarene host must be functionalized with chiral moieties that define a 3-D chiral distribution of binding sites complementary to that of the guest. The structures of the host calix[4]arenes (**L1**, **L2**) are given in Figure 1. The molecular design components are broadly similar in that they both possess the following: (1) a calix[4]arene backbone (4-repeat units in the macrocycle); (2) hydrogen-bonding sites defined by carbonyl oxygen, amide nitrogen, and hydroxy groups at roughly similar positions with respect to the phenoxy oxygen at each pendant group; (3) a chiral center (starred in Figure 1) located in the vicinity of the hydrogen-bonding sites; (4) naphthyl groups sited at the bottom of the pendant groups to provide a fluoresence signaling capability; (5)

* To whom correspondence should be addressed: (e-mail) dermot.diamond@dcu.ie.

[†] Dublin City University.

[‡] The Queen's University.

(1) Hacksell, U.; Ahlenius, S. *Tibtech* **1993**, *11* (March,), 73–74.
(2) Cope, M. J. *Anal. Proc.* **1993**, *30* (Dec), 498–500.
(3) Shamsi, S. A.; Warner, I. M. *Electrophoresis* **1997**, *18*, 853–872.
(4) Bojarski, J.; Aboul-Enein, H. Y. *Electrophoresis* **1997**, *18*, 965–967.
(5) Jung, M.; Mayer, S.; Schurig, V. *LC-GC* **1994**, *12*, 458–468.
(6) Mayer, S.; Schurig, V. *J. Liq. Chromatogr.* **1993**, *16*, 915–931.
(7) Diamond, D.; Nolan, K. *Anal. Chem.* **2001**, *73*, 22A–29A.

10.1021/ac010153k CCC: $22.00
Published on Web 11/30/2001

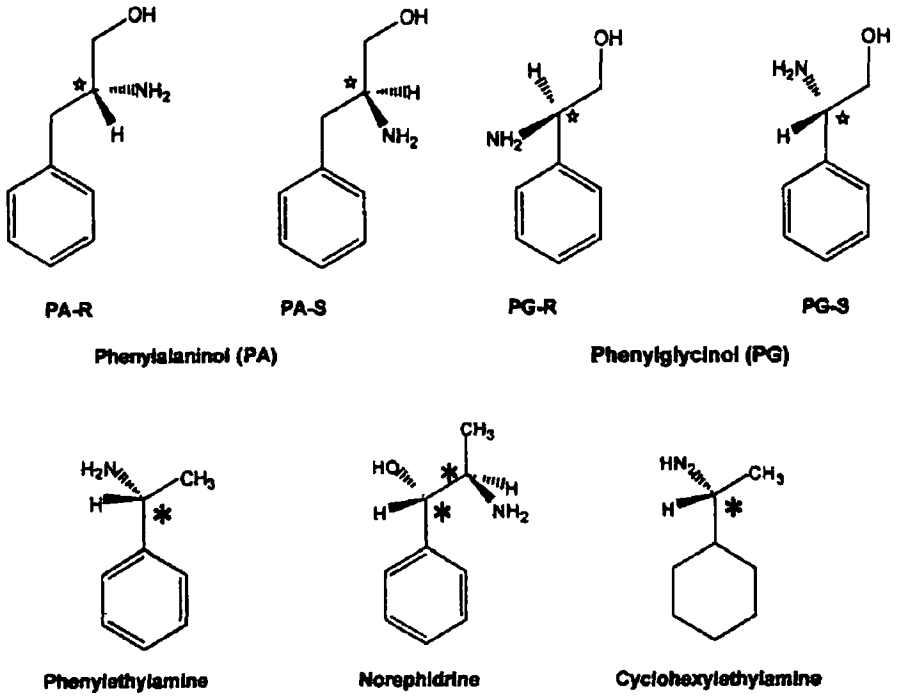

Figure 2 Structures of phenylamines (*R*) and (*S*) phenylalaninol (PA R and PA S respectively) (*R*) and (*S*) phenylglycinol (PG R and PG S respectively) phenylethylamine norephidrine and cyclohexylamine (chiral centers indicated by astensks)

allyl groups positioned at the end of the calix[4]arene opposite to the chiral binding sites (the upper rim) in order to facilitate immobilization on a polymer substrate with minimal effect on the host–guest characteristics and fluorescence properties (**L1** only)

In previous work [8,9] it has been shown that ligand **2** can discriminate between the enantiomers of phenylethylamine norephedrine and phenylglycinol (Figure 2) In these guest molecules the common feature is the positioning of hydrogen bonding sites and a chiral center immediately adjacent to an aryl ring The aryl ring is known to be a crucial feature as cyclohexyl ethylamine (Figure 2) the nonaromatic analogue of phenylethyl amine has no quenching effect at all [10]

Although the two calixarene hosts contain similar design features and their structures are broadly similar we are interested in the effect of subtle differences in these molecular receptors in particular the effect of the relative spacing between the naphthyl signaling groups and the 3 D chiral distribution of binding sites within the calixarene cavity **L1** has therefore been designed to have these binding sites and the chiral center separated from the naphthyl groups by an additional ether group compared to **L2** (Figure 1)

Key questions to be addressed are as follows Does the chiral discrimination depend on the separation of the aryl group and the chiral binding centers? If so can this separation be tuned in hosts and guests to provide sensitive molecular recognition as well as chiral discrimination? As calix[4]arenes have well known ion binding properties will ion complexes have different host–guest behavior compared to the free calix[4]arene host?

To examine these questions the enantiomers of phenylglycinol and phenylalaninol were used as target guests Phenylalaninol differs from the other amines in that it has the chiral binding sites separated from the aryl group by a methylene spacer (Figure 2)

EQUIPMENT AND MATERIALS

All experiments were performed using a Perkin Elmer luminescence spectrometer LS 50B (Beaconsfield Buckinghamshire U K) Postrun data processing was performed using Microsoft Excel 97 Both enantiomers of phenylalaninol (*R*) (+) phenyl alaninol and (*S*) (−) phenylalaninol and both enantiomers of phenylglycinol (*R*) (−) 2 phenylglycinol and (*S*) (+) 2 phenylglycinol were obtained in 99% purity (ee >99 1 HPLC) from Fluka Biochemika (Gillingham Dorset U K) The methanol (HPLC grade solvent) was obtained from Labscan (Stillorgan Co Dublin Ireland)

Synthesis of the Propranolol Amide Calix[4]arene Derivative The dealkylated tetramer **I** was prepared as described previously (See Figure 3) [11] From this calix[4]arene **II** was subsequently reacted with allyl bromide in a Williamson ether synthesis as previously described [12] This delivered the tetrakis (allyloxy)calix[4]arene **III** a solution of which (3 15 g 5 4 mmol) in 25 mL of *N*,*N*-diethylaniline was refluxed for 2 h under N_2 After acidification with concentrated HCl and filtration the crude product was recrystallized from 2 propanol to give colorless needles in 80% yield (2 55 g) [13] The Claisen rearrangement product **IV** [12] the *p*-allylcalix[4]arene (2 55 g 4 4 mmol) was subsequently refluxed in 30 mL of dry acetone with anhydrous K_2CO_3 (3 65 g

(8) Grady T Joyce T Smith M R Harris S J Diamond D *Anal Commun* **1998** *35* 123–125
(9) Grady T Harris, S J Smyth M R Diamond D *Anal Chem* **1996** *68* 3775–3782
(10) Jennings K Diamond D *Analyst* **2001** *126* 1063–1067
(11) Gutsche C D Levine J A *J Am Chem Soc* **1982** *104* 2652–2653
(12) Gutshce C D Dhawan B Levine J A Hyun No K Bauer L J *Tetrahedron* **1983** *39* 409–426
(13) Gutsche C D Levine J A Sujeeth P K *J Org Chem* **1985** *50* 5802–5806

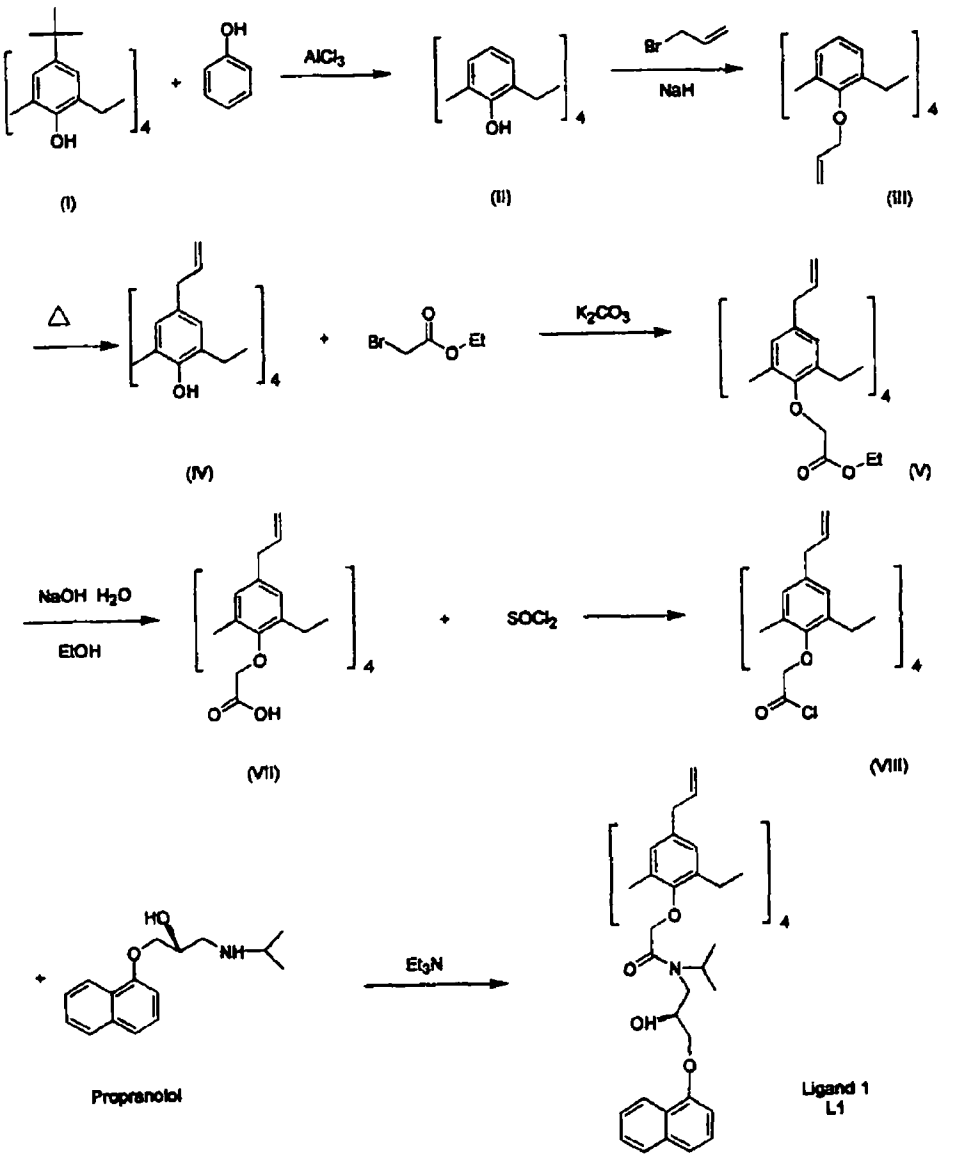

Figure 3 Reaction scheme outlining the synthesis of **L1** the propranolol amide derivative of *p*-allylcalix[4]arene

26 4 mmol) and ethyl bromoacetate (9 4 mL 37 4 mmol) under N_2 for 5 days The reaction mixture was filtered concentrated and redissolved in $CHCl_3$ which was then washed dried filtered and concentrated and the residue recrystallized from dichlo romethane/methanol to give a white crystalline solid **V** in 50% yield (2 03 g) The *p*-allyl tetraethylester **V** (2 03 g 2 2 mmol) was then hydrolyzed to its carboxylic acid sodium salt by refluxing with NaOH (1 67 g 0 042 mol) in 50 mL of ethanol followed by acidification with 50% aqueous H_2SO_4 and filtration to give 87% of the corresponding acid **VII** (1 55 g) A 310 mg sample of this acid was subsequently converted to the acid chloride by a 2 h reflux in 10 mL of thionyl chloride followed by removal of volatiles to give **VIII** in quantitative yield which was used immediately To 300 mg (0 4 mmol) of the acid chloride **VIII** in 5 mL of dry THF was added 0 435 g (1 6 mmol) of (*S*) propranolol and 0 24 mL (1 6 mmol) of triethylamine with stirring at room temperature for 24 h A pale yellow product was isolated by filtration and purified by column chromatography (silica EtOAc/MeOH) This yielded a yellow solid in 40% yield (**L1** Figure 1) mp decomposes above 190 °C IR λ_{max} (cm^{-1}) 1654 (C=O str (amide)) 3435 (OH str) ^{1}H NMR 400 MHz ($CDCl_3$) (ppm) δ 1 13 and 1 37 (12H each $NCH(CH_3)_2$) 3 15 (d 8H allyl) 3 3 (m 8H NCH_2) 3 4 (m 4H NCH) 4 09 (d 4H Ar-CH_A Ar) 4 2 (4H chiral CH) 4 4 (8H CH_2O naphth) 4 69(d 4H Ar-CH_B Ar) 4 94 (8H Ar OCH_2) 4 96 and 4 98 (4H each $CHCH_2$(allyl)) 5 8 (m 4H $CH_2CH{=}CH_2$) 6 62 (d 4H naphthyl) 6 8 (d 4H naphthyl) 7 19 (d 8H phenolic benzene) 7 35 (m 12H naphthyl) 7 66 (d 4H naphthyl) 8 19 (d 4H naphthyl) ESIMS (in acetonitrile) *m/e* (rel intensity) 1805 (MNa^+ 100)

Procedure for Fluorescence Measurements Solutions giving concentrations of the propranolol amide calix[4]arene (**L1**) of 0 7 μmol dm^{-3} and phenylalaninol in the range 0−25 mmol dm^{-3} in methanol were prepared as follows A 0 1 mmol dm^{-3} stock solution of **L1** was prepared by dissolving 8 9 mg in 50 mL

of methanol A 0 25 mol dm^{-3} stock solution of phenylalaninol was prepared by dissolving the required combination of the two enantiomers totaling 0 945 g in 25 mL of methanol Test solutions were prepared by taking 70 μL of the calixarene stock solution in a 10 mL volumetric flask adding 0 2 0 4 0 6 0 8 and 1 0 mL of phenylalaninol stock solution and making up to volume with methanol Measurements were repeated a minimum of three times for each addition The fluorescence intensities of the solutions were measured at an excitation wavelength of 227 nm (see Results and Discussion) The fluorescent intensity readings were compared to that of a solution containing 0 7 μmol dm^{-3} **L1** and no phenylalaninol

Solutions giving concentrations of phenylglycinol in the range 0−15 mmol dm^{-3} in methanol were prepared in a manner similar to that described above

Solutions of **L2** and phenylglycinol in methanol were prepared by transferring 0 5 1 0 and 1 5 mL of 0 025 mol dm^{-3} stock solutions of 100% *R* 100% *S* and a racemic mixture of phenyl glycinol to 10-mL volumetric flasks To each of these 100 μL of a 50 μmol dm^{-3} of **L2** methanol solution was added and made up to the mark using methanol This gave final concentrations of 0−3 75 mmol dm^{-3} phenylglycinol and 0 5 μmol dm^{-3} **L2** Each experiment was repeated a minimum of three times Emission spectra were measured at an excitation wavelength of 274 nm The fluorescence intensity readings were compared to that of a reference solution containing 0 5 μmol dm^{-3} **L1** and no phenyl glycinol

Solutions of **L2** and phenylalaninol were prepared in a manner identical to that for phenylglycinol and **L2**

Solutions of the sodium complexes of **L1** and phenylalanmol were prepared by dissolving 8 9 mg of **L1** in 50 mL of methanol and adding a 10-fold excess of sodium iodide and sodium perchlorate respectively to ensure complexation The various test solutions were then prepared in a manner identical to that of free **L1** and phenylalaninol described above Solutions containing phenylglycinol and the sodium complex of **L1** were prepared in a manner similar to that described above Test solutions for the potassium complexes of **L1** and phenylalaninol and phenylglycinol were prepared in a manner identical to that for the sodium complexes

Procedure for Molecular Modeling Studies The modeling calculations were carried out using Spartan[14] SGI version 5 1 1 The simulations were run on a Silicon Graphics O2 workstation with a MIPS R10000 rev 2 7 195 MHz CPU running an IRIX operating system release 6 3 with 128 MB RAM

Monte Carlo conformational searches were carried out on the sodium complex Each conformer found was geometry optimized in vacuo with molecular mechanics using the Merck molecular force field (MMFF) [15] The models shown correspond to the conformer found with the lowest energy

The model shown for the free ligand and the potassium complex were obtained by in vacuo geometry optimizations with molecular mechanics using MMFF

(14) Spartan Wavefunction Inc 18401 Von Karman Ave Suite 370 Irvine CA 92612 http //www wavefun com/

(15) Halgren T *J Am Chem Soc* **1992** *114* 7827−7843

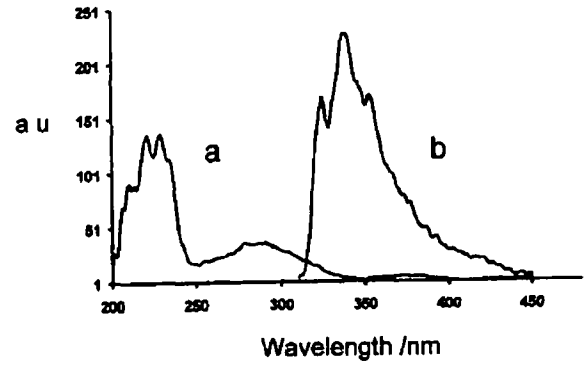

Figure 4 Excitation (a) and emission (b) spectra of **L1** in methanol

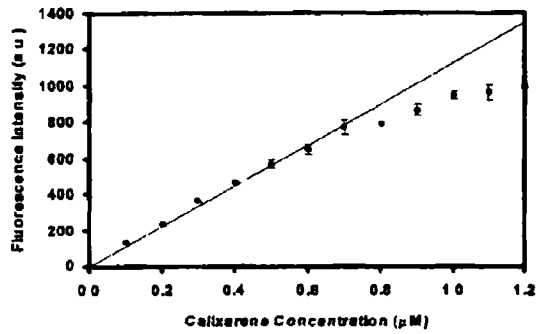

Figure 5 Linear concentration range of **L1** in methanol at 227 nm

RESULTS AND DISCUSSION

The excitation and emission spectra of the propranolol amide **L1** at a concentration of 0 7 μmol dm^{-3} are shown in Figure 4 The maximum of the excitation spectrum is at 227 nm and the maximum of the emission spectrum obtained using an excitation wavelength of 227 nm is at 338 nm Due to the fact that the guest species absorb in the region 235−275 nm 227 nm is a suitable excitation wavelength

The linear response range of fluorescence intensity to con centration of **L1** in methanol was determined to be between 0 1 and 0 7μmol dm^{-3} as shown in Figure 5 It is important to use a concentration of the calixarene within the linear range in order to ensure that no self quenching occurs and therefore that no alternative quenching mechanisms are present A concentration of 0 7 μmol dm^{-3} was chosen for subsequent experiments to examine the effects of phenylalaninol and phenylglycinol and hence any quenching observed can be related to the effect of the amine on the ligand

The efficiency of the quenching processes between the fluorophore (calixarene) and the quenching species (guest enan tiomer) follows the Stern−Volmer relationship provided both are present in the appropriate concentrations

$$I_0/I = 1 + K_{SV}[Q] \qquad (1)$$

where I_0 is the Fluorescence of the fluorophore in the absence of quencher I is the Fluorescence of the fluorophore in the presence of quencher [Q] is the concentration of the quenching species and K_{SV} is the Stern−Volmer constant A plot of I_0/I versus [Q] yields a straight line the slope of which gives the Stern−Volmer

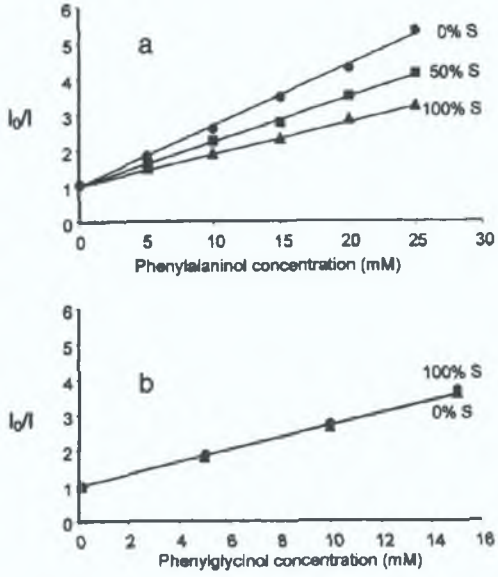

Figure 6. (a) Stern–Volmer plots for the quenching of **L1** upon addition of 0, 50, and 100% (*S*)-phenylalaninol in methanol; (b) Stern–Volmer plots for the quenching of **L1** upon addition of 100 and 0% (*S*)-phenylglycinol. Standard deviations are shown as error bars ($n = 3$), which may be masked by symbols.

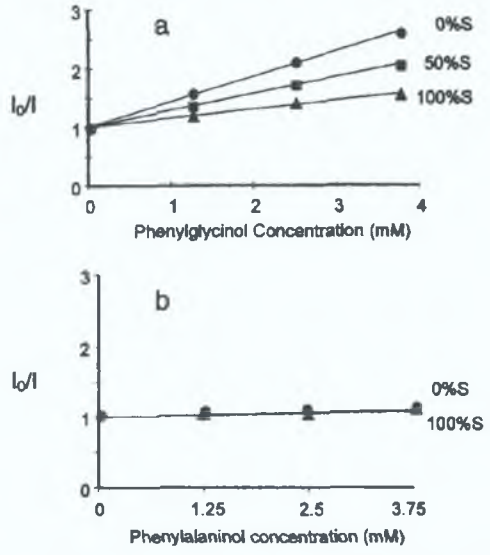

Figure 7. (a) Stern Volmer plot for the quenching of the fluorescence emission of **L2** upon addition of 0, 50, and 100% (*S*)-phenylglycinol; (b) Stern–Volmer plot for the quenching of the fluorescence of **L2** upon addition of 0, 50, and 100% (*S*)-phenylalaninol. Standard deviations are shown as error bars ($n = 3$), which may be masked by symbols.

constant (K_{SV}) and whose intercept is 1. The greater the K_{SV} value, the greater the quenching efficiency of the guest enantiomer.

The Stern–Volmer plot of **L1** was found to be linear over the range 0–25 mmol dm^{-3} racemic phenylalaninol. Figure 6 illustrates the Stern–Volmer plots for the quenching of the fluorescence of **L1** upon addition of 0, 50, and 100% (*S*)-phenylalaninol, respectively, at a concentration range of 0–25 mmol dm^{-3}. The values for the Stern–Volmer constants (K_{SV}) are 0.172, 0.124, and 0.0888 after the addition of 0, 50, and 100% (*S*)-phenylalaninol, respectively, and the (K_{SV}) ratio (100% *R*/100% *S*) is 1.937. Because the Stern–Volmer plots show such a large difference in the K_{SV} values of each enantiomer, it can be concluded that **L1** exhibits significant ability to discriminate between the enantiomers of phenylalaninol. Although the observation of linear Stern–Volmer plots usually indicates that collisional (or dynamic) quenching has occurred, static quenching can also result in a linear Stern–Volmer plot. In general, static and dynamic quenching can be distinguished by their differing dependence on temperature and viscosity, or preferably by lifetime measurements. An additional method to distinguish static and dynamic quenching is by careful examination of the absorption spectra of the fluorophore. Collisional quenching only affects the fluorophores' excited states and therefore no changes in their absorption spectra are predicted. Preliminary studies of the absorption spectra of ligand **L1** would seem to indicate a collisional quenching mechanism, due to the absence of changes in the spectrum in the presence of a guest molecule.

Figure 6 illustrates the Stern–Volmer plots for the quenching of the fluorescence of **L1** upon addition of 0 and 100% (*S*)-phenylglycinol at a concentration range of 0–15 mmol dm^{-3}. The values for the Stern–Volmer constants (K_{SV}) are 0.1615 and 0.1683 after the addition of 0, and 100% phenylglycinol respectively, and the (K_{SV}) ratio (100% *R*/100% *S*) is 0.959. Clearly, there is virtually no difference between the K_{SV} values for the *R* and *S* enantiomers. It can therefore be concluded that approximately equal interactions takes place between **L1** and both enantiomers of phenylglycinol. Enantiomeric discrimination of phenylglycinol is therefore not possible with this calix[4]arene. However, the K_{SV} values are virtually the same as the (*R*)-phenylalaninol enantiomer, implying that both phenylglycinol enantiomers quench **L1** to the same degree as (*R*)-phenylalaninol.

The synthesis of **L2** was previously described, and the linear range of this ligand in methanol is known to be 0.1–0.5 μmol dm^{-3} at an excitation wavelength of 274 nm and emission wavelength of 340 nm.[9] Therefore, a concentration of 0.5 μmol dm^{-3} was chosen to examine the quenching effects of phenylglycinol and phenylalaninol. Over the range of 0–3.75 mmol dm^{-3} racemic phenylglycinol, a linear Stern–Volmer plot was observed (not shown). The Stern–Volmer plots for the quenching of **L2** after addition of 0, 50, and 100% (*S*)-phenylglycinol at a concentration range of 0–3.75 mmol dm^{-3} are illustrated in Figure 7a. The values for the Stern–Volmer constants are 0.4338, 0.2854, and 0.1501 for the addition of 0, 50, and 100% (*S*)-phenylglycinol, respectively. The K_{SV} ratio is 2.89, and from this it can be concluded that the (*S*)-dinaphthylprolinol calix[4]arene (**L2**) exhibits excellent ability to discriminate between the enantiomers of phenylglycinol.

The quenching effect of phenylalaninol on **L2** over the same concentration range is shown in Figure 7b. The Stern–Volmer constants were calculated to be 0.025, 0.0246, and 0.0195 after the addition of 0, 50, and 100% (*S*)-phenylalaninol. From these results, it can be concluded that neither of the enantiomers of phenylalaninol exhibits a significant quenching effect on **L2**, compared to that of (*R*)-phenylglycinol in particular, which is ~20 times more effective.

From these results, we can conclude that **L2** can successfully discriminate between enantiomers of phenylglycinol, whose chiral

center is immediately adjacent to its aromatic ring. However, when a methylene spacer is present between the chiral center and aromatic ring of the guest amino alcohol, as in phenylalaninol, no discrimination is observed.

In contrast to **L2**, **L1** was designed to have a spacer group between the chiral center and the fluorescent naphthyl moiety. This ligand was found to successfully discriminate between the enantiomers of phenylalaninol, which possesses a methylene spacer between its aromatic moiety and chiral center. However, discrimination between the enantiomers of phenylglycinol was not observed with this calixarene.

Our interpretation of these results is as follows. **L1** and **L2** both possess relatively well-defined 3-D chiral spaces in the calixarene cavity. It is almost certain that the guest amines approach from the more open end of the molecule (i.e., that defined by the fluorescent naphthyl groups) and hydrogen bond with the appropriate groups within the cavity of the host molecules. Association between the aryl groups of the guest and the naphthyl groups on the host is the source of the quenching effect, and this will be most efficient if (1) hydrogen bonding is favored (depends on the host and the guest), (2) distance to the aromatic groups corresponds (depends on presence or absence of appropriate spacer groups in the host and guest), and (3) orientation of the guest during hydrogen bonding is such that the aryl group interacts with the naphthyl group of the host.

The almost total absence of quenching of **L2** by either enantiomer of phenylalaninol is probably due to a combination of (2) and (3) above, as, if hydrogen bonding occurs, the methylene spacer leaves the aryl group sitting below the naphthyl groups, unable to effectively quench the emission. However, with phenylglycinol, both enantiomers have the correct spacing between the hydrogen-bonding groups and the aryl group (quenching is much more apparent than for the phenylalaninol enantiomers), and the *R* enantiomer of phenylglycinol is favored under (1) and (3), above.

As the host molecules are themselves chiral in nature, each bearing (*S*)-amide substituents, the *R* enantiomers in each case should be better predisposed to interact than the *S* enantiomers. This would lead to a more efficient energy transfer from the host naphthyl groups and therefore a greater slope for the Stern–Volmer plot. This is observed experimentally, as the *R* enantiomers have the larger quenching effect, with greater K_{SV} values than the corresponding *S* enantiomers. The importance of the spacing between the hydrogen-bonding sites and the aromatic groups is also clearly demonstrated in this study. The fact that the "shorter" **L2** cannot discriminate between the "longer" guest enantiomers, and the "longer" **L1** cannot differentiate between the "shorter" guest enantiomers, demonstrates the important molecular recognition capabilities of these hosts. They are very selective in their interactions with guest molecules and can successfully recognize a difference as small as a methylene spacer.

Effect of Ion Complexation on Enantiomeric Discrimination by L1. The histogram in Figure 8 shows a dramatic improvement in enantiomeric discrimination of phenylalaninol when the Na^+–**L1** and K^+–**L1** complexes are substituted for the free ligand. It should be noted that the presence of a metal ion causes no change in the fluorescence spectrum of the free ligand. It is only in the presence of guest molecules that the effect of

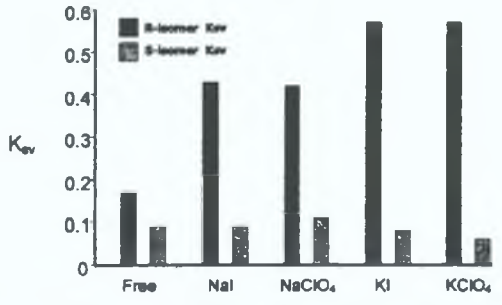

Figure 8. Histogram comparing Stern–Volmer constants of phenylalaninol in methanol with free **L1** and the Na^+–**L1** and K^+–**L1** complexes.

metal ion complexation is observed. The chiral selectivity of the free ligand, expressed as K_{SV} ratio (100% *R*/100% *S*) is calculated to be 1.9, whereas the sodium iodide and perchlorate complexes of **L1** return K_{SV} ratios of 4.8 and 3.8, respectively. This indicates a huge increase in chiral selectivity of the Na^+–**L1** complexes which is independent of the anion. When the equivalent plots are examined for the K^+–**L1** complexes, it can be seen that the K_{SV} ratios amount to 7.1 and 9.5 for the iodide and perchlorate complexes, respectively.

We believe that the reason for this dramatic increase in enantiomeric selectivity lies in the well-known tendency of calix[4]arenes to adopt a more regular C_{4V} symmetry, in which the pendent groups are held in a much more rigid conformation compared to the free ligand. In a calix[4]arene like **L1**, the metal ion will be positioned between the planes defined by the carbonyl and phenoxy oxygen atoms of the calixarene macrocycle. The main electrostatic interaction is with the carbonyl oxygen atoms, and the ion therefore tends to lie nearer these than the phenoxy oxygen atoms.[16] In contrast, the free ligand **L1** is dependent solely on hydrogen bonding to define the lower cavity, and this will therefore be less rigid, with a greater tendency to open and accommodate various guests but with corresponding loss of enantiomeric and molecular selectivities.

Important experimental evidence in favor of this hypothesis is presented in the ^1H NMR spectra of the free ligand **L1** (top), the Na^+–**L1** complex (middle), and the K^+–**L1** complex (bottom) shown in Figure 9. Three significant differences between the spectra of the complexes and the free ligand are highlighted: (1) The allyl proton resonances are split into two main resonances at 5.1 and 6.0 ppm in the free ligand. This merges into a single multiplet at ~5.85 ppm in both complexes. (2) The H_A and H_B protons of the *p*-allyl system (CH_2–CH=CH_2) and the two methylene protons of the allyl group (CH_2–CH=CH_2), which typically occur around 4.69 and 4.09 ppm, are poorly resolved complex multiplets in the free ligand spectrum compared to the complexes. (3) The isopropyl protons resonances 1.25 and 1.46 ppm merge and shift to ~1.55 ppm as a result of electron density changes arising from coordination to an electropositive metal. The apparent triplet is actually two doublets, which is to be expected since each diastereotopic methyl group is split by one proton on the adjacent carbon. The coupling constants of the apparent triplets are not equal in value, further proving that these peaks are in fact doublets.

(16) Kane, P.; Fayne, D.; Diamond, D.; McKervey, A. M. *J. Mol. Mod.* **2000**, *6*, 272–281.

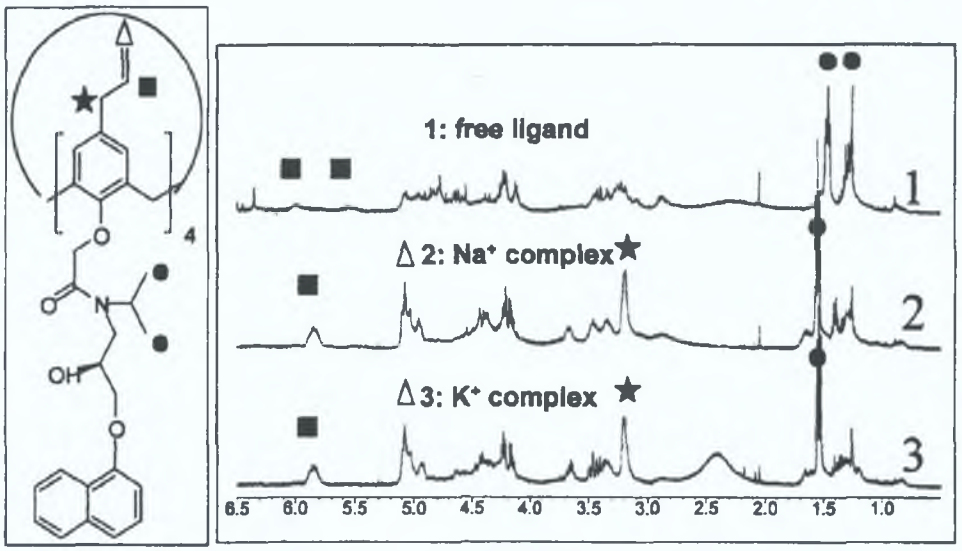

Figure 9. ^{1}H NMR spectra of (1) **L1** in $CDCl_3$, (2) **L1**−Na^+ complex in $CDCl_3$, and (3) **L1**−K^+ complex in $CDCl_3$.

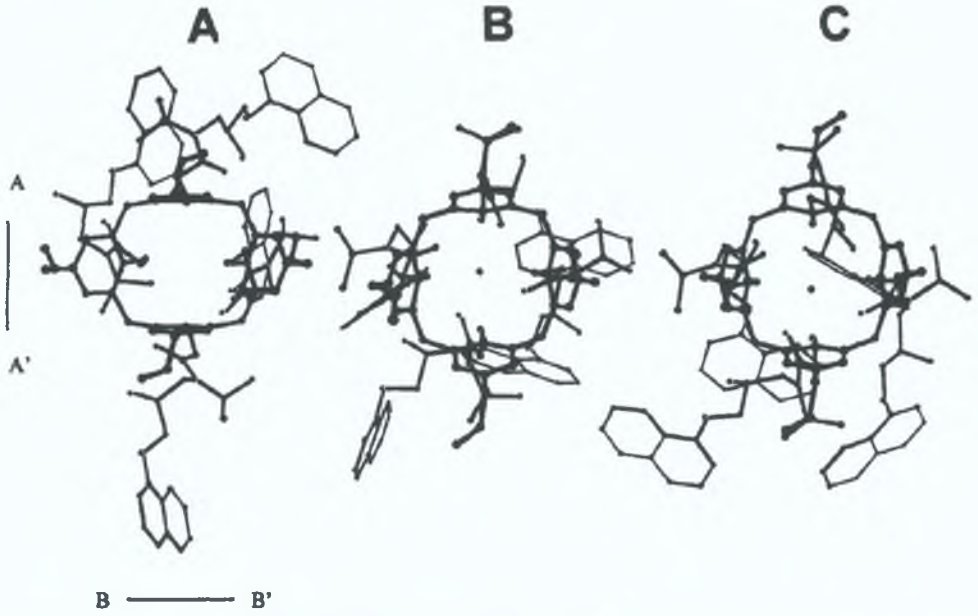

Figure 10. Energy optimized structures of (A) the free ligand **L1**, (B) the **L1**−Na^+ complex, and (C) the **L1**−K^+ complex.

These spectra prove that the metal ion complexes do form and that the calix[4]arene adopts a more symmetrical cone conformation in the process, since simplification in NMR spectra is associated with an increase in symmetry in the molecule.[17,18] It is known that in calix[4]aryl tetraesters and tetraamides the four carbonyls are turned outward to reduce electrostatic repulsion among carbonyl oxygens, whereas bound Na^+ induces the carbonyls to point inward in order to bind the Na^+ ion.[19] The merging and upfield shift of the isopropyl proton peaks show that this rearrangement is indeed occurring and that the carbonyl oxygen atoms are strongly interacting with the Na^+ ion.

Figure 10 shows views through the macrocycle cavity of **L1** and the Na^+−**L1** and the K^+−**L1** complexes generated by molecular modeling calculations. The free ligand (left) clearly has a more rectangular C_{2V} symmetry compared to the square C_{4V} symmetry of the complexes.

Table 1 summarizes important data from the molecular modeling calculations that support the evidence of the adoption of a highly symmetrical cone conformation induced by metal ion complexation provided by the H^1 NMR spectra. In the free ligand, opposing phenoxy groups of the **L1** macrocycle are almost parallel, and at right angles, respectively (11.2° and 87.4°), whereas in the Na^+−**L1** complex, they are approximately symmetrical at 56.1° and 49.9° to each other. Interestingly, with the K^+−**L1**

(17) Jin, T.; Ichikawa, K.; Koyama, T. *J. Chem. Soc. Chem. Commun.* **1992**, 499−501.

(18) Aoki, I.; Sakaki, T.; Shinkai, S. *J. Chem. Soc., Chem. Commun.* **1992**, 730−732.

(19) Ikeda, A.; Shinkai, S. *Chem. Rev.* **1997**, *97*, 1713−1734.

Table 1 Summary Data Extracted from Energy Minimized Structures[a]

		free ligand	Na^+ complex	K^+ complex
distance between opposite phenyl rings /Å	A–A	5 957	7 762	7 776
	B–B	9 561	8 116	7 996
distance between opposite phenolic oxygens/Å	A–A	5 341	4 625	4 759
	B–B′	3 692	4 599	4 771
angles made by planes/deg	A–A	11 2	56 1	52 7
	B–B	87 4	49 9	49

[a] A–A and B–B are shown in Figure 10

complex this induced symmetry is even more developed (52 7° and 49 0°) which is in agreement with the results in Figure 8 which show that the K^+–L1 complex has a greater effect than the Na^+–L1 complex Other data in Table 1 support the conclusion that the K^+ has a greater effect on the symmetry of the ligand than Na^+

CONCLUSION

It has been proven experimentally that L1 can successfully discriminate between the enantiomers of phenylalaninol with fluorescence-quenching techniques but fails to discriminate between the shorter chain enantiomers of phenylglycinol as no quenching is observed On the other hand L2 can very successfully discriminate between enantiomers of phenylglycinol but cannot discriminate the enantiomers of phenylalaninol due to equal fluorescence quenching by each enantiomer A dramatic enhancement of chiral selectivity of the enantiomers of phenyl alaninol observed with the K^+–L1 and Na^+–L1 complexes compared to the free ligand is attributed to the adoption of a more rigid and more symmetrical cavity into which the *R* enantiomer preferably fits Previously we have shown that these receptors can be used to estimate enantiomeric composition with better than 5% accuracy on the basis of a single fluorescence measurement These results suggest that an array of such receptors could provide simultaneous chiral and molecular recognition of a range of guest amines

ACKNOWLEDGMENT

We acknowledge support for this research from Enterprise Ireland under the Basic Research Program (grant SC/ 99/ 131) the Higher Education Authority PRTLI program and Westmeath County Council

Received for review February 5 2001 Accepted July 25, 2001

AC010153K

REFERENCE